Amino acid regulation of mTORC1

by

Liron Bar-Peled
B.S. Biochemistry
University of Georgia

SUBMITTED TO THE DEPARTMENT OF BIOLOGY IN PARTIAL FULFILLMENT OF THE REQUIREMENTS FOR THE DEGREE OF

DOCTOR OF PHILOSOPHY IN BIOLOGY

AT THE

MASSACHUSETTS INSTITUTE OF TECHNOLOGY

SEPTEMBER 2013

Signature of Author: _____
Department of Biology
June 14, 2013

Certified by: _____
David M. Sabatini
Member Whitehead Institute
Professor of Biology
Thesis Supervisor

Accepted by: _____
Stephen P. Bell
Professor of Biology
Chair, Committee for Graduate Students

Amino acid regulation of mTORC1

by

Liron Bar-Peled

Submitted to the Department of Biology on June 14, 2013 in Partial Fulfillment of the Requirements of the Degree of Philosophy in Biology

Abstract

Mammalian target of rapamycin complex I (mTORC1) is an atypical Ser/Thr kinase that regulates cellular and organismal growth. Accordingly, mTORC1 has substantial roles in regulating insulin sensitivity and lifespan, and when deregulated, it is implicated in the pathogenesis of common cancers. mTORC1 responds to a diverse set of stimuli, including growth factors, oxygen availability, energy and amino acid levels in order to control essential anabolic and catabolic processes. Amino acids promote mTORC1 shuttling to the lysosomal surface, its site of activation. This translocation is mediated by a family of heterodimeric GTPases known as the Rags that reside on the lysosomal surface. Unique among the small GTPases, the Rags are obligate heterodimers: the highly related RagA and RagB are functionally redundant and bind to RagC or RagD, which are also very similar to each other. Amino acids regulate the binding of nucleotides to RagB, such that amino acid stimulation increases its GTP loading, leading to the recruitment and binding of mTORC1. In the work described here, we identify two Rag interacting complexes termed 'Ragulator' and 'GATOR' that form a lysosome based signaling platform that controls the activity of the Rags. We find that Ragulator is a pentameric complex that is both necessary and sufficient to determine the intracellular localization of Rags. Moreover, we find that Ragulator functions as a guanine nucleotide exchange factor (GEF) for RagA and RagB stimulating GTP-loading, a key event in the amino-acid dependent activation of mTORC1. Additionally, we describe the function of GATOR, an octomeric complex that is defined by two distinct subcomplexes termed GATOR1 and GATOR2. We find that GATOR2 functions as a positive regulator of mTORC1 whereas GATOR1 negatively controls this pathway. Epistasis analysis reveals GATOR2 functions upstream of GATOR1, which inhibits the Rags through its GTPase activating protein (GAP) activity towards RagA and RagB. GATOR1 components are mutated in gliolbastoma and ovarian tumors and GATOR1 deficient cancer cells are hypersensitive to the mTORC1 inhibitor rapamycin. Thus, we define the molecular mechanisms regulating the function of Rags and propose a model for the activation of the mTORC1 pathway by amino acids.

Acknowledgements

David Sabatini is everything I could have asked for in a mentor: insightful, adventurous, creative, meticulous and frank. My meetings with David were usually impromptu and happened at my bench. While they would begin with science (where his infectious curiosity is evident) they would often meander into other areas such as cycling and politics. I owe David a great deal of gratitude for helping me to develop into the scientist that I am today.

Throughout my years as a graduate student Hidde Ploegh and Iain Cheeseman have served as my thesis committee members. Though both have incredibly busy schedules, they have always left a door open for spontaneous meetings and their advice has helped propel my research forward. I would also like to thank Matt Vander Heiden and Brendan Manning whose work I've long admired for serving on my thesis defense committee.

When I first arrived in the Sabatini lab, Yasemin Sancak guided me through the ropes of molecular biology. Not only have we had wonderful collaborations but a lasting friendship, which I am truly thankful for. I was also very fortunate to have Lynne Chantranupong as a bay mate for these past two years and I am delighted to have had the opportunity to work with her during this time. I've had fruitful collaborations with Roberto Zoncu and Larry Schweitzer, whose scientific ideas have guided me in new directions. More often than not, room 359 has felt like home and this could only made possible by Yasemin, Lynne, Nada, Nora, Tony, Tim, Zhi, Shuyu and Naama. I would also like to thank Dohoon Kim for his generosity and our lengthy conversations that were rarely about science. Edie Valeri and Kathleen Ottina have kept the lab running and made my research possible. Finally, the Sabatini lab, would not be such a special place to work in if it were not for its members and I would like to thank them all, past and present.

I met many of my graduate school classmates before we were even officially enrolled at MIT and in the past six years we've shared the ups and downs of research. I have made some lasting friends at MIT and I have greatly enjoyed both our scientific and non scientific adventures. I would especially like to thank: Mohini Jangi, Keren Higleldorf, Zach Whitfield, David Weinberg, Lauren Surface, Emily Rosowski, Sejal Vyas and Albert Alaamada for their continued friendship and advice.

I cannot even begin to thank my family (Aba, Ema, Tal and Yael) for providing unconditional love and support. My parents have always been there for me and I cherish their wisdom. My first research experience was in my father's lab, and it was here that I received my first training in, and appreciation for biochemistry. My father continues to serve as a great inspiration and is one of the reasons I will pursue a career in science.

Finally, there is my fiancée Fei. I cannot imagine making it through these past few years without her. Fei's compassion and joy that has kept me going through the perils of research in lab and has been a steadying force with the ever increasing stress of research. I am extraordinarily lucky to have met Fei and I am grateful for her companionship on the journey ahead.

Table of Contents

Chapter 1

Introduction

Cell growth is a fundamental biological process and at its simplest form entails the accumulation of biomass– an increase in carbohydrates, lipids, proteins and nucleic acids. Not surprisingly, the pathways regulating growth control are conserved across the vast swath of eukaryotic life. A master regulator of cell growth can be though of as a rheostat, gauging environmental and intracellular conditions and in turn modulating pathways responsible for growth. When conditions are favorable for cellular growth (adequate supplies of nutrients and low stress levels) anabolic programs such as translation, transcription and metabolism are activated leading to an increase in cell size. However, when growth-promoting conditions are reversed, a cell must rapidly shut down these anabolic programs and instead promote restorative catabolic programs in order to survive.

Today we know this master growth regulator to be the evolutionarily conserved target of rapamycin (TOR) pathway. In the twenty years since its discovery, the study of this pathway has transformed the field of growth regulation; not only providing a deeper molecular understanding of growth control but making important advances in the treatment of numerous human diseases. In this introductory chapter, I will provide a signaling centric description of the TOR pathway, with an emphasis on areas relevant to the presented work.

The Discovery of TOR

Our understanding of the TOR pathway began with the discovery of rapamycin, a polyketide macrolide produced by a soil bacteria on Rapa Nui, a small sunny island in the middle of the south Pacific (*3*). Rapamycin was initially characterized as a powerful fungicide inducing a striking G_1 arrest in *Saccharomyces cerevisiae* (*4*). Its antiproliferative properties also extend to

some human cancer cell lines. This spurred initial interest in its application as a chemotherapeutic– an idea that would only be realized decades later in the treatment of advanced renal cell carcinoma (*5, 6*). Notably, rapamycin treatment of a variety of cell types resulted in a dramatic reduction in cell size, implicating its role in growth control (*3*). Rapamycin was also appreciated as a potent immunosuppressant (*7*), efficiently blocking IL-2 mediated lymphocyte proliferation at low nanogram doses (*8*), while maintaining immune surveillance (*8*) and thus avoiding additional complications associated with other immunosuppressants. Today, rapamycin (also known as serolimus) is a mainstay in organ transplantation (*9*) and rapamycin-coated stents are used during angioplasties to inhibit restenosis of arteries (*10*). These therapeutic properties of rapamycin fueled great interest in understanding the molecular mechanisms underlying its function.

Initial insights into the cellular targets of rapamycin came from *Saccharomyces cerevisiae*. Elegant genetic screens in this organism uncovered that mutations in three genes completely blocked the antiproliferative effects of rapamycin (*11, 12*). The first gene identified was FRP1, which encodes the evolutionarily conserved prolyl-hydroxylase FKBP12 that forms a stable complex with rapamycin in cells (*11*). While knockout of FRP1 mediates complete resistance to rapamycin-induced G_1 arrest, loss of FKBP12 did not have an overt growth phenotype. This suggests that while FRP1 is necessary for the function of rapamycin it was not the relevant cellular target (*12*).

The two remaining genes contained dominant active mutations resulting in corresponding protein products that cannot interact with the FKBP12-rapamycin complex. The two genes are over 7000 base pairs in size and were renamed target of rapamycin 1 and target of rapamycin 2 (TOR1 and TOR2, respectively) (*12*). Deletion of TOR1 results in smaller cells and is synthetic lethal with rapamycin treatment, yet proves dispensable for yeast viability. In contrast deletion of TOR2 is lethal (*13*). These results indicated that although TOR1 and TOR2 share substantial homology they also have non-overlapping functions.

While genetic approaches in yeast identified the genes that replicate the cellular effects of rapamycin, it would be biochemical approaches in mammalian cell lines that would uncover this compound's physical target.

In parallel efforts to uncover the function of rapamycin in mammalian cells, multiple research groups undertook protein purification campaigns to identify FKBP12-rapamycin interacting proteins. This yielded the discovery of a massive protein (289 kDa) of unknown function that was named the apropos mammalian TOR or mTOR (*14-16*). Unlike budding yeast, higher eukaryotes as well as *Saccharomyces pombe* only contain one ortholog of TOR.

mTOR is a founding member of the phosphatidylinositol-3 kinase related kinase (PIKK) family which also includes ATM, ATR, DNA-PK and SGM-1L (*17*). The PIKKs are characterized by their large size and a C-terminal Ser/Thr kinase domain which resemble the catalytic domain of the lipid kinase PI3K (*18*). A sixth member of the PIKK family, TRRAP, lost its kinase activity. The mTOR consensus phosphorylation motif is poorly defined, compared to other members of the PIKK family, making bioinformatic identification of mTOR substrates difficult. Two recent phospho-proteomic studies revealed that the mTOR phosphorylation site is enriched at the +1 position for proline, aliphatic (Leu, Val) and hydrophobic (Phe, Tyr, Trp, His) residues (*19, 20*). The PIKK family members also share additional domains including a FRAP, ATM and TRRAP (FAT) domain and a C-terminal FAT domain that together flank the kinase domain of mTOR and are both required for its activity (*17, 21*). At the N-terminus of mTOR are two Huntington, elongation factor 3, the A subunit of phosphatase 2A and TOR (HEAT) domains necessary for protein-protein interactions (*22*). Finally, sandwiched between the TOR kinase domain and FAT domain is the FKBP12-rapamycin binding (FRB) domain (*23, 24*), which covers the catalytic cleft and functions as a gate keeper for substrate entry (*25*) (**Figure 1, A and B**).

The two faces of TOR

In cells, mTOR does not function on its own but rather in two distinct multicomponent complexes commonly referred to as mTOR complex 1 and mTOR complex 2 (mTORC1 and mTORC2, respectively) (*6*). These complexes are conserved to yeast, where TORC1 is nucleated by either TOR1 or TOR2 and TORC2 only by TOR2 (*26*). The identification of these two complexes explains the original observations that TOR1 and TOR2 have non-overlapping functions.

mTORC1

mTORC1 is a pentameric complex (**Figure 1C**), which homodimerizes to form a 2 MDa rhomboid. This massive complex contains a central cavity that is presumed to be important for substrate phosphorylation (*27*). Affinity purifications of mTOR (the mainstay for finding mTORC1 complex members) identified regulatory associated protein of mTOR (raptor) as an mTOR binding protein (*28, 29*). Raptor is the defining member of mTORC1 and contains multiple WD40 interaction domains and HEAT motifs making it a highly effective protein scaffold. Raptor not only serves as a docking site for many mTORC1 substrates through its interaction with their TOR signaling (TOS) motifs (*30, 31*) but is also essential for the intracellular localization of mTORC1 (*32, 33*). mTORC1 is known as the rapamycin sensitive complex and is rapidly inactivated by acute rapamycin treatments. The rapamycin-FKPB12 complex is thought to block mTORC1 function by disrupting the mTOR-raptor interaction (*27*) in addition to preventing substrate entry into its catalytic cleft (*25*). Intuitively, mTOR is essential for life and mice null for this protein die during implantation (*34*). Similarly, mouse embryos lacking raptor expire shortly after e6.5 (*35*).

The second mTORC1 member identified was mLST8 (*36*), whose budding yeast ortholog (LST8) was originally characterized as a gene that was synthetic lethal with the COPII and nucleopore member Sec13 (*37*). Like raptor and many GATOR proteins (see chapter 4), mLST8 also contains a WD40 domain and in cultured mammalian cells is required for proper mTORC1 function (*36*). Deletion of mLST8 is lethal at embryonic day e10.5 (*35*), however loss of this protein does not alter mTORC1 activity in cells obtained from knockout animals, further

complicating our understanding of its function (*35*). Proline rich Akt substrate of 40 kDa (PRAS40) is one of two endogenous mTORC1 inhibitors and interacts directly with raptor to inhibit mTORC1 kinase activity both in vitro and in vivo (*38, 39*). As its name suggests, PRAS40 is phosphorylated by Akt (*40*), which promotes its dissociation from raptor and relieves its inhibitory activity towards mTORC1 (*38*). DEPTOR rounds out the remaining members of mTORC1. Like PRAS40, DEPTOR also inhibits mTORC1 kinase activity (*41*).

In yeast, TORC1 contains two othrologs of its mammalian counterpart: KOG1 the ortholog of raptor and LST8 (*26*). Additionally, TORC1 also contains the yeast specific TCO89, whose function appears important for cell wall maintenance (*42*). Curiously, unlike other TORC1 components (with the exception of TOR2), deletion of KOG1 is lethal illustrating its non-redundant functions in yeast (*26*). As described below, mTORC1 serves as a master regulator of cell and organismal growth.

mTORC2

Unlike mTORC1, the cellular functions of mTORC2 remain poorly understood. Like mTORC1, mTORC2 is also a zaftig of a complex, however it is currently unknown whether it adopts a higher order structure. Rapamycin-insensitive companion of mTOR (rictor) is an essential component of mTORC2 (*43, 44*), and serves as a scaffold that is required for the phosphorylation and activation of the mTORC2 substrates: Akt, PKCα and SGK1 (*35, 45, 46*). The rictor-mTOR interaction is not perturbed by short-term rapamycin treatments, thus defining mTORC2 as the rapamycin insensitive complex (*43*). However, in certain cancer cell lines, prolonged treatment with rapamycin disrupts mTORC2 stability leading to a decrease in Akt phosphorylation (*47*). In other cell lines Akt phosphorylation is increased upon rapamycin treatment due to inhibition of the S6K-IRS1 feedback loop discussed below. Like raptor, rictor is necessary for murine viability, however mice lacking rictor die at e10.5 compared to the much earlier death for raptor-null mice (*35*). In addition to rictor, a troika of additional mTORC2 specific components exist: protein associated with rictor 1 or 2

(PROTOR1, PROTOR2) (*48*) and mammalian stress-activated protein kinase interacting protein 1 (mSIN1) (*49, 50*). Binding of PROTOR1 or PROTOR2 to rictor is mutually exclusive and the function of their remains elusive. mSIN1 is required for mTORC2 stability and Akt phosphorylation (*49*). mLST8 and DEPTOR are shared with mTORC2 and maintain their functions in this complex as well (*41, 43*).

Yeast TORC2 contains three orthologs of mTORC2: AVO1 (mSIN1) (*51*), AVO3 (Rictor) and LST8 (*26*). Additionally, AVO2 is also a TORC2 component, but its function is poorly understood (*26*). While mTORC1 promotes cell growth, mTORC2 is responsible for cell proliferation and survival, making this pathway an enticing therapeutic target.

Pharmacological Inhibitors of mTOR

While rapamycin serves as both a useful discovery tool and pharmacological agent, it has long been appreciated that this allosteric inhibitor only partially blocks mTOR kinase activity. Recent pharmacological screens resulted in several ATP-competitive inhibitors (Torin, PP242 and PP30) that specifically target the mTOR kinase domain (*52-54*). With median inhibitory concentrations (IC_{50}) in the low nanomolar range toward mTORC1 in vitro and in cells, these catalytic inhibitors have begun to reveal many novel functions for mTORC1 (*19, 55, 56*). Importantly, this new class of mTOR inhibitors also disrupts the function of mTORC2, notably the phosphorylation of Akt (*52*). Thus, these catalytic inhibitors may be more clinically beneficial than rapamycin in treatment of certain cancers. Indeed, recent pre-clinical studies revealed a striking decrease in PI3K driven tumors after treatment with catalytic site inhibitors when compared to rapamycin treatment (*57*),(*58*). However, the full therapeutic benefits of these mTOR catalytic inhibitors will only be realized upon identification of biomarkers that can predict which tumors are addicted to deregulation of the mTORC1 and mTORC2 pathways.

The research presented in this thesis pertains to mTORC1 and the remainder of the introduction will describe signaling pathways upstream and downstream of this complex as well as the deregulation of this pathway in human disease.

Making a cell grow: Downstream pathways regulated by mTORC1.

As a master regulator of growth, mTORC1 increases cell biomass by promoting anabolic programs including translation, transcription, mitochondrial biogenesis, and lipid and nucleic acid biosynthesis, while inhibiting catabolic pathways such as autophagy (**Figure 2**).

Protein synthesis

Proteins account for roughly 50% of the dry weight of a cell, making regulation of protein synthesis by mTORC1 critical to cell growth (*59*),(*60*). mTORC1-mediated translational control is best understood at the level of its effectors S6 Kinase1 (S6K1) and eIF-4E binding proteins (4EBPs) and by promoting ribosome biogenesis and translation of transcripts containing a 5' terminal oligopyrimidine (TOP) sequence.

S6K

Early investigations with rapamycin revealed that phosphorylation of the ubiquitous S6 ribosomal protein was sensitive to this drug (*61-63*). S6 forms part of the 40S ribosomal subunit and is phosphorylated on multiple residues by the protein kinase A, G, C (AGC) family member S6K1 (*64, 65*), a direct mTORC1 substrate (*66, 67*). In mammalian cells S6K1 exists as a two isoforms: cytosolic p70 and nuclear p85. A second S6K, S6K2, was discovered inadvertently by the generation of the $S6K1^{-/-}$ mouse (*68*). Although it is a substrate of mTORC1 and partially overlaps with S6K1 function, the cellular role of S6K2 is unclear (*68*). mTORC1 regulates S6K1 activity by phosphorylating its C-terminal loop (*66*). This forms a docking site for another AGC kinase, PDK1, which subsequently

phosphorylates and activates S6K1 (*69*). How the phosphorylation of S6 by S6K regulates translation remains controversial. Cells taken from transgenic mice in which all five phosphorylation sites on S6 have been mutated to Ala are smaller and insensitive to further reductions in cell size in response to rapamycin treatment (*70*). This demonstrates that mTORC1-dependent cell size regulation is directly dependent on S6 phosphorylation. Paradoxically these mutant cells show an increase in protein synthesis caused by an increase in translation initiation (*70*), underscoring a poorly defined feedback loop.

In addition to S6 phosphorylation, S6K1 exerts its effects on translation by phosphorylation of eIF4B (*71*), which promotes its association with the pre-initiation complex and stimulates the translation initiation helicase eIF4A. S6K1 further supports translation initiation, by relieving the PDCD4-mediated inhibition of eIF4A. S6K1 directly phosphorylates PDCD4 (*72*), which is then ubiquitinated and undergoes proteasomal degradation. S6K1 also impinges on elongation through its phosphorylation and inhibition of eEF2K (*73*). Although not directly part of protein synthesis, S6K1 increases nascent transcript splicing by activating the exon junction protein SKAR, which in combination with S6K1 enhances splicing efficiency (*74*).

4EBPs

The rate-limiting step in protein synthesis is translation initiation. Hence, multiple layers of regulation exist for this step, many of which, including cap-dependent translation, are controlled by mTORC1,. Covalent modification of a majority of nascent transcripts with a 7-methyl guanosine cap on the 5' end ensures message stability. The initiation factor eIF4E binds to the capped mRNA and recruits eIF4G1 facilitating translation initiation. 4EBPs sequester eIF4E preventing its interaction with the initiation scaffold eIF4G1 and formation of the initiation complex (*59*). Phosphorylation of 4EBPs by mTORC1 prevents 4EBPs from binding to eIF4E thus allowing the initiation complex to be assembled (*75, 76*). In mammals, three 4EBP proteins exist: 4EBP1 and 4EBP2 appear to have redundant functions as a single deletion of either does not increase total protein

synthesis (*77*), while the function of 4EBP3 is cryptic. MEFs collected from double 4EBP1 and 4EBP2 knockout mice are completely resistant to mTORC1-dependent translational regulation (*55*) implying that 4EBP1 and 2 are the major translational effectors for this pathway.

Translation of TOP mRNAs

mTORC1 also impacts protein synthesis by modulating the translation of a subset of mRNAs containing a TOP motif (*59*). TOP motifs consist of pyrimidine rich tracts, located in the 5' UTR of a transcript and are enriched in mRNAs encoding protein synthesis factors (*59*). How mTORC1 selectively regulated the translation of TOP mRNAs remained largely unknown until two groups (including our own) applied high-throughput ribosome profiling techniques to this question (*55, 78*). These studies revealed that eIF4E binds selectively to TOP mRNAs and mTORC1 promotes translation of these messages by inhibiting the function of 4EBP1 and 4EBP2 (*55*). Both studies also provided an unparalleled view of the translational landscape regulated by mTORC1 and identified new regulatory elements including TOP-like (*55*) and pyrimidine rich translational element (PRTE) (*78*) motifs important for translation control.

Ribosome biogenesis

At the most basic level, translational output can be influenced by the total number of ribosomes. Early studies with rapamycin showed a dramatic decrease in the transcription of ribosomal RNA, ribosomal proteins and tRNAs (*79*). Subsequent studies clarified this relationship by identifying the TIF-1A as a downstream effector of mTORC1. mTORC1 promotes the nuclear localization of TIF-1A (*80*), which functions as a co-factor for RNA polymerase I that is critical for rRNA biosynthesis. Additionally, mTORC1 phosphorylates and inhibits MAF1 (*81, 82*), an inhibitor of RNA polyemerase III, which is required for 5S rRNA and tRNA transcription.

Metabolism

In addition to regulating protein synthesis, mTORC1 plays a critical role in the synthesis of other macromolecules such as lipids (*83*) and nucleic acids (*84*). mTORC1 also exerts its control over glycolytic metabolism and energy production by modulating key metabolic transcription factors such as HIF1α.

Lipid Biosynthesis

A growing cell demands an ever-increasing supply of lipids to maintain continued expansion of the plasma membrane and organogenesis. Sterol response element binding protein 1 (SREBP1) functions as a master transcriptional regulator of lipid and cholesterol biosynthesis (*85*). SREBP1 lies dormant in the ER membranes until a decrease in sterol levels or activation of the insulin pathway stimulates its proteolytic processing and ensuing release from the ER. Activated SREBP1 translocates to the nucleus and promotes expression of key genes required for lipid biosynthesis, cholesterol biosynthesis and the oxidative arm of the pentose phosphate pathway (*85*). mTORC1 regulates SREBP1 nuclear translocation through its effector S6K1, which is required for efficient SREBP1-dependent gene expression (*86-88*). Additionally, mTORC1 activates SREBP1 by inhibiting Lipin-1, a lipid phosphatase and suppressor of SREBP1 signaling (*56*). By directly phosphorylating Lipin-1, mTORC1 prevents its nuclear shuttling, where Lipin-1 promotes redistribution of SREBP1 to the nuclear lamina resulting in a decrease in SREBP1 activity (*56*). Interestingly, depletion of SREBP1 results in smaller cells (*89*), suggesting that one mechanism by which mTORC1 regulates cell size is through lipid/sterol synthesis.

When mammals undergo starvation, ketone bodies are used as an alternative energy currency for the brain. In a recent study from our lab (*90*), mTORC1 was found to inactivate hepatic ketogenesis by inhibiting the function of PPARα, a nuclear receptor that controls the expression of genes required for fatty acid and ketone body synthesis (*91*). mTORC1, via S6K2 activation (*92*), promotes the nuclear accumulation of the histone deacetylase (HDAC) nCoR1 (*90*), which blocks the transcriptional activity of PPARα.

Mitochondrial biogenesis and Glycolysis

The anabolic programs driven by mTORC1 are tremendously energy consuming (i.e. the synthesis of one peptide bond requires hydrolysis of four phosphoanhydride bonds). It is therefore not surprising that mTORC1 accommodates these energy demands by promoting mitochondrial function and biogenesis through a concerted increase in mitochondrial DNA content and in expression of oxidative phosphorylation genes (*93*). mTORC1 is thought to promote the interaction of PGC-1α, a master regulator of mitochondrial biogenesis, with the transcription factor YinYang1 (*94*). However this model must be reconciled with the fact that mTORC1 does not reside in the nucleus (*32, 33*). Thus, additional mTORC1-dependent mechanisms likely exist to increase mitochondrial biogenesis.

HIF1α is a transcription factor induced under hypoxic conditions to help a cell cope with reduced oxidative phosphorylation (*95, 96*). By increasing the expression of key glycolytic genes and glucose transporters and driving pyruvate flux towards lactate, HIF1α guarantees a steady supply of ATP under low oxygen conditions (*97*). mTORC1 promotes ATP production and glycolytic flux by positively regulating the transcription and translation of HIF1α (*98-101*).

Pyrimidine biosynthesis

Two recent studies uncovered a critical role for mTORC1 in the regulation of pyrimidine biosynthesis, a key component of nucleic acids. By utilizing metabolic profiling, Manning and colleagues discovered that mTORC1 upregulates synthesis of N-carbomyl-aspartate, a critical substrate required for pyrimidine biosynthesis (*102*). Through a phosphoproteomics approach, Hall and colleagues converged on S6K1 as the key intermediary between pyrimidine biosynthesis and mTORC1 (*103*). The Manning and Hall labs went on to demonstrate that S6K1 phosphorylates and activates CAD, the rate-limiting enzyme in pyrimidine biosynthesis, responsible for N-carbomyl-aspartate

production, potentially linking mTORC1 activation to progression through S-phase.

Autophagy

While enabling anabolic programs to increase cellular growth, mTORC1 shuts down catabolic programs such as autophagy to prevent a futile cycle of synthesis and degradation. Autophagy is best characterized as a cellular recycling program. It encompasses the sequestration and break down of cytosolic proteins (microautophagy) and organelles (macroautophagy) to replenish the cell with key macromolecules under nutrient starvation (*104*). Upon mTORC1 inhibition, double membrane vesicles originating from the ER engulf cytosolic proteins and organelles and fuse with lysosomes where degradative enzymes rapidly digest these cellular products into simpler molecules (*105*). mTORC1 primarily regulates autophagy by inhibiting key regulators of this process. Specifically, mTORC1 phosphorylates and inhibits the kinase complex of ULK1-ATG13-FIP200 (*106-108*), required for autophagasome formation. Recently, mTORC1 was also shown to activate DAP1 a negative regulator of autophagy (*109*).

Lysosome biogenesis

As discussed below, the lysosomal surface is the site of mTORC1 activation. It is therefore not surprising that mTORC1 has a critical role in lysosome biogenesis through its regulation of transcription factor EB (TFEB). mTORC1 directly phosphorylates TFEB1 promoting 14-3-3 protein binding and its sequestration in the cytoplasm (*110-112*). When mTORC1 is inactivated, TFEB is rapidly dephosphorylated, sheds its 14-3-3 proteins and shuttles to the nucleus. There, TFEB controls the expression of lysosome maintenance (*113*) and autophagasome formation genes (*114*), resulting in an increase in lysosome number, size and function.

Regulating the Regulator: Signaling pathways upstream of mTORC1

As a master regulator of cell growth mTORC1 must be keenly aware of the nutrient conditions inside the cell as well as those in the extracellular milieu., The pathway has therefore evolved to sense a wide variety of inputs including energy, amino acid and oxygen levels, genotoxic stress, and metazoan specific signals such as growth factors and hormones (**Figure 2**). All upstream inputs that funnel onto mTORC1 can be divided into two branches: those that modulate the activity of its main activator ras homolog enriched in brain (Rheb) and those required for its movement to the lysosomal surface, where it is activated.

Rheb

The small GTPase Rheb was initially identified as a protein upregulated in rat brains during seizures (*115*). Its connection to the TORC1 pathway was first discovered in flies, where gain of function screens in the fly eye placed dRheb upstream of dTORC1 and established its role as a positive regulator of this pathway (*116, 117*). Subsequent biochemical studies in mammalian cells indicated that GTP-bound Rheb functions as a potent stimulator of mTORC1 kinase activity (*38*). In vivo, the localization of Rheb is just as important as its nucleotide state in activating this pathway. Like other small GTPases, Rheb relies on a lipid modification (farnesylation) (*118*) for its proper localization to late endosomes/lysosomes (*119*). Mutation of the cysteine required for C-terminal Rheb farnesylation, reduces mTORC1 activity (*119*), whereas flooding the cytoplasm by overexpressing Rheb, uncouples mTORC1 activation from its lysosomal localization (*33, 120*). Curiously, while Rheb is absolutely required for mTORC1 activation in all metazoans and the yeast *S. pombe* (*121*), it is not required for pathway activation in *S. cerevisiae* (*122*). This difference likely stems from the need to integrate new signaling inputs such as growth factors (see below) in metazoans but not in *cerevisiae*.

Tuberous sclerosis complex

Mutation in the genes encoding tuberous sclerosis complex 1 and 2 (TSC1 and TSC2, TSC1/2) were originally identified as the causative agents in

the hamaratomatous syndrome of the same name (*123, 124*). Pioneering studies in flies and mammalian cells defined TSC1/2 as a negative upstream regulator of TORC1 (*125, 126*). The discovery of Rheb and its function downstream to TSC1/2, heralded biochemical investigations which revealed that TSC2 harbors GTPase activating protein (GAP) activity toward Rheb (*127-129*). TSC2 utilizes an asparagine thumb to accelerate Rheb GTP hydrolysis, however key residues utilized by other small GTPases for hydrolysis are not conserved in Rheb, suggesting a novel mechanism by which GTP is hydrolyzed (*130*). Recently, TBC1D7 was identified as a third member of TSC, required for maintaining the TSC1-TSC2 interaction. Like TSC1 and TSC2, depletion of TBC1D7 increases mTORC1 activity, however this member has yet to be found mutated in patients (*131*). To inactivate Rheb, TSC1/2 localizes to the lysosomal surface, a process thought to be dependent on TSC2 (*132*).

The identification of the Rheb-TSC1/2 axis greatly clarified the regulation of mTORC1 and revealed that TSC1/2 functions as a central hub for a multitude of different inputs that converge onto this pathway (*133*).

Growth factor and Cytokine signaling

Binding of growth factors such as insulin or EGF to their cognate receptor tyrosine kinases triggers complex signal transduction pathways ultimately leading to the activation of Ras and PI3K. GTP bound Ras activates a kinase cascade turning on the RSK and ERK kinases, which phosphorylate and inactivate TSC2 (*134, 135*). Active PI3K generates 3,4,5-phosphoinositol (PIP3) recruiting Akt to the plasma membrane where it is activated by PDK1. Akt both directly and indirectly activates mTORC1 by phosphorylating and inhibiting TSC2 (*126, 136-138*) and PRAS40 (*38*). To temper the activating signals generated by Ras and PI3K, cell rely on the tumor suppressors NF1 (*139*) and PTEN (*140*) whose function as a Ras GAP and a PIP3 phosphatase, respectively, inhibit downstream pathway signaling. Notably, cancers driven by mutations in these tumor suppressors are marked by hyperactivation of mTORC1. The mTORC1 pathway has also evolved its own safety valve in the form of two negative

feedback loops with insulin receptor signaling. Active S6K1 phosphorylates IRS1, a key component of the insulin receptor, leading to its degradation and attenuation of PIP3 signaling (*141, 142*). In the second feedback loop, mTORC1 activates GRB10 a negative regulator of the insulin receptor (*19, 20*). These two negative feedback loops have important ramifications for diabetes and cancer (see below).

The WNT and NFκB pathways are the remaining extracellular signaling pathways that funnel onto TSC1/2. Binding of the WNT ligand to its cognate GPCR results in the inhibition of GSK3, which activates TSC2 (*143*). Conversely, the death ligand TNFα activates the IKKβ kinase, which phosphorylates TSC1 leading to the inactivation of the complex (*144*). It has become apparent that phosphorylation of TSC1 or TSC2 serves as the preeminent form of TSC1/2 regulation. Phosphorylation either activates or inactivates this complex (*143, 145*), with the latter being modulated by complex destabilization or 14-3-3 binding to TSC2 which prevents its localization with Rheb (*126, 132, 138*).

Energy sensing

Unlike growth factor signaling which activates mTORC1, a drop in energy levels as detected by a decrease in the ratio of ATP:AMP negatively regulates this pathway. AMP kinase (AMPK) functions as a master sensor of cellular energy levels (*146*). AMP competes with ATP for a binding pocket in the regulatory γ subunit of the obligate heterotrimer. Upon AMP binding the γ subunit undergoes a conformational change that activates the catalytic α subunit (*147*). When active, AMPK phosphorylates TSC2 (*145*) as well as raptor (*148*) and both events down regulate mTORC1 activity. Because mitochondria produce the majority of ATP in the cell, the regulation of AMPK is intimately connected to the function of this organelle. Reducing ATP levels by treating cells with the anti-diabetic drugs metformin or phenformin (complex I inhibitors) (*149-152*), the anti-aging polyphenol resveratrol (F_1F_0 mitochondrial ATPase inhibitor) (*152*) or by reducing oxygen and glucose levels all increase AMPK activity. The tumor

suppressor LKB1 also stimulates AMPK through direct phosphorylation of its β regulatory subunit of AMPK (*153, 154*). Finally, genotoxic stress (DNA damage) regulates AMPK through p53-mediated up regulation of sestrins, which in turn activate AMPK (*155*).

Oxygen sensing

A short-term drop in oxygen levels is sufficient to inhibit mTORC1 (*156*), a process that is independent of AMPK function. Genetic screens in flies identified the orthologs of regulated in development and DNA damage response 1 (REDD1) as a protein induced under short term hypoxic conditions that functions downstream of PI3K signaling but upstream of TSC (*157, 158*). REDD1 is thought to activate TSC, by binding 14-3-3 proteins that otherwise are destined to sequester TSC2 away from Rheb (*158, 159*). How REDD1 senses oxygen is currently is unknown.

Amino acid sensing

Early investigations revealed that amino acids were required to stimulate protein synthesis in rat skeletal muscles (*160*). Later studies confirmed that a mixture of all 20 amino acids directly activated the mTORC1 pathway and along with growth factor signaling was absolutely required for the phosphorylation of S6K1 and the 4EBPs (*76, 161*). Whether all amino acids, one particular amino acid or an amino acid byproduct is being sensed by the mTORC1 pathway remains to be elucidated. Seminal studies established that leucine as well as arginine were necessary for mTORC1 activation but were not sufficient to activate mTORC1 in cells deprived of all amino acids (*76*). Dissecting the amino acid signal is further complicated by the fact that some plasma membrane amino acid transporters require additional amino acids to pump their cargo into the cytoplasm (*162*); thus blurring the singular importance of any one amino acid. The development of cell-free assays used to measure amino acid activation of mTORC1 promises to help answer this outstanding question (*163*).

Amino acid stimulation of the TORC1 pathway is evolutionarily conserved to yeast where it is reduced to the more primitive form of nitrogen sensing (*164-166*). Depending on the yeast strain, growth on nitrogen poor substrates inactivates TORC1. This leads to a transcriptional up regulation of key metabolic enzymes required for production of glutamine as well as a shuttling of amino acid permeases to the plasma membrane to help the cell scavenge for nitrogen rich sources (*164*). In flies, mutation of amino acid transporter genes *pathetic*, *minidiscs* and *slimfast* decrease animal size (*167-169*), indicating the necessity of amino acid signaling during development.

Although it was clear for over a decade that amino acids were required for mTORC1 activation, precisely how they functioned remained a mystery. Recently, our lab along with others have identified that amino acids regulate the intracellular localization of mTORC1 (*32, 33*). When cells are starved of amino acids, mTORC1 is found in a poorly defined cytoplasmic compartment. Upon amino acid stimulation mTORC1 rapidly shuttles to the lysosomal surface where it is presumed to interact with Rheb (*32*). The raptor component of mTORC1 is critical to its lysosomal targeting (*32, 33*) and curiously it also contains a domain shared by many vesicle coat proteins (*170*). Targeting mTORC1 constitutively to the lysosmal surface eliminates the need for the amino acid signal to activate the pathway as does localizing this complex along with Rheb to the plasma membrane (*170*). Thus, the purpose of the amino acid signal is to bring mTORC1 and Rheb together. In yeast, TORC1 is localized to the vacuole and does not shuttle in response to amino acids (*171*). The lack of a functional Rheb homolog in budding yeast likely makes TORC1 movement unnecessary.

Where amino acid sensing occurs is still a matter of debate. While extracellular amino acids must enter the cell to activate mTORC1 during amino acid starvation (*162*), the use of the translation inhibitor cyclohexamide to generate intracellular pools of amino acids reveals that sensing occurs inside the cell and not at the plasma membrane (*32*). Clarifying the site of sensing, Zoncu et al. used cell free reconstitution assays to establish that amino acid sensing

initiates from within the lysosomal lumen (*163*). Disruption of the lysosomal membrane with detergents or ionophores also inhibits amino acid sensing, however changes in luminal pH appear dispensable for this process. Luminal amino acid sensing was further corroborated in cells by over-expression of the PAT1 transporter, a lysosomal amino acid exporter which drains the lysosomal lumen of amino acids and efficiently turns off mTORC1 signaling even in the presence of extracellular amino acids (*163*). Collectively these studies demonstrate that lysosomal accumulation of amino acids is critical for the sensing mechanism.

While it was long believed that the amino acid signal funneled through the TSC1/2-Rheb axis, the development of $TSC2^{-/-}$ mice proved otherwise. mTORC1 remained sensitive to amino acid regulation in MEFs obtained from these animals (*172, 173*), implicating an alternative pathway. The identification of the Rag GTPases as mTORC1 interacting proteins (*32, 174*) completely changed our understanding of how this pathway senses amino acids.

The Rag GTPases

Rags are unique among all small GTPases as they function as obligate heterodimers (*32, 174-177*). Mammalian cells contain four Rag GTPases: RagA and RagB are functionally redundant and bind to the highly similar RagC and RagD (*175-177*). While RagA, RagC and RagD are ubiquitously expressed, RagB expression is restricted to the brain, suggesting a specialized function for this protein (*177*). It is currently unknown if a preferred Rag heterodimer exists, however the existence of only two Rags (RagA and RagC) in all other eukaryotes (with the exception of plants that do not encode these genes) suggests a functional redundancy for the other Rags. This hypothesis will be tested with the generation Rag knockout mice. The yeast ortholog of RagA/B is GTR1 whereas GTR2 is the ortholog of RagC/D (*171, 178, 179*). The GTRs were first connected to the TORC1 pathway in a screen that identified negative regulators of macroautophagy (*178*). While the GTRs are not essential genes, their deletion is synthetic lethal in the presence of rapamycin (*171*), a phenotype that extends to

other TORC1 components. The crystal structures of the GTR1-GTR2 reveals that the two G proteins are tied together by their C-terminal roadblock domains (*180, 181*); a domain that is curiously found in four other components of the amino acid sensing pathway (Chapter 3) (*182*). In the GTP loaded state, the G domain of the GTRs face away from each other, however when GTR2 is bound to GDP its G domain undergoes a dramatic rearrangement and leans into the G domain of GTR1 (*180, 181*). The functional significance of this rearrangement remains to be determined (Chapter 5), nevertheless, the nucleotide bound state of the Rags is key to their function (discussed below).

Loss of function studies in mammalian, fly and yeast cells established that the Rags GTPases were critical in mediating the amino acid signal to mTORC1 (*32, 171, 174*). In cells depleted of Rags, mTORC1 cannot translocate to the lysosomal surface (*33*). Rags interact with raptor in an amino acid dependent manner, and their localization to the lysosomal surface defines their role as a docking site for mTORC1 on this organelle (*32*). Unlike other small GTPases, the Rags do contain lipid modifications that are commonly used to indicate a protein's intracellular home. As will be discussed in Chapters 2 and 3, the Rags rely on the pentameric Ragulator complex for their localization (*33, 182*) whose function is conserved to the EGO complex in yeast (*171, 179*).

Metabolic labeling studies have demonstrated that during amino acid starvation RagB is bound to GDP and upon amino acid stimulation GDP is exchanged for GTP (*32*). Rag mutants thought to mimic different nucleotide bound states demonstrate that a GTP-locked RagA heterodimer strongly interacts with raptor whereas the Rag complex with the opposite nucleotide bound state does not (*32*). In mice or cells expressing RagA or RagB GTP mutants, mTORC1 is constitutively localized to the lysosomal surface and the pathway is insensitive to regulation by amino acids (*32, 183*). Rags do not directly sense amino acids and the identification of a RagA/B guanine nucleotide exchange factor (GEF) (Chapter 3) (*182*) and GAP (Chapter 4) illustrates that a

complex signal transduction pathway lies between the amino acid signal and these GTPases.

mTORC1 and disease

Given the ubiquity of the cellular processes under the control of mTORC1 and the multitude of signaling pathways that regulate its activity, it is not surprising that this pathway is often deregulated in numerous human diseases (*6*). The most prominent examples of mTORC1 deregulation in disease are discussed below.

Cancer

The genetic hamaratomatous syndrome TSC, characterized by large benign tubers was the first and is the best described cancer prone syndrome driven by aberrant mTORC1 signaling (*184*). Deletion or loss-of-function mutations in either TSC1 or TSC2 underlie a majority of these cases. Although this syndrome is rare (1:6000 live births) the location of tumors in the lungs, brain, kidney and heart can disrupt normal physiological operations leading to severe complications (*184*). Treatment of TSC induced subependymal giant cell astrocytomas with the rapamycin analog everolimus leads to a near complete remission of this tumor. A related cancer caused by TSC1/2 loss and exclusively affecting women is lymphangiomyomatosis (LAM) characterized by lung cysts that destroy the lung parenchyma. The disease is fatal because even after lung transplantation the cysts return (*185*). Recent clinical trials with rapamycin, although preliminary, appear to be promising in the treatment of LAM (*186*).

In addition to TSC, other hamaratomatous cancers are defined by loss of tumor suppressors that lie upstream of mTORC1 and include: Peut-Jeghers (LKB1) (*186*), Neurofibromatosis (NF1) (*187*), Cowden syndrome (PTEN) (*186*) and Birt-Hoog-Dube syndrome caused by mutations in Folliculin a tumor suppressor proposed to be part of the mTORC1 pathway (*188*). Finally, expression of DEPTOR is also found to be unregulated in multiple myelomas

(*41*). By inhibiting mTORC1 activity, DEPTOR relieves the negative feedback loop between S6K1 and IRS1 allowing for continued activation of Akt (*41*).

Functioning downstream of many classical oncogenic pathways such as the PI3K/Pten/Akt and the Ras/Raf pathways, aberrant mTORC1 activation is a staple in many cancers (*6, 41, 189*). Although mTORC1 promotes cell growth through a variety of mechanisms, regulation of translation represents an especially important oncogenic avenue for this signaling pathway. Depletion of the protein synthesis inhibitors 4E-BPs is pro-proliferative (*190*) and is important for tumorigenicity (*191*), whereas over-expression of 4EBP-1 in Akt driven lymphoma reduces tumor volume (*58*). Moreover, eIF4E has emerged as an important oncogene by promoting the translation of factors important for cell survival and proliferation such as cyclin D and c-Myc (*190, 192*). Finally, the up regulation and stabilization of HIF1α by mTORC1 (*98-101*) promotes angiogenesis by increasing VEGF expression and adapting tumors to a hypoxic environment (*101*).

Diabetes

Targeting core components of the mTORC1 pathway in transgenic mice has revealed a prominent role for mTORC1 in diabetes (*6*). Mice with a conditional knockout of raptor in adipose tissue have increased blood glucose tolerance, insulin sensitivity and resistance to diet induced obesity (*193*). Given the requirement of mTORC1 for adipogenesis (*83*), these mice are leaner owing to a decrease in adipose tissue. These results are mirrored in whole body S6K1 knockout mice as well (*194*). Conversely, TSC2 deficient cells are extraordinarily insulin and IGF1 resistant (*141*) and these results are explained by the S6K-IRS1 and GRB10 negative feedback loops.

Aging

For over a century, caloric restriction has been demonstrated to extend lifespan in numerous model organisms including mice and rhesus monkeys (*195, 196*). Studies in yeast and in worms have indicated that caloric restriction funnels

through mTORC1 although the molecular mechanisms underlying this pathway have yet to be established. Furthermore, depletion of key mTORC1 components in yeast, worms, flies and mice all show an increase in lifespan (*196, 197*). In worms, TORC1 appears to regulate longevity through its control of the Pha4 and Skn1 transcription factors (*198, 199*). Excitingly, treatment of middle-aged mice with rapamycin significantly increased their lifespan (~16% in females and 8% in males) (*200*).

Immune disorders

The discovery of rapamycin as a potent immunosuppressant highlighted the importance of the mTORC1 pathway in the immune system (*3*). While rapamycin is known to be a potent inhibitor of many immune cells, only recently was a primary immunodeficiency linked to this pathway. Mutation in the 3'UTR of the transcript encoding a Ragulator protein (p14) results in decreased protein expression and causes a severe reduction in neutrophil counts (*201*). Interestingly, patients diagnosed with this disorder were below the first percentile in height compared to their age-matched peers (*201*) and cells isolated from these patients display a marked reduction in mTORC1 activity (*33*). This syndrome represents the first in what promises to be a large class of immune disorders with aberrant mTORC1 signaling underlying their etiology.

Introduction to the work presented in the thesis

Initial studies first described the stimulation of mTORC1 by amino acids over fifteen years ago, but for much of this time how amino acids regulate this pathway has remained enigmatic. The discovery that the Rag GTPases mediate the amino acid signal to mTORC1 represents a significant step forward not only in our grasp of mTORC1 signaling but also its role in normal and diseased states. For my doctoral thesis I studied how amino acids control the function of the Rags by addressing the following questions:

1. How do the Rags localize to the lysosomal surface?

Because the Rags do not contain lipid modifications to direct their intracellular localization, we hypothesized that additional proteins must directly interact and tether them to the lysosomal surface. By purifying the Rags under several conditions, we identified five proteins (p14, MP1, p18, HBXIP and C7orf59) that form a novel complex, which we named 'Ragulator'. Ragulator is found at the lysosomal surface and specifically interacts with the Rags on this organelle. Loss of function and mislocalization studies revealed that Ragulator is both necessary and sufficient for Rag localization. In cells null for or highly depleted of Ragulator proteins mTORC1 is no longer found at the lysosomes and remains inactive.

2. What factors are required to activate Rags upon amino acid stimulation?

Several key experiments revealed that the Rag-Ragulator interaction is regulated by amino acids suggesting that Ragulator may also control the nucleotide loading of the Rag GTPases. The Rags pose a unique experimental challenge for identifying factors that regulate the nucleotide state of a single Rag given that they exist as obligate heterodimers. To circumvent this problem, we developed several methods that allowed us to analyze the nucleotide binding state of one Rag at a time. This led to the discovery of Ragulator as a GEF for RagA and RagB. GEFs lead to the activation of their cognate GTPase by increasing GTP binding through displacement of GDP from the GTPase.

Interestingly, the GEF activity of Ragulator is not localized to one Ragulator subunit, but requires the complete pentameric complex, indicating that Ragulator belongs to a new family of multi-protein GEFs.

3. What factors are required to inactivate Rags upon amino acid withdrawal?

To identify negative regulators of the Rags, we purified them in the presence of a chemical crosslinker that preserves transiently interacting proteins. This approach led to the identification of a complex of eight Rag-interacting proteins that we refer to as 'GATOR' (GAP Activity TOwards Rags). GATOR is defined by two distinct subcomplexes, GATOR1 and GATOR2, where GATOR1 negatively regulates mTORC1 while GATOR2 positively regulates this pathway by inhibiting GATOR1. GATOR1 directly interacts with the Rag GTPases and inhibits their function through its GAP activity towards RagA and RagB. Upstream negative regulators of mTORC1 are commonly mutated in cancer and, indeed, in a subset of glioblastoma and ovarian tumors, we find inactivating mutations in GATOR1 genes. Moreover, in cancer cell lines missing GATOR1 components the mTORC1 pathway is insensitive to amino acid starvation and hypersensitive to treatment with the mTORC1 inhibitor rapamycin.

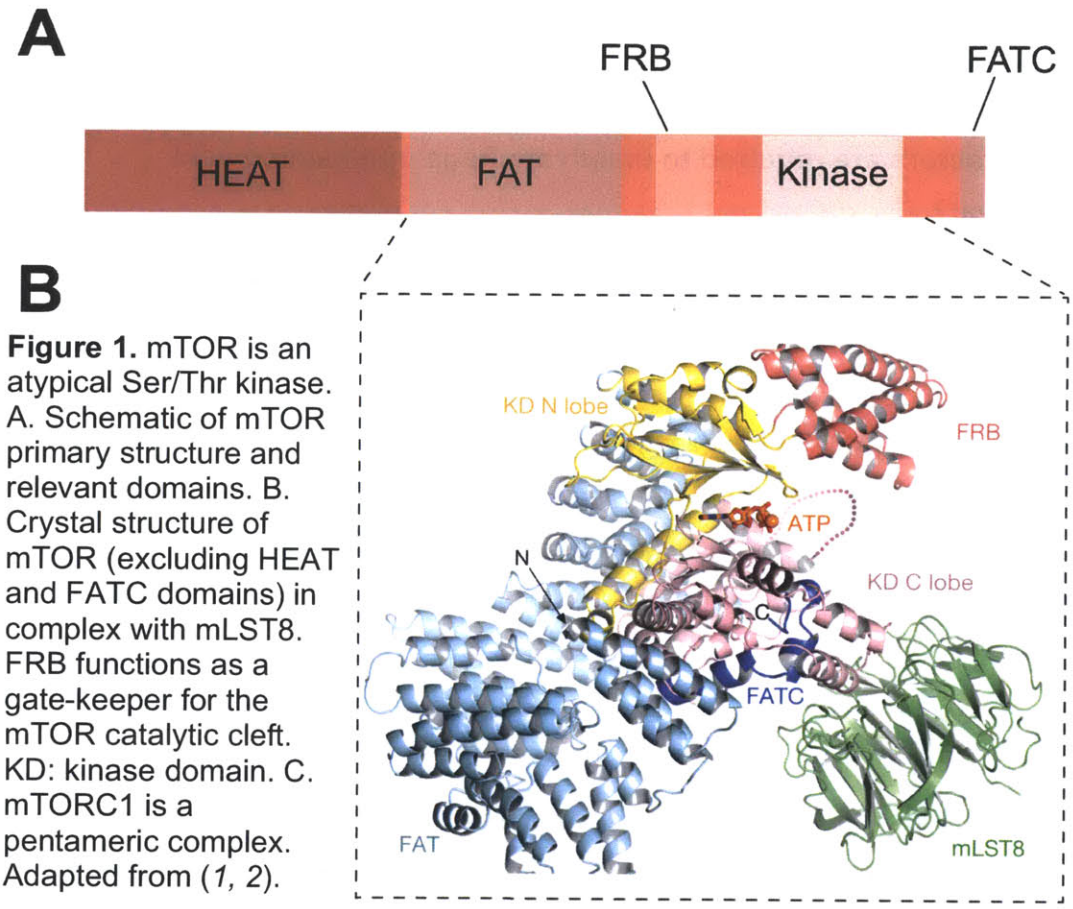

Figure 1. mTOR is an atypical Ser/Thr kinase. A. Schematic of mTOR primary structure and relevant domains. B. Crystal structure of mTOR (excluding HEAT and FATC domains) in complex with mLST8. FRB functions as a gate-keeper for the mTOR catalytic cleft. KD: kinase domain. C. mTORC1 is a pentameric complex. Adapted from (*1, 2*).

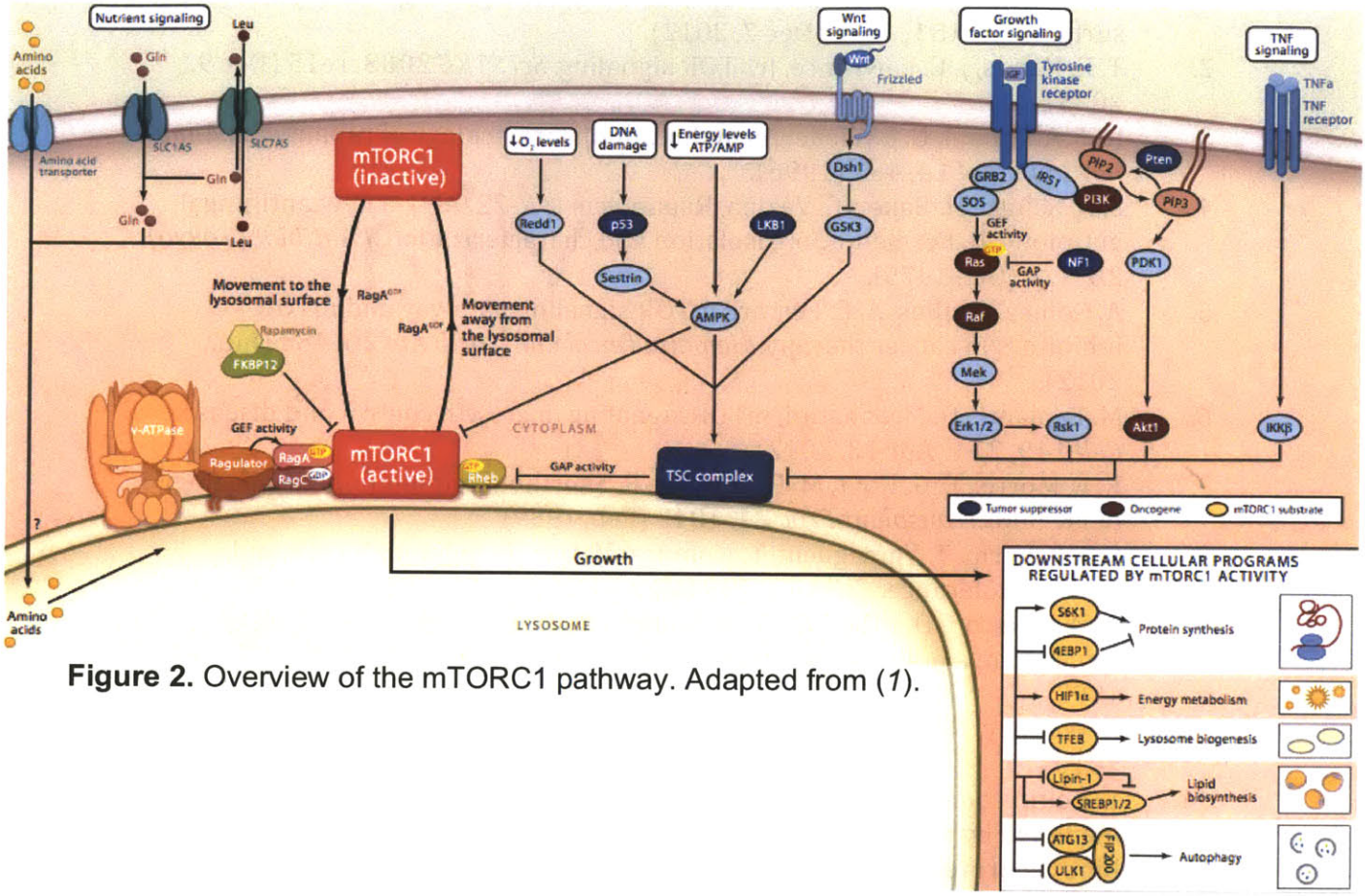

Figure 2. Overview of the mTORC1 pathway. Adapted from (*1*).

References

1. L. Bar-Peled, D. M. Sabatini, SnapShot: mTORC1 signaling at the lysosomal surface. *Cell* **151**, 1390 (Dec 7, 2012).
2. T. E. Harris, J. C. Lawrence, Jr., TOR signaling. *Sci STKE* **2003**, re15 (Dec 9, 2003).
3. R. T. Abraham, G. J. Wiederrecht, Immunopharmacology of rapamycin. *Annu Rev Immunol* **14**, 483 (1996).
4. S. N. Sehgal, H. Baker, C. Vezina, Rapamycin (AY-22,989), a new antifungal antibiotic. II. Fermentation, isolation and characterization. *J Antibiot (Tokyo)* **28**, 727 (Oct, 1975).
5. A. Gomez-Pinillos, A. C. Ferrari, mTOR signaling pathway and mTOR inhibitors in cancer therapy. *Hematol Oncol Clin North Am* **26**, 483 (Jun, 2012).
6. M. Laplante, D. M. Sabatini, mTOR signaling in growth control and disease. *Cell* **149**, 274 (Apr 13, 2012).
7. R. E. Morris, E. G. Hoyt, M. P. Murphy, R. Shorthouse, Immunopharmacology of FK-506. *Transplant Proc* **21**, 1042 (Feb, 1989).
8. S. Sakaguchi, T. Yamaguchi, T. Nomura, M. Ono, Regulatory T cells and immune tolerance. *Cell* **133**, 775 (May 30, 2008).
9. R. W. Yatscoff, D. F. LeGatt, N. M. Kneteman, Therapeutic monitoring of rapamycin: a new immunosuppressive drug. *Ther Drug Monit* **15**, 478 (Dec, 1993).
10. R. Wessely, New drug-eluting stent concepts. *Nat Rev Cardiol* **7**, 194 (Apr, 2010).
11. Y. Koltin *et al.*, Rapamycin sensitivity in Saccharomyces cerevisiae is mediated by a peptidyl-prolyl cis-trans isomerase related to human FK506-binding protein. *Mol Cell Biol* **11**, 1718 (Mar, 1991).
12. J. Heitman, N. R. Movva, M. N. Hall, Targets for cell cycle arrest by the immunosuppressant rapamycin in yeast. *Science* **253**, 905 (Aug 23, 1991).
13. J. Kunz *et al.*, Target of rapamycin in yeast, TOR2, is an essential phosphatidylinositol kinase homolog required for G1 progression. *Cell* **73**, 585 (May 7, 1993).
14. E. J. Brown *et al.*, A mammalian protein targeted by G1-arresting rapamycin-receptor complex. *Nature* **369**, 756 (Jun 30, 1994).
15. D. M. Sabatini, H. Erdjument-Bromage, M. Lui, P. Tempst, S. H. Snyder, RAFT1: a mammalian protein that binds to FKBP12 in a rapamycin-dependent fashion and is homologous to yeast TORs. *Cell* **78**, 35 (Jul 15, 1994).
16. C. J. Sabers *et al.*, Isolation of a protein target of the FKBP12-rapamycin complex in mammalian cells. *J Biol Chem* **270**, 815 (Jan 13, 1995).
17. H. Lempiainen, T. D. Halazonetis, Emerging common themes in regulation of PIKKs and PI3Ks. *Embo J* **28**, 3067 (Oct 21, 2009).
18. G. Manning, D. B. Whyte, R. Martinez, T. Hunter, S. Sudarsanam, The protein kinase complement of the human genome. *Science* **298**, 1912 (Dec 6, 2002).

19. P. P. Hsu *et al.*, The mTOR-regulated phosphoproteome reveals a mechanism of mTORC1-mediated inhibition of growth factor signaling. *Science* **332**, 1317 (Jun 10, 2011).
20. Y. Yu *et al.*, Phosphoproteomic analysis identifies Grb10 as an mTORC1 substrate that negatively regulates insulin signaling. *Science* **332**, 1322 (Jun 10, 2011).
21. R. Bosotti, A. Isacchi, E. L. Sonnhammer, FAT: a novel domain in PIK-related kinases. *Trends Biochem Sci* **25**, 225 (May, 2000).
22. J. Perry, N. Kleckner, The ATRs, ATMs, and TORs are giant HEAT repeat proteins. *Cell* **112**, 151 (Jan 24, 2003).
23. J. Chen, X. F. Zheng, E. J. Brown, S. L. Schreiber, Identification of an 11-kDa FKBP12-rapamycin-binding domain within the 289-kDa FKBP12-rapamycin-associated protein and characterization of a critical serine residue. *Proc Natl Acad Sci U S A* **92**, 4947 (May 23, 1995).
24. J. Choi, J. Chen, S. L. Schreiber, J. Clardy, Structure of the FKBP12-rapamycin complex interacting with the binding domain of human FRAP. *Science* **273**, 239 (Jul 12, 1996).
25. H. Yang *et al.*, mTOR kinase structure, mechanism and regulation. *Nature* **497**, 217 (May 9, 2013).
26. R. Loewith *et al.*, Two TOR complexes, only one of which is rapamycin sensitive, have distinct roles in cell growth control. *Mol Cell* **10**, 457 (Sep, 2002).
27. C. K. Yip, K. Murata, T. Walz, D. M. Sabatini, S. A. Kang, Structure of the human mTOR complex I and its implications for rapamycin inhibition. *Mol Cell* **38**, 768 (Jun 11, 2010).
28. D. H. Kim *et al.*, mTOR interacts with raptor to form a nutrient-sensitive complex that signals to the cell growth machinery. *Cell* **110**, 163 (Jul 26, 2002).
29. K. Hara *et al.*, Raptor, a binding partner of target of rapamycin (TOR), mediates TOR action. *Cell* **110**, 177 (Jul 26, 2002).
30. H. Nojima *et al.*, The mammalian target of rapamycin (mTOR) partner, raptor, binds the mTOR substrates p70 S6 kinase and 4E-BP1 through their TOR signaling (TOS) motif. *J Biol Chem* **278**, 15461 (May 2, 2003).
31. S. S. Schalm, D. C. Fingar, D. M. Sabatini, J. Blenis, TOS motif-mediated raptor binding regulates 4E-BP1 multisite phosphorylation and function. *Curr Biol* **13**, 797 (May 13, 2003).
32. Y. Sancak *et al.*, The Rag GTPases bind raptor and mediate amino acid signaling to mTORC1. *Science* **320**, 1496 (Jun 13, 2008).
33. Y. Sancak *et al.*, Ragulator-Rag complex targets mTORC1 to the lysosomal surface and is necessary for its activation by amino acids. *Cell* **141**, 290 (Apr 16, 2010).
34. Y. G. Gangloff *et al.*, Disruption of the mouse mTOR gene leads to early postimplantation lethality and prohibits embryonic stem cell development. *Mol Cell Biol* **24**, 9508 (Nov, 2004).

35. D. A. Guertin *et al.*, Ablation in mice of the mTORC components raptor, rictor, or mLST8 reveals that mTORC2 is required for signaling to Akt-FOXO and PKCalpha, but not S6K1. *Dev Cell* **11**, 859 (Dec, 2006).
36. D. H. Kim *et al.*, GbetaL, a positive regulator of the rapamycin-sensitive pathway required for the nutrient-sensitive interaction between raptor and mTOR. *Mol Cell* **11**, 895 (Apr, 2003).
37. E. J. Chen, C. A. Kaiser, LST8 negatively regulates amino acid biosynthesis as a component of the TOR pathway. *J Cell Biol* **161**, 333 (Apr 28, 2003).
38. Y. Sancak *et al.*, PRAS40 is an insulin-regulated inhibitor of the mTORC1 protein kinase. *Mol Cell* **25**, 903 (Mar 23, 2007).
39. K. Thedieck *et al.*, PRAS40 and PRR5-like protein are new mTOR interactors that regulate apoptosis. *PLoS One* **2**, e1217 (2007).
40. K. S. Kovacina *et al.*, Identification of a proline-rich Akt substrate as a 14-3-3 binding partner. *J Biol Chem* **278**, 10189 (Mar 21, 2003).
41. T. R. Peterson *et al.*, DEPTOR is an mTOR inhibitor frequently overexpressed in multiple myeloma cells and required for their survival. *Cell* **137**, 873 (May 29, 2009).
42. A. Reinke *et al.*, TOR complex 1 includes a novel component, Tco89p (YPL180w), and cooperates with Ssd1p to maintain cellular integrity in Saccharomyces cerevisiae. *J Biol Chem* **279**, 14752 (Apr 9, 2004).
43. D. D. Sarbassov *et al.*, Rictor, a novel binding partner of mTOR, defines a rapamycin-insensitive and raptor-independent pathway that regulates the cytoskeleton. *Curr Biol* **14**, 1296 (Jul 27, 2004).
44. E. Jacinto *et al.*, Mammalian TOR complex 2 controls the actin cytoskeleton and is rapamycin insensitive. *Nat Cell Biol* **6**, 1122 (Nov, 2004).
45. D. D. Sarbassov, D. A. Guertin, S. M. Ali, D. M. Sabatini, Phosphorylation and regulation of Akt/PKB by the rictor-mTOR complex. *Science* **307**, 1098 (Feb 18, 2005).
46. J. M. Garcia-Martinez, D. R. Alessi, mTOR complex 2 (mTORC2) controls hydrophobic motif phosphorylation and activation of serum- and glucocorticoid-induced protein kinase 1 (SGK1). *Biochem J* **416**, 375 (Dec 15, 2008).
47. D. D. Sarbassov *et al.*, Prolonged rapamycin treatment inhibits mTORC2 assembly and Akt/PKB. *Mol Cell* **22**, 159 (Apr 21, 2006).
48. L. R. Pearce *et al.*, Identification of Protor as a novel Rictor-binding component of mTOR complex-2. *Biochem J* **405**, 513 (Aug 1, 2007).
49. M. A. Frias *et al.*, mSin1 is necessary for Akt/PKB phosphorylation, and its isoforms define three distinct mTORC2s. *Curr Biol* **16**, 1865 (Sep 19, 2006).
50. E. Jacinto *et al.*, SIN1/MIP1 maintains rictor-mTOR complex integrity and regulates Akt phosphorylation and substrate specificity. *Cell* **127**, 125 (Oct 6, 2006).
51. D. Berchtold, T. C. Walther, TORC2 plasma membrane localization is essential for cell viability and restricted to a distinct domain. *Mol Biol Cell* **20**, 1565 (Mar, 2009).
52. D. A. Guertin, D. M. Sabatini, The pharmacology of mTOR inhibition. *Sci Signal* **2**, pe24 (2009).

53. C. C. Thoreen *et al.*, An ATP-competitive mammalian target of rapamycin inhibitor reveals rapamycin-resistant functions of mTORC1. *J Biol Chem* **284**, 8023 (Mar 20, 2009).
54. M. E. Feldman *et al.*, Active-site inhibitors of mTOR target rapamycin-resistant outputs of mTORC1 and mTORC2. *PLoS Biol* **7**, e38 (Feb 10, 2009).
55. C. C. Thoreen *et al.*, A unifying model for mTORC1-mediated regulation of mRNA translation. *Nature* **485**, 109 (May 3, 2012).
56. T. R. Peterson *et al.*, mTOR complex 1 regulates lipin 1 localization to control the SREBP pathway. *Cell* **146**, 408 (Aug 5, 2011).
57. C. M. Chresta *et al.*, AZD8055 is a potent, selective, and orally bioavailable ATP-competitive mammalian target of rapamycin kinase inhibitor with in vitro and in vivo antitumor activity. *Cancer Res* **70**, 288 (Jan 1, 2010).
58. A. C. Hsieh *et al.*, Genetic dissection of the oncogenic mTOR pathway reveals druggable addiction to translational control via 4EBP-eIF4E. *Cancer Cell* **17**, 249 (Mar 16, 2010).
59. X. M. Ma, J. Blenis, Molecular mechanisms of mTOR-mediated translational control. *Nat Rev Mol Cell Biol* **10**, 307 (May, 2009).
60. S. Ferrari, G. Thomas, S6 phosphorylation and the p70s6k/p85s6k. *Crit Rev Biochem Mol Biol* **29**, 385 (1994).
61. J. Chung, C. J. Kuo, G. R. Crabtree, J. Blenis, Rapamycin-FKBP specifically blocks growth-dependent activation of and signaling by the 70 kd S6 protein kinases. *Cell* **69**, 1227 (Jun 26, 1992).
62. C. J. Kuo *et al.*, Rapamycin selectively inhibits interleukin-2 activation of p70 S6 kinase. *Nature* **358**, 70 (Jul 2, 1992).
63. D. J. Price, J. R. Grove, V. Calvo, J. Avruch, B. E. Bierer, Rapamycin-induced inhibition of the 70-kilodalton S6 protein kinase. *Science* **257**, 973 (Aug 14, 1992).
64. J. Blenis, C. J. Kuo, R. L. Erikson, Identification of a ribosomal protein S6 kinase regulated by transformation and growth-promoting stimuli. *J Biol Chem* **262**, 14373 (Oct 25, 1987).
65. D. J. Price, R. A. Nemenoff, J. Avruch, Purification of a hepatic S6 kinase from cycloheximide-treated Rats. *J Biol Chem* **264**, 13825 (Aug 15, 1989).
66. P. E. Burnett, R. K. Barrow, N. A. Cohen, S. H. Snyder, D. M. Sabatini, RAFT1 phosphorylation of the translational regulators p70 S6 kinase and 4E-BP1. *Proc Natl Acad Sci U S A* **95**, 1432 (Feb 17, 1998).
67. S. Isotani *et al.*, Immunopurified mammalian target of rapamycin phosphorylates and activates p70 S6 kinase alpha in vitro. *J Biol Chem* **274**, 34493 (Nov 26, 1999).
68. M. Pende *et al.*, S6K1(-/-)/S6K2(-/-) mice exhibit perinatal lethality and rapamycin-sensitive 5'-terminal oligopyrimidine mRNA translation and reveal a mitogen-activated protein kinase-dependent S6 kinase pathway. *Mol Cell Biol* **24**, 3112 (Apr, 2004).
69. A. Mora, D. Komander, D. M. van Aalten, D. R. Alessi, PDK1, the master regulator of AGC kinase signal transduction. *Semin Cell Dev Biol* **15**, 161 (Apr, 2004).

70. I. Ruvinsky *et al.*, Ribosomal protein S6 phosphorylation is a determinant of cell size and glucose homeostasis. *Genes Dev* **19**, 2199 (Sep 15, 2005).
71. B. Raught *et al.*, Phosphorylation of eucaryotic translation initiation factor 4B Ser422 is modulated by S6 kinases. *Embo J* **23**, 1761 (Apr 21, 2004).
72. N. V. Dorrello *et al.*, S6K1- and betaTRCP-mediated degradation of PDCD4 promotes protein translation and cell growth. *Science* **314**, 467 (Oct 20, 2006).
73. X. Wang *et al.*, Regulation of elongation factor 2 kinase by p90(RSK1) and p70 S6 kinase. *Embo J* **20**, 4370 (Aug 15, 2001).
74. X. M. Ma, S. O. Yoon, C. J. Richardson, K. Julich, J. Blenis, SKAR links pre-mRNA splicing to mTOR/S6K1-mediated enhanced translation efficiency of spliced mRNAs. *Cell* **133**, 303 (Apr 18, 2008).
75. G. J. Brunn *et al.*, Phosphorylation of the translational repressor PHAS-I by the mammalian target of rapamycin. *Science* **277**, 99 (Jul 4, 1997).
76. K. Hara *et al.*, Amino acid sufficiency and mTOR regulate p70 S6 kinase and eIF-4E BP1 through a common effector mechanism. *J Biol Chem* **273**, 14484 (Jun 5, 1998).
77. O. Le Bacquer *et al.*, Elevated sensitivity to diet-induced obesity and insulin resistance in mice lacking 4E-BP1 and 4E-BP2. *J Clin Invest* **117**, 387 (Feb, 2007).
78. A. C. Hsieh *et al.*, The translational landscape of mTOR signalling steers cancer initiation and metastasis. *Nature* **485**, 55 (May 3, 2012).
79. P. B. Mahajan, Modulation of transcription of rRNA genes by rapamycin. *Int J Immunopharmacol* **16**, 711 (Sep, 1994).
80. C. Mayer, J. Zhao, X. Yuan, I. Grummt, mTOR-dependent activation of the transcription factor TIF-IA links rRNA synthesis to nutrient availability. *Genes Dev* **18**, 423 (Feb 15, 2004).
81. T. Kantidakis, B. A. Ramsbottom, J. L. Birch, S. N. Dowding, R. J. White, mTOR associates with TFIIIC, is found at tRNA and 5S rRNA genes, and targets their repressor Maf1. *Proc Natl Acad Sci U S A* **107**, 11823 (Jun 29, 2010).
82. B. Shor *et al.*, Requirement of the mTOR kinase for the regulation of Maf1 phosphorylation and control of RNA polymerase III-dependent transcription in cancer cells. *J Biol Chem* **285**, 15380 (May 14, 2010).
83. M. Laplante, D. M. Sabatini, An emerging role of mTOR in lipid biosynthesis. *Curr Biol* **19**, R1046 (Dec 1, 2009).
84. G. R. Buel, S. G. Kim, J. Blenis, mTORC1 Signaling Aids in CADalyzing Pyrimidine Biosynthesis. *Cell Metab* **17**, 633 (May 7, 2013).
85. J. D. Horton, J. L. Goldstein, M. S. Brown, SREBPs: activators of the complete program of cholesterol and fatty acid synthesis in the liver. *J Clin Invest* **109**, 1125 (May, 2002).
86. K. Duvel *et al.*, Activation of a metabolic gene regulatory network downstream of mTOR complex 1. *Mol Cell* **39**, 171 (Jul 30, 2010).
87. S. Li *et al.*, Role of S6K1 in regulation of SREBP1c expression in the liver. *Biochem Biophys Res Commun* **412**, 197 (Aug 26, 2011).

88. B. T. Wang *et al.*, The mammalian target of rapamycin regulates cholesterol biosynthetic gene expression and exhibits a rapamycin-resistant transcriptional profile. *Proc Natl Acad Sci U S A* **108**, 15201 (Sep 13, 2011).
89. T. Porstmann *et al.*, SREBP activity is regulated by mTORC1 and contributes to Akt-dependent cell growth. *Cell Metab* **8**, 224 (Sep, 2008).
90. S. Sengupta, T. R. Peterson, M. Laplante, S. Oh, D. M. Sabatini, mTORC1 controls fasting-induced ketogenesis and its modulation by ageing. *Nature* **468**, 1100 (Dec 23, 2010).
91. P. Lefebvre, G. Chinetti, J. C. Fruchart, B. Staels, Sorting out the roles of PPAR alpha in energy metabolism and vascular homeostasis. *J Clin Invest* **116**, 571 (Mar, 2006).
92. K. Kim, S. Pyo, S. H. Um, S6 kinase 2 deficiency enhances ketone body production and increases peroxisome proliferator-activated receptor alpha activity in the liver. *Hepatology* **55**, 1727 (Jun, 2012).
93. M. Koyanagi *et al.*, Ablation of TSC2 enhances insulin secretion by increasing the number of mitochondria through activation of mTORC1. *PLoS One* **6**, e23238 (2011).
94. J. T. Cunningham *et al.*, mTOR controls mitochondrial oxidative function through a YY1-PGC-1alpha transcriptional complex. *Nature* **450**, 736 (Nov 29, 2007).
95. A. J. Majmundar, W. J. Wong, M. C. Simon, Hypoxia-inducible factors and the response to hypoxic stress. *Mol Cell* **40**, 294 (Oct 22, 2010).
96. W. G. Kaelin, Jr., The von Hippel-Lindau tumour suppressor protein: O2 sensing and cancer. *Nat Rev Cancer* **8**, 865 (Nov, 2008).
97. J. R. Cantor, D. M. Sabatini, Cancer cell metabolism: one hallmark, many faces. *Cancer Discov* **2**, 881 (Oct, 2012).
98. J. B. Brugarolas, F. Vazquez, A. Reddy, W. R. Sellers, W. G. Kaelin, Jr., TSC2 regulates VEGF through mTOR-dependent and -independent pathways. *Cancer Cell* **4**, 147 (Aug, 2003).
99. C. C. Hudson *et al.*, Regulation of hypoxia-inducible factor 1alpha expression and function by the mammalian target of rapamycin. *Mol Cell Biol* **22**, 7004 (Oct, 2002).
100. E. Laughner, P. Taghavi, K. Chiles, P. C. Mahon, G. L. Semenza, HER2 (neu) signaling increases the rate of hypoxia-inducible factor 1alpha (HIF-1alpha) synthesis: novel mechanism for HIF-1-mediated vascular endothelial growth factor expression. *Mol Cell Biol* **21**, 3995 (Jun, 2001).
101. N. Ferrara, VEGF and the quest for tumour angiogenesis factors. *Nat Rev Cancer* **2**, 795 (Oct, 2002).
102. I. Ben-Sahra, J. J. Howell, J. M. Asara, B. D. Manning, Stimulation of de novo pyrimidine synthesis by growth signaling through mTOR and S6K1. *Science* **339**, 1323 (Mar 15, 2013).
103. A. M. Robitaille *et al.*, Quantitative phosphoproteomics reveal mTORC1 activates de novo pyrimidine synthesis. *Science* **339**, 1320 (Mar 15, 2013).
104. Z. Yang, D. J. Klionsky, Mammalian autophagy: core molecular machinery and signaling regulation. *Curr Opin Cell Biol* **22**, 124 (Apr, 2010).

105. J. D. Rabinowitz, E. White, Autophagy and metabolism. *Science* **330**, 1344 (Dec 3, 2010).
106. I. G. Ganley *et al.*, ULK1.ATG13.FIP200 complex mediates mTOR signaling and is essential for autophagy. *J Biol Chem* **284**, 12297 (May 1, 2009).
107. N. Hosokawa *et al.*, Nutrient-dependent mTORC1 association with the ULK1-Atg13-FIP200 complex required for autophagy. *Mol Biol Cell* **20**, 1981 (Apr, 2009).
108. C. H. Jung *et al.*, ULK-Atg13-FIP200 complexes mediate mTOR signaling to the autophagy machinery. *Mol Biol Cell* **20**, 1992 (Apr, 2009).
109. I. Koren, E. Reem, A. Kimchi, DAP1, a novel substrate of mTOR, negatively regulates autophagy. *Curr Biol* **20**, 1093 (Jun 22, 2010).
110. J. A. Martina, Y. Chen, M. Gucek, R. Puertollano, MTORC1 functions as a transcriptional regulator of autophagy by preventing nuclear transport of TFEB. *Autophagy* **8**, 903 (Jun, 2012).
111. A. Roczniak-Ferguson *et al.*, The transcription factor TFEB links mTORC1 signaling to transcriptional control of lysosome homeostasis. *Sci Signal* **5**, ra42 (Jun 12, 2012).
112. C. Settembre *et al.*, A lysosome-to-nucleus signalling mechanism senses and regulates the lysosome via mTOR and TFEB. *Embo J* **31**, 1095 (Mar 7, 2012).
113. M. Palmieri *et al.*, Characterization of the CLEAR network reveals an integrated control of cellular clearance pathways. *Hum Mol Genet* **20**, 3852 (Oct 1, 2011).
114. C. Settembre *et al.*, TFEB links autophagy to lysosomal biogenesis. *Science* **332**, 1429 (Jun 17, 2011).
115. K. Yamagata *et al.*, rheb, a growth factor- and synaptic activity-regulated gene, encodes a novel Ras-related protein. *J Biol Chem* **269**, 16333 (Jun 10, 1994).
116. L. J. Saucedo *et al.*, Rheb promotes cell growth as a component of the insulin/TOR signalling network. *Nat Cell Biol* **5**, 566 (Jun, 2003).
117. H. Stocker *et al.*, Rheb is an essential regulator of S6K in controlling cell growth in Drosophila. *Nat Cell Biol* **5**, 559 (Jun, 2003).
118. G. J. Clark *et al.*, The Ras-related protein Rheb is farnesylated and antagonizes Ras signaling and transformation. *J Biol Chem* **272**, 10608 (Apr 18, 1997).
119. C. Buerger, B. DeVries, V. Stambolic, Localization of Rheb to the endomembrane is critical for its signaling function. *Biochem Biophys Res Commun* **344**, 869 (Jun 9, 2006).
120. X. Long, Y. Lin, S. Ortiz-Vega, K. Yonezawa, J. Avruch, Rheb binds and regulates the mTOR kinase. *Curr Biol* **15**, 702 (Apr 26, 2005).
121. K. E. Mach, K. A. Furge, C. F. Albright, Loss of Rhb1, a Rheb-related GTPase in fission yeast, causes growth arrest with a terminal phenotype similar to that caused by nitrogen starvation. *Genetics* **155**, 611 (Jun, 2000).
122. D. E. Martin, M. N. Hall, The expanding TOR signaling network. *Curr Opin Cell Biol* **17**, 158 (Apr, 2005).
123. Identification and characterization of the tuberous sclerosis gene on chromosome 16. *Cell* **75**, 1305 (Dec 31, 1993).
124. M. van Slegtenhorst *et al.*, Identification of the tuberous sclerosis gene TSC1 on chromosome 9q34. *Science* **277**, 805 (Aug 8, 1997).

125. X. Gao *et al.*, Tsc tumour suppressor proteins antagonize amino-acid-TOR signalling. *Nat Cell Biol* **4**, 699 (Sep, 2002).
126. K. Inoki, Y. Li, T. Zhu, J. Wu, K. L. Guan, TSC2 is phosphorylated and inhibited by Akt and suppresses mTOR signalling. *Nat Cell Biol* **4**, 648 (Sep, 2002).
127. K. Inoki, Y. Li, T. Xu, K. L. Guan, Rheb GTPase is a direct target of TSC2 GAP activity and regulates mTOR signaling. *Genes Dev* **17**, 1829 (Aug 1, 2003).
128. Y. Zhang *et al.*, Rheb is a direct target of the tuberous sclerosis tumour suppressor proteins. *Nat Cell Biol* **5**, 578 (Jun, 2003).
129. A. R. Tee, B. D. Manning, P. P. Roux, L. C. Cantley, J. Blenis, Tuberous sclerosis complex gene products, Tuberin and Hamartin, control mTOR signaling by acting as a GTPase-activating protein complex toward Rheb. *Curr Biol* **13**, 1259 (Aug 5, 2003).
130. M. T. Mazhab-Jafari *et al.*, An autoinhibited noncanonical mechanism of GTP hydrolysis by Rheb maintains mTORC1 homeostasis. *Structure* **20**, 1528 (Sep 5, 2012).
131. C. C. Dibble *et al.*, TBC1D7 is a third subunit of the TSC1-TSC2 complex upstream of mTORC1. *Mol Cell* **47**, 535 (Aug 24, 2012).
132. S. L. Cai *et al.*, Activity of TSC2 is inhibited by AKT-mediated phosphorylation and membrane partitioning. *J Cell Biol* **173**, 279 (Apr 24, 2006).
133. D. J. Kwiatkowski, B. D. Manning, Tuberous sclerosis: a GAP at the crossroads of multiple signaling pathways. *Hum Mol Genet* **14 Spec No. 2**, R251 (Oct 15, 2005).
134. P. P. Roux, B. A. Ballif, R. Anjum, S. P. Gygi, J. Blenis, Tumor-promoting phorbol esters and activated Ras inactivate the tuberous sclerosis tumor suppressor complex via p90 ribosomal S6 kinase. *Proc Natl Acad Sci U S A* **101**, 13489 (Sep 14, 2004).
135. L. Ma, Z. Chen, H. Erdjument-Bromage, P. Tempst, P. P. Pandolfi, Phosphorylation and functional inactivation of TSC2 by Erk implications for tuberous sclerosis and cancer pathogenesis. *Cell* **121**, 179 (Apr 22, 2005).
136. A. R. Tee *et al.*, Tuberous sclerosis complex-1 and -2 gene products function together to inhibit mammalian target of rapamycin (mTOR)-mediated downstream signaling. *Proc Natl Acad Sci U S A* **99**, 13571 (Oct 15, 2002).
137. C. J. Potter, L. G. Pedraza, T. Xu, Akt regulates growth by directly phosphorylating Tsc2. *Nat Cell Biol* **4**, 658 (Sep, 2002).
138. H. C. Dan *et al.*, Phosphatidylinositol 3-kinase/Akt pathway regulates tuberous sclerosis tumor suppressor complex by phosphorylation of tuberin. *J Biol Chem* **277**, 35364 (Sep 20, 2002).
139. F. McCormick, Ras signaling and NF1. *Curr Opin Genet Dev* **5**, 51 (Feb, 1995).
140. Y. Shi, B. E. Paluch, X. Wang, X. Jiang, PTEN at a glance. *J Cell Sci* **125**, 4687 (Oct 15, 2012).
141. O. J. Shah, Z. Wang, T. Hunter, Inappropriate activation of the TSC/Rheb/mTOR/S6K cassette induces IRS1/2 depletion, insulin resistance, and cell survival deficiencies. *Curr Biol* **14**, 1650 (Sep 21, 2004).
142. L. S. Harrington *et al.*, The TSC1-2 tumor suppressor controls insulin-PI3K signaling via regulation of IRS proteins. *J Cell Biol* **166**, 213 (Jul 19, 2004).

143. K. Inoki *et al.*, TSC2 integrates Wnt and energy signals via a coordinated phosphorylation by AMPK and GSK3 to regulate cell growth. *Cell* **126**, 955 (Sep 8, 2006).
144. D. F. Lee *et al.*, IKK beta suppression of TSC1 links inflammation and tumor angiogenesis via the mTOR pathway. *Cell* **130**, 440 (Aug 10, 2007).
145. K. Inoki, T. Zhu, K. L. Guan, TSC2 mediates cellular energy response to control cell growth and survival. *Cell* **115**, 577 (Nov 26, 2003).
146. M. M. Mihaylova, R. J. Shaw, The AMPK signalling pathway coordinates cell growth, autophagy and metabolism. *Nat Cell Biol* **13**, 1016 (Sep, 2011).
147. D. G. Hardie, D. Carling, S. J. Gamblin, AMP-activated protein kinase: also regulated by ADP? *Trends Biochem Sci* **36**, 470 (Sep, 2011).
148. D. M. Gwinn *et al.*, AMPK phosphorylation of raptor mediates a metabolic checkpoint. *Mol Cell* **30**, 214 (Apr 25, 2008).
149. J. A. Dykens *et al.*, Biguanide-induced mitochondrial dysfunction yields increased lactate production and cytotoxicity of aerobically-poised HepG2 cells and human hepatocytes in vitro. *Toxicol Appl Pharmacol* **233**, 203 (Dec 1, 2008).
150. G. Zhou *et al.*, Role of AMP-activated protein kinase in mechanism of metformin action. *J Clin Invest* **108**, 1167 (Oct, 2001).
151. R. J. Shaw *et al.*, The kinase LKB1 mediates glucose homeostasis in liver and therapeutic effects of metformin. *Science* **310**, 1642 (Dec 9, 2005).
152. S. A. Hawley *et al.*, Use of cells expressing gamma subunit variants to identify diverse mechanisms of AMPK activation. *Cell Metab* **11**, 554 (Jun 9, 2010).
153. R. J. Shaw *et al.*, The LKB1 tumor suppressor negatively regulates mTOR signaling. *Cancer Cell* **6**, 91 (Jul, 2004).
154. S. A. Hawley *et al.*, Complexes between the LKB1 tumor suppressor, STRAD alpha/beta and MO25 alpha/beta are upstream kinases in the AMP-activated protein kinase cascade. *J Biol* **2**, 28 (2003).
155. A. V. Budanov, M. Karin, p53 target genes sestrin1 and sestrin2 connect genotoxic stress and mTOR signaling. *Cell* **134**, 451 (Aug 8, 2008).
156. A. M. Arsham, J. J. Howell, M. C. Simon, A novel hypoxia-inducible factor-independent hypoxic response regulating mammalian target of rapamycin and its targets. *J Biol Chem* **278**, 29655 (Aug 8, 2003).
157. J. H. Reiling, E. Hafen, The hypoxia-induced paralogs Scylla and Charybdis inhibit growth by down-regulating S6K activity upstream of TSC in Drosophila. *Genes Dev* **18**, 2879 (Dec 1, 2004).
158. J. Brugarolas *et al.*, Regulation of mTOR function in response to hypoxia by REDD1 and the TSC1/TSC2 tumor suppressor complex. *Genes Dev* **18**, 2893 (Dec 1, 2004).
159. M. P. DeYoung, P. Horak, A. Sofer, D. Sgroi, L. W. Ellisen, Hypoxia regulates TSC1/2-mTOR signaling and tumor suppression through REDD1-mediated 14-3-3 shuttling. *Genes Dev* **22**, 239 (Jan 15, 2008).
160. V. R. Preedy, P. J. Garlick, The response of muscle protein synthesis to nutrient intake in postabsorptive rats: the role of insulin and amino acids. *Biosci Rep* **6**, 177 (Feb, 1986).

161. X. Wang, L. E. Campbell, C. M. Miller, C. G. Proud, Amino acid availability regulates p70 S6 kinase and multiple translation factors. *Biochem J* **334 (Pt 1)**, 261 (Aug 15, 1998).
162. P. Nicklin *et al.*, Bidirectional transport of amino acids regulates mTOR and autophagy. *Cell* **136**, 521 (Feb 6, 2009).
163. R. Zoncu *et al.*, mTORC1 senses lysosomal amino acids through an inside-out mechanism that requires the vacuolar H(+)-ATPase. *Science* **334**, 678 (Nov 4, 2011).
164. B. Magasanik, C. A. Kaiser, Nitrogen regulation in Saccharomyces cerevisiae. *Gene* **290**, 1 (May 15, 2002).
165. J. L. Jewell, R. C. Russell, K. L. Guan, Amino acid signalling upstream of mTOR. *Nat Rev Mol Cell Biol* **14**, 133 (Mar, 2013).
166. P. Gulati, G. Thomas, Nutrient sensing in the mTOR/S6K1 signalling pathway. *Biochem Soc Trans* **35**, 236 (Apr, 2007).
167. J. Colombani *et al.*, A nutrient sensor mechanism controls Drosophila growth. *Cell* **114**, 739 (Sep 19, 2003).
168. D. C. Goberdhan, D. Meredith, C. A. Boyd, C. Wilson, PAT-related amino acid transporters regulate growth via a novel mechanism that does not require bulk transport of amino acids. *Development* **132**, 2365 (May, 2005).
169. J. F. Martin, E. Hersperger, A. Simcox, A. Shearn, minidiscs encodes a putative amino acid transporter subunit required non-autonomously for imaginal cell proliferation. *Mech Dev* **92**, 155 (Apr, 2000).
170. D.-H. Kim *et al.*, mTOR Interacts with Raptor to Form a Nutrient-Sensitive Complex that Signals to the Cell Growth Machinery. *Cell* **110**, 163 (2002).
171. M. Binda *et al.*, The Vam6 GEF controls TORC1 by activating the EGO complex. *Mol Cell* **35**, 563 (Sep 11, 2009).
172. M. Roccio, J. L. Bos, F. J. Zwartkruis, Regulation of the small GTPase Rheb by amino acids. *Oncogene* **25**, 657 (Feb 2, 2006).
173. E. M. Smith, S. G. Finn, A. R. Tee, G. J. Browne, C. G. Proud, The tuberous sclerosis protein TSC2 is not required for the regulation of the mammalian target of rapamycin by amino acids and certain cellular stresses. *J Biol Chem* **280**, 18717 (May 13, 2005).
174. E. Kim, P. Goraksha-Hicks, L. Li, T. P. Neufeld, K. L. Guan, Regulation of TORC1 by Rag GTPases in nutrient response. *Nat Cell Biol* **10**, 935 (Aug, 2008).
175. E. Hirose, N. Nakashima, T. Sekiguchi, T. Nishimoto, RagA is a functional homologue of S. cerevisiae Gtr1p involved in the Ran/Gsp1-GTPase pathway. *J Cell Sci* **111 (Pt 1)**, 11 (Jan, 1998).
176. T. Sekiguchi, E. Hirose, N. Nakashima, M. Ii, T. Nishimoto, Novel G proteins, Rag C and Rag D, interact with GTP-binding proteins, Rag A and Rag B. *J Biol Chem* **276**, 7246 (Mar 9, 2001).
177. A. Schurmann, A. Brauers, S. Massmann, W. Becker, H. G. Joost, Cloning of a novel family of mammalian GTP-binding proteins (RagA, RagBs, RagB1) with remote similarity to the Ras-related GTPases. *J Biol Chem* **270**, 28982 (Dec 1, 1995).

178. F. Dubouloz, O. Deloche, V. Wanke, E. Cameroni, C. De Virgilio, The TOR and EGO protein complexes orchestrate microautophagy in yeast. *Mol Cell* **19**, 15 (Jul 1, 2005).
179. M. Gao, C. A. Kaiser, A conserved GTPase-containing complex is required for intracellular sorting of the general amino-acid permease in yeast. *Nat Cell Biol* **8**, 657 (Jul, 2006).
180. R. Gong *et al.*, Crystal structure of the Gtr1p-Gtr2p complex reveals new insights into the amino acid-induced TORC1 activation. *Genes Dev* **25**, 1668 (Aug 15, 2011).
181. J. H. Jeong *et al.*, Crystal structure of the Gtr1p(GTP)-Gtr2p(GDP) protein complex reveals large structural rearrangements triggered by GTP-to-GDP conversion. *J Biol Chem* **287**, 29648 (Aug 24, 2012).
182. L. Bar-Peled, L. D. Schweitzer, R. Zoncu, D. M. Sabatini, Ragulator Is a GEF for the Rag GTPases that Signal Amino Acid Levels to mTORC1. *Cell* **150**, 1196 (Sep 14, 2012).
183. A. Efeyan *et al.*, Regulation of mTORC1 by the Rag GTPases is necessary for neonatal autophagy and survival. *Nature* **493**, 679 (Jan 31, 2013).
184. P. B. Crino, K. L. Nathanson, E. P. Henske, The tuberous sclerosis complex. *N Engl J Med* **355**, 1345 (Sep 28, 2006).
185. E. P. Henske, F. X. McCormack, Lymphangioleiomyomatosis - a wolf in sheep's clothing. *J Clin Invest* **122**, 3807 (Nov 1, 2012).
186. J. J. Bissler *et al.*, Sirolimus for angiomyolipoma in tuberous sclerosis complex or lymphangioleiomyomatosis. *N Engl J Med* **358**, 140 (Jan 10, 2008).
187. E. Pasmant, M. Vidaud, D. Vidaud, P. Wolkenstein, Neurofibromatosis type 1: from genotype to phenotype. *J Med Genet* **49**, 483 (Aug, 2012).
188. F. H. Menko *et al.*, Birt-Hogg-Dube syndrome: diagnosis and management. *Lancet Oncol* **10**, 1199 (Dec, 2009).
189. D. M. Sabatini, mTOR and cancer: insights into a complex relationship. *Nat Rev Cancer* **6**, 729 (Sep, 2006).
190. H. G. Wendel *et al.*, Survival signalling by Akt and eIF4E in oncogenesis and cancer therapy. *Nature* **428**, 332 (Mar 18, 2004).
191. E. Petroulakis *et al.*, p53-dependent translational control of senescence and transformation via 4E-BPs. *Cancer Cell* **16**, 439 (Nov 6, 2009).
192. D. Ruggero *et al.*, The translation factor eIF-4E promotes tumor formation and cooperates with c-Myc in lymphomagenesis. *Nat Med* **10**, 484 (May, 2004).
193. P. Polak *et al.*, Adipose-specific knockout of raptor results in lean mice with enhanced mitochondrial respiration. *Cell Metab* **8**, 399 (Nov, 2008).
194. S. H. Um *et al.*, Absence of S6K1 protects against age- and diet-induced obesity while enhancing insulin sensitivity. *Nature* **431**, 200 (Sep 9, 2004).
195. G. P. Fadini, G. Ceolotto, E. Pagnin, S. de Kreutzenberg, A. Avogaro, At the crossroads of longevity and metabolism: the metabolic syndrome and lifespan determinant pathways. *Aging Cell* **10**, 10 (Feb, 2011).
196. C. J. Kenyon, The genetics of ageing. *Nature* **464**, 504 (Mar 25, 2010).
197. M. N. Stanfel, L. S. Shamieh, M. Kaeberlein, B. K. Kennedy, The TOR pathway comes of age. *Biochim Biophys Acta* **1790**, 1067 (Oct, 2009).

198. S. Robida-Stubbs *et al.*, TOR signaling and rapamycin influence longevity by regulating SKN-1/Nrf and DAF-16/FoxO. *Cell Metab* **15**, 713 (May 2, 2012).
199. K. L. Sheaffer, D. L. Updike, S. E. Mango, The Target of Rapamycin pathway antagonizes pha-4/FoxA to control development and aging. *Curr Biol* **18**, 1355 (Sep 23, 2008).
200. D. E. Harrison *et al.*, Rapamycin fed late in life extends lifespan in genetically heterogeneous mice. *Nature* **460**, 392 (Jul 16, 2009).
201. G. Bohn *et al.*, A novel human primary immunodeficiency syndrome caused by deficiency of the endosomal adaptor protein p14. *Nat Med* **13**, 38 (Jan, 2007).

Chapter 2

The Ragulator-Rag complex mediates translocation of mTORC1 to the lysosomal surface, which is necessary and sufficient for its activation by amino acids

Yasemin Sancak[1,2,*], Liron Bar-Peled[1,2,*], Roberto Zoncu[1,2], Andrew L. Markhard[1], Shigeyuki Nada[4], and David M. Sabatini[1,2,3]

[1]Whitehead Institute for Biomedical Research and Massachusetts Institute of Technology, Department of Biology, Nine Cambridge Center, Cambridge, MA 02142, USA

[2]The David H. Koch Institute for Integrative Cancer Research at MIT, 77 Massachusetts Avenue, Cambridge, MA 02139, USA

[3] Howard Hughes Medical Institute, Department of Biology, Massachusetts Institute of Technology, Cambridge, MA 02139, USA

[4]Department of Oncogene Research, Research Institute for Microbial Diseases, Osaka University, 3-1 Yamadaoka, Suita, Osaka 565-0871, Japan

* These authors contributed equally to this work

This work has been published in:
Sancak, Y., Bar-Peled, L., Zoncu, R., Markhard, A.L., Nada, S., and Sabatini, D.M. (2010). Ragulator-Rag complex targets mTORC1 to the lysosomal surface and is necessary for its activation by amino acids. Cell *141*, 290-303.

Experiments shown in figures 2, 3, 4, 7, S3, S4 and S5 were preformed by LBP. Experiments shown in figures 1, 5, 6, 7, S1, S2, S6 and S7 were preformed by YS. Experiments shown in figures 1, 3, S1, S3, S4 and S7 were preformed by RZ.

Summary

The mTORC1 kinase promotes growth in response to growth factors, energy levels, and amino acids and its activity is often deregulated in disease. The Rag GTPases interact with mTORC1 and are proposed to activate it in response to amino acids by promoting the translocation of mTORC1 to a membrane-bound compartment that contains the mTORC1 activator Rheb. We show that amino acids induce the movement of mTORC1 to lysosomal membranes, where the Rag proteins reside in an amino acid-independent fashion. The Ragulator, a complex encoded by the MAPKSP1, ROBLD3, and c11orf59 genes, interacts with the Rag GTPases, localizes them to lysosomes, and is essential for mTORC1 activation. Constitutive targeting of mTORC1 to the lysosomal surface is sufficient to render the mTORC1 pathway resistant to amino acid deprivation and independent of Rag and Ragulator, but not Rheb, function. Thus, Rag-Ragulator mediated translocation of mTORC1 to lysosomal membranes is the key event governing amino acid signaling to mTORC1.

Introduction

The multi-component kinase mTORC1 (mammalian target of rapamycin complex 1) regulates cell growth by coordinating upstream signals from growth factors, intracellular energy levels, and amino acid availability, and is deregulated in diseases such as cancer and diabetes (reviewed in (Guertin and Sabatini 2007)). The TSC1 and TSC2 proteins form a tumor suppressor complex that transmits growth factor and energy signals to mTORC1 by regulating the GTP-loading state of Rheb, a Ras-related GTP-binding protein. When bound to GTP, Rheb interacts with and activates mTORC1(Inoki et al., 2003; Long et al., 2005; Sancak et al., 2007; Saucedo et al., 2003; Stocker et al., 2003; Tee et al., 2003) and appears to be necessary for the activation of mTORC1 by all signals, including amino acid availability (Avruch et al., 2006; Nobukuni et al., 2005; Sancak et al., 2008; Saucedo et al., 2003; Tee et al., 2005; Tee et al., 2003; Zhang et al., 2003). In contrast, TSC1-TSC2 is dispensable for the regulation of mTORC1 by amino acids and, in cells lacking TSC2, the mTORC1 pathway is sensitive to amino acid starvation but resistant to growth factor withdrawal (Roccio et al., 2006; Smith et al., 2005.).

Recently, the Rag GTPases, which are also members of the Ras-family of GTP-binding proteins, were shown to be amino acid-specific regulators of the mTORC1 pathway (Kim et al., 2008; Sancak et al., 2008). Mammals express four Rag proteins—RagA, RagB, RagC, and RagD—that form heterodimers consisting of RagA or RagB with RagC or RagD. RagA and RagB, like RagC and RagD, are highly similar to each other and are functionally redundant (Hirose et al., 1998; Sancak et al., 2008; Schurmann et al., 1995; Sekiguchi et al., 2001). Rag heterodimers containing GTP-bound RagB interact with mTORC1, and amino acids induce the mTORC1-Rag interaction by promoting the loading of RagB with GTP, which enables it to directly interact with the raptor component of mTORC1 (Sancak et al., 2008). The activation of the mTORC1 pathway by amino acids correlates with the movement of mTORC1 from an undefined location to a compartment containing Rab7 (Sancak et al., 2008), a marker of

both late endosomes and lysosomes (Chavrier et al., 1990; Luzio et al., 2007). How the Rag proteins regulate mTORC1 is unknown, but, in cells expressing a RagB mutant that is constitutively bound to GTP ($RagB^{GTP}$), the mTORC1 pathway is insensitive to amino acid starvation and mTORC1 resides in the Rab7-positive compartment even in the absence of amino acids (Sancak et al., 2008). We previously proposed that amino acids promote the translocation of mTORC1—in a Rag-dependent fashion—to the surface of an endomembrane compartment where mTORC1 can find its well-known activator Rheb. Here, we show that the lysosomal surface is the compartment where the Rag proteins reside and to which mTORC1 moves in response to amino acids. We identify the trimeric Ragulator protein complex as a new component of the mTORC1 pathway that interacts with the Rag GTPases, is essential for localizing them and mTORC1 to the lysosomal surface, and is necessary for the activation of the mTORC1 pathway by amino acids. In addition, by expressing in cells a modified raptor protein that targets mTORC1 to the lysosomal surface, we provide evidence that supports our model of mTORC1 pathway activation by amino acids.

Results

Amino acids cause the translocation of mTORC1 to lysosomal membranes, where the Rag GTPases are already present

To better define the compartment to which mTORC1 moves upon amino acid stimulation, we co-stained human cells with antibodies to endogenous mTOR, raptor, or RagC as well as to various endomembrane markers (data not shown). This revealed that in the presence, but not the absence, of amino acids mTOR and raptor co-localized with LAMP2 (Figures 1A and 1B), a well-characterized lysosomal marker (reviewed in (Eskelinen, 2006)). Amino acid stimulation also resulted in an appreciable increase in the average size of lysosomes, which, as determined by live cell imaging, was most likely caused by lysosome-lysosome fusion (R.Z., unpublished results). The amino acid-induced movement of mTOR to the LAMP2-positive compartment depends on the Rag GTPases as it was eliminated by the RNAi mediated co-knockdown of RagA and RagB (Figure S1A and S1B). Endogenous RagC also co-localized extensively with LAMP2, but, unlike mTORC1, this co-localization was unaffected by amino acid availability (Figure 1C). Consistent with amino acids not regulating the interaction between RagC and RagA or RagB (Figure 1D), an antibody that recognizes RagA and RagB stained lysosomes in both amino acid-starved and replete cells (Figure 1E). Lastly, GFP-tagged wild-type and GTP-bound mutants of RagB ($RagB^{GTP}$) and RagD ($RagD^{GTP}$) behaved identically to their endogenous counterparts (Figures 1F and 1G). Thus, amino acids stimulate the translocation of mTORC1 to the lysosomal surface, where the Rag GTPases reside irrespective of their GTP-loaded states or amino acid availability. Given that mTORC1 interacts with the Rag heterodimers in an amino acid-dependent fashion (Sancak et al., 2008), the mTORC1 and Rag localization data are consistent with the Rag GTPases serving as an amino acid-regulated docking site for mTORC1 on lysosomes.

Figure 1

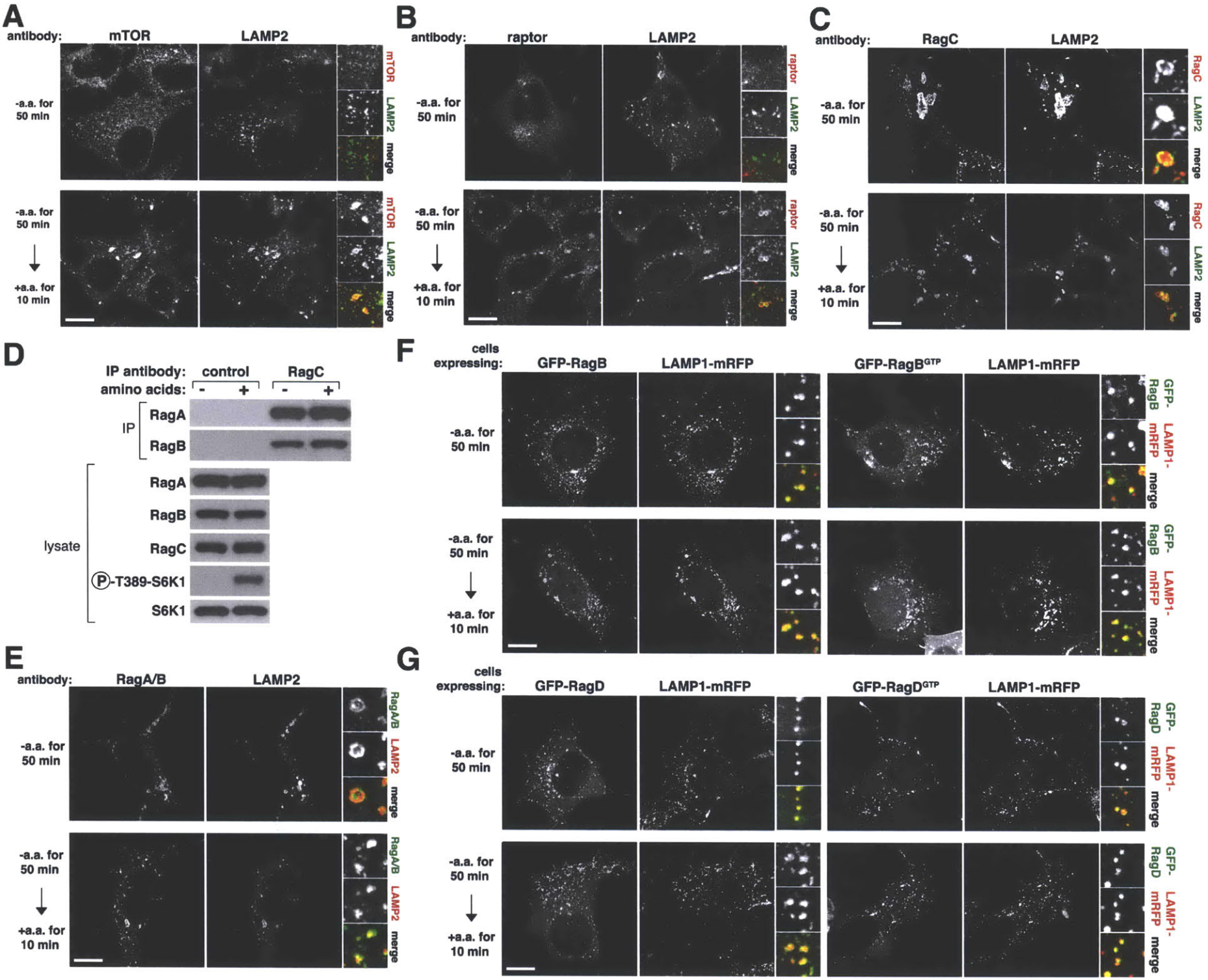
A
antibody:
mTOR
LAMP2
-a.a. for 50 min
+a.a. for 10 min
mTOR
LAMP2
merge
B
antibody:
raptor
LAMP2
-a.a. for 50 min
+a.a. for 10 min
raptor
LAMP2
merge
C
antibody:
RagC
LAMP2
-a.a. for 50 min
+a.a. for 10 min
RagC
LAMP2
merge
D
IP antibody:
control
RagC
amino acids:
- + - +
IP
RagA
RagB
lysate
RagA
RagB
RagC
Ⓟ-T389-S6K1
S6K1
E
antibody:
RagA/B
LAMP2
-a.a. for 50 min
+a.a. for 10 min
RagA/B
LAMP2
merge
F
cells expressing:
GFP-RagB
LAMP1-mRFP
GFP-RagB^{GTP}
LAMP1-mRFP
-a.a. for 50 min
+a.a. for 10 min
GFP-RagB
LAMP1-mRFP
merge
G
cells expressing:
GFP-RagD
LAMP1-mRFP
GFP-RagD^{GTP}
LAMP1-mRFP
-a.a. for 50 min
+a.a. for 10 min
GFP-RagD
LAMP1-mRFP
merge

Figure. 1. mTORC1 localizes to lysosomal membranes in an amino acid-dependent fashion while the Rag GTPases are constitutively localized to the same compartment.

(A) Images of HEK-293T cells co-immunostained for lysosomal protein LAMP2 (green) and mTOR (red). Cells were starved of and restimulated with amino acids for the indicated times before processing and imaging.
(B) Images of HEK-293T cells co-immunostained for LAMP2 (green) and raptor (red). Cells were treated and processed as in (A).
(C) Images of HEK-293T cells co-immunostained for LAMP2 (green) and RagC (red). Cells were treated and processed as in (A).
(D) RagC interacts with RagA and RagB independently of amino acid availability. RagC-immunoprecipitates were prepared from HEK-293T cells starved or stimulated with amino acids as in (A), and immunoprecipitates and lysates were analyzed by immunoblotting for the indicated proteins.
(E) Images of HEK-293T cells co-immunostained for RagA/B (green) and LAMP2 (red). Cells were treated, processed, and imaged as in (A).
(F) GFP-RagB and GFP-RagB^{GTP} co-localize with co-expressed LAMP1-mRFP independently of amino acid availability. HEK-293T cells transfected with the indicated cDNAs were treated and processed as in (A).
(G) GFP-RagD and GFP-RagD^{GTP} co-localize with co-expressed LAMP1-mRFP independently of amino acid availability. HEK-293T cells transfected with the indicated cDNAs were treated and processed as in (A). In all images, insets show selected fields that were magnified five times and their overlays. Scale bar is 10 μm.

The translocation of mTORC1 to lysosomes does not depend on growth factors, Rheb, or mTORC1 activity

The movement of mTORC1 to lysosomes is a specific response to amino acids. In wild-type mouse embryonic fibroblasts (MEFs), amino acids promoted the translocation of mTORC1 to lysosomes even when cells were cultured in the absence of serum (Figure S2A), a condition in which mTORC1 signaling, as detected by phosphorylated S6K1, is not active (Figure S2B). Conversely, in the absence of amino acids, neither serum stimulation nor constitutive activation of Rheb caused by the loss of TSC2, led to the lysosomal translocation of mTORC1 (Figure S2A). In both wild-type and TSC2-null MEFs, RNAi-mediated suppression of Rheb1 expression inhibited mTORC1 activation by amino acids (Figure S2C), but did not interfere with the amino acid-induced movement of mTOR to lysosomes (Figure S2D). Thus, the amino acid-induced translocation of mTORC1 to the lysosomal surface occurs independently of mTORC1 activity and does not require TSC2, Rheb, or growth factors.

The trimeric Ragulator complex interacts with the Rag GTPases and co-localizes with them on lysosomal membranes

Inspection of the amino acid sequence of the Rag GTPases did not reveal any obvious lipid modification signals that might mediate Rag recruitment to lysosomal membranes. Thus, we pursued the possibility that unknown Rag-interacting proteins are needed to localize the Rag GTPases to lysosomes and play a role in mTORC1 signaling. To identify such proteins we used protein purification approaches that have led to the discovery of other mTOR pathway components (see supp. methods). Mass spectrometric analysis of anti-FLAG immunoprecipitates prepared from human HEK-293T cells stably expressing FLAG-RagB or FLAG-RagD, but not FLAG-Rap2a, consistently revealed the presence of proteins encoded by the MAPKSP1, ROBLD3, and c11orf59 genes (Figure 2A). Furthermore, the same proteins were also detected in immunoprecipitates of endogenous RagC but not control proteins like p53 or

Figure S1

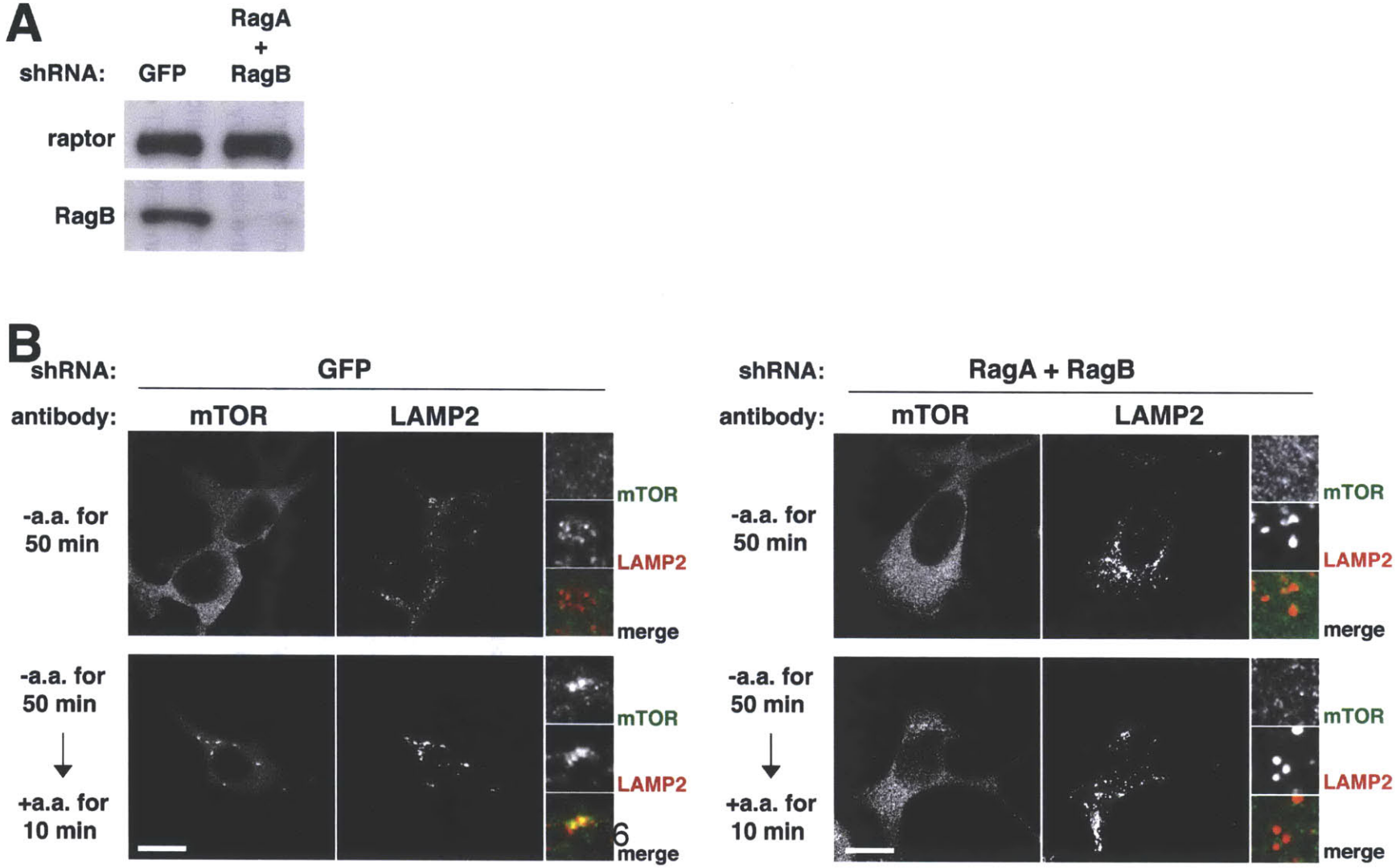
A
shRNA:
GFP
RagA + RagB
raptor
RagB
B
shRNA:
GFP
antibody:
mTOR
LAMP2
-a.a. for 50 min
+a.a. for 10 min
mTOR
LAMP2
merge
shRNA:
RagA + RagB
antibody:
mTOR
LAMP2
-a.a. for 50 min
+a.a. for 10 min
mTOR
LAMP2
merge

Supplementary Figure 1, related to Figure 1. Movement of mTORC1 to lysosomal membranes in response to amino acids depends on the Rag GTPases.

(A) Immunoblot analysis of RagB and raptor protein levels in HEK-293T cells with an RNAi-mediated knockdown of a control protein or RagA and RagB.

(B) Images of cells with knockdowns of RagA and RagB and co-immunostained for mTOR (green) and LAMP2 (red) after starvation and restimulation with amino acids for the indicated times. HEK-293T cells expressing the indicated shRNAs were starved and restimulated with amino acids as indicated and processed in the immunofluorescence assay. In all images, insets show selected fields that were magnified five times and their overlay. Scale bar is 10 μm.

Figure S2

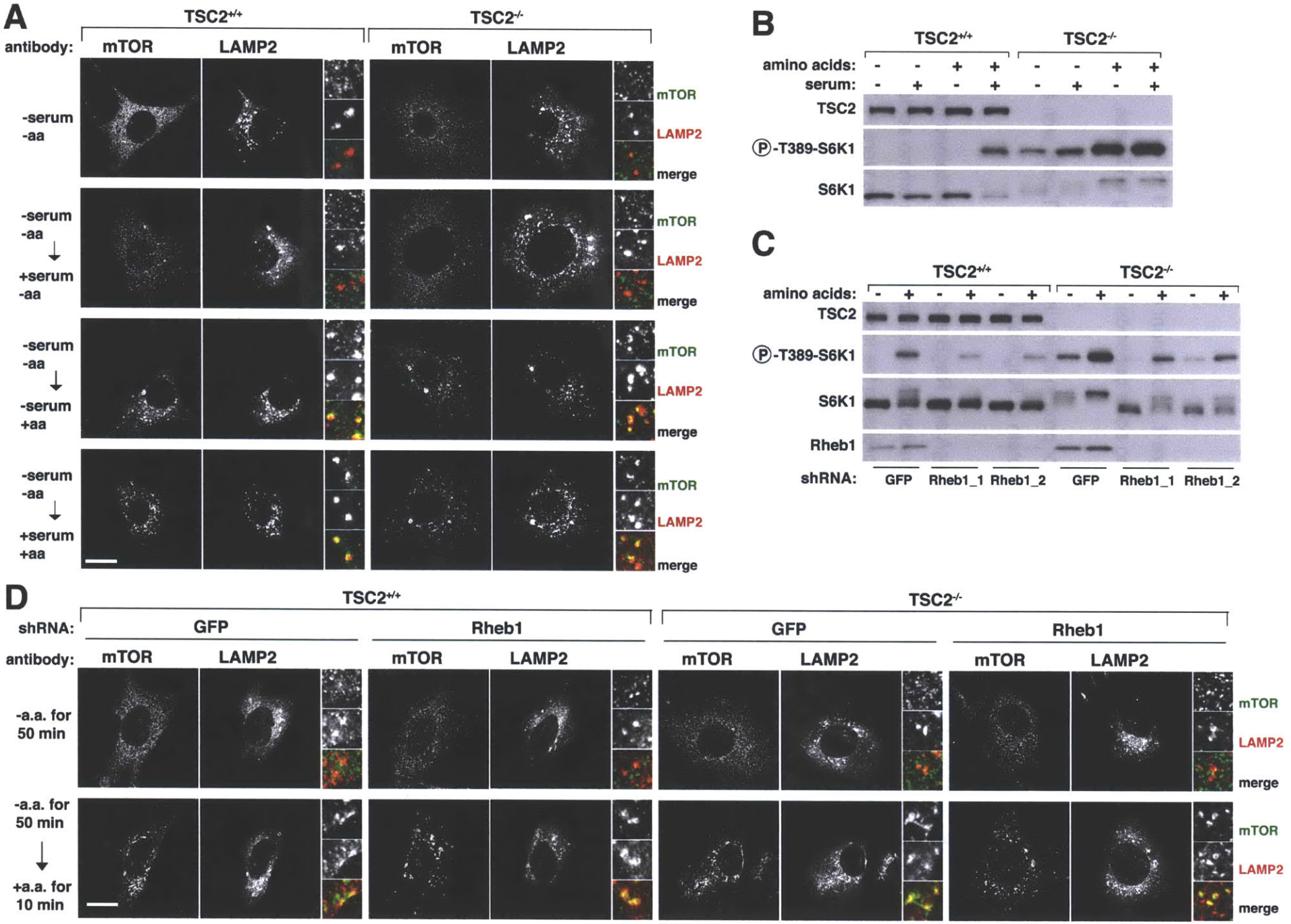
A
TSC2+/+
TSC2-/-
antibody:
mTOR
LAMP2
-serum
-aa
+serum
merge
B
amino acids:
serum:
TSC2
Ⓟ-T389-S6K1
S6K1
C
Rheb1
shRNA:
GFP
Rheb1_1
Rheb1_2
D
-a.a. for
50 min
+a.a. for
10 min

Supplementary Figure 2, related to Figure 1. TSC1/2, Rheb and growth factors do not regulate the lysosomal localization of mTORC1.

(A) mTOR co-localizes with LAMP2 only in the presence of amino acids and independently of serum stimulation. Images show co-immunostaining of mTOR (green) and LAMP2 (red) in $TSC2^{+/+}$ and $TSC2^{-/-}$ MEFs after indicated treatments. Cells were starved for serum and amino acids, and stimulated with dialyzed serum, amino acids, or both before processing in the immunofluorescence assay.

(B) Lysates from $TSC2^{+/+}$ and $TSC2^{-/-}$ MEFs starved and stimulated as in (A) were analyzed by immunobloting for the activity of the mTORC1 pathway.

(C) Loss of Rheb expression inhibits mTORC1 signaling in $TSC2^{+/+}$ and $TSC2^{-/-}$ MEFs. Cells expressing the indicated shRNAs were starved for amino acids or starved and restimulated with amino acids and lysates analyzed by immunobloting for mTORC1 pathway activity and Rheb1 levels.

(D) mTOR co-localizes with LAMP2 only in the presence of amino acids and independently of Rheb or TSC2. Images show co-immunostaining of mTOR (green) and LAMP2 (red) in $TSC2^{+/+}$ and $TSC2^{-/-}$ MEFs treated as in (C). In all images, insets show selected fields that were magnified five times and their overlays. Scale bar is 10 μm.

Figure 2

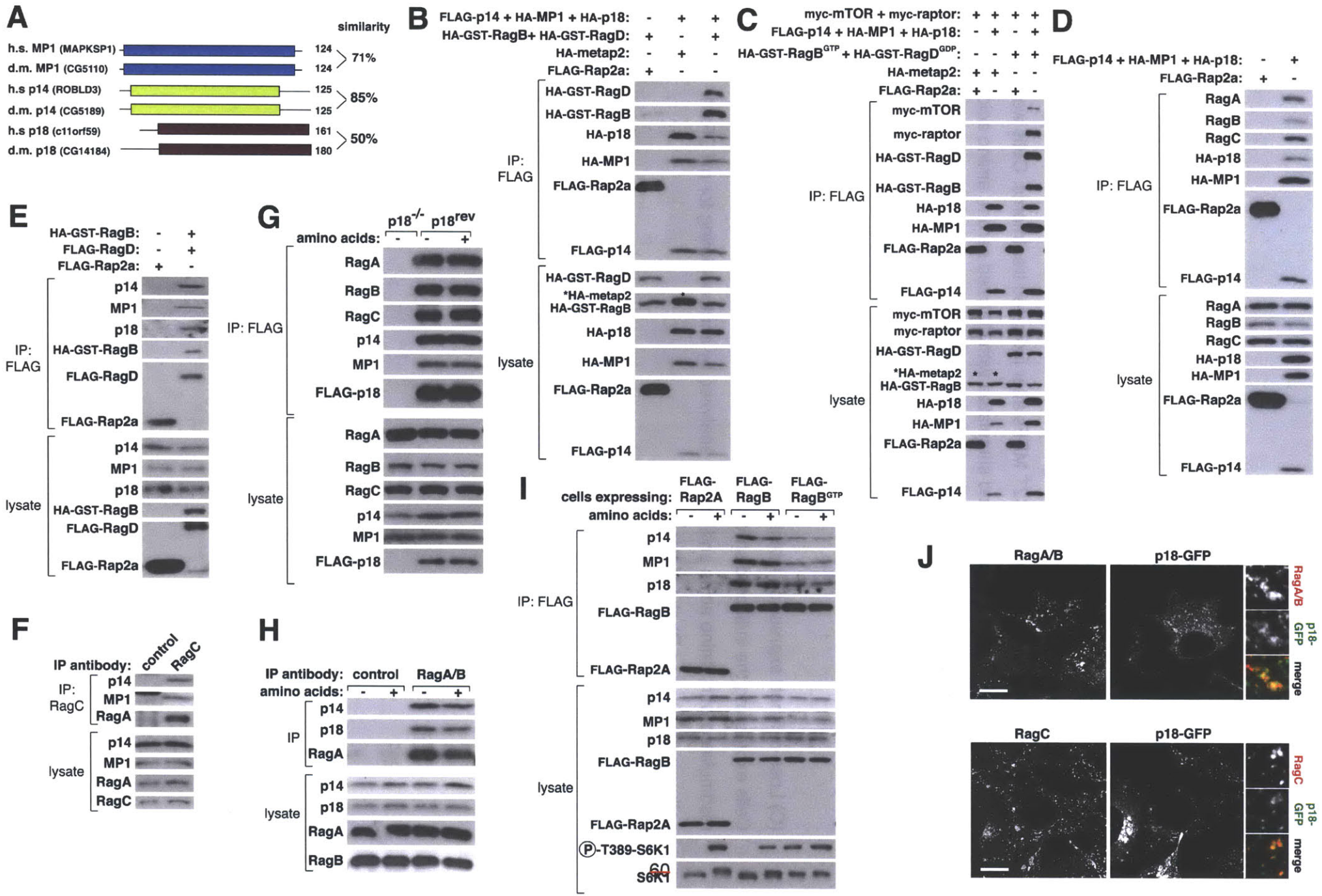
A
similarity
h.s. MP1 (MAPKSP1)
d.m. MP1 (CG5110)
h.s p14 (ROBLD3)
d.m. p14 (CG5189)
h.s p18 (c11orf59)
d.m. p18 (CG14184)
124
124
125
125
161
180
71%
85%
50%
B
FLAG-p14 + HA-MP1 + HA-p18:
HA-GST-RagB+ HA-GST-RagD:
HA-metap2:
FLAG-Rap2a:
IP: FLAG
lysate
HA-GST-RagD
HA-GST-RagB
HA-p18
HA-MP1
FLAG-Rap2a
FLAG-p14
*HA-metap2
C
myc-mTOR + myc-raptor:
FLAG-p14 + HA-MP1 + HA-p18:
HA-GST-RagB^GTP + HA-GST-RagD^GDP:
HA-metap2:
FLAG-Rap2a:
IP: FLAG
lysate
myc-mTOR
myc-raptor
HA-GST-RagD
HA-GST-RagB
HA-p18
HA-MP1
FLAG-Rap2a
FLAG-p14
*HA-metap2
D
FLAG-p14 + HA-MP1 + HA-p18:
FLAG-Rap2a:
IP: FLAG
lysate
RagA
RagB
RagC
HA-p18
HA-MP1
FLAG-Rap2a
FLAG-p14
E
HA-GST-RagB:
FLAG-RagD:
FLAG-Rap2a:
IP: FLAG
lysate
p14
MP1
p18
HA-GST-RagB
FLAG-RagD
FLAG-Rap2a
F
IP antibody:
control
RagC
IP: RagC
lysate
p14
MP1
RagA
RagC
G
p18^-/-
p18^rev
amino acids:
IP: FLAG
lysate
RagA
RagB
RagC
p14
MP1
FLAG-p18
H
IP antibody:
control
RagA/B
amino acids:
IP
lysate
p14
p18
RagA
RagB
I
cells expressing:
FLAG-Rap2A
FLAG-RagB
FLAG-RagB^GTP
amino acids:
IP: FLAG
lysate
p14
MP1
p18
FLAG-RagB
FLAG-Rap2A
(P)-T389-S6K1
S6K1
60
J
RagA/B
p18-GFP
RagA/B
p18-GFP
merge
RagC
p18-GFP
RagC
p18-GFP
merge

Figure 2. The trimeric Ragulator complex interacts and co-localizes with the Rag GTPases

(A) Schematic amino acid sequence alignment of human MP1, p14, and p18 and their corresponding *Drosophila* orthologs.
(B) Recombinant epitope-tagged Ragulator co-immunoprecipitates recombinant RagB and RagD. Anti-FLAG immunoprecipitates were prepared from HEK-293T cells co-transfected with the indicated cDNAs in expression vectors and cell lysates and immunoprecipitates analyzed by immunoblotting for levels of indicated proteins. The * indicates the band corresponding to the metap2 protein as it has the same apparent molecular weight as HA-GST-RagB.
(C) Recombinant Ragulator co-immunoprecipitates mTORC1 when it is co-expressed with the GTP-bound mutant of RagB. HEK-293T cells were co-transfected with the indicated cDNAs in expression vectors and analyzed as in (B). The * indicates the bands corresponding to metap2 as it has the same apparent molecular weight as HA-GST-RagB.
(D) Recombinant Ragulator co-immunoprecipitates endogenous RagA, RagB, and RagC. HEK-293T cells were co-transfected with indicated cDNAs in expression vectors and anti-FLAG immunoprecipitates analyzed as in (B).
(E) Recombinant RagB-RagD heterodimers co-immunoprecipitate endogenous p14, MP1, and p18. HEK-293T cells were co-transfected with indicated cDNAs in expression vectors and anti-FLAG immunoprecipitates analyzed as in (B).
(F) Endogenous RagC co-immunoprecipitates endogenous p14 and MP1. Anti-RagC immunoprecipitates were prepared from HEK-293T cells and analyzed for the levels of the indicated proteins.
(G) Amino acids do not regulate the amounts of endogenous MP1, p14, RagA, or RagB that co-immunoprecipitate with recombinant p18. p18-null cells ($p18^{-/-}$) or p18-null cells stably expressing FLAG-p18 ($p18^{rev}$) were starved for amino acids for 50 min or starved and restimulated with amino acids for 10 min. After in-cell cross-linking, anti-FLAG immunoprecipitates were prepared from cell lysates and analyzed for the levels of the indicated proteins by immunoblotting.

(H) Amino acids do not affect the amounts of endogenous p14 and p18 that co-immunoprecipitate with endogenous RagA/B. HEK-293T cells were treated as in (G) and anti-RagA/B immunoprecipitates analyzed by immunoblotting for the indicated proteins.

(I) Endogenous Ragulator co-immunoprecipitates with FLAG-RagB independently of amino acid availability and GTP-loading of RagB. HEK-293T cells stably expressing FLAG-RagB or FLAG-RagB^{GTP} were starved and restimulated with amino acids as in (G) and anti-FLAG immunoprecipitates analyzed for the levels of indicated proteins.

(J) The Rag GTPases co-localize with GFP-tagged p18. HEK-293T cells were transfected with a cDNA encoding p18-GFP, processed for immunostaining for endogenous RagA/B or RagC, and imaged for the RagA/B (red) or RagC (red) signal as well as for p18-GFP fluorescence (green). Note: not all cells express p18-GFP. In all images, insets show selected fields that were magnified five times and their overlays. Scale bar is 10 μm.

tubulin. Previous work indicates that these three small proteins interact with each other, localize to endosomes and lysosomes, and play positive roles in the MAPK pathway (Lunin et al., 2004; Nada et al., 2009; Schaeffer et al., 1998; Teis et al., 2006; Teis et al., 2002; Wunderlich et al., 2001). The proteins encoded by MAPKSP1, ROBLD3, and c11orf59 have been called MP1, p14, and p18, respectively, and we use these names throughout this study. For convenience and because MP1, p14, and p18 are Rag and mTORC1 regulators (see below) we refer to the trimeric complex as the 'Ragulator'.

Orthologues of MP1, p14, and p18 are readily detectable in vertebrates as well as in *Drosophila* (Figure 2A), but extensive database searches did not reveal any potential orthologues in budding or fission yeast. The amino acid sequences of MP1, p14, and p18 reveal little about their function and other than p14, which has a roadblock domain of unknown function (Koonin and Aravind, 2000), the proteins do not share sequence homology amongst themselves or with any other proteins in the databases besides their direct orthologues. In particular, they do not share any sequence similarity with the Ego1p or Ego3p, proteins, which interact with Gtr1p and Gtr2p (Dubouloz et al., 2005; Gao and Kaiser, 2006), the orthologues of the Rag proteins in budding yeast (Gao and Kaiser, 2006; Schurmann et al., 1995). The lysosomal localization of p18 requires its lipidation through N-terminal myristoylation and palmitoylation sites and p18 likely serves as a platform for keeping MP1 and p14 on the lysosomal surface (Nada et al., 2009).

In humans a mutation that leads to a partial reduction in the expression of p14 causes a pronounced growth defect so that individuals carrying the mutation are below the third percentile in age-adjusted height (Bohn et al., 2006). Furthermore, mice engineered to lack either p14 or p18 die around embryonic day 7-8 and exhibit severe growth retardation (Nada et al., 2009; Teis et al., 2006). Given the major role of the mTORC1 pathway in growth control, these loss of function phenotypes were of interest to us.

As an initial step in verifying our mass spectrometric identification of MP1, p14, and p18 as Rag-interacting proteins, we co-expressed them along with

RagB and RagD in HEK-293T cells and found that the Ragulator, but not the control Rap2A protein, co-immunoprecipitated both Rag GTPases but not the metap2 protein that has the same molecular weight as tagged RagB (Figure 2B). Furthermore, when co-expressed with a RagB mutant ($RagB^{GTP}$) that binds constitutively to GTP, the Ragulator co-immunoprecipitated the mTORC1 components raptor and mTOR (Figure 2C), consistent with the GTP-loading of RagB promoting the interaction of the Rag heterodimers with mTORC1 (Sancak et al., 2008). Furthermore, endogenous RagA, RagB, and RagC co-purified with recombinant Ragulator (Figure 2D) and endogenous Ragulator components co-purified with the recombinant RagB-RagD heterodimer (Figure 2E). Lastly, endogenous p14 and MP1 were present in immunoprecipitates prepared with an antibody directed against endogenous RagC that readily co-immunoprecipitates RagA (Figure 2F).

Amino acids did not appreciably regulate the interaction of recombinant p18 with endogenous p14, MP1 or the Rag GTPases (Figure 2G). Similarly, amino acids did not affect the interaction of endogenous Ragulator with endogenous Rag A/B (Figure 2H). The amounts of p14, p18, and MP1 that co-immunoprecipitated with the GTP-bound RagB mutant ($RagB^{GTP}$) were slightly less than with wild-type RagB (Figure 2I). Because mTORC1 pathway activity is high in cells expressing $RagB^{GTP}$ (Sancak et al., 2008) the reduced Ragulator-Rag interaction in these cells may reflect a compensatory mechanism to reduce mTORC1 activity. To test if the Rag GTPases interact with one or more Ragulator components directly, we performed *in vitro* binding assays between purified RagB-RagD heterodimers and individual Ragulator proteins. p18 interacted with RagB-RagD *in vitro*, but not with the Rap2a control protein (Figure S3A). In contrast, we did not detect a direct interaction between either p14 or MP1 and the Rag GTPases (data not shown), suggesting that p18 is the principal Rag-binding subunit of the Ragulator. Lastly, within HEK-293T cells, GFP-tagged p18 co-localized with endogenous RagA/B and RagC (Figure 2J). Collectively, these results show that the Ragulator interacts with the Rag GTPases and that a super-complex consisting of Ragulator, a Rag heterodimer, and mTORC1 can

Figure S3

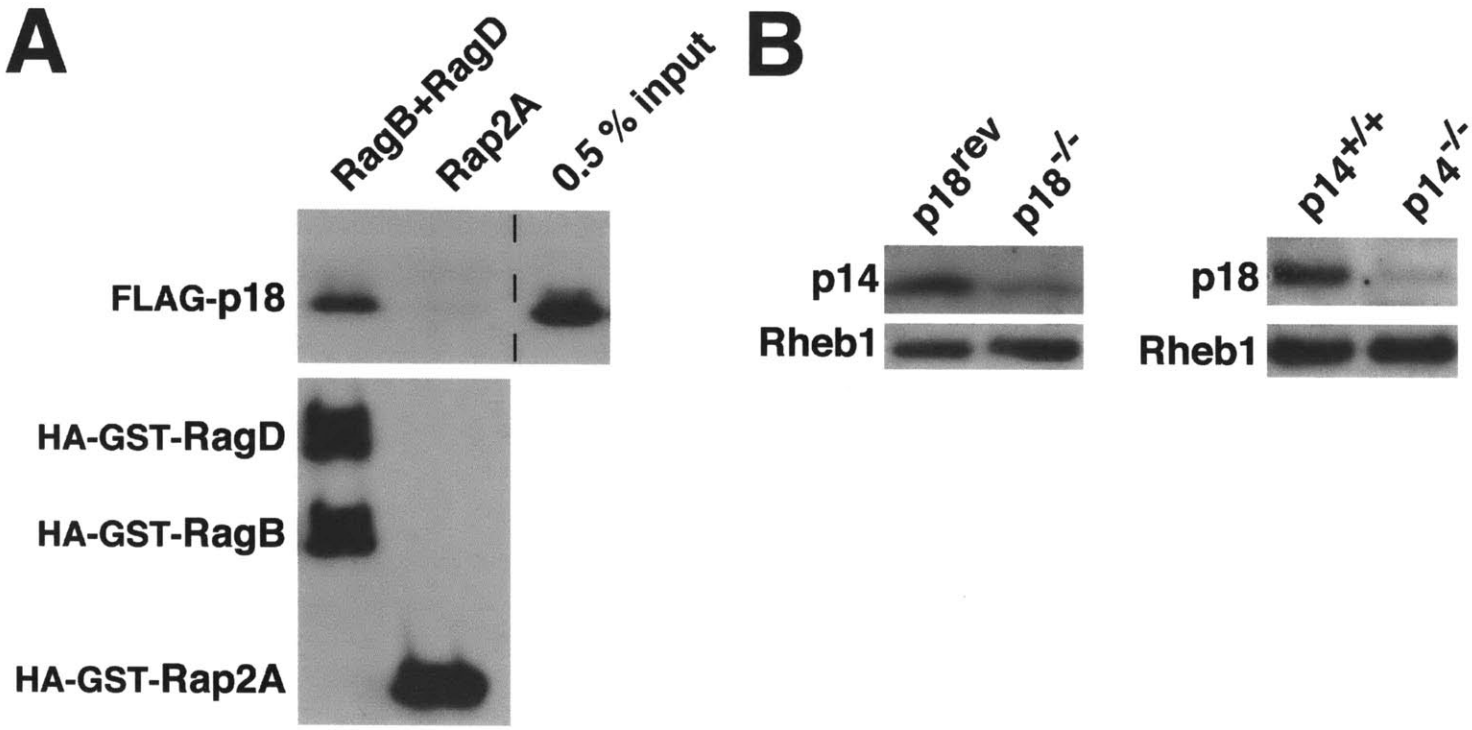
A
RagB+RagD
Rap2A
0.5 % input
FLAG-p18
HA-GST-RagD
HA-GST-RagB
HA-GST-Rap2A
B
p18rev
p18-/-
p14
Rheb1
p14+/+
p14-/-
p18
Rheb1

Supplementary Figure 3, related to Figure 2. The expression of Ragulator proteins is co-regulated and purified FLAG-p18 interacts with purified HA-GST-RagB/HA-GST-RagD dimer *in vitro*.

(A) *In vitro* binding assay using purified soluble FLAG-p18 and HA-GST-RagB/HA-GST-RagD heterodimer bound to glutathione beads was performed as described in the methods.

(B) p14 protein levels are lower in p18-null cells than in p18-null cells expressing FLAG-p18 ($p18^{rev}$). Similarly, in cells that lack p14 ($p14^{-/-}$), p18 expression is reduced compared to control cells ($p14^{+/+}$). Cells were grown to confluency, lysates were prepared, and the levels of the indicated proteins analyzed by immunoblotting.

exist within cells.

Ragulator localizes the Rag proteins to the lysosomal surface and is necessary for the amino acid-dependent recruitment of mTORC1 to the same compartment

Because the Rag GTPases interact with Ragulator and given the function of p18 in localizing MP1 and p14 to lysosomes (Nada et al., 2009), it seemed possible that the Ragulator is necessary for localizing the Rag proteins to the lysosomal surface. Indeed, in cells lacking p14 or p18 (Nada et al., 2009; Teis et al., 2006), endogenous RagC was localized in small puncta throughout the cytoplasm of the cells rather than to lysosomes (Figure 3A), the morphology of which was not obviously affected by the loss of either protein. In contrast, in $p14^{+/+}$ cells or p18-null cells reconstituted with wild-type p18 ($p18^{rev}$), RagC constitutively co-localized with the LAMP2 lysosomal marker (Figure 3A). Analogous results were obtained in HEK-293T cells with an RNAi-mediated reduction in MP1 expression (Figure S4A). Consistent with the essential role of the Rag proteins in the translocation of mTORC1 to the lysosomal surface (Figure S1), in cells lacking p14 or p18 or in HEK-293T cells with p14, p18, or MP1 knockdowns, amino acids failed to induce lysosomal recruitment of mTOR, which was found throughout the cytoplasm in both amino acid starved and stimulated cells (Figures 3B, S4B, and S4D). Thus, all Ragulator subunits are required for lysosomal targeting of the Rag GTPases and mTORC1.

To determine if Ragulator is sufficient to control the intracellular localization of the Rag proteins, it was necessary to target Ragulator to a location that is distinct from the lysosomal surface. As p18 binds both p14 and MP1 and is necessary for targeting them to the lysosomal surface (Nada et al., 2009), we chose to manipulate the intracellular localization of p18. To accomplish this we generated a variant of p18, called $p18^{mito}$, which lacks its N-terminal lipidation sites but is fused at its C-terminus to the transmembrane region of OMP25, which is sufficient to target heterologous proteins to the mitochondrial surface (Nemoto and De Camilli, 1999). When expressed in p18-null cells, $p18^{mito}$ was

Figure 3

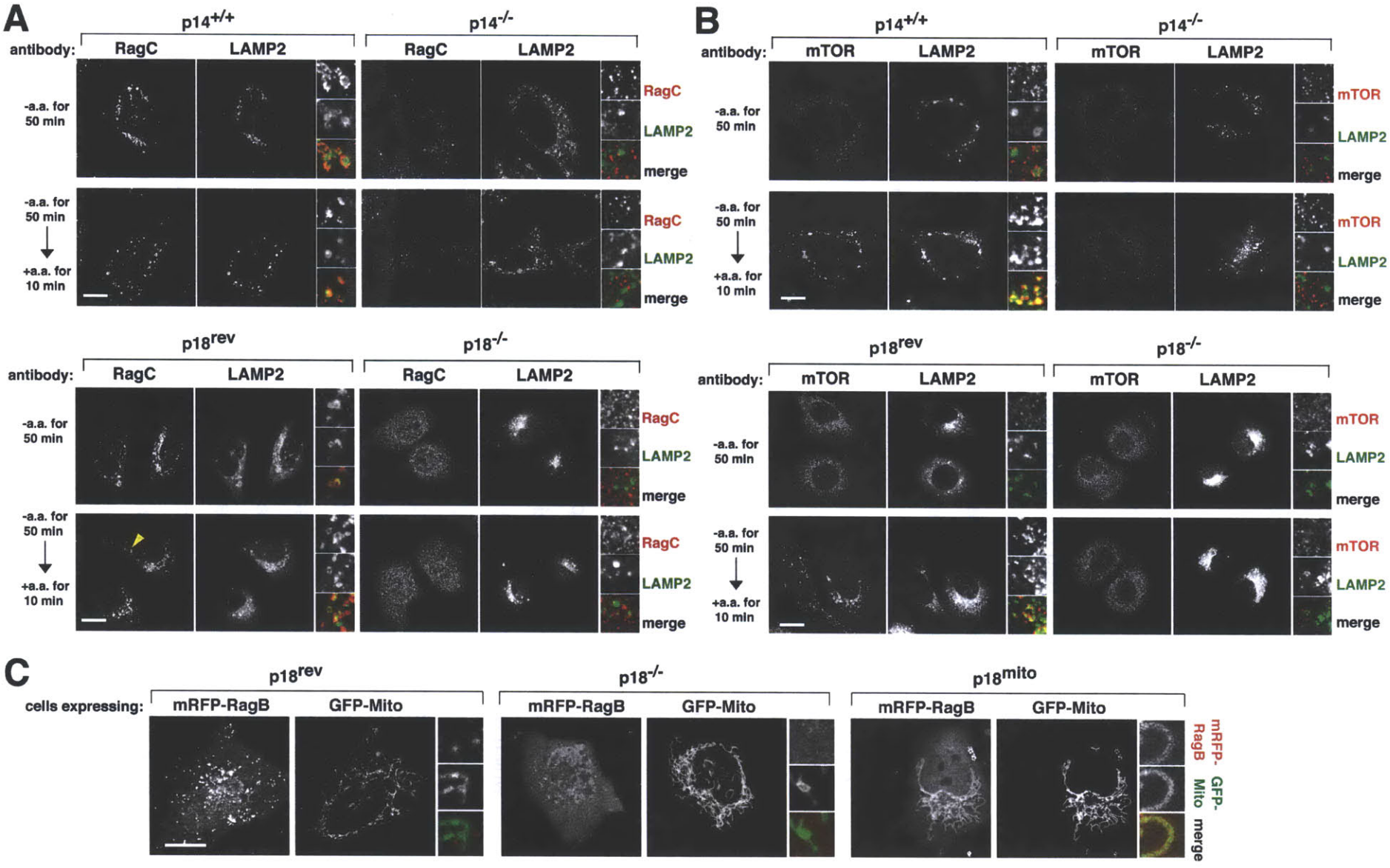
A
p14+/+
p14-/-
antibody:
RagC
LAMP2
-a.a. for 50 min
+a.a. for 10 min
RagC
LAMP2
merge
B
mTOR
p18rev
p18-/-
C
cells expressing:
mRFP-RagB
GFP-Mito
p18mito
mRFP-RagB
GFP-Mito
merge

Figure 3. The Ragulator is necessary to localize the Rag GTPases and mTORC1 to lysosomal membranes

(A) Images of p14-null or p18-null cells or their respective controls co-immunostained for RagC (red) and LAMP2 (green). Cells were starved of and restimulated with amino acids for the indicated times before processing for the immunofluorescence assay and imaging.
(B) Images of p14-null or p18-null cells or their respective controls co-immunostained for mTOR (red) and LAMP2 (green). Cells were treated and processed as in (A).
(C) Co-localization of mRFP-RagB (red) with GFP-Mito (green) in cells expressing mitochondrially-localized p18. p18-null cells ($p18^{-/-}$), or p18-null cells expressing wild type p18 ($p18^{rev}$) or mitochondrially-localized p18 ($p18^{mito}$), were transiently transfected with the indicated cDNAs in expression plasmids and imaged. In all images, insets show selected fields that were magnified five times and their overlays. Scale bar is 10 μm.

Figure S4

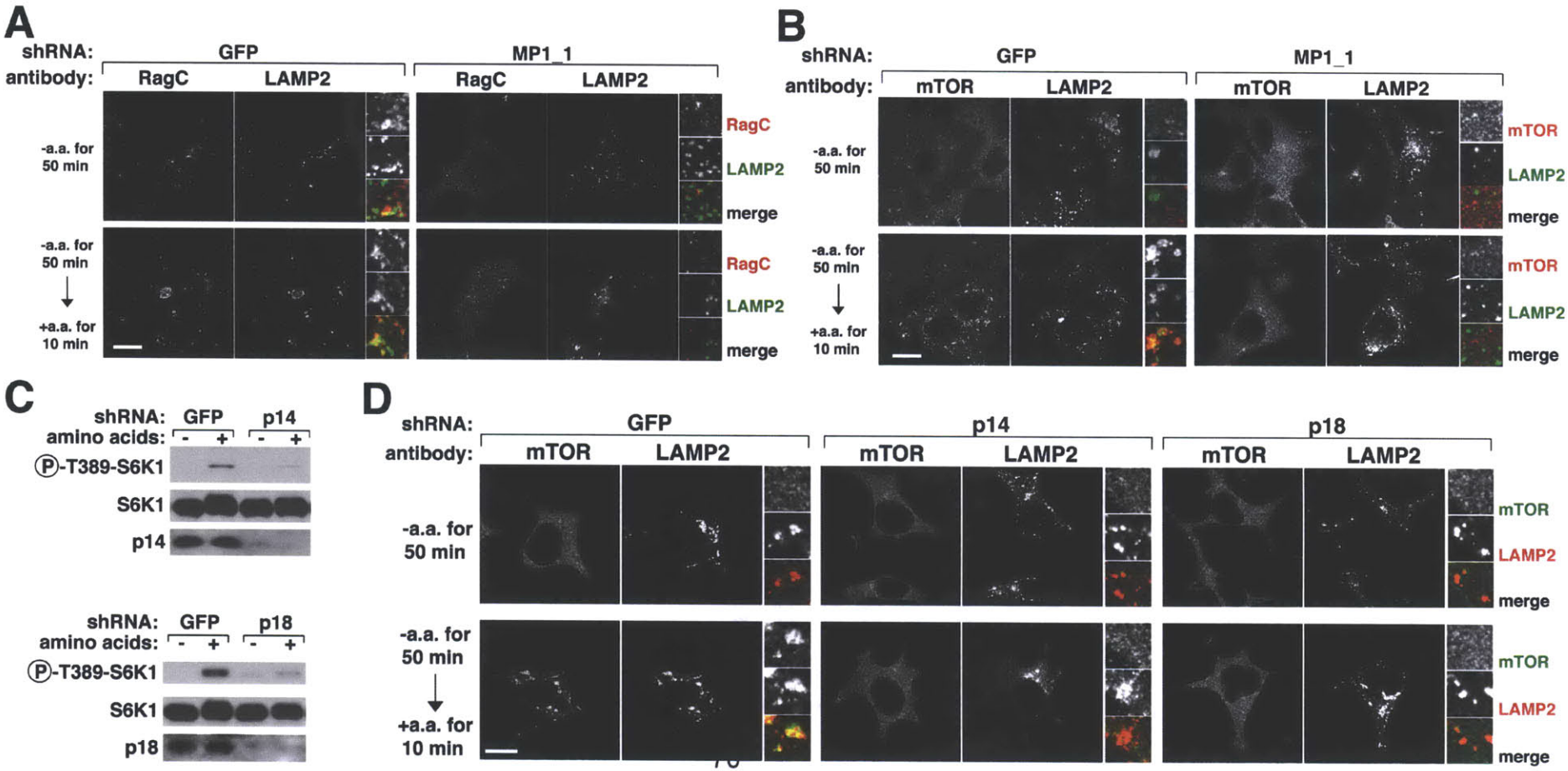
A
shRNA:
GFP
MP1_1
antibody:
RagC
LAMP2
RagC
LAMP2
-a.a. for 50 min
-a.a. for 50 min
+a.a. for 10 min
RagC
LAMP2
merge
RagC
LAMP2
merge
B
shRNA:
GFP
MP1_1
antibody:
mTOR
LAMP2
mTOR
LAMP2
-a.a. for 50 min
-a.a. for 50 min
+a.a. for 10 min
mTOR
LAMP2
merge
mTOR
LAMP2
merge
C
shRNA:
GFP
p14
amino acids:
- + - +
Ⓟ-T389-S6K1
S6K1
p14
shRNA:
GFP
p18
amino acids:
- + - +
Ⓟ-T389-S6K1
S6K1
p18
D
shRNA:
GFP
p14
p18
antibody:
mTOR
LAMP2
mTOR
LAMP2
mTOR
LAMP2
-a.a. for 50 min
-a.a. for 50 min
+a.a. for 10 min
mTOR
LAMP2
merge
mTOR
LAMP2
merge

Supplementary Figure 4, related to Figure 3. The Ragulator is required for RagC localization to lysosomal membranes and, in response to amino acids, association of mTOR with lysosomes and mTORC1 activation.

(A) An MP1 knockdown displaces RagC from the lysosomal surface. Images of cells with shRNA-mediated knockdowns of a control protein or MP1 and co-immunostained for RagC (red) and LAMP2 (green). HEK-293T cells expressing the indicated shRNAs were starved of and restimulated with amino acids for the stated times and then processed in the immunofluorescence assay.

(B) An MP1 knockdown impairs the recruitment of mTOR to the lysosomal surface in response to amino acid stimulation. Images of cells with shRNA-mediated knockdowns of a control protein or MP1 and co-immunostained for mTOR (red) and LAMP2 (green). HEK-293T cells expressing the indicated shRNAs were starved of and restimulated with amino acids for the stated times and then processed in the immunofluorescence assay.

(C) Knockdown of p18 or p14 in HEK-293T cells impair amino acid-induced mTORC1 activation. HEK-293T cells with RNAi-mediated knockdown of p14 or p18, or control cells, were starved for amino acids for 50 min or starved and restimulated with amino acid for 10 min. Cell lysates were prepared and analyzed by immunoblotting for the phosphorylation states and levels of indicated proteins.

(D) Knockdown of p18 or p14 in HEK-293T cells impairs amino acid-induced lysosomal recruitment of mTOR. Control cells and cells with p14 or p18 knockdown were treated as in (C) and immunostained for mTOR (green) and LAMP2 (red). In all images, insets show selected fields that were magnified five times and their overlays. Scale bar is 10 μm.

associated with mitochondria as verified by co-localization with the established mitochondrial protein Cytochrome c (Figure S5A). Remarkably, in the p18-null cells expressing $p18^{mito}$, RFP-tagged RagB co-localized with the mitochondrial marker GFP-mito (Figure 3C). In contrast, RFP-RagB did not co-localize with GFP-mito in p18-null cells ($p18^{-/-}$) or $p18^{rev}$ cells, and instead was present in a cytoplasmic or lysosomal pattern, respectively (Figure 3C). In cell expressing $p18^{mito}$, mTORC1 activity remained very low and mTOR was not recruited to the mitochondria (Figure S5A and S5B), likely because the mitochondrial surface does not contain the machinery necessary to load the Rag GTPases with the appropriate nucleotides. These results indicate that the location of p18 is sufficient to define that of the Rag proteins and are consistent with Ragulator serving as a constitutive docking site on lysosomes for the Rag heterodimers, which, in amino acid-replete cells, have an analogous function for mTORC1.

Ragulator is necessary for TORC1 activation by amino acids in mammalian and *Drosophila* cells

We employed the cells lacking p14 or p18 to determine if Ragulator is necessary for mTORC1 activation by amino acids. Strikingly, in both p14- and p18-null cells, but not in control cells, amino acids were incapable of activating the mTORC1 pathway as detected by the phosphorylation of S6K1 (Figures 4A and 4B) and 4E-BP1 (Figure S6A). Similarly, cells derived from patients with a homozygous mutation in the p14 gene that causes a reduction in p14 expression (Bohn et al., 2006) showed a defect in amino acid-induced mTORC1 activation compared to cells derived from a healthy donor (Figure 4E). In addition, autophagy, a process normally inhibited by mTORC1, was activated in p14-null cells, as detected by an increase compared to in control cells in the size and number of GFP-LC3-II puncta (Figure S6B). mTORC1 activity was also suppressed in HEK-293T cells with RNAi-induced reductions in p14, p18, or MP1 levels (Figures 4C and S4C). Consistent with the known requirement of amino acids and Rag function for growth factors to activate mTORC1 (Sancak et al., 2008), serum was also incapable of activating the mTORC1 pathway in cells null

Figure S5

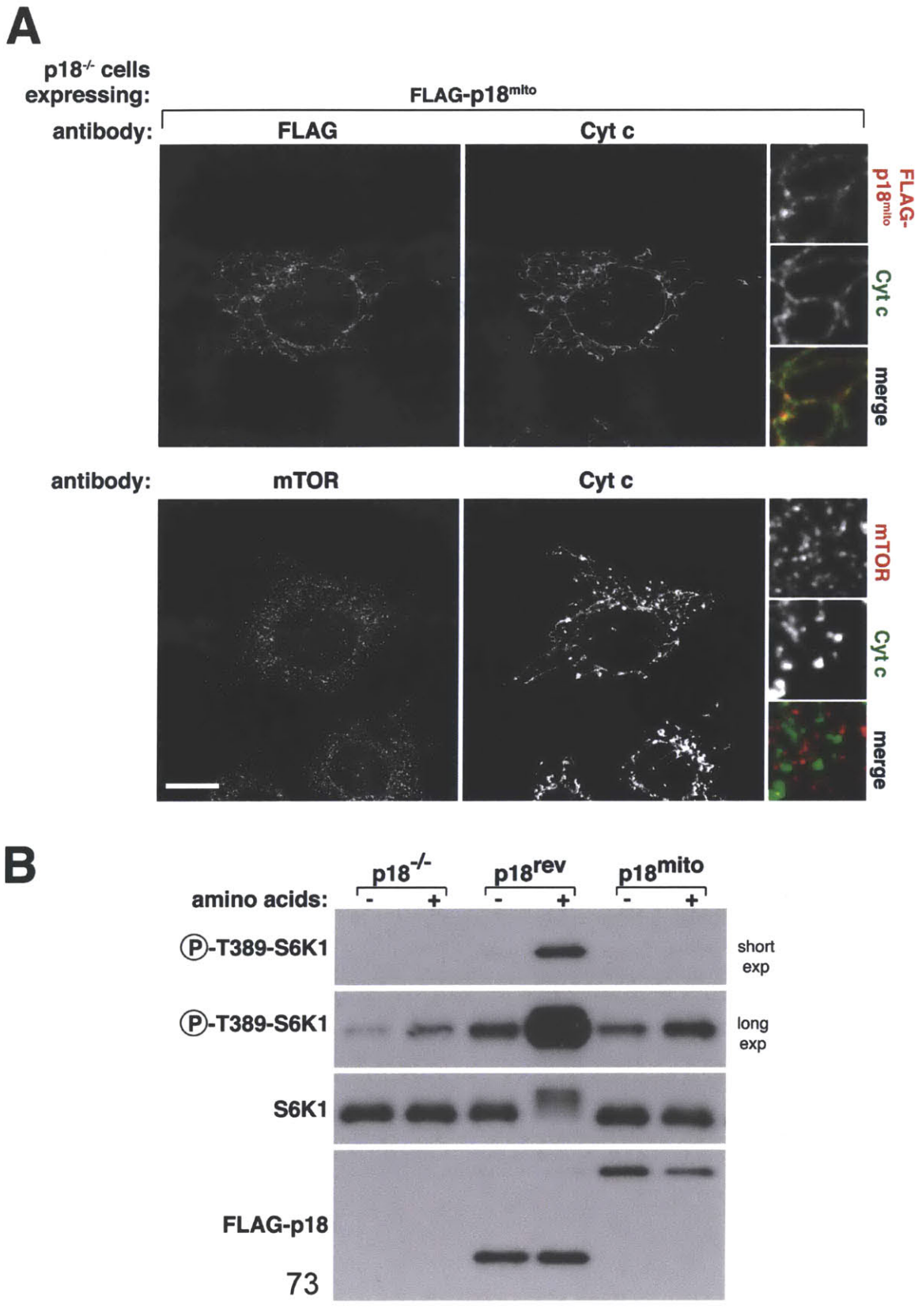
A
p18-/- cells expressing:
FLAG-p18mito
antibody:
FLAG
Cyt c
FLAG-p18mito
Cyt c
merge
antibody:
mTOR
Cyt c
mTOR
Cyt c
merge
B
p18-/-
p18rev
p18mito
amino acids:
- + - + - +
Ⓟ-T389-S6K1
short exp
Ⓟ-T389-S6K1
long exp
S6K1
FLAG-p18
73

Supplementary Figure 5, related to Figure 3. In p18-null cells mitochondrially-targeted p18 ($p18^{mito}$) localizes to mitochondria, but does not recruit mTOR to mitochondria or restore mTORC1 signaling.

(A) Images of $p18^{-/-}$ cells stably expressing FLAG-$p18^{mito}$ and co-immunostained for FLAG-$p18^{mito}$ or mTOR (red) and Cytochrome c (Cyt c) (green).

(B) The mTORC1 pathway can be activated by amino acids in p18-null cells expressing wild-type p18 ($p18^{rev}$), but not mitochondrially-targeted p18 ($p18^{mito}$). Cells were starved for amino acids in the presence of dialyzed serum for 50 min, or starved and restimulated with amino acids for 10 min. Lysates were prepared and phosphorylation states and levels of indicated proteins were analyzed by immunoblotting.

Figure 4

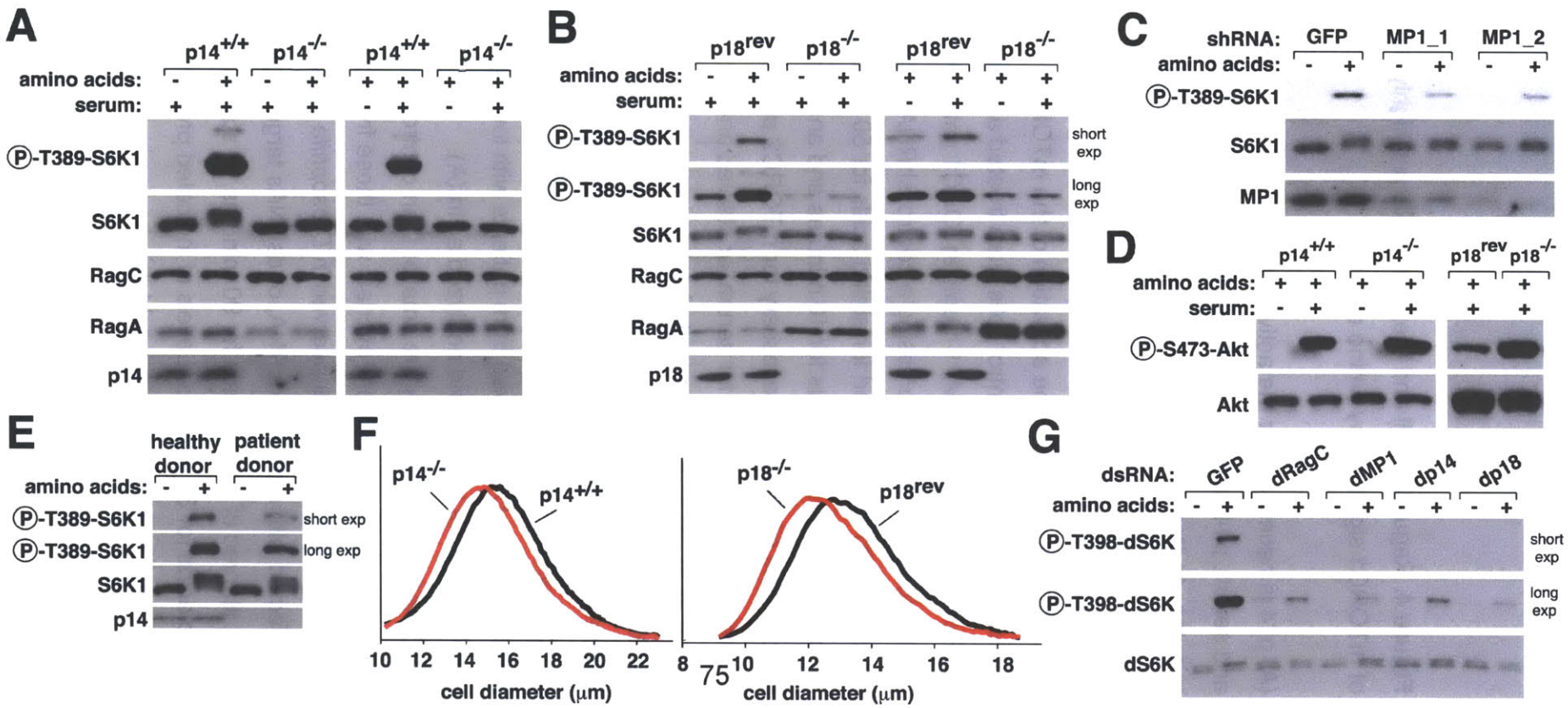
A
p14+/+
p14-/-
p14+/+
p14-/-
amino acids:
serum:
Ⓟ-T389-S6K1
S6K1
RagC
RagA
p14
B
p18rev
p18-/-
p18rev
p18-/-
amino acids:
serum:
Ⓟ-T389-S6K1
short exp
Ⓟ-T389-S6K1
long exp
S6K1
RagC
RagA
p18
C
shRNA:
GFP
MP1_1
MP1_2
amino acids:
Ⓟ-T389-S6K1
S6K1
MP1
D
p14+/+
p14-/-
p18rev
p18-/-
amino acids:
serum:
Ⓟ-S473-Akt
Akt
E
healthy donor
patient donor
amino acids:
Ⓟ-T389-S6K1
short exp
Ⓟ-T389-S6K1
long exp
S6K1
p14
F
p14-/-
p14+/+
10 12 14 16 18 20 22
cell diameter (μm)
p18-/-
p18rev
8 10 12 14 16 18
cell diameter (μm)
G
dsRNA:
GFP
dRagC
dMP1
dp14
dp18
amino acids:
Ⓟ-T398-dS6K
short exp
Ⓟ-T398-dS6K
long exp
dS6K

Figure 4. Ragulator-null and -depleted cells are highly deficient in the activation of mTORC1 signaling by amino acids.

(A) p14 is necessary for the activation of the mTORC1 pathway by amino acids and serum. p14-null or control cells were starved of amino acids or serum for 50 minutes, or starved and re-stimulated with amino acids or serum for 10 minutes. Immunoblot analyses were used to measure the levels of the indicated proteins and phosphorylation states.
(B) p18 is necessary for the activation of the mTORC1 pathway by amino acids and serum. p18-null or control cells were treated and analyzed as in (A).
(C) Partial knockdown of MP1 blunts mTORC1 pathway activation by amino acids. HEK-293T cells expressing a control shRNA or two distinct shRNAs targeting MP1 were starved for amino acids for 50 minutes, or starved and stimulated with amino acids for 10 minutes and analyzed as in (A).
(D) p14 and p18 are not necessary for mTORC2 pathway activity. p14-null or control cells were starved for serum, or starved and then re-stimulated with serum as in (A). p18-null or control cells were grown in complete media. Cell lysates were prepared and analyzed by immunobloting for the levels of Akt1 and Akt phosphorylation at the S473 site phosphorylated by mTORC2.
(E) Decreased p14 expression impairs amino acid-induced mTORC1 activation in human cells. Cells derived from patients with lower p14 expression or healthy individuals were treated and analyzed as in (A).
(F) Cells lacking Ragulator are smaller than control cells. Cell size distributions of p14-null or p18-null cells are overlaid with those from corresponding control cells.
(G) Ragulator function is conserved in *Drosophila* cells. *Drosophila* S2 cells were transfected with a control dsRNA, or dsRNAs targeting dRagC, dMP1, dp14, or dp18, starved of amino acids for 90 minutes, or starved and restimulated with amino acids for 30 minutes. Levels of indicated proteins and phosphorylation states were analyzed by immunobloting.

Figure S6

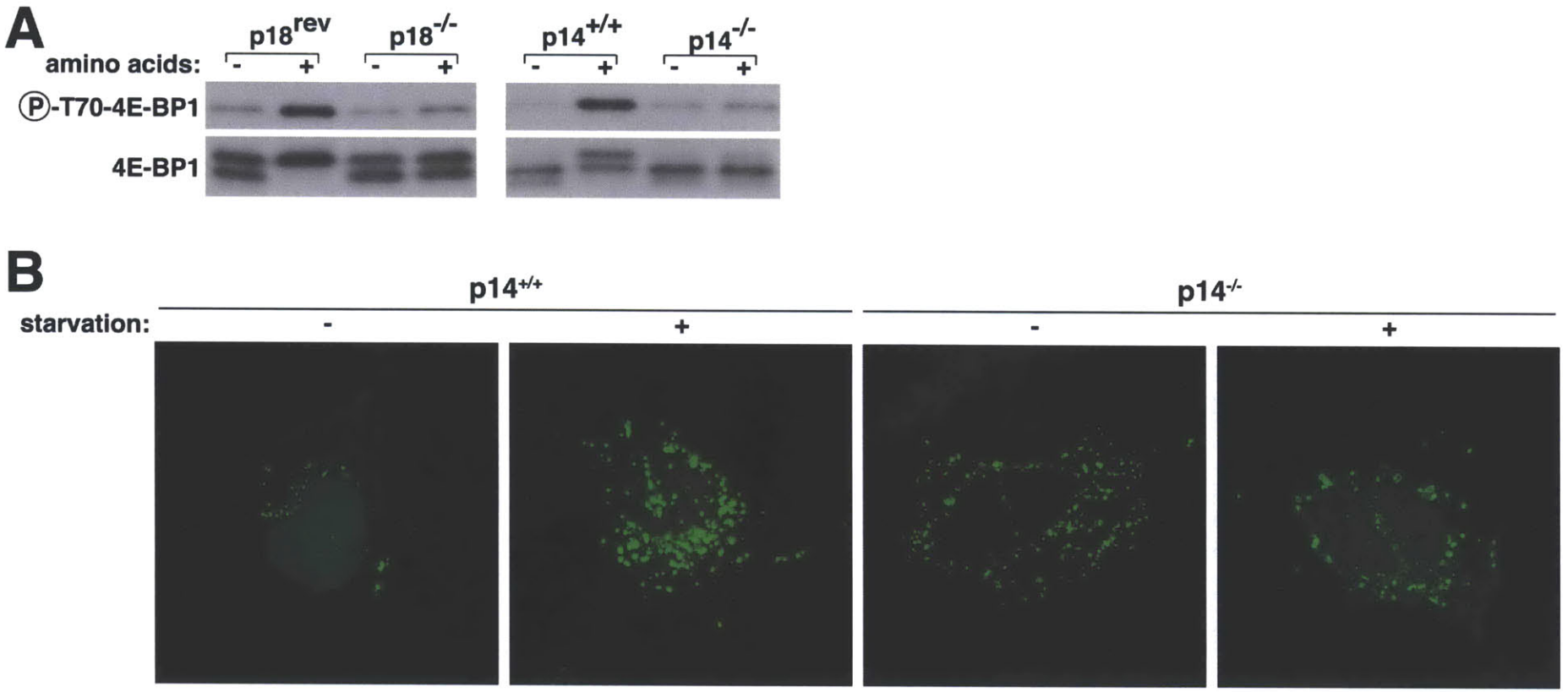
A
p18rev
p18-/-
p14+/+
p14-/-
amino acids:
- + - + - + - +
Ⓟ-T70-4E-BP1
4E-BP1
B
p14+/+
p14-/-
starvation:
- + - +

Supplementary Figure 6, related to Figure 4. 4E-BP1 phosphorylation is inhibited and autophagy is induced in cells lacking Ragulator components.

(A) Amino acids fail to stimulate 4E-BP1 phosphoryation in cells lacking p14 or p18. Cells were starved for amino acids in the presence of dialyzed serum for 50 min, or starved and restimulated with amino acids for 10 min. Lysates were prepared and 4E-BP1 phosphorylation and levels analyzed by immunoblotting.

(B) Autophagy is induced in p14-null cells. Images of cells transiently expressing GFP-LC3 and starved for amino acids and serum for 3 hours or growing in complete media. Accumulation of GFP-LC3 in large puncta in starved control cells and in the non-starved p14-null cells indicates increased levels of autophagy in these cells.

for p14 or p18 (Figures 4A and 4B). In contrast, no defect was observed in the level of S473 phosphorylation of Akt (Figure 4D). In fact, Akt phosphoylation was slightly higher in the p14-null and p18-null cells than in controls cells, which likely results from the lack of the well-appreciated inhibitory input from mTORC1 to the PI3K pathway in these cells (reviewed in (Manning, 2004)). As mTORC2 is the growth factor-regulated S473 kinase of Akt (Sarbassov et al., 2005), these results also indicate that the Ragulator does not play a detectable positive role in mTORC2 signaling. Interestingly, in the p18-null cells the expression of RagA and RagC was higher than in control cells (Figure 4B), suggesting that feedback signals in these cells may be trying to overcome the defect in mTORC1 activity by boosting Rag expression or that Ragulator also negatively controls Rag GTPase levels. Consistent with p18, p14, and MP1 forming a complex, the expression or stability of the Ragulator proteins seems to be co-regulated because in cells that lack p14, p18 protein levels are also reduced, and, similarly, in cells that lack p18, p14 protein levels are also low (Figure S3B). A well-known function of the mTORC1 pathway is the positive regulation of cell growth, so that inhibition of the pathway leads to a reduction in cell size (Fingar et al., 2002; Kim et al., 2002). Consistent with Ragulator being a positive component of the mTORC1 pathway, the p14- and p18-null cells were smaller in size than their respective controls (Figure 4F).

Many components of the TORC1 pathway, such as the Rag proteins, have conserved roles in mammalian and *Drosophila* cells (Kim et al., 2008; Sancak et al., 2008). RNAi-inducing dsRNAs that target the *Drosophila* orthologues of MP1 (CG5110), p14 (CG5189), and p18 (CG14184) were as effective at blocking amino acid-stimulated activation of dTORC1 in *Drosophila* S2 cells as dsRNAs targeting dRagC (Figure 4G). Our loss of function experiments indicate that Ragulator is a component of the TORC1 pathway that, like the Rag GTPases, is essential for amino acids to activate TORC1 signaling in mammalian and *Drosophila* cells.

Forced targeting of mTORC1 to the lysosomal surface eliminates the amino

acid sensitivity of the mTORC1 pathway

The findings we have presented so far are consistent with the amino acid-induced movement of mTORC1 to the lysosomal surface being necessary for the activation of mTORC1 by amino acids. To test if the placement of mTORC1 on lysosomal membranes is sufficient to mimic the amino acid input to mTORC1, it was necessary to force mTORC1 onto these membranes in the absence of amino acids. To accomplish this we expressed in HEK-293T cells modified raptor proteins that consist of epitope-tagged raptor fused to the intracellular targeting signals of Rheb1 or Rap1b, small GTPases that localize, in part, to the lysosomal surface (Pizon et al., 1994; Saito et al., 2005; Sancak et al., 2008). Because the targeting signals of these proteins are in their C-terminal tails, we added the last 15 or 17 amino acids of Rheb1 or Rap1b, respectively, to the C-terminus of raptor (Figure 5A). For simplicity, we refer to these fusion proteins as raptor-Rheb15 and raptor-Rap1b17. As a control we generated a raptor fusion protein that lacks the CAAX box of the Rheb1 targeting signal (raptor-Rheb15ΔCAAX) and so cannot associate with membranes (Buerger et al., 2006; Clark et al., 1997; Takahashi et al., 2005).

When expressed in cells together with myc-mTOR, raptor-Rheb15 and raptor-Rap1b17 localized to lysosomes in the presence or absence of amino acids, as judged by co-staining with LAMP2 (Figure 5B). In contrast, raptor-Rheb15ΔCAAX behaved like wild-type raptor and localized to lysosomes only upon amino acid stimulation (Figure 5B). In all cases the localization of the co-expressed myc-mTOR mirrored that of the wild-type or altered forms of raptor, indicating that C-terminal modifications of raptor do not perturb its interaction with mTOR (Figure 5C), which was confirmed in co-immunoprecipitation experiments (Figure S7A).

Remarkably, transient expression of raptor-Rheb15 or raptor-Rap1b17 in HEK-293T cells was sufficient to render the mTORC1 pathway, as judged by the phosphorylation of S6K1, resistant to amino acid starvation (Figure 6A). In contrast, the expression of wild-type raptor or raptor-Rheb15ΔCAAX did not affect the amino acid sensitivity of the pathway (Figure 6A). In HEK-293E cells,

Figure 5

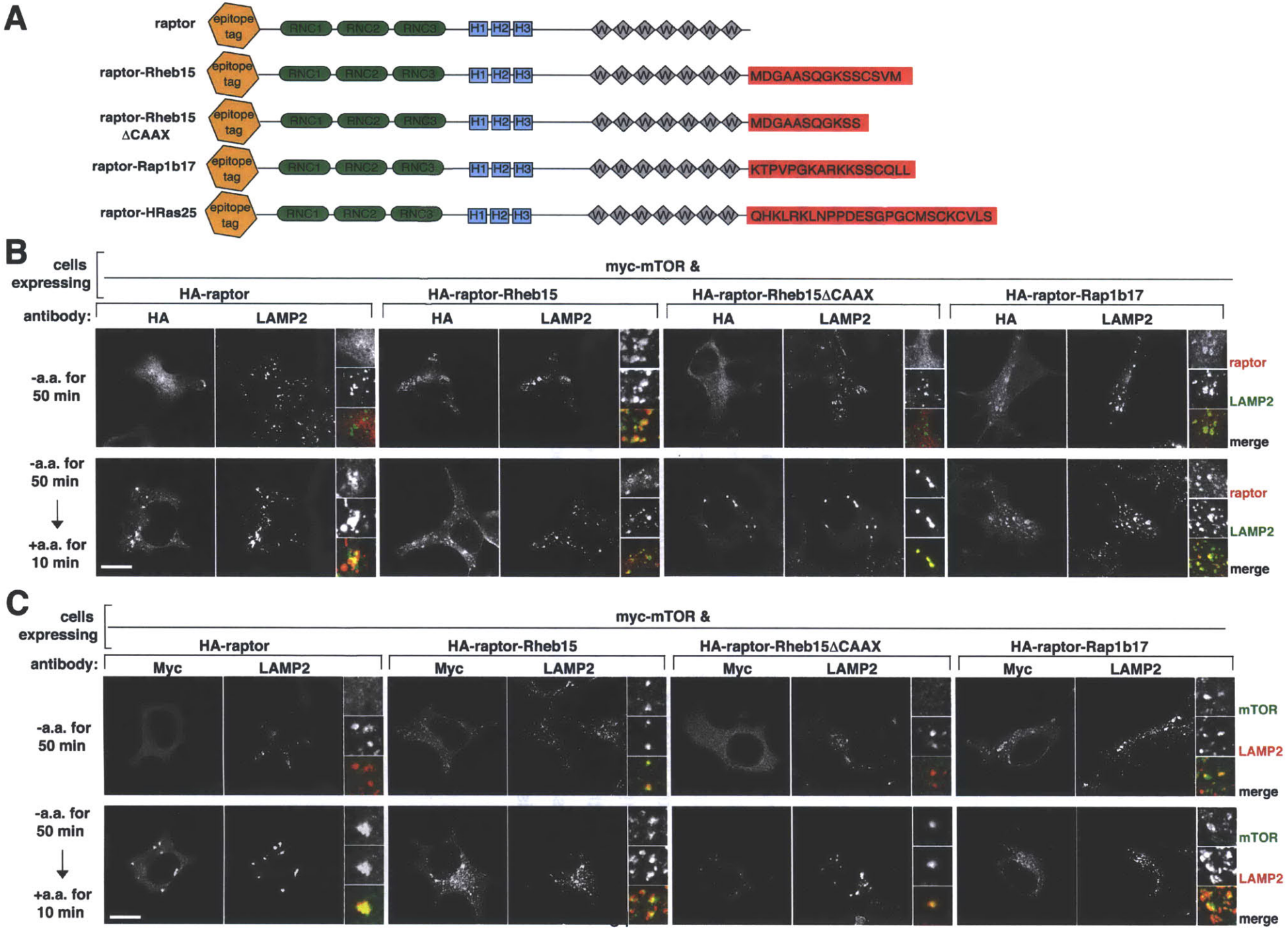
A
raptor
epitope tag
RNC1
RNC2
RNC3
H1
H2
H3
raptor-Rheb15
MDGAASQGKSSCSVM
raptor-Rheb15 ΔCAAX
MDGAASQGKSS
raptor-Rap1b17
KTPVPGKARKKSSCQLL
raptor-HRas25
QHKLRKLNPPDESGPGCMSCKCVLS
B
cells expressing
myc-mTOR &
HA-raptor
HA-raptor-Rheb15
HA-raptor-Rheb15ΔCAAX
HA-raptor-Rap1b17
antibody:
HA
LAMP2
-a.a. for 50 min
+a.a. for 10 min
raptor
LAMP2
merge
C
cells expressing
myc-mTOR &
HA-raptor
HA-raptor-Rheb15
HA-raptor-Rheb15ΔCAAX
HA-raptor-Rap1b17
antibody:
Myc
LAMP2
-a.a. for 50 min
+a.a. for 10 min
mTOR
LAMP2
merge

Figure 5. In cells expressing raptor variants fused to the targeting signals of Rheb1 or Rap1b, mTORC1 localizes to lysosomal membranes in an amino acid-independent fashion.

(A) Schematic of raptor fusion proteins that target mTORC1 to lysosomal membranes (raptor-Rheb15; raptor-Rap1b17) or to the plasma membrane (Raptor-HRas25) as well as proteins used as controls (wild-type raptor; raptor-Rheb15ΔCAAX).
(B) Images of amino acid starved or replete cells expressing lysosomally-targeted or control HA-tagged raptor proteins and co-immunostained for the HA epitope (red) and endogenous LAMP2 (green). HEK-293T cells were transfected with the indicated cDNAs, starved of and restimulated with amino acids for the indicated times, and processed in the immunofluorescence assay.
(C) Images of amino acid starved or replete cells co-expressing myc-mTOR and the indicated raptor fusion proteins and co-immunostained for the myc epitope (green) and endogenous LAMP2 (red). HEK-293T cells were co-transfected with the indicated cDNAs and treated and processed as in (B). In all images, insets show selected fields that were magnified five times and their overlays. Scale bar is 10 μm.

Figure S7

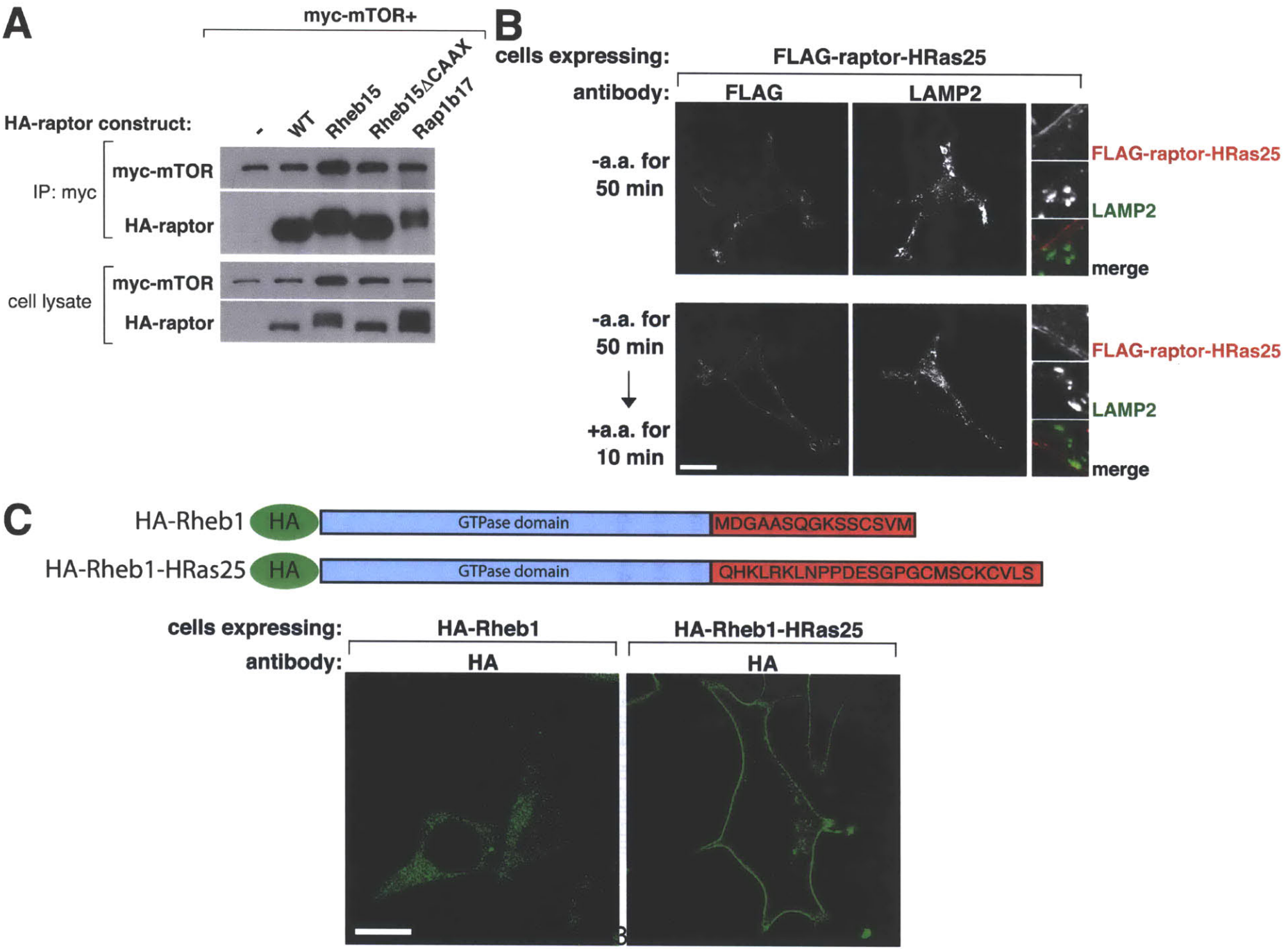
A
myc-mTOR+
HA-raptor construct:
-
WT
Rheb15
Rheb15ΔCAAX
Rap1b17
IP: myc
myc-mTOR
HA-raptor
cell lysate
myc-mTOR
HA-raptor
B
cells expressing:
FLAG-raptor-HRas25
antibody:
FLAG
LAMP2
-a.a. for 50 min
FLAG-raptor-HRas25
LAMP2
merge
-a.a. for 50 min
+a.a. for 10 min
FLAG-raptor-HRas25
LAMP2
merge
C
HA-Rheb1
HA
GTPase domain
MDGAASQGKSSCSVM
HA-Rheb1-HRas25
HA
GTPase domain
QHKLRKLNPPDESGPGCMSCKCVLS
cells expressing:
HA-Rheb1
HA-Rheb1-HRas25
antibody:
HA
HA

Supplementary Figure 7, related to Figure 7. Addition of Rheb1 and Rap1b targeting signals to raptor does not interfere with its binding to mTOR and raptor-HRas25 and Rheb-HRas25 localize to the plasma membrane.

(A) HEK-293T cells were co-transfected with plasmids encoding myc-mTOR and the indicated HA-raptor variants. Anti-myc immunoprecipitates as well as lysates were analyzed by immunobloting for the indicated proteins.

(B) Raptor fused at its C-terminus with the localization signal of HRas localizes to the plasma membrane. Images of cells expressing FLAG-raptor-HRas25 and starved of and restimulated with amino acid for the indicated times and co-immunostained with antibodies to the FLAG epitope (red) and endogenous LAMP2 (green).

(C) Rheb1 localizes to the plasma membrane when its localization signal is swapped for that of HRas. Schematic shows composition of the HA-Rheb1-HRas25 variant. Images of cells expressing HA-Rheb1 or HA-Rheb1-HRas25 (green).

Figure 6

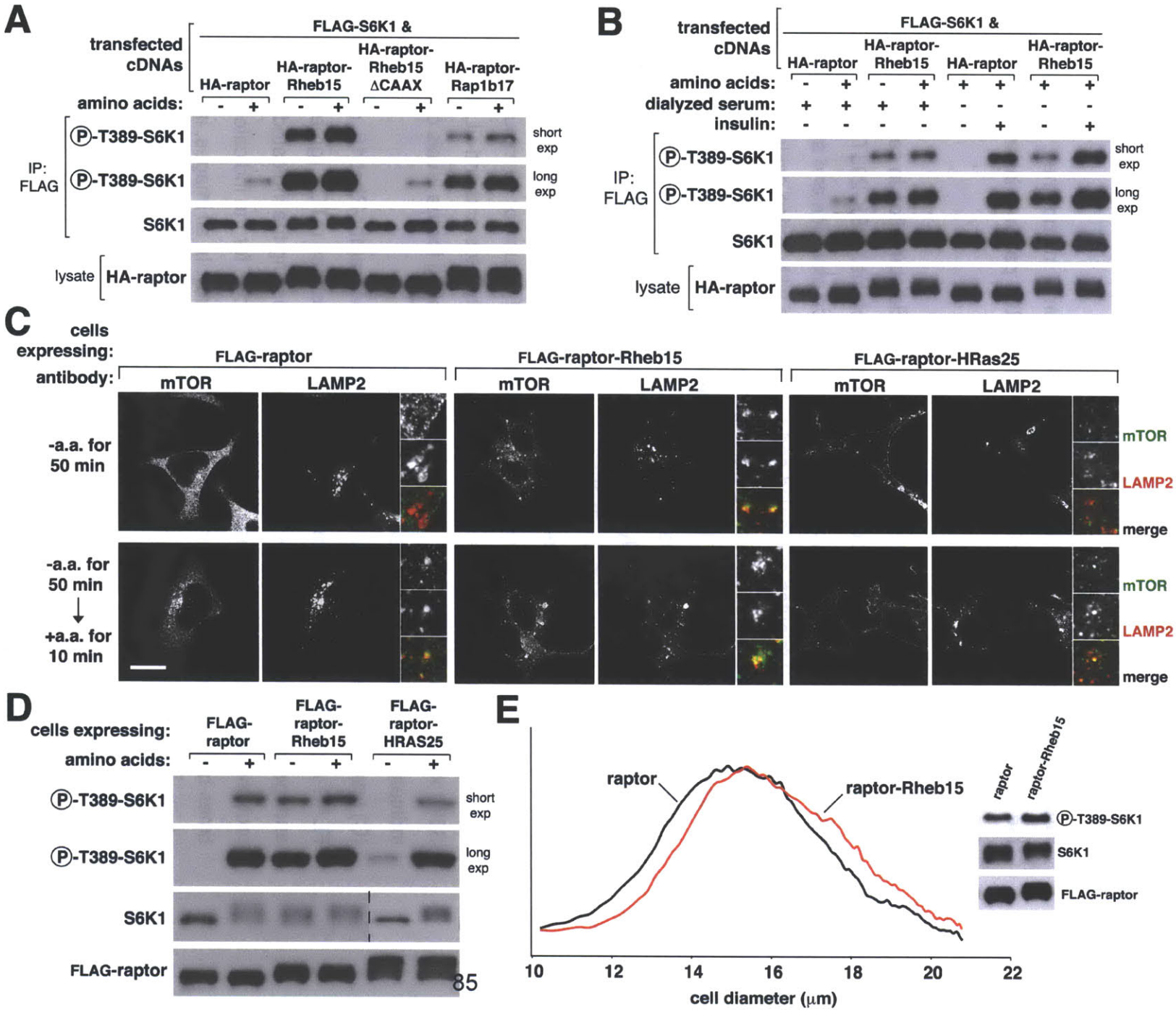
A
transfected cDNAs
FLAG-S6K1 &
HA-raptor
HA-raptor-Rheb15
HA-raptor-Rheb15 ΔCAAX
HA-raptor-Rap1b17
amino acids:
IP: FLAG
Ⓟ-T389-S6K1
short exp
Ⓟ-T389-S6K1
long exp
S6K1
lysate
HA-raptor
B
transfected cDNAs
FLAG-S6K1 &
HA-raptor
HA-raptor-Rheb15
HA-raptor
HA-raptor-Rheb15
amino acids:
dialyzed serum:
insulin:
IP: FLAG
Ⓟ-T389-S6K1
short exp
Ⓟ-T389-S6K1
long exp
S6K1
lysate
HA-raptor
C
cells expressing:
FLAG-raptor
FLAG-raptor-Rheb15
FLAG-raptor-HRas25
antibody:
mTOR
LAMP2
-a.a. for 50 min
-a.a. for 50 min
+a.a. for 10 min
mTOR
LAMP2
merge
D
cells expressing:
FLAG-raptor
FLAG-raptor-Rheb15
FLAG-raptor-HRAS25
amino acids:
Ⓟ-T389-S6K1
short exp
Ⓟ-T389-S6K1
long exp
S6K1
FLAG-raptor
E
raptor
raptor-Rheb15
10
12
14
16
18
20
22
cell diameter (μm)
raptor
raptor-Rheb15
Ⓟ-T389-S6K1
S6K1
FLAG-raptor

Figure 6. Constitutive association of raptor with lysosomal membranes, but not the plasma membrane, is sufficient to make the mTORC1 pathway insensitive to amino acid starvation.

(A) The mTORC1 pathway is not sensitive to amino acid starvation in cells that express lysosomally-targeted but not control raptor proteins. HEK-293T cells were co-transfected with the indicated cDNA expression plasmids and starved of amino acids for 50 minutes or starved and restimulated with amino acids for 10 minutes. Cell lysates and anti-FLAG-S6K1 immunoprecipitates were analyzed by immunobloting for the levels of the indicated proteins and phosphorylation states.
(B) The mTORC1 pathway is sensitive to serum starvation and insulin stimulation in cells that express lysosomally-targeted as well as control raptor proteins. HEK-293E cells were co-transfected with the indicated cDNA expression plasmids, starved of amino acids for 50 minutes or starved and restimulated with amino acids for 10 minutes. Duplicate cultures were starved of serum for 50 minutes or starved and stimulated with insulin for 10 minutes. Cell lysates and anti-FLAG-S6K1 immunoprecipitates were analyzed by immunobloting for the levels of the indicated proteins and phosphorylation states.
(C) Images of cells stably expressing FLAG-raptor, FLAG-raptor-Rheb15, or FLAG-raptor-HRas25 and co-immunostained for endogenous mTOR (green) and endogenous LAMP2 (red). HEK-293T cells stably expressing the indicated proteins were starved of and restimulated with amino acids for the indicated times before processing in the immunofluorescence assay. In all images, insets show selected fields that were magnified five times and their overlays. Scale bar is 10 μm.
(D) Targeting of mTORC1 to the lysosomal but not the plasma membrane makes the mTORC1 pathway insensitive to amino acid starvation. HEK-293T cells stably expressing FLAG-raptor, FLAG-raptor-Rheb15, or FLAG-raptor-HRas25 were starved of and restimulated with amino acids as in (C) and analyzed by immunoblotting for the levels of the indicated proteins and phosphorylation states.

(E) Targeting of mTORC1 to the lysosomal membrane increases cell size and pathway activity in cells under normal growth conditions. Cell size distributions of cells that stably express FLAG-raptor or FLAG-raptor-rheb15 as well as immunoblot analyses of the mTORC1 pathway in the same cells.

the expression of raptor-Rheb15 made S6K1 phosphorylation insensitive to amino acid starvation, but did not affect its regulation by insulin (Figure 6B). Thus, lysosomal targeting of mTORC1 can substitute for the amino acid, but not growth factor, input to mTORC1. This is consistent with previous work showing that growth factors signal to mTORC1 in large part through the TSC1-TSC2-Rheb axis (Dan et al., 2002; Gao and Pan, 2001; Garami et al., 2003; Inoki et al., 2002; Ma et al., 2005; Manning et al., 2002; Potter et al., 2001; Potter et al., 2002), and not through the Rag GTPases (Sancak et al., 2008).

To verify the effects of lysosomally-targeted mTORC1 in a more physiological setting than that achieved by transient cDNA expression, we generated HEK-293T cell lines stably expressing FLAG-tagged raptor-Rheb15 or wild-type raptor. In cells expressing the lysosomally-targeted but not wild-type raptor, mTOR was always associated with lysosomes, irrespective of amino acids (Figure 6C). As with the transient expression of raptor-Rheb15, its stable expression rendered the mTORC1 pathway fully resistant to amino acid starvation (Figure 6D). Furthermore, under normal growth conditions these cells had an increase in mTORC1 activity and were larger than controls (Figure 6E).

We next examined if the targeting of mTORC1 to membranes other than lysosomal membranes could also eliminate the amino acid sensitivity of the mTORC1 pathway. This was not the case because although the stable expression of a raptor variant consisting of raptor fused to the last 25 amino acids of H-Ras (raptor-HRas25) (Figures 5A and S7B) was sufficient to target a fraction of cellular mTOR to the plasma membrane (Figure 6C), it did not render the mTORC1 pathway resistant to amino acid starvation (Figure 6D).

Forced targeting of mTORC1 to the lysosomal surface eliminates the requirement in mTORC1 signaling for Rag and Ragulator, but not Rheb, function

The ability to constitutively localize mTORC1 to lysosomal membranes enabled us to probe in more detail the role of the Rag and Rheb GTPases, as well as Ragulator, in the activation of mTORC1 by amino acids. We hypothesized

that if the major role of the Rag GTPases is to allow mTORC1 to localize to lysosomes, then in cells that express raptor-Rheb15, mTORC1 activity should be independent of Rag function. Indeed, while in control cells the RNAi-mediated knockdown of both RagA and RagB strongly blunted the activation of mTORC1 by amino acids, it did not reduce the amino acid-insensitive mTORC1 activity observed in raptor-Rheb15 expressing cells (Figure 7A). As an additional approach to inhibit Rag function, we exploited the fact that co-expression of a GDP-bound RagB mutant ($RagB^{GDP}$) and a GTP-bound RagD mutant ($RagD^{GTP}$) eliminates mTORC1 pathway activity within cells (Kim et al., 2008; Sancak et al., 2008). Expression of $RagB^{GDP}$-$RagD^{GTP}$ completely prevented mTORC1 activation by amino acids in control cells, but had no effect on the amino acid-insensitive mTORC1 activity of cells expressing raptor-Rheb15 (Figure 7B).

If the main function of Ragulator in the mTORC1 pathway is to localize the Rag GTPases to the lysosomes then it should be possible to reactivate the mTORC1 pathway in Ragulator-null cells by expressing raptor-Rheb15. Remarkably, the stable expression of raptor-Rheb15, but not wild-type raptor, in p14- or p18-null cells reactivated mTORC1 signaling and made it insensitive to amino acid deprivation (Figure 7C and 7D). Furthermore, expression of raptor-Rheb15 in the p18-null cells was sufficient to increase their size (Figure 7E). In contrast to the results observed with the Rag GTPases and Ragulator, RNAi-mediated suppression of Rheb1 blocked amino acid-induced mTORC1 activation in cells expressing raptor-Rheb15 to the same extent as it did in control cells (Figure 7F).

To test whether the presence of mTORC1 and Rheb on the same membrane compartment is sufficient to render the mTORC1 pathway insensitive to amino acid levels, we generated cells in which mTORC1 and Rheb are both present on the plasma membrane. To accomplish this we prepared a Rheb1 variant, called Rheb1-HRas25, that localizes to the plasma-membrane (Figure S7C) because it contains the C-terminal 25 amino acids of H-Ras instead of the normal Rheb1 localization signal. When Rheb1-HRas25 was stably co-expressed with raptor-HRas25, but not wild-type raptor, the mTORC1 pathway became

insensitive to amino acid starvation (Figure 7G). Importantly, mTORC1 signaling remained amino acid-sensitive in cells in which either Rheb or mTORC1, but not both, was targeted to the plasma membrane (Figure 7G).

Figure 7

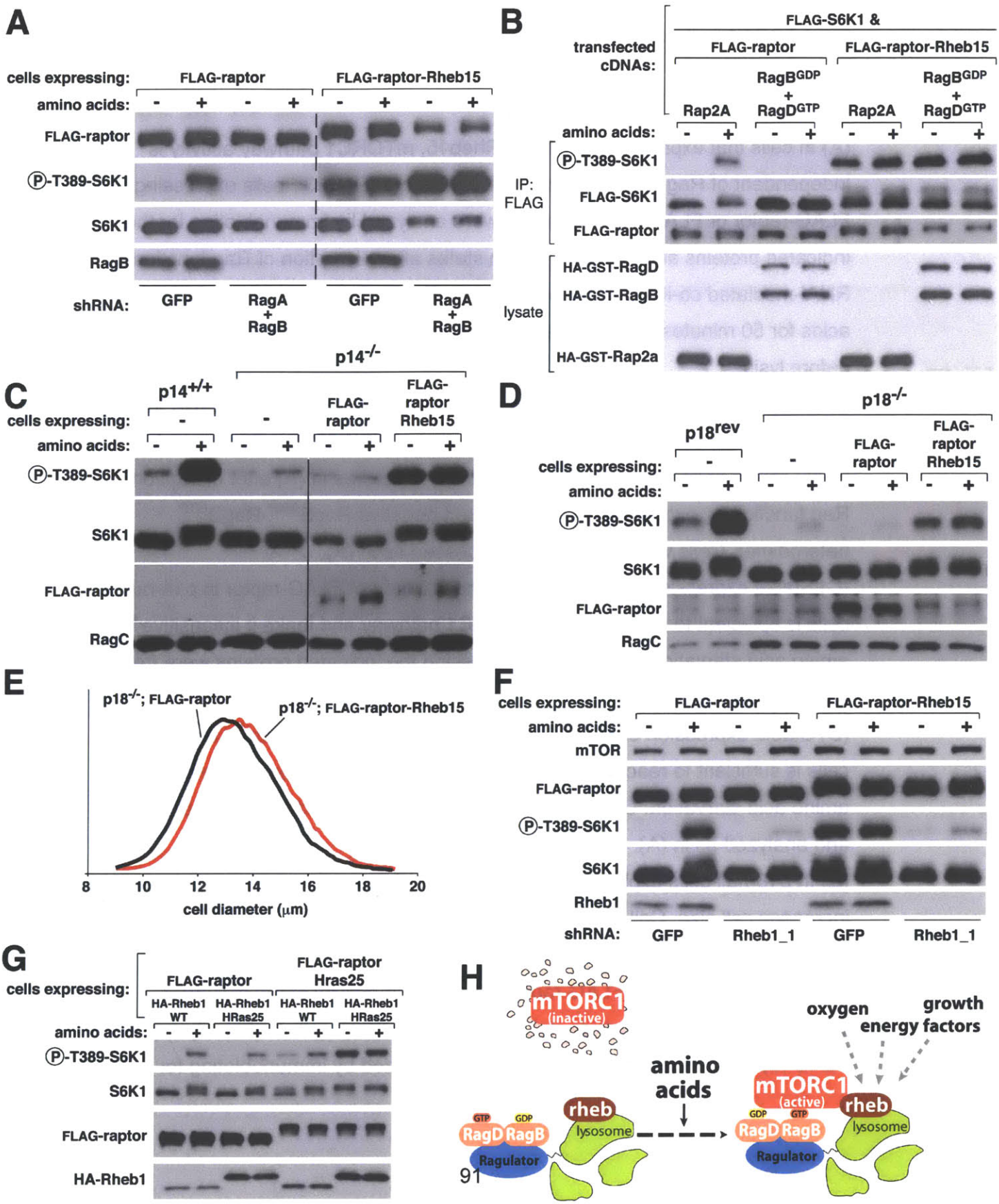
A
cells expressing:
FLAG-raptor
FLAG-raptor-Rheb15
amino acids:
FLAG-raptor
Ⓟ-T389-S6K1
S6K1
RagB
shRNA:
GFP
RagA + RagB
B
transfected cDNAs:
FLAG-S6K1 &
FLAG-raptor
FLAG-raptor-Rheb15
Rap2A
RagB^GDP + RagD^GTP
amino acids:
IP: FLAG
Ⓟ-T389-S6K1
FLAG-S6K1
FLAG-raptor
lysate
HA-GST-RagD
HA-GST-RagB
HA-GST-Rap2a
C
p14+/+
p14-/-
FLAG-raptor
FLAG-raptor Rheb15
cells expressing:
amino acids:
Ⓟ-T389-S6K1
S6K1
FLAG-raptor
RagC
D
p18rev
p18-/-
cells expressing:
amino acids:
Ⓟ-T389-S6K1
S6K1
FLAG-raptor
RagC
E
p18-/-; FLAG-raptor
p18-/-; FLAG-raptor-Rheb15
8
10
12
14
16
18
20
cell diameter (μm)
F
cells expressing:
FLAG-raptor
FLAG-raptor-Rheb15
amino acids:
mTOR
FLAG-raptor
Ⓟ-T389-S6K1
S6K1
Rheb1
shRNA:
GFP
Rheb1_1
G
cells expressing:
FLAG-raptor
FLAG-raptor Hras25
HA-Rheb1 WT
HA-Rheb1 HRas25
amino acids:
Ⓟ-T389-S6K1
S6K1
FLAG-raptor
HA-Rheb1
H
mTORC1 (inactive)
oxygen
growth factors
energy
amino acids
mTORC1 (active)
rheb
lysosome
GTP
GDP
RagD
RagB
Ragulator

Figure 7. Targeting of mTORC1 to the lysosomal surface makes the activity of the mTORC1 pathway independent of Rag and Ragulator, but not, Rheb function.

(A) In cells that express FLAG-raptor-Rheb15, mTORC1 pathway activity is independent of Rag GTPase function. Lysates of HEK-293T cells expressing FLAG-raptor or FLAG-raptor-Rheb15 were analyzed by immunobloting for the indicated proteins and phosphorylation states after disruption of Rag function by RNAi-mediated co-knockdown of RagA and RagB. Cells were starved of amino acids for 50 minutes or starved and restimulated with amino acids for 10 minutes before lysis.
(B) In cells that express FLAG-raptor-Rheb15, mTORC1 pathway activity is independent of Rag GTPase function. Lysates of HEK-293T cells expressing FLAG-raptor or FLAG-raptor-Rheb15 were analyzed as in (A) after disruption of Rag function by expression of the dominant negative $RagB^{GDP}$-$RagD^{GTP}$ heterodimer. Cells were treated and processed as in (A).
(C) Stable expression of FLAG-raptor-Rheb15 but not FLAG-raptor in p14-null cells is sufficient to reactivate the mTORC1 pathway and make it insensitive to amino acid starvation. Cells stably expressing the indicated proteins were treated and analyzed as in (A).
(D) Stable expression of FLAG-raptor-Rheb15 but not FLAG-raptor in p18-null cells is sufficient to reactivate the mTORC1 pathway and make it insensitive to amino acid starvation. Cells stably expressing the indicated proteins were treated and analyzed as in (A).
(E) In p18-null cells expression of raptor-Rheb15, but not wild-type raptor, increases cell size. Cell size distributions of p18-null cells that stably express FLAG-raptor or FLAG-raptor-Rheb15.
(F) In cells that express FLAG-raptor-Rheb15, the activity of the mTORC1 pathway is still Rheb-dependent. Lysates of HEK-293T cells that stably express FLAG-raptor or FLAG-raptor-Rheb15 were analyzed by immunobloting for the

indicated proteins and phosphorylation states after disruption of Rheb function by an RNAi-mediated knockdown of Rheb1. Cells were treated as in (A).
(G) Co-expression of plasma membrane-targeted raptor and plasma membrane-targeted Rheb1 renders the mTORC1 pathway insensitive to amino acid starvation. HEK-293T cells stably expressing the indicated proteins were treated and analyzed as in (A).
(H) Model for amino-acid induced mTORC1 activation. In the absence of amino acids, mTORC1 cannot associate with the endomembrane system, and has no access to its activator Rheb. In the presence of amino acids, the Rag GTPases, which are tethered to the lysosomal surface by the Ragulator, serve as a docking site for mTORC1, allowing mTORC1 to associate with endomembranes and thus encounter and become activated by Rheb.

Discussion

Our findings, together with previous work showing that Rheb is required for amino acids to activate the mTORC1 pathway (Avruch et al., 2006; Nobukuni et al., 2005; Sancak et al., 2008; Saucedo et al., 2003; Tee et al., 2005; Tee et al., 2003) and can localize to late endosomes/lysosomes (Saito et al., 2005; Sancak et al., 2008), is consistent with a model in which amino acids induce mTORC1 to associate with the endomembrane system of the cell and thus allow it to encounter its activator Rheb. In this model the essential role of the Ragulator-Rag complex is to serve as an amino acid-regulated docking site for mTORC1 on lysosomal membranes (see schematic in Figure 7H). The proposed link between the Rag and Rheb GTPases in the regulation of the mTORC1 pathway provides an explanation for why activation of mTORC1 occurs only when activators of both Rheb (e.g., growth factors and energy) and the Rags (i.e., amino acids) are available. For technical reasons (Buerger et al., 2006; Sancak et al., 2008), it has not been possible to determine the intracellular localization of endogenous Rheb and work using overexpressed GFP-tagged Rheb1 has placed it on various endomembrane compartments, including endosomes and lysosomes (Buerger et al., 2006; Saito et al., 2005; Sancak et al., 2008; Takahashi et al., 2005). Our results suggests that at some point in its life cycle Rheb must traverse the lysosomal surface in order to encounter mTORC1 and so in our model we have chosen to place Rheb on this compartment (Figure 7H). However, at any given time only a small fraction of cellular Rheb may actually be on the lysosomal surface or, alternatively, some of the mTORC1 within the cell may move to a non-lysosomal endomembrane compartment that also contains Rheb. These issues will only be answered once a definitive location for endogenous Rheb can be determined.

The trimeric p14, p18, and MP1 protein complex, which we call Ragulator, is a Rag-interacting complex that is essential for amino acid signaling to mTORC1 and represents an additional critical component of the TORC1 signaling pathway in mammals and flies. p18 directly interacts with the Rag

GTPases (Figure S3A) as well as with p14 and MP1 (Nada et al., 2009) and so may serve as a scaffold to bring the Rag GTPases and MP1-p14 next to each other. In vitro we have not detected a direct interaction between the Rag GTPases and either MP1 or p14, but both proteins are, like p18, necessary for localizing the Rag GTPases to the lysosomal surface. p14 is required to maintain normal p18 expression levels (Figure S3B), suggesting that within cells p14 and MP1 form a crucial part of the Ragulator structure. Given the non-specific nature of the p14 and p18 names, in the future it may be best to rename these proteins, perhaps to names that reflect their essential roles in the mTORC1 pathway.

The location of the Rag GTPases, the Ragulator, and mTORC1 on the lysosomal surface implicates this organelle as the site of a yet to be discovered sensing system that signals amino acid availability to the Ragulator-Rag complex. The lysosomal location of the amino acid sensing branch of the mTORC1 pathway is consistent with increasing evidence that lysosomes, and their yeast counterparts, vacuoles, are at the nexus of amino acid metabolism within cells. Lysosomes are a major site of protein degradation and amino acid recycling and vacuoles store amino acids at high concentrations (reviewed in (Li and Kane, 2009)). Thus, mTORC1 and its regulators may reside on the lysosomal surface so as to sense a currently unknown aspect of lysosomal function that reflects the intracellular pools of amino acids.

It is interesting to consider the differences and similarities between the still poorly understood amino acid signaling mechanisms employed by the mTORC1 and yeast TORC1 pathways. Consistent with previous work in mammalian cells (Sancak et al., 2008), the Gtr1p-Gtr2p heterodimer that is orthologous to RagA/B-RagC/D, interacts with yeast TORC1 when Gtr1p is GTP-loaded (Binda et al., 2009). TORC1 and the Gtr proteins are located on the surface of the vacuole (Berchtold and Walther, 2009; Binda et al., 2009), the yeast equivalent of lysosomes, but, unlike in mammals, yeast TORC1 does not leave the vacuolar surface upon amino acid deprivation although amino acids do control the interaction of TORC1 with Gtr1p-Gtr2p (Binda et al., 2009). This finding suggests that there must exist a distinct mechanism for retaining TORC1

at the vacuolar surface and that in yeast the interaction between TORC1 and Gtr1p-Gtr2p serves other purposes besides controlling the intracellular location of TORC1. In contrast, our current work argues that in mammals the main role of the Rag GTPase and the associated Ragulator complex is to control the association of mTORC1 with the cellular endomembrane system, in particular, lysosomes. Rheb, which is essential for the activation of mTORC1 by all upstream signals (Avruch et al., 2006; Nobukuni et al., 2005; Sancak et al., 2008; Saucedo et al., 2003; Tee et al., 2005; Tee et al., 2003), does not appear to be part of the TORC1 pathway in yeast (reviewed in (Berchtold and Walther, 2009)). As we suggest that the Rag-dependent and amino acid-regulated translocation of mTORC1 to the lysosomal surface may ultimately be a mechanism for controlling the access of mTORC1 to Rheb, the absence of Rheb in the yeast TORC1 pathway may make regulation of TORC1 localization unnecessary. That known Rag- and Gtr-interacting proteins share no sequence homology also suggests that the mechanisms through which the Rag and Gtr GTPases regulate mTORC1 and yeast TORC1, respectively, have diverged. Although it is clear that the Ragulator and EGO complexes both control the intracellular localization of the Rag (this paper) and Gtr (Gao and Kaiser, 2006) GTPases, respectively, whether these complexes have additional functions remains to be determined.

Previous studies suggest that MP1-p14-p18 complex plays an adaptor role in the MAP Kinase (MAPK) pathway (reviewed in (Dard and Matthias, 2006)) and our current findings do not contradict these results. However, considering the very strong inhibition of the mTORC1 pathway that occurs in cells lacking p14 or p18, it seems possible that some of the impairment in MAPK signaling observed in those cells reflects an altered feedback signaling from Akt to the MAPK pathway. For example, in Ragulator-null cells, Akt is slightly activated, almost certainly because the well-known inhibitory signal from mTORC1 to PI3K is absent. As Akt suppresses MAPK signaling by phosphorylating and inhibiting Raf (Zimmermann and Moelling, 1999), it is conceivable that the activation of Akt that occurs in Ragulator-null cells could account, at least in part, for the inhibition of MAPK signaling that has been observed in these cells.

Mice lacking either p14 or p18 die around embryonic day 7.5-8 and have obvious growth defects (Nada et al., 2009; Teis et al., 2006). We would not be surprised if, when generated, mice lacking the Rag proteins die at around the same age and present similar defects. On the other hand, mice lacking the core mTORC1 component raptor die earlier (before embryonic day 6.5) than p14- and p18-null mice (Guertin et al., 2006). This may be expected because although loss of p14 or p18 completely blocks mTORC1 activation by amino acids, cells lacking the Ragulator proteins are likely to retain a low residual level of mTORC1 activity that may be sufficient to support development further than in embryos completely lacking mTORC1 function. Lastly, our results suggest that the strong growth retardation observed in humans with a mutation that reduces p14 expression (Bohn et al., 2006), is a result of partial suppression of the mTORC1 pathway. If this turns out to be the case, it would represent the first human example of a loss of function mutation in a positive component of the mTORC1 pathway.

Materials and Methods

Cell Lines and Tissue Culture

HEK-293E cells; HEK-293T cells; $TSC2^{+/+}$, $TSC2^{-/-}$, $p14^{+/+}$, and $p14^{-/-}$ MEFs were cultured in DMEM with 10% IFS. $p18^{rev}$, $p18^{mito}$, and $p18^{-/-}$ cells were cultured in DMEM with 10% FBS. HEK-293E and HEK-293T cells express E1a and SV40 large T antigen, respectively. In HEK-293E, but not HEK-293T, cells the mTORC1 pathway is strongly regulated by serum and insulin (Sancak et al., 2007). $TSC2^{-/-}$, $p53^{-/-}$ and $TSC2^{+/+}$, $p53^{-/-}$ MEFs were kindly provided by Dr. David Kwiatkowski (Harvard Medical School). The HEK-293E cell line was kindly provided by Dr. John Blenis (Harvard Medical School). $p14^{-/-}$ and control MEFs were kindly provided by Dr. Lukas A. Huber (Innsbruck Medical University) and described in (Teis et al., 2006). $p18^{-/-}$ cells are epithelial in nature and $p18^{rev}$ cells are $p18^{-/-}$ cells in which wild-type p18 has been re-expressed (Nada et al., 2009). Patient-derived cells with a homozygous mutation in the p14 gene and control healthy donor-derived cells were kindly provided by Dr. Christoph Klein (Universität München) and have been described in (Bohn et al., 2006)

Amino Acid and Serum Starvation and Stimulation of Cells

Serum and/or amino acid starvation of HEK-293T cells, HEK-293E cells, p14-null and control cells, p18-null and control cells, MEFs, patient-derived and healthy donor-derived cells were performed essentially as described (Sancak et al., 2008). Serum was dialyzed against PBS in dialysis cassettes (Thermo Scientific) having a 3,500 molecular weight cut off.

Preparation of Cell Lysates and Immunoprecipitations

Cell lysate preparation, cell lysis and immunoprecipitations were done as described (Sancak et al., 2008).

For co-transfection experiments, 2 million HEK-293T or HEK-293E cells were plated in 10 cm culture dishes. 24 hours later, cells were transfected with the indicated plasmids as follows: 50 ng or 1500 ng myc-mTOR in pRK5; 20 ng

or 500 ng HA-, myc- or FLAG-Raptor in pRK5 or pLJM1 with or without the targeting signals; 100 ng HA-GST-Rap2a in pRK5; 100 ng HA-GST-Rheb1 in pRK5; 100 ng HA-GST-RagB in pRK5, 100 ng HA-GST-RagD in pRK5; 1 ng FLAG-S6K1 in pRK7; 50 ng or 600 ng HA- or FLAG-p14 in pRK5; 75 ng or 600 ng HA-MP1 in pRK5; 50 ng or 800 ng HA-p18 in pRK5. The total amount of plasmid DNA in each transfection was normalized to 2 μg using empty pRK5.

Cell Size Determinations

To measure cell size, 2 million HEK-293T cells or 200,000 of other cell types were plated into 10 cm culture dishes. 24 hours later the cells were harvested by trypsinization in a 4 ml volume and diluted 1:20 with counting solution (Isoton II Diluent, Beckman Coulter). Cell diameters were determined using a particle size counter (Coulter Z2, Beckman Coulter) running Coulter Z2 AccuComp software.

Mammalian Lentiviral shRNAs and cDNAs

Lentiviral shRNAs targeting human Rheb1, RagB, and RagC have been described (Sancak et al., 2008). Lentiviral shRNAs targeting mouse Rheb1 and human p14 were obtained from Sigma-Aldrich. Lentiviral shRNAs targeting the mRNA for human MP1 and human p18 were cloned into pLKO.1 vector as described (Sarbassov et al., 2005). The target sequences are as follows:

MP1_1: GAGATGGAGTACCTGTTATTA
MP1_2: ATATCAATCCAGCAATCTTTA
p18: AGACAGCCAGCAACATCATTG

Virus generation and infection was done as previously described (Sancak et al., 2008).

Raptor was cloned into the AgeI and BamHI sites of a modified pLKO.1 vector (pLJM1) (Sancak et al., 2008) with or without the Rheb1, Rap1b and HRas targeting signals or cloned into the pRK5 vector with or without the same localization signals. After sequence verification, pLJM1 based plasmids were used in transient cDNA transfections or to produce lentivirus needed to generate

cell lines stably expressing these proteins. pRK5 based plasmids were also used for transient transfection experiments. The $p18^{mito}$ expression plasmid was generated by cloning a mutant p18 with amino acids 2-5 changed to alanines into a modified version of the pLKO.1 vector that added, to the C-terminus of p18, the mitochondrial localization signal of OMP25 protein. This plasmid was used in transient cDNA transfections or to produce lentivirus needed to generate stable cell lines. HA-Rheb1 and HA-Rheb1-HRas25 were cloned into pLJM5, a derivative of pLJM1 carrying a hygromycin instead of puromycin resistance gene. The vectors were used as above for lentivirus production.

Immunofluorescence Assays

50,000 HEK-293T cells or 20,000 of other cell types were plated on fibronectin coated glass coverslips in 12-well tissue culture plates. 24 hours later, the slides were rinsed with PBS once and fixed for 15 minutes with 4% paraformaldehyde in PBS warmed to 37°C. The slides were rinsed twice with PBS and cells were permealized with 0.05% Triton X-100 in PBS for 30 seconds. After rinsing twice with PBS, the slides were incubated with primary antibody in 5% Normal Donkey Serum for 2 hours at room temperature, rinsed four times with PBS and incubated with secondary antibodies produced in donkey (diluted 1:1000 in 5% Normal Donkey Serum) for one hour at room temperature in the dark, washed four times with PBS. Slides were mounted on glass coverslips using Vectashield (Vector Laboratories) and imaged.

Materials

Reagents were obtained from the following sources: antibodies to phospho-T389 S6K1, S6K1, mTOR, raptor, RagA/B, RagC, p14, p18, MP1, the myc epitope, the HA epitope, the FLAG epitope (unconjugated and alexa fluor conjugated), TSC2, phospho-T398 dS6K, phospho-S473 Akt, Akt1, phospho-T70 4E-BP1, 4E-BP1, and Rheb from Cell Signaling Technology; antibodies to LAMP2 from Abcam (ab25631 and ab13524); antibody to raptor (for immunostaining) from Millipore; antibody to Cytochrome c from BD Biosciences;

HRP-labeled anti-mouse, anti-goat, and anti-rabbit secondary antibodies from Santa Cruz Biotechnology; FLAG M2 affinity gel, FLAG M2 antibody, human recombinant insulin, from Sigma Aldrich; protein G-sepharose and dialysis cassettes from Thermo Scientific; DMEM from SAFC Biosciences; FuGENE 6 and Complete Protease Cocktail from Roche; alexa fluor conjugated secondary antibodies from Invitrogen; 16% paraformaldehyde solution from Electron Microscopy Sciences; fibronectin from Jackson Immunoresearch Laboratories; 35 mm glass bottom dishes from Mattek Corporation; glass coverslips from Ted Pella, Inc; amino acid and glucose-free RPMI from United States Biological; Schneider's medium, Drosophila-SFM, and Inactivated Fetal Calf Serum (IFS) from Invitrogen. The dS6K antibody was a generous gift from Mary Stewart (North Dakota State University).

Identification of Ragulator Components as Rag-associated Proteins

Ragulator components (MP1, p14, and p18) were detected in anti-FLAG immunoprecipitates prepared from HEK-293T cells stably expressing FLAG-RagB or FLAG-RagD as well as in immunoprecipitates of endogenous RagC prepared from HEK-293T cells. Immunoprecipitates were prepared as described (Sancak et al., 2008). Proteins were eluted with the FLAG peptide from the anti-FLAG affinity matrix or recovered from the protein G-sepharose by boiling with sample buffer, resolved by SDS-PAGE, and stained with simply blue stain (Invitrogen). Each gel lane was sliced into 10-12 pieces and the proteins in each gel slice digested overnight with trypsin. The resulting digests were analyzed by mass spectrometry as described (Sancak et al., 2008). 2-3 peptides corresponding to each Ragulator component were identified in the FLAG-RagB and endogenous RagC immunoprecipitates, while no peptides corresponding to any of the proteins were ever found in the FLAG-Rap2a, p53, or α-tubulin immunoprecipitates that served as controls.

Amino Acid Starvation and Stimulation and dsRNA-mediated Knockdowns in *Drosophila* Cells

Amino acid starvation and stimulation of *Drosophila* S2 cells was performed as described(Sancak et al., 2008). The design and synthesis of dsRNAs has also been described (Sancak et al., 2008).

Primer sequences used to amplify DNA templates for dsRNA synthesis for dp14, dp18, and dMP1, including underlined 5' and 3' T7 promoter sequences, are as follows:

dp14 (CG5189) dsRNA forward primer:

GAATTAATACGACTCACTATAGGGAGACTCTATTGGCCTACTCCGGTTAT

dp14 (CG5189) dsRNA reverse primer:

GAATTAATACGACTCACTATAGGGAGATATGAGGCCGAGATCTGCTTA

dp18 (CG14184) dsRNA forward primer:

GAATTAATACGACTCACTATAGGGAGAGCAGAATACTGCGATAAACATGATA

dp18 (CG14184) dsRNA reverse primer:

GAATTAATACGACTCACTATAGGGAGATGGATAGGTTGGCTTAGACAGATAG

dMP1 (CG5110) dsRNA forward primer:

GAATTAATACGACTCACTATAGGGAGAGTCGGACGACATCAAGAAGTATTTA

dMP1 (CG5110) dsRNA reverse primer:

GAATTAATACGACTCACTATAGGGAGAAGTACATGGAGATGATGGTCTTGTT

In vitro Binding Assay

2 million HEK-293T cells were transfected with 2 µg FLAG-p18 (lipidation mutant G2A), 2 µg HA-GST-Rap2a, or 2 µg HA-GST-RagB together with 2 µg of HA-GST-RagC. 2 days after transfection, the cells were lysed in lysis buffer containing 1% Triton X-100 as described (Sancak et al., 2007) and cleared lysates were incubated with glutathione- or FLAG-beads for 3 hours at 4°C with rotation. The beads were washed 3 times with lysis buffer and two times with lysis buffer containing 0.3% CHAPS. FLAG-p18 was eluted from FLAG beads with the FLAG peptide and 1/8 of the eluate was incubated with 1/4 of the Rag-containing glutathione beads in lysis buffer with 0.3% CHAPS for 45 min at 4°C. The glutathione beads were washed three times with lysis buffer containing 0.3% CHAPS and 150 mM NaCl. Proteins were denatured by the addition of 20 µl of

sample buffer and boiling for 5 minutes and analyzed by SDS-PAGE and immunoblotting.

Transient Transfections for Immunofluorescence Assays

For myc-mTOR and HA-raptor co-transfection experiments, HEK-293T cells were seeded in 60 mm culture plates. 24 hours later, cells were transfected with 500 ng myc-mTOR and 50 ng HA-Raptor. 24 hours after transfections, cells were split and plated on fibronectin coated glass coverslip in 12-well culture plates and processed as above.

For GFP-RagB, GFP-RagD, p18-GFP, GFP-Mito, RFP-RagB, and LAMP1-mRFP co-transfection experiments, HEK-293T cells (250,000 cells/dish) or $p18^{-/-}$, $p18^{rev}$ or $p18^{mito}$ cells (50,000 cells/dish) were plated on 35 mm, glass-bottom Mattek dishes. The next day, each dish was transfected with 100 ng of GFP-RagB or GFP-RagD, p18-GFP, GFP-mito, RFP-RagB or LAMP1-mRFP using fugene. At 18-24 hours post transfections, cells were fixed and imaged. GFP-Mito has been described (Nemoto and De Camilli, 1999).

For GFP-LC3 localization experiments, 2 million cells were transfected by electroporation with 1 µg of GFP-LC3 plasmid, and plated on 35 mm glass-bottom Mattek dishes. The next day the cells were starved for 3 hours in serum- and amino acid-free RPMI to induce autophagy and processed for imaging as above.

All images were acquired with a spinning disk confocal microscope (Perkin Elmer) equipped with a Hamamatsu 1k X 1k EM-CCD camera. For each image, 8-10 optical slices were acquired and displayed as maximum projections.

Acknowledgements

We thank all members of the Sabatini Lab for helpful suggestions and Eric Spooner for the mass spectrometric analysis of samples. We thank Dr. Lukas A. Huber for providing p14-null and control cells and Dr. Christoph Klein for providing patient-derived and healthy donor-derived cells. This work was supported by grants from the NIH (CA103866 and AI47389) and Department of Defense (W81XWH-07-0448) to D.M.S., awards from the W.M. Keck Foundation and LAM Foundation to D.M.S, and fellowship support from the LAM Foundation and from the Jane Coffin Childs Memorial Fund for Medical Research to R.Z. D.M.S. is an investigator of the Howard Hughes Medical Institute.

References

Avruch, J., Hara, K., Lin, Y., Liu, M., Long, X., Ortiz-Vega, S., and Yonezawa, K. (2006). Insulin and amino-acid regulation of mTOR signaling and kinase activity through the Rheb GTPase. Oncogene *25*, 6361-6372.

Berchtold, D., and Walther, T.C. (2009). TORC2 plasma membrane localization is essential for cell viability and restricted to a distinct domain. Mol Biol Cell, 1565-1575.

Binda, M., Péli-Gulli, M., Bonfils, G., Panchaud, N., Urban, J., Sturgill, T., Loewith, R., and De Virgilio, C. (2009). The Vam6 GEF controls TORC1 by activating the EGO complex. Mol Cell *35*, 563-573.

Bohn, G., Allroth, A., Brandes, G., Thiel, J., Glocker, E., Schäffer, A.A., Rathinam, C., Taub, N., Teis, D., Zeidler, C., *et al.* (2006). A novel human primary immunodeficiency syndrome caused by deficiency of the endosomal adaptor protein p14. Nat Med *13*, 38-45.

Buerger, C., DeVries, B., and Stambolic, V. (2006). Localization of Rheb to the endomembrane is critical for its signaling function. Biochem Biophys Res Commun *344*, 869-880.

Chavrier, P., Parton, R.G., Hauri, H.P., Simons, K., and Zerial, M. (1990). Localization of low molecular weight GTP binding proteins to exocytic and endocytic compartments. Cell *62*, 317-329.

Clark, G.J., Kinch, M.S., Rogers-Graham, K., Sebti, S.M., Hamilton, A.D., and Der, C.J. (1997). The Ras-related protein Rheb is farnesylated and antagonizes Ras signaling and transformation. J Biol Chem *272*, 10608-10615.

Dard, N., and Matthias, P. (2006). Scaffold proteins in MAP kinase signaling: more than simple passive activating platforms. BioEssays *28*, 146-156.

Dubouloz, F., Deloche, O., Wanke, V., Cameroni, E., and De Virgilio, C. (2005). The TOR and EGO protein complexes orchestrate microautophagy in yeast. Mol Cell *19*, 15-26.

Eskelinen, E.L. (2006). Roles of LAMP-1 and LAMP-2 in lysosome biogenesis and autophagy. Mol Aspects Med *27*, 495-502.

Fingar, D.C., Salama, S., Tsou, C., Harlow, E., and Blenis, J. (2002). Mammalian cell size is controlled by mTOR and its downstream targets S6K1 and 4EBP1/eIF4E. Genes Dev *16*, 1472-1487.

Gao, M., and Kaiser, C. (2006). A conserved GTPase-containing complex is required for intracellular sorting of the general amino-acid permease in yeast. Nat Cell Biol *8*, 657-667.

Guertin, D.A., and Sabatini , D.M. (2007). Defining the role of mTOR in cancer. Cancer Cell *12*, 9-22.

Guertin, D.A., Stevens, D.M., Thoreen, C.C., Burds, A.A., Kalaany, N.Y., Moffat, J., Brown, M., Fitzgerald, K.J., and Sabatini, D.M. (2006). Ablation in mice of the mTORC components raptor, rictor, or mLST8 reveals that mTORC2 is required for signaling to Akt-FOXO and PKCalpha, but not S6K1. Dev Cell *11*, 859-871.

Kim, D.H., Sarbassov, D.D., Ali , S.M., King, J.E., Latek, R.R., Erdjument-Bromage, H., Tempst, P., and Sabatini, D.M. (2002). mTOR interacts with raptor to form a nutrient-sensitive complex that signals to the cell growth machinery. Cell *110*, 163-175.

Kim, E., Goraksha-Hicks, P., Li , L., Neufeld, T.P., and Guan, K.L. (2008). Regulation of TORC1 by Rag GTPases in nutrient response. Nat Cell Biol *10*, 395-345.

Koonin, E.V., and Aravind, L. (2000). Dynein light chains of the Roadblock/LC7 group belong to an ancient protein superfamily implicated in NTPase regulation. Curr Biol *10*, 774-776.

Li, S.C., and Kane, P.M. (2009). The yeast lysosome-like vacuole: endpoint and crossroads. Biochim Biophys Acta *1793*, 650-663.

Luzio, J.P., Pryor, P.R., and Bright, N.A. (2007). Lysosomes: fusion and function. Nat Rev Mol Cell Biol *8*, 622-632.

Manning, B.D. (2004). Balancing Akt with S6K: implications for both metabolic diseases and tumorigenesis. J Cell Biol *167*, 399-403.

Nada, S., Hondo, A., Kasai, A., Koike, M., Saito, K., Uchiyama, Y., and Okada, M. (2009). The novel lipid raft adaptor p18 controls endosome dynamics by anchoring the MEK–ERK pathway to late endosomes. EMBO J *28*, 477-489.

Nemoto, Y., and De Camilli, P. (1999). Recruitment of an alternatively spliced form of synaptojanin 2 to mitochondria by the interaction with the PDZ domain of a mitochondrial outer membrane protein. EMBO J *18*, 2991-3006.

Nobukuni, T., Joaquin, M., Roccio, M., Dann, S.G., Kim, S.Y., Gulati, P., Byfield, M.P., Backer, J.M., Natt, F., Bos, J.L., *et al.* (2005). Amino acids mediate mTOR/raptor signaling through activation of class 3 phosphatidylinositol 3OH-kinase. PNAS *102*, 14238-14243.

Pizon, V., Desjardins, M., Bucci, C., Parton, R.G., and Zerial, M. (1994). Association of Rap1a and Rap1b proteins with late endocytic/phagocytic compartments and Rap2a with the Golgi complex. J Cell Sci *107*, 1661-1670.

Roccio, M., Bos, J.L., and Zwartkruis, F.J.T. (2006). Regulation of the small GTPase Rheb by amino acids. Oncogene *25*, 657-664.

Saito, K., Araki, Y., Kontani, K., Nishina, H., and Katada, T. (2005). Novel Role of the Small GTPase Rheb: Its Implication in Endocytic Pathway Independent of the Activation of Mammalian Target of Rapamycin. J Biochem *137*, 429-430.

Sancak, Y., Peterson, T.R., Shaul, Y.D., Lindquist , R.A., Thoreen, C.C., Bar-Peled, L., and Sabatini, D.M. (2008). The Rag GTPases bind raptor and mediate amino acid signaling to mTORC1. Science *320*, 1496-1501.

Sancak, Y., Thoreen, C.C., Peterson, T.R., Lindquist, R.A., Kang, S.A., Spooner, E., Carr, S.A., and Sabatini, D.M. (2007). PRAS40 is an insulin-regulated inhibitor of the mTORC1 protein kinase. Mol Cell *25*, 903-915.

Sarbassov, D.D., Guertin, D.A., Ali , S.M., and Sabatini , D.M. (2005). Phosphorylation and Regulation of Akt/PKB by the Rictor-mTOR Complex. Science *307*, 1098-1101.

Saucedo, L.J., Gao, X., Chiarelli, D.A., Li, L., Pan, D., and Edgar, B.A. (2003). Rheb promotes cell growth as a component of the insulin/TOR signalling network. Nat Cell Bio *5*, 566-571.

Schurmann, A., Brauers, A., Maßmann, S., Becker, W., and Joost, H. (1995). Cloning of a Novel Family of Mammalian GTP-binding Proteins (RagA, RagBs, RagBl) with Remote Similarity to the Ras-related GTPases. J Biol Chem *270*, 28982-28988.

Smith, E.M., Finn, S.G., Tee, A.R., Browne, G.J., and Proud, C.G. (2005.). The tuberous sclerosis protein TSC2 is not required for the regulation of the mammalian target of rapamycin by amino acids and certain cellular stresses. J Biol Chem *280*, 18717–18727.

Takahashi, K., Nakagawa, M., Young, S.G., and S, Y. (2005). Differential Membrane Localization of ERas and Rheb, Two Ras-related Proteins Involved in the Phosphatidylinositol 3-Kinase/mTOR Pathway. J Biol Chem *280*, 32768-32774.

Tee, A.R., Blenis, J., and Proud, C.G. (2005). Analysis of mTOR signaling by the small G-proteins, Rheb and RhebL1. Febs Letters *579*, 4763-4768.

Tee, A.R., Manning, B.D., Roux, P.P., Cantley, L.C., and Blenis, J. (2003). Tuberous sclerosis complex gene products, Tuberin and Hamartin, control mTOR signaling by acting as a GTPase-activating protein complex toward Rheb. Curr Biol *13*, 1259-1268.

Teis, D., Taub, N., Kurzbauer, R., Hilber, D., Araujo, M.E., Erlacher, M., Offterdinger, M., Villunger, A., Geley, S., Bohn, G., *et al.* (2006). p14–MP1-MEK1 signaling regulates endosomal traffic and cellular proliferation during tissue homeostasis. J Cell Biol *175*, 861-868.

Zhang , Y., Gao, X., Saucedo, L.J., Ru, B., Edgar, B.A., and Pan, D. (2003). Rheb is a direct target of the tuberous sclerosis tumour suppressor proteins. Nat Cell Bio *5*, 578-581.

Zimmermann, S., and Moelling, K. (1999). Phosphorylation and Regulation of Raf by Akt (Protein Kinase B). Science *286*, 1741-1744.

Chapter 3

Ragulator is a GEF for the Rag GTPases that signal amino acid levels to mTORC1

Liron Bar-Peled[1,2], Lawrence D. Schweitzer[1,2], Roberto Zoncu[1,2], and David M. Sabatini[1,2,3]

[1]Whitehead Institute for Biomedical Research and Massachusetts Institute of Technology, Department of Biology, Nine Cambridge Center, Cambridge, MA 02142, USA

[2]Koch Institute for Integrative Cancer Research, 77 Massachusetts Avenue, Cambridge, MA 02139, USA

[3] Howard Hughes Medical Institute, Department of Biology, Massachusetts Institute of Technology, Cambridge, MA 02139, USA

This work has been published in:

Bar-Peled L., Schweitzer L. D., Zoncu R., Sabatini D. M. (2012). Ragulator Is a GEF for the Rag GTPases that Signal Amino Acid Levels to mTORC1. *Cell* **150**, 1196-1208.

Experiments in figures 1, 2, 3, 4, 5, 6, S1, S2, S3, S4, S5 and S6 were preformed by LBP. Analysis and experiments in figures 1, 2, 3, and S1 were preformed by LDS. Experiments in figures 6 and S6 were preformed by RZ.

Summary

The mTOR Complex 1 (mTORC1) pathway regulates cell growth in response to numerous cues, including amino acids, which promote mTORC1 translocation to the lysosomal surface, its site of activation. The heterodimeric RagA/B-RagC/D GTPases, the Ragulator complex that tethers the Rags to the lysosome, and the v-ATPase form a signaling system that is necessary for amino acid sensing by mTORC1. Amino acids stimulate the binding of GTP to RagA and RagB but the factors that regulate Rag nucleotide loading are unknown. Here, we identify HBXIP and C7orf59 as novel Ragulator components that are required for mTORC1 activation by amino acids. The expanded Ragulator has nucleotide exchange activity towards RagA and RagB and interacts with the Rag heterodimers in an amino acid- and v-ATPase-dependent fashion. Thus, we provide mechanistic insight into how mTORC1 senses amino acids by identifying Ragulator as a guanine nucleotide exchange factor (GEF) for the Rag GTPases.

Introduction

Mechanistic target of rapamycin complex I (mTORC1) is a master growth regulator that couples nutrient availability to the control of cell growth and proliferation. When active, mTORC1 stimulates anabolic processes, such as translation, transcription, lipid biosynthesis, and ribosome biogenesis, and inhibits catabolic processes, such as autophagy (reviewed in (Howell and Manning, 2011; Ma and Blenis, 2009; Zoncu et al., 2011b)). Consistent with its growth-promoting function, many of the oncogenes and tumor suppressors that underlie familial tumor syndromes and sporadic cancers are upstream of mTORC1. mTORC1 responds to a variety of stimuli, including growth factors, oxygen availability, and energy levels, all of which impinge on mTORC1 through the tuberous sclerosis heterodimer (TSC1-TSC2). TSC1-TSC2 negatively regulates the mTORC1 pathway by acting as a GTPase activating protein (GAP) for Rheb1, a small GTPase that when bound to GTP is an essential activator of mTORC1 kinase activity.

One mTORC1 stimulus that does not funnel through the TSC1-TSC2-Rheb axis is amino acid sufficiency (Roccio et al., 2006; Smith et al., 2005). Recent findings indicate that amino acid signaling initiates within the lysosomal lumen (Zoncu et al., 2011a) and induces the translocation of mTORC1 to the lysosomal surface, where it comes in contact with Rheb and becomes activated. How mTORC1 moves to the lysosomal membrane is poorly understood, but another family of GTPases, known as the Rag GTPases, play an integral role (Kim et al., 2008; Sancak et al., 2008). Unique among the small GTPases, the Rags are obligate heterodimers: the highly related RagA and RagB are functionally redundant and bind to RagC or RagD, which are also very similar to each other (Hirose et al., 1998; Schurmann et al., 1995; Sekiguchi et al., 2001). The Rags localize to lysosomal membranes and bind to the raptor component of mTORC1, a process that depends on the binding of GTP to RagA or RagB. Amino acids regulate the binding of nucleotides to RagB, such that amino acid stimulation increases its GTP loading (Sancak et al., 2008). In cells expressing a RagA or RagB mutant that is constitutively bound to GTP, mTORC1 interacts with the Rags and localizes to the lysosome irrespective of amino acid levels, making the mTORC1 pathway immune to amino acid starvation (Kim et al., 2008; Sancak et al., 2008). Thus, a key event in the

amino acid-dependent activation of mTORC1 is the conversion of RagA or RagB from a GDP- to GTP-bound state, yet the putative guanine nucleotide exchange factors (GEFs) that mediate this transition have yet to be identified.

Unlike the many GTPases that rely on a lipid moiety for their subcellular localization, the Rags use the recently identified Ragulator complex as their tether to the lysosomal surface. Three proteins that localize to lysosomal membranes make up Ragulator: p18, p14, and MP1, which are encoded by the *LAMTOR1, LAMTOR2,* and *LAMTOR3* genes, respectively. In cells depleted of these proteins, the Rags and mTORC1 no longer reside at the lysosome, and, consequently, the mTORC1 pathway is inactive (Sancak et al., 2010).

The lysosomal v-ATPase is a newly characterized Ragulator-interacting complex and required for amino acid activation of mTORC1 (Zoncu et al. 2011). The mechanisms through which the v-ATPase activates the mTORC1 pathway and whether or not Ragulator has additional regulatory functions remain unknown. Here, we identify two novel components of Ragulator, the proteins encoded by the *HBXIP* and *C7orf59* genes. These proteins interact with the Rag GTPases and together with p18, p14, and MP1 form a pentameric Ragulator complex. HBXIP and C7orf59 are necessary for both Rag and mTOR lysosomal localization and mTORC1 activation. Surprisingly, the pentameric Ragulator, but not individual subunits or the trimeric Ragulator, has GEF activity towards RagA and RagB. Furthermore, modulation of the Ragulator-Rag interaction by amino acids requires the v-ATPase, suggesting that v-ATPase activity is upstream of the GEF activity of Ragulator.

Results

HBXIP and *C7orf59* encode components of an expanded Ragulator complex

We previously identified p14, MP1, and p18, collectively named Ragulator, as proteins that interact with the Rag GTPases within cells (Sancak et al., 2010). However, in cell-free assays, Rag heterodimers interact relatively weakly with purified, recombinantly-produced Ragulator (Sancak et al., 2010), suggesting that proteins responsible for stabilizing the interaction within cells are missing from our in vitro preparations. To identify such proteins, we used a purification strategy involving immunoprecipitation followed by mass spectrometry that previously led to the discovery of other mTORC1 pathway components (see Methods). Immunoprecipitates prepared from HEK-293T cells stably expressing FLAG-tagged p18, p14, or RagB, but not the Metap2 control, consistently contained HBXIP and the protein product of the *C7orf59* gene, hereafter called C7orf59. Several studies implicate HBXIP in the regulation of cell cycle progression, proliferation, apoptosis, and Hepatitis B virus replication (Fujii et al., 2006; Marusawa et al., 2003; Melegari et al., 1998; Wang et al., 2007; Wen et al., 2008), while C7orf59 has no described functions.

Orthologs of HBXIP and C7orf59 exist in mammals besides humans and in *Drosophila* (Figure S1A). Like other Ragulator components, HBXIP and C7orf59 lack protein sequence homology with any fission or budding yeast proteins, including Ego1p and Ego3p, which tether the yeast orthologs of the Rag GTPases to the vacuole (Binda et al., 2009; Dubouloz et al., 2005; Gao and Kaiser, 2006). High-resolution crystal structures of MP1 and p14 reveal the presence of a roadblock domain in each (Kurzbauer et al., 2004; Lunin et al., 2004), and secondary structure predictions suggest that the C-terminal regions of RagB and RagC also contain this domain (Gong et al., 2011) (Figure S1B). While the function of the domain is unknown, it is interesting to note that HBXIP also contains a roadblock domain (Garcia-Saez et al., 2011), and our secondary structure analyses predict the same for C7orf59 (Figure S1B). Thus, the Rag-Ragulator complex is likely to contain six roadblock domains.

Figure S1

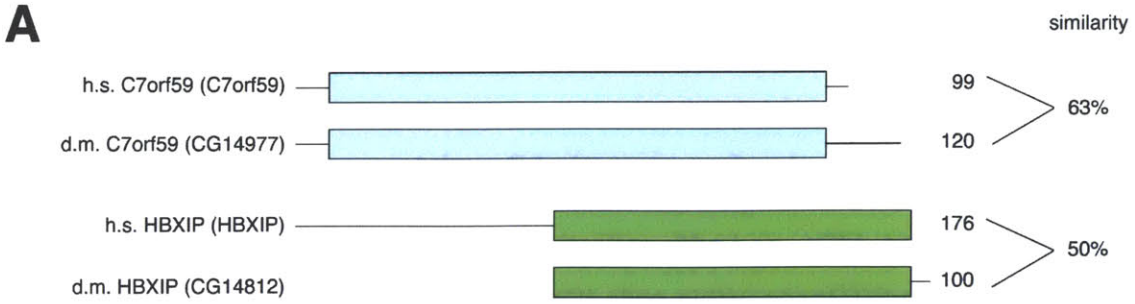

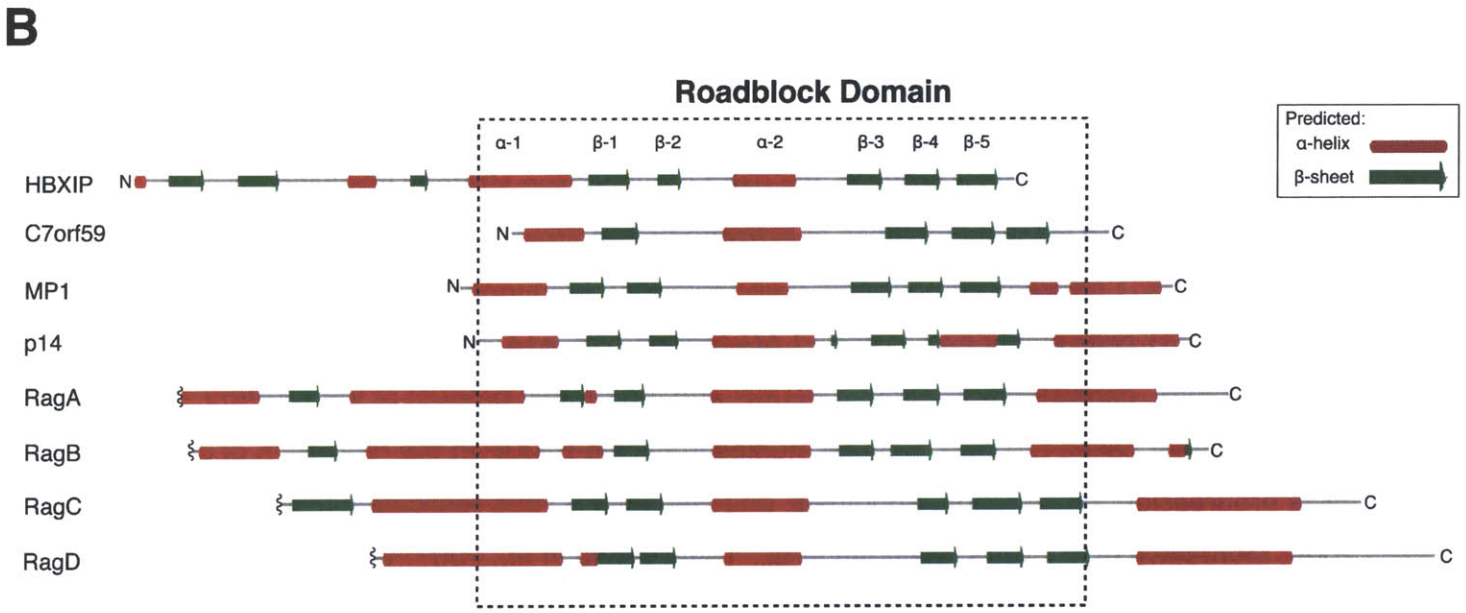

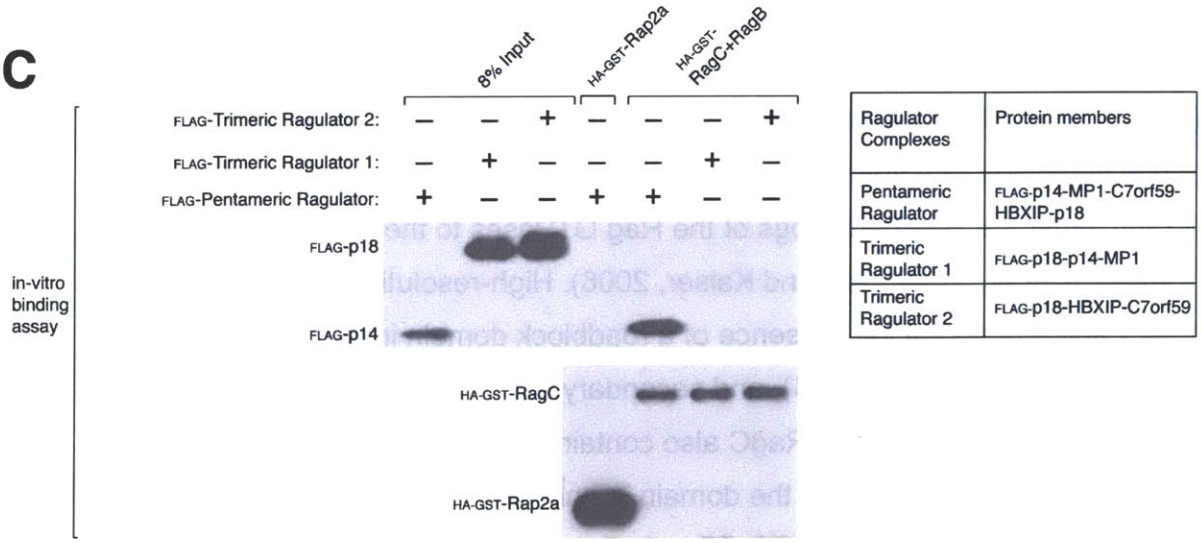

Ragulator Complexes	Protein members
Pentameric Ragulator	FLAG-p14-MP1-C7orf59-HBXIP-p18
Trimeric Ragulator 1	FLAG-p18-p14-MP1
Trimeric Ragulator 2	FLAG-p18-HBXIP-C7orf59

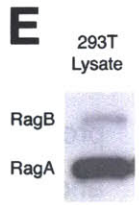

D

```
RagA                                                  PNTAMKKVLLMGKSGSGKTSMRSIIFANYIARDTRRLGATIDVEHSHVRFLGNLVLNLWDCGGQDTFMENYFTS 76
RagB  MEESDSEKTTEKENLGPRMDPPLGEPEGSLGWVLPNTAMKKVLLMGKSGSGKTSMRSIIFANYIARDTRRLGATIDVEHSHVRFLGNLVLNLWDCGGQDTFMENYFTS 109
                                                      ************************************************************

RagA  QRDNIFRNVEVLIYVFDVESRELEKDMHYYQSCLEAILQNSPDAKIFCLVHKMDLVQEDQRDLIFKEREEDLRRLSRPLECACFRTSIWDETLYKAWSSIVYQLIPNVQ 185
RagB  QRDNIFRNVEVLIYVFDVESRELEKDMHYYQSCLEAILQNSPDAKIFCLVHKMDLVQEDQRDLIFKEREEDLRRLSRPLECSCFRTSIWDETLYKAWSSIVYQLIPNVQ 218
      ************************************************************.***********************

RagA  QLEMNLRNFAQIIEADEVLLFERATFLVISHYQCKEQRDVHRFEKISNIIKQFKLSCSKLAASFQSMEVRNSNFAAFIDIFTSNTYVMVVMSDPSIPSAATLINIRNAR 294
RagB  QLEMNLRNFAEIIEADEVLLFERATFLVISHYQCKEQRDAHRFEKISNIIKQFKLSCSKLAASFQSMEVRNSNFAAFIDIFTSNTYVMVVMSDPSIPSAATLINIRNAR 327
      **********.**************************** ************************************************************

RagA  KHFEKLERVDGPKHSLLMR 313
RagB  KHFEKLERVDGPFQCLLMR 346
      ************..****
```

98% identity in highlighted region that excludes the first 30 amino acids in the n-terminus of RagB

Supplemental Figure 1: Secondary structure predictions of Rag and Ragulator proteins indicate the presence of the roadblock domain and Rags preferentially interact with a pentameric Ragulator complex, related to Figure 1

A) Schematic amino acid alignment of human HBXIP and C7orf59 with their corresponding *Drosophila* orthologs.

B) The presence of roadblock domains in Ragulator and Rag proteins. Secondary structure predictions of the indicated proteins using Jpred 3 secondary structure prediction server (Cole et al., 2008). The dashed box outlines the canonical roadblock domain predicted in each protein.

C) Rags preferentially interact with a pentameric Ragulator complex. In vitro binding assay in which recombinant HA-GST-tagged-RagB-RagC, were incubated with the indicated purified FLAG-tagged Ragulator complexes. HA-GST precipitates were analyzed by immunoblotting for levels of the indicated proteins.

D) RagA and RagB are highly similar. Amino acid sequence alignment of RagA and RagB indicates that the two proteins are 98% identical. RagB contains an N-terminal extension that increases its molecular weight compared to RagA.

E) RagA is much more abundant than RagB in HEK-293T cells. HEK-293T cell lysate was analyzed by immunoblotting for RagA and RagB with an antibody from CST that recognizes the same epitope in both proteins.

Experiments in cells and in cell-free systems indicate that that HBXIP and C7orf59 are new Ragulator components. When expressed in HEK-293T cells, FLAG-tagged HBXIP or C7orf59, but not Rap2a, co-immunoprecipitated endogenous RagA, which is highly similar but far more abundant than RagB (Figure S1D, S1E), RagC, p18, and MP1 at similar levels as FLAG-p14 (Figures 1A,B). Gratifyingly, endogenous HBXIP and C7orf59 co-immunoprecipitated with an antibody to endogenous p18, but not a control protein (Figure 1C). When co-expressed along with Ragulator proteins in HEK-293T cells, HBXIP and C7orf59 co-localized with p18 (Figure 1D), consistent with the lysosomal localization of other Ragulator components (Nada et al., 2009; Sancak et al., 2010; Wunderlich et al., 2001). In an in vitro binding assay, HBXIP bound to C7orf59 in the absence of other proteins, and the HBXIP-C7orf59 heterodimer, but neither protein alone, bound the established Ragulator components (MP1, p14 and p18) (Figure 1E). These results indicate that Ragulator is a pentameric complex in which HBXIP and C7orf59 form a heterodimer that interacts, through p18, with the MP1-p14 heterodimer (Figure 1F).

Consistent with our initial hypothesis that the original Ragulator lacked components required to bind strongly to the Rag GTPases, in HEK-293T cells the pentameric Ragulator interacted to a much greater degree with the Rags than the trimeric one (Figure 1G, S1C). Likewise, in an in vitro binding assay, Rags interacted with an intact pentameric Ragulator, but not one lacking p18 (Figure 1H). It is likely that in previous work, the two new Ragulator components were present in binding experiments in sub-stoichiometric amounts, explaining the weaker interactions we had observed (Sancak et al., 2010). Collectively, our results show that HBXIP and C7orf59 are part of an expanded Ragulator that requires all its subunits to bind strongly to the Rag GTPases.

HBXIP and C7orf59 are necessary for TORC1 activation by amino acids in mammalian and *Drosophila* cells

Figure 1

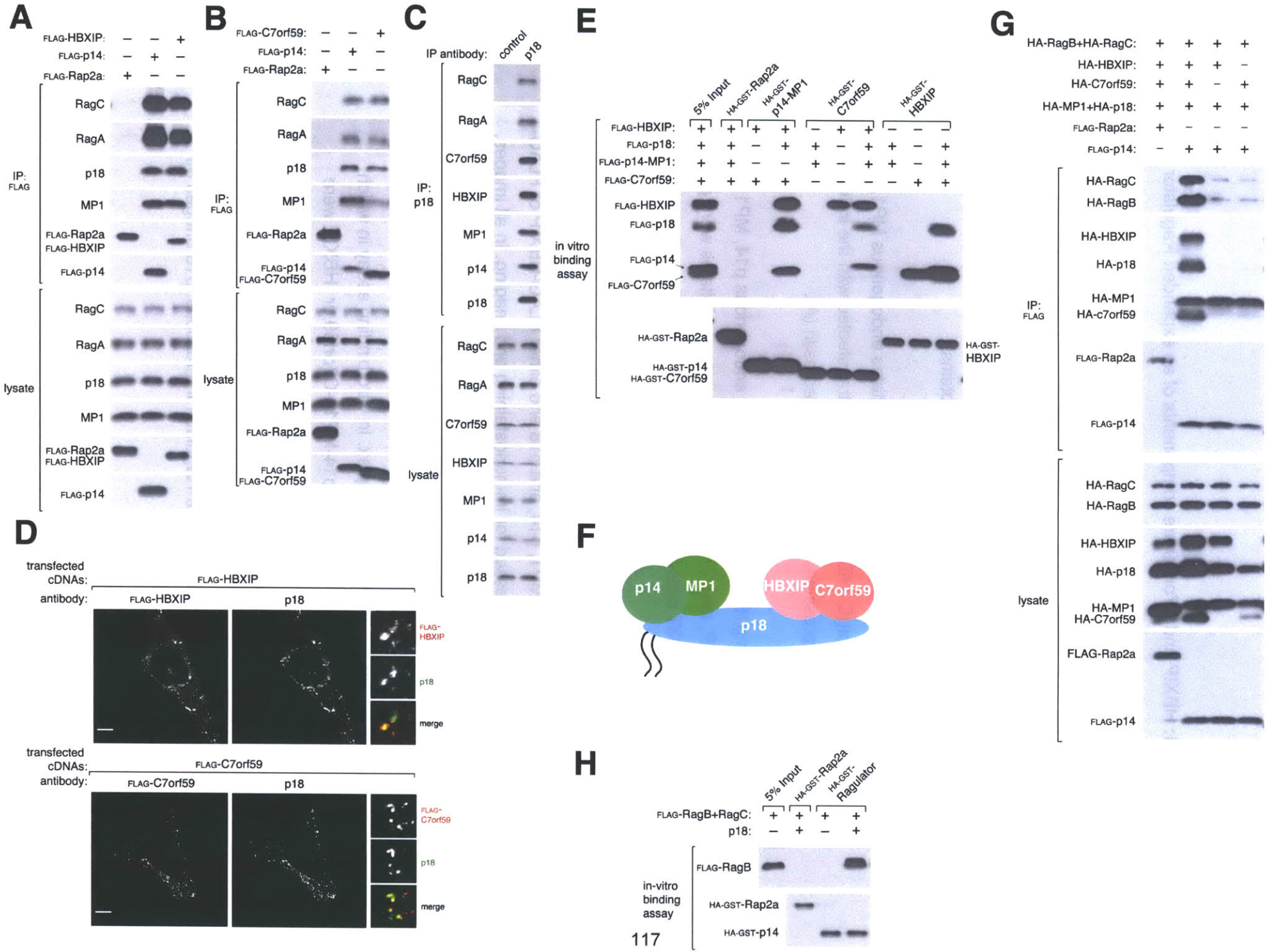
A
FLAG-HBXIP: – – +
FLAG-p14: – + –
FLAG-Rap2a: + – –
IP: FLAG
RagC
RagA
p18
MP1
FLAG-Rap2a
FLAG-HBXIP
FLAG-p14
lysate
RagC
RagA
p18
MP1
FLAG-Rap2a
FLAG-HBXIP
FLAG-p14
B
FLAG-C7orf59: – – +
FLAG-p14: – + –
FLAG-Rap2a: + – –
IP: FLAG
RagC
RagA
p18
MP1
FLAG-Rap2a
FLAG-p14
FLAG-C7orf59
lysate
RagC
RagA
p18
MP1
FLAG-Rap2a
FLAG-p14
FLAG-C7orf59
C
IP antibody: control p18
IP: p18
RagC
RagA
C7orf59
HBXIP
MP1
p14
p18
lysate
RagC
RagA
C7orf59
HBXIP
MP1
p14
p18
D
transfected cDNAs: FLAG-HBXIP
antibody: FLAG-HBXIP p18
FLAG-HBXIP
p18
merge
transfected cDNAs: FLAG-C7orf59
antibody: FLAG-C7orf59 p18
FLAG-C7orf59
p18
merge
E
5% Input
HA-GST-Rap2a
HA-GST-p14-MP1
HA-GST-C7orf59
HA-GST-HBXIP
FLAG-HBXIP: + + + + – + + – – –
FLAG-p18: + + – + + – + + – +
FLAG-p14-MP1: + + – – + – + + – +
FLAG-C7orf59: + + + + – – – – + +
in vitro binding assay
FLAG-HBXIP
FLAG-p18
FLAG-p14
FLAG-C7orf59
HA-GST-Rap2a
HA-GST-p14
HA-GST-C7orf59
HA-GST-HBXIP
F
p14
MP1
HBXIP
C7orf59
p18
G
HA-RagB+HA-RagC: + + + +
HA-HBXIP: + + + –
HA-C7orf59: + + – +
HA-MP1+HA-p18: + + + +
FLAG-Rap2a: + – – –
FLAG-p14: – + + +
IP: FLAG
HA-RagC
HA-RagB
HA-HBXIP
HA-p18
HA-MP1
HA-c7orf59
FLAG-Rap2a
FLAG-p14
lysate
HA-RagC
HA-RagB
HA-HBXIP
HA-p18
HA-MP1
HA-C7orf59
FLAG-Rap2a
FLAG-p14
H
5% Input
HA-GST-Rap2a
HA-GST-Ragulator
FLAG-RagB+RagC: + + + +
p18: – + – +
in-vitro binding assay
FLAG-RagB
HA-GST-Rap2a
HA-GST-p14

Figure 1: HBXIP and C7orf59 are components of an expanded Ragulator complex

A) Recombinant epitope-tagged HBXIP co-immunoprecipitates endogenous MP1, p18, RagA, and RagC. Anti-FLAG immunoprecipitates were prepared from HEK-293T cells transfected with the indicated cDNAs in expression vectors. Cell lysates and immunoprecipitates were analyzed by immunoblotting for levels of indicated proteins.

B) Recombinant C7orf59 co-immunoprecipitates endogenous MP1, p18, RagA, and RagC. HEK-293T cells were transfected with the indicated cDNAs in expression vectors and analyzed as in (A).

C) Endogenous p18 co-immunoprecipitates endogenous p14, MP1, RagA, RagC, HBXIP, and C7orf59. Anti-p18 immunoprecipitates were prepared from HEK-293T cells and analyzed for the levels of the indicated proteins.

D) Images of HEK-293T cells co-immunostained for p18 (green) and FLAG-HBXIP (red) or FLAG-C7orf59 (red). Cells were co-transfected with cDNAs encoding MP1, p14, and p18 and either FLAG-HBXIP or FLAG-C7orf59 and processed for immunostaining and imaging. In all images, insets show selected fields that were magnified five times and their overlays. Scale bar represents 10 μm.

E) Ragulator is a pentameric complex. In vitro binding assay in which recombinant HA-GST-tagged-p14-MP1, -C7orf59 or -HBXIP were incubated with the indicated purified FLAG-tagged Ragulator proteins. HA-GST precipitates were analyzed for levels of the indicated proteins.

F) Schematic summarizing intra-Ragulator interactions: p18 bridges MP1-p14 with HBXIP-C7orf59.

G) The pentameric Ragulator complex co-immunoprecipitates recombinant RagB and RagC. HEK-293T cells were co-transfected with the indicated cDNAs in expression vectors and analyzed as in (A).

H) Requirement for a pentameric Ragulator complex to interact with Rags. In vitro binding assay in which recombinant HA-GST Ragulator with or without p18 was incubated with purified FLAG-RagB-RagC and analyzed as in (E). See also Figure S1.

We next examined the functions of the novel Ragulator components in mTORC1 signaling. In HEK-293T cells, RNAi-mediated reductions in HBXIP or C7orf59 expression blunted mTORC1 activation by amino acids, as detected by S6K1 phosphorylation, to similar extents as knockdowns of the established Ragulator proteins p18 and p14 (Figure 2A). As expected for positive regulators of the growth-promoting mTORC1 pathway (Fingar et al., 2002; Kim et al., 2008; Sancak et al., 2010; Sancak et al., 2008; Stocker et al., 2003), reductions in HBXIP and C7orf59 levels also decreased the size of HEK-293T cells (Figure 2B). As the components of obligate heterodimers often behave (Cortez et al., 2001; Sancak et al., 2008), loss of either HBXIP or C7orf59 reduced the expression of its partner, but not of p14 (Figure 2A). Finally, consistent with the conserved functions of the Rag and Ragulator proteins in *Drosophila* (Kim et al., 2008; Sancak et al., 2010; Sancak et al., 2008), treatment of S2 cells with dsRNAs targeting the HBXIP (CG14812) or C7orf59 (CG14977) fly orthologs strongly inhibited dTORC1 activation by amino acids (Figure 2C). These results establish that HBXIP and C7orf59 are positive components in mammalian and *Drosophila* cells of the amino acid sensing branch of the TORC1 pathway.

Localization of the Rag GTPases and mTOR to the lysosomal surface requires HBXIP and C7orf59

Upon amino acid stimulation, the Rag GTPases recruit mTORC1 to the lysosomal surface (Sancak et al., 2010). In the absence of Ragulator, the Rags detach from the lysosome and cannot target mTORC1 to this organelle. The inability of amino acids to activate mTORC1 in cells depleted of HBXIP and C7orf59 suggested that HBXIP and C7orf59, like p14, MP1, and p18, might also localize the Rags, and thus mTORC1, to the lysosome. Indeed, in HEK-293T cells treated with siRNAs targeting C7orf59 and HBXIP, RagA and RagC localized in a diffuse pattern throughout the cytoplasm and did not co-localize with the lysosomal marker LAMP2 (Figure 2D, S2A). The lysosomal localization of p18 was unaffected by depletion of HBXIP or C7orf59 (Figure S2B), consistent with its function as a lysosomal tether for the Ragulator complex that does not require other Ragulator components for its own lysosomal localization (Sancak et al., 2010, Nada et al., 2009). As expected from the mis-localization of the Rags, in cells depleted of HBXIP

Figure 2

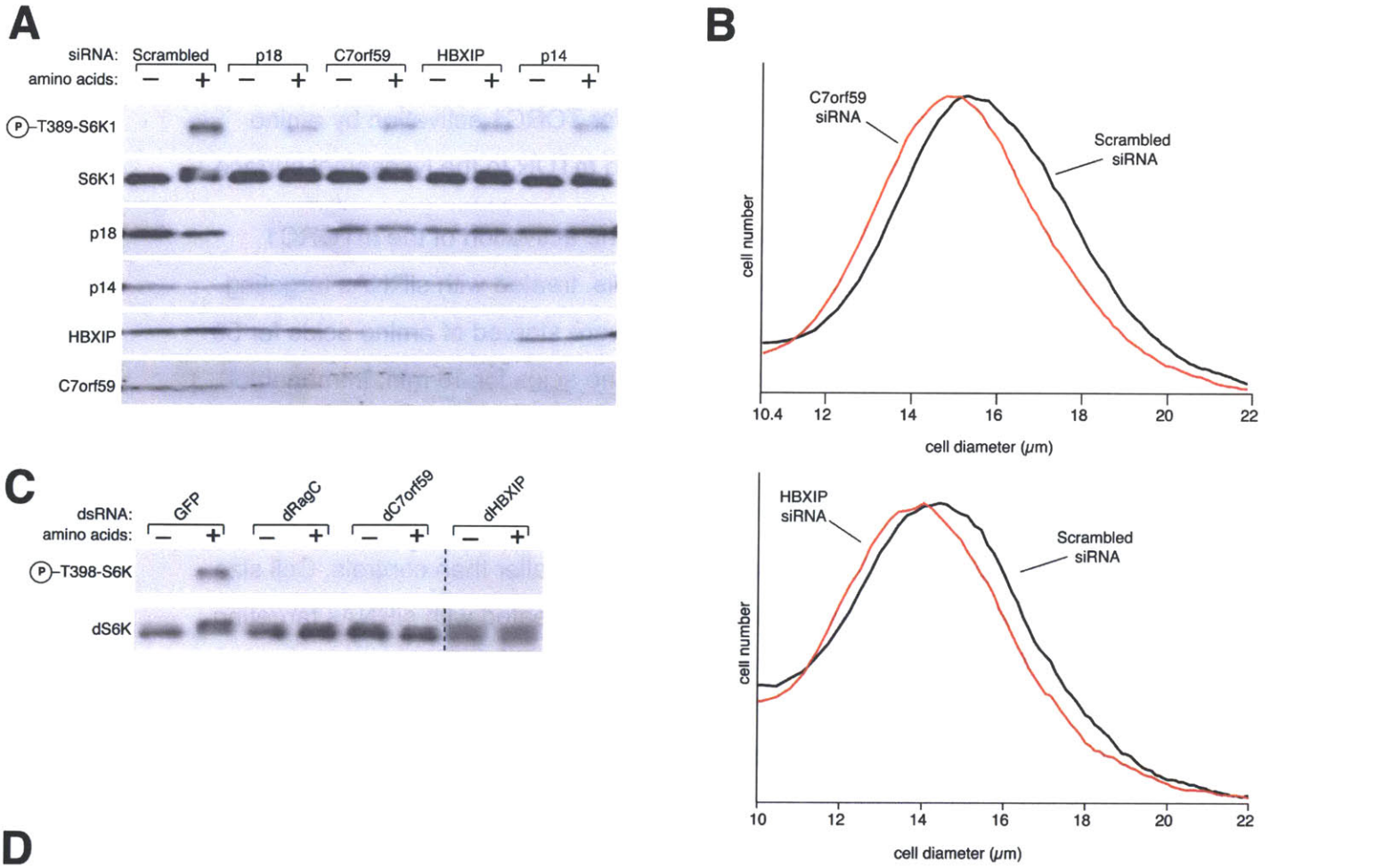
A
siRNA: Scrambled p18 C7orf59 HBXIP p14
amino acids: – + – + – + – + – +
P–T389-S6K1
S6K1
p18
p14
HBXIP
C7orf59
B
C7orf59 siRNA
Scrambled siRNA
cell number
10.4 12 14 16 18 20 22
cell diameter (μm)
HBXIP siRNA
Scrambled siRNA
cell number
10 12 14 16 18 20 22
cell diameter (μm)
C
dsRNA: GFP dRagC dC7orf59 dHBXIP
amino acids: – + – + – + – +
P–T398-S6K
dS6K
D
siRNA: Scrambled C7orf59
antibody: RagA Lamp2 RagA Lamp2
-a.a. for 50 min
-a.a. for 50 min
+a.a. for 10 min
RagA
LAMP2
merge
siRNA: Scrambled HBXIP
antibody: RagA Lamp2 RagA Lamp2
E
siRNA: Scrambled C7orf59
antibody: mTOR Lamp2 mTOR Lamp2
siRNA: Scrambled HBXIP
antibody: mTOR Lamp2 mTOR Lamp2
mTOR
LAMP2
merge

Figure 2: HBXIP and C7orf59 are necessary for TORC1 activation by amino acids and localization of the Rag GTPases and mTOR to the lysosomal surface

A) C7orf59 and HBXIP are necessary for the activation of the mTORC1 pathway by amino acids. HEK-293T cells, treated with siRNAs targeting the mRNAs for the indicated proteins, were starved of amino acids for 50 min, or starved and stimulated with amino acids for 10 min. Immunoblot analyses were used to measure the levels of the indicated proteins and phosphorylation states.

B) Cells depleted of C7orf59 and HBXIP are smaller than controls. Cell size distributions are shown for HEK-293T cells treated with siRNAs targeting C7orf59, HBXIP, or a scrambled non-targeting control.

C) *Drosophila* orthologs of HBXIP and C7orf59 are required for the activation of the TORC1 pathway. *Drosophila* S2 cells were transfected with a control dsRNA or dsRNAs targeting dRagC, dC7orf59, or dHBXIP, starved for amino acids for 90 min or starved and stimulated with amino acids for 30 min and analyzed as in (A).

D) Images of HEK-293T cells, treated with a non-targeting siRNA or siRNAs targeting HBXIP or C7orf59, co-immunostained for RagA (red) and LAMP2 (green). Cells were starved for amino acids or starved and stimulated for the indicated times before processing for the immunofluorescence assay and imaging.

E) Images of HEK-293T cells, treated with a non-targeting siRNA or siRNAs targeting HBXIP or C7orf59, co-immunostained for mTOR (red) and LAMP2 (green). Cells were treated and processed as in (A). In all images, insets show selected fields that were magnified five times and their overlays. Scale bars represent 10 μm. See also Figure S2.

Figure S2

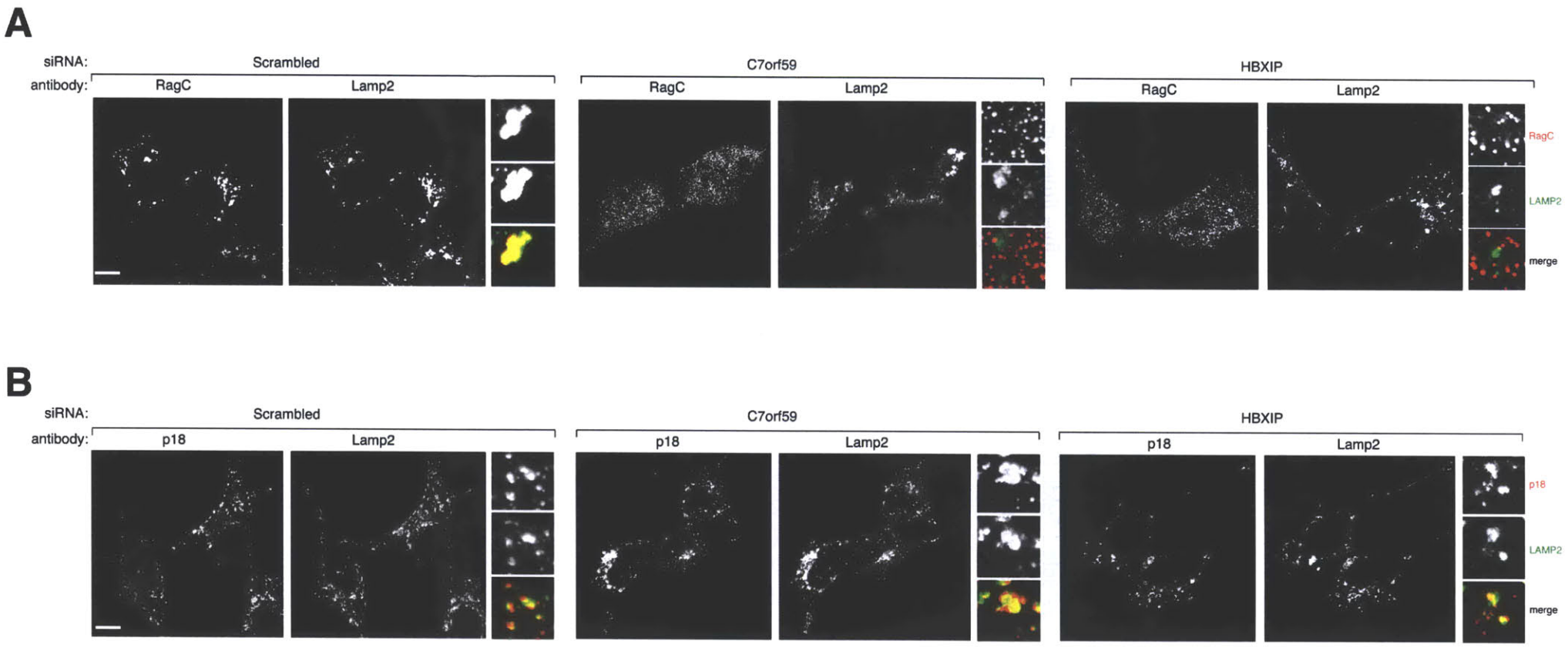
A
siRNA:
Scrambled
C7orf59
HBXIP
antibody:
RagC
Lamp2
RagC
Lamp2
RagC
Lamp2
RagC
LAMP2
merge
B
siRNA:
Scrambled
C7orf59
HBXIP
antibody:
p18
Lamp2
p18
Lamp2
p18
Lamp2
p18
LAMP2
merge

Supplemental Figure 2: HBXIP and C7orf59 are required for the localization of RagC but not p18 to the lysosomal surface, related to Figure 2

A) Images of HEK-293T cells, treated with a non-targeting siRNA or siRNAs targeting HBXIP or C7orf59, co-immunostained for RagC (red) and LAMP2 (green) and processed for imaging.

B) Images of HEK-293T cells, treated with a non-targeting siRNA or siRNAs targeting HBXIP or C7orf59, co-immunostained for p18 (red) and LAMP2 (green). Cells were treated and processed as in (A). In all images, insets show selected fields that were magnified five times and their overlays. Scale bars represent 10 μm. See also Figure S2.

and C7orf59, mTOR also did not co-localize with lysosomes, irrespective of whether or not they had been stimulated with amino acids (Figure 2E). These results indicate that both HBXIP and C7or59 have similar functions to p14, MP1, and p18 and confirm that the pentameric Ragulator complex acts as a scaffold for the Rag GTPases and mTORC1 at the lysosomal membrane (Sancak et al., 2010). Thus, throughout the remainder of this paper, we use the name 'Ragulator' to refer to the pentameric complex.

Amino acids regulate the Rag-Ragulator interaction

Multimeric signaling complexes often engage in regulated interactions as a mechanism to control downstream signaling events (Good et al., 2011). Because the Rag GTPases interact with mTORC1 in an amino-acid dependent manner, we wondered if the binding of Ragulator to the Rags might also be amino acid sensitive. In order to detect the endogenous Rag-Ragulator interaction using the antibodies available in the past, we had found it necessary to use cross-linked conditions that would have prevented detection of a regulated interaction (Sancak et al., 2010). Using optimized cell lysis conditions and improved antibodies, we find that amino acid starvation strengthens the interaction between endogenous Rags and the Ragulator isolated through p14, p18, HBXIP, or C7orf59 (Figures 3A, 3B, S3D, S3E). Similarly, amino acid stimulation decreased the amounts of endogenous Ragulator that co-immunoprecipitated with RagB (Figure 3C, S3F). Leucine is necessary for mTORC1 activation (Hara et al., 1998) and the Rag-Ragulator as well as the Ragulator-v-ATPase interactions, were both strengthened in cells deprived of leucine (Figure 3D), consistent with a mixture of all 20 amino acids regulating Ragulator-v-ATPase binding (Zoncu et al., 2011a). Amino acids only slightly regulated the interaction between p18 and other endogenous Ragulator proteins (Figure S3C), whereas the amount of mTORC1 that co-immunoprecipitated with Ragulator substantially increased upon amino acid stimulation (Figures S3A, S3B). Because amino acids also modulate the nucleotide loading of RagB (Sancak et al., 2008), the regulated interaction between Ragulator and the Rag heterodimers suggested that Ragulator might have additional functions towards the Rags besides simply being their lysosomal scaffold.

Ragulator preferentially interacts with nucleotide-free Rag GTPases

Figure 3

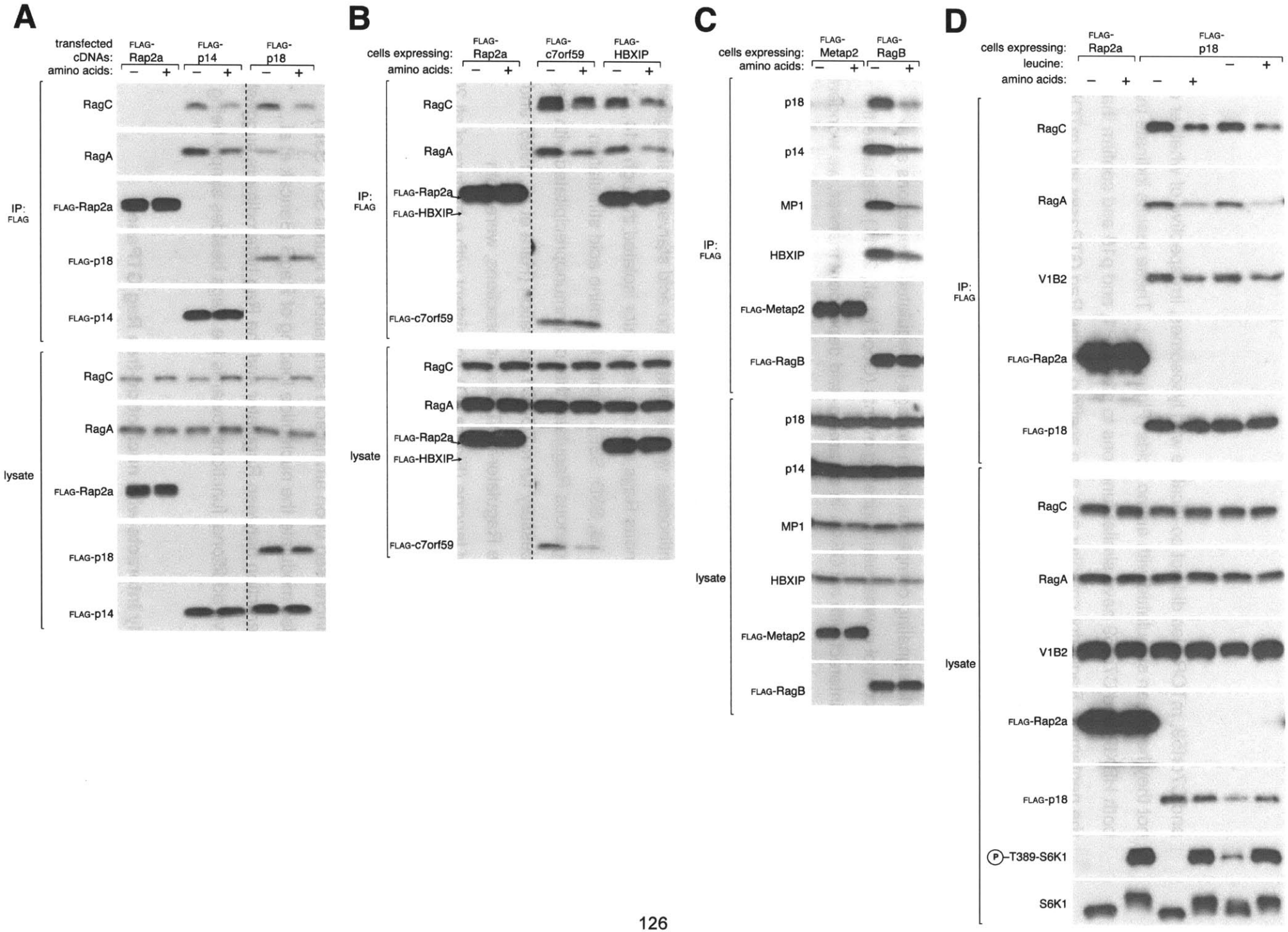
A
transfected cDNAs:
FLAG-Rap2a
FLAG-p14
FLAG-p18
amino acids:
IP: FLAG
RagC
RagA
FLAG-Rap2a
FLAG-p18
FLAG-p14
lysate
B
cells expressing:
FLAG-Rap2a
FLAG-c7orf59
FLAG-HBXIP
amino acids:
IP: FLAG
FLAG-HBXIP
FLAG-c7orf59
lysate
C
cells expressing:
FLAG-Metap2
FLAG-RagB
amino acids:
IP: FLAG
p18
p14
MP1
HBXIP
FLAG-Metap2
FLAG-RagB
lysate
D
cells expressing:
FLAG-Rap2a
FLAG-p18
leucine:
amino acids:
IP: FLAG
RagC
RagA
V1B2
FLAG-Rap2a
FLAG-p18
lysate
P-T389-S6K1
S6K1

Figure 3: Amino acids regulate the Rag-Ragulator interaction

A) Amino acids regulate the amounts of endogenous RagA and RagC that co-immunoprecipitate with recombinant p14 and p18. HEK-293T cells, transfected with the indicated cDNAs in expression vectors, were starved for amino acids for 2 hours or starved and stimulated with amino acids for 15 min. Anti-FLAG immunoprecipitates were prepared from cell lysates and analyzed by immunoblotting for levels of indicated proteins.

B) Amino acid starvation strengthens the interaction between endogenous Rags and recombinant C7orf59 and HBXIP. HEK-293T cells stably expressing FLAG-C7orf59 or FLAG-HBXIP were starved and re-stimulated with amino acids. Anti-FLAG immunoprecipitates were analyzed as in (A).

C) FLAG-RagB co-immunoprecipitation of endogenous Ragulator is dependent on amino acids. HEK-293T cells stably expressing FLAG-RagB were starved and re-stimulated with amino acids as in (A). Anti-FLAG immunoprecipitates were analyzed for the levels of the indicated proteins.

D) Leucine starvation strengthens the binding of Ragulator to endogenous Rags and the V1 domain of the v-ATPase. HEK-293T cells stably expressing FLAG-p18 were starved and re-stimulated with total amino acids as in (A) or starved for leucine for 2 hours or starved and stimulated with leucine for 20 min. Anti-FLAG immunoprecipitates were analyzed for the levels of the indicated proteins. See also Figure S3.

Figure S3

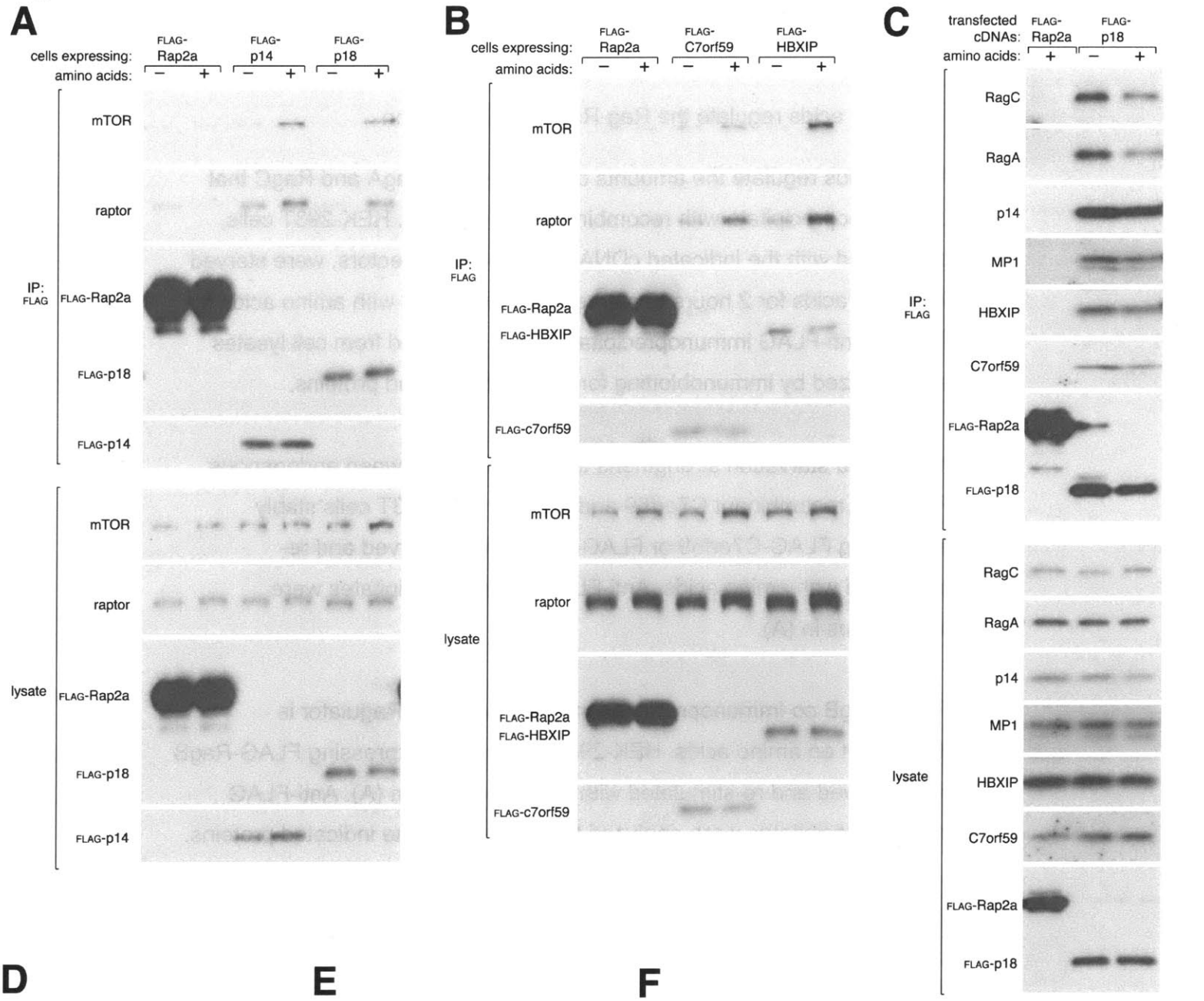
A
cells expressing:
FLAG-Rap2a
FLAG-p14
FLAG-p18
amino acids:
IP: FLAG
mTOR
raptor
FLAG-Rap2a
FLAG-p18
FLAG-p14
lysate
B
cells expressing:
FLAG-Rap2a
FLAG-C7orf59
FLAG-HBXIP
amino acids:
IP: FLAG
mTOR
raptor
FLAG-Rap2a
FLAG-HBXIP
FLAG-c7orf59
lysate
C
transfected cDNAs:
FLAG-Rap2a
FLAG-p18
amino acids:
IP: FLAG
RagC
RagA
p14
MP1
HBXIP
C7orf59
FLAG-Rap2a
FLAG-p18
lysate

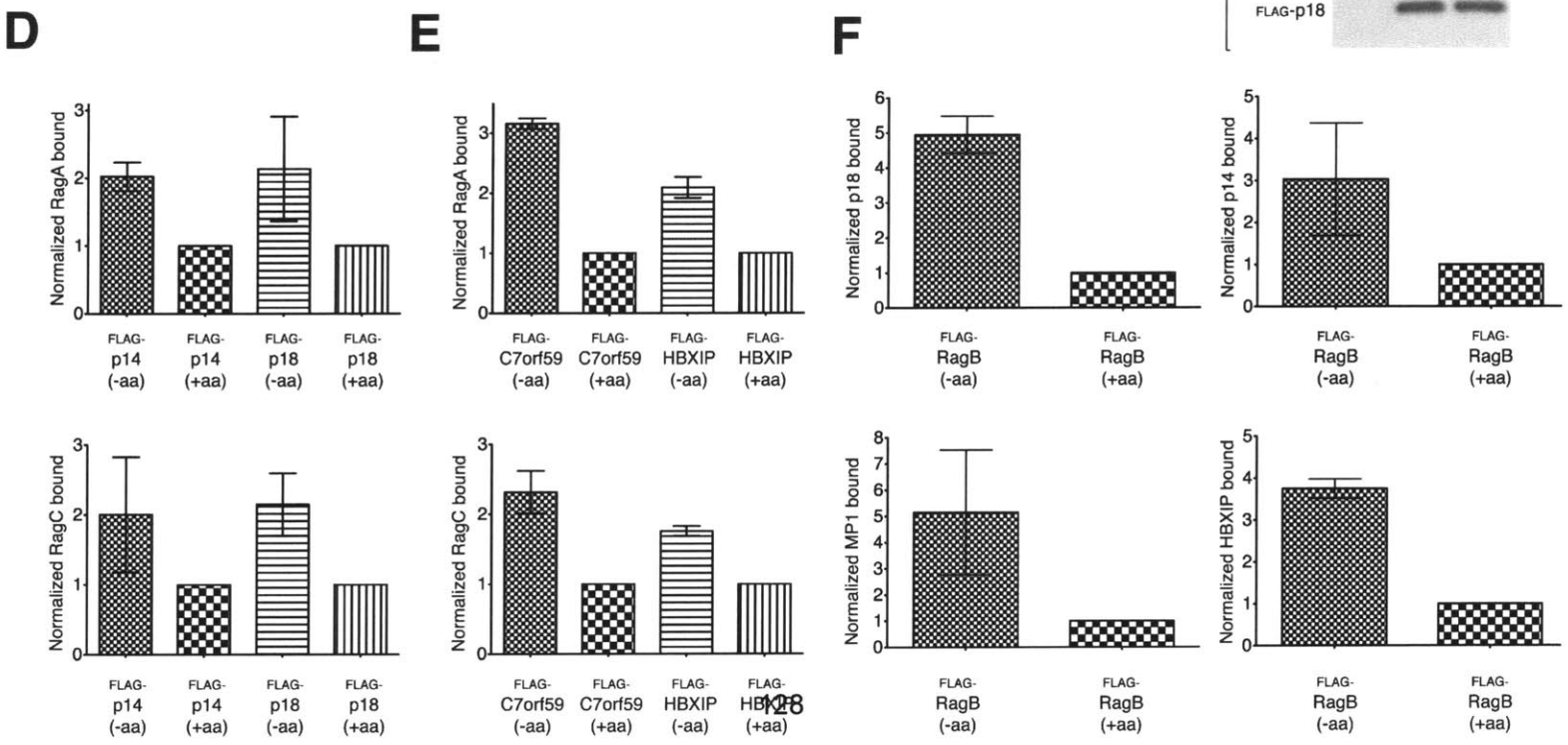
D
Normalized RagA bound
Normalized RagC bound
FLAG-p14 (-aa)
FLAG-p14 (+aa)
FLAG-p18 (-aa)
FLAG-p18 (+aa)
E
Normalized RagA bound
Normalized RagC bound
FLAG-C7orf59 (-aa)
FLAG-C7orf59 (+aa)
FLAG-HBXIP (-aa)
FLAG-HBXIP (+aa)
F
Normalized p18 bound
Normalized p14 bound
Normalized MP1 bound
Normalized HBXIP bound
FLAG-RagB (-aa)
FLAG-RagB (+aa)

Supplemental Figure 3: Amino acids regulate the Ragulator-mTORC1 interaction, related to Figure 3

A) Amino acid stimulation increases the amount of endogenous mTORC1 that co-immunoprecipitates with recombinant p14 and p18. HEK-293T cells stably expressing FLAG-p14 or FLAG-p18 were starved for amino acids for 2 hours or starved and stimulated with amino acids for 15 min. After in-cell crosslinking, anti-FLAG immunoprecipitates were prepared from cell lysates and analyzed by immunoblotting for levels of indicated proteins.

B) Amino acids regulate the amount of endogenous mTORC1 that co-immunoprecipitates with recombinant C7orf59 and HBXIP. HEK-293T cells stably expressing FLAG-C7orf59 or FLAG-HBXIP were treated as in (A) and anti-FLAG immunoprecipitates were analyzed for the levels of the indicated proteins.

C) Inter-Ragulator interactions are moderately regulated by amino acids. HEK-293T cells, transfected with the indicated cDNAs in expression vectors, were starved for amino acids for 2 hours or starved and stimulated for 15 min and anti-FLAG immunoprecipitates were analyzed for the levels of the indicated proteins.

D) Quantification of endogenous RagA and RagC binding to recombinant p14 and p18 upon amino acid starvation and re-stimulation. Each value represents the normalized mean ±SE for n=2.

E) Quantification of endogenous RagA and RagC binding to recombinant C7orf59 and HBXIP upon amino acid starvation and re-stimulation. Each value represents the normalized mean ±SE for n=2.

F) Quantification of endogenous Ragulator proteins binding to recombinant RagB upon amino acid starvation and re-stimulation. Each value represents the normalized mean ±SE for n=2.

Regulation of the Rag nucleotide-binding state is not understood, but is key for amino acid signaling to mTORC1. The amino acid-sensitive interaction between Rags and Ragulator prompted us to examine whether Ragulator might also regulate nucleotide binding to the Rags. Intriguingly, many proteins that regulate nucleoside triphosphatase (NTPases) have roadblock domains (Bowman et al., 1999; Koonin and Aravind, 2000; Miertzschke et al., 2011; Wanschers et al., 2008) which four of the five Ragulator components are likely to contain. Preliminary experiments indicated that Ragulator does not have GTPase activating protein (GAP) activity towards the Rag GTPases, and so we examined whether it might have the activity of a guanine nucleotide exchange factor (GEF). A characteristic of GEFs is their strong preference for binding nucleotide-free over nucleotide-loaded GTPases (Bos et al., 2007; Feig, 1999). Incubation with buffers containing EDTA, which chelates the magnesium ion necessary for nucleotide binding, is a common way to generate largely nucleotide-free GTPases (Wang et al., 2000). Interestingly, the presence of EDTA in the cell lysis buffer significantly increased the interaction of recombinant RagB and endogenous Ragulator proteins (Figure 4A, S4A) as well as the binding of recombinant p18 to endogenous RagA and RagC (Figure 4B). In vitro binding assays proved useful in dissecting the effects of nucleotides on the Rag-Ragulator interaction. Ragulator readily bound to the Rags in vitro, likely by displacing their nucleotides (see below), but the addition of GTP significantly weakened the interaction (Figure S4B). In a complementary experiment, highly purified Ragulator had a clear preference for interacting with a recombinant Rag heterodimer stripped of its nucleotides rather than nucleotide-bound, indicating that both in cells and in vitro Ragulator prefers binding to nucleotide-free Rags (Figure 4C). It is important to note that even when nucleotide-loaded, the Rag GTPases interact to a significant extent with Ragulator, consistent with its role as a scaffold and suggesting that the Rag-Ragulator complex can exist in interaction states of differing strengths.

To study a potential regulatory function for Ragulator, it was necessary to first determine if the nucleotide binding state of RagB or RagC is the dominant determinant of the interaction between Rag heterodimers and Ragulator. To address this issue, we generated two different classes of Rag nucleotide binding mutants (Figure 4D). In the first, a critical Thr/Ser that is necessary for stabilizing magnesium was changed to Asn,

Figure 4

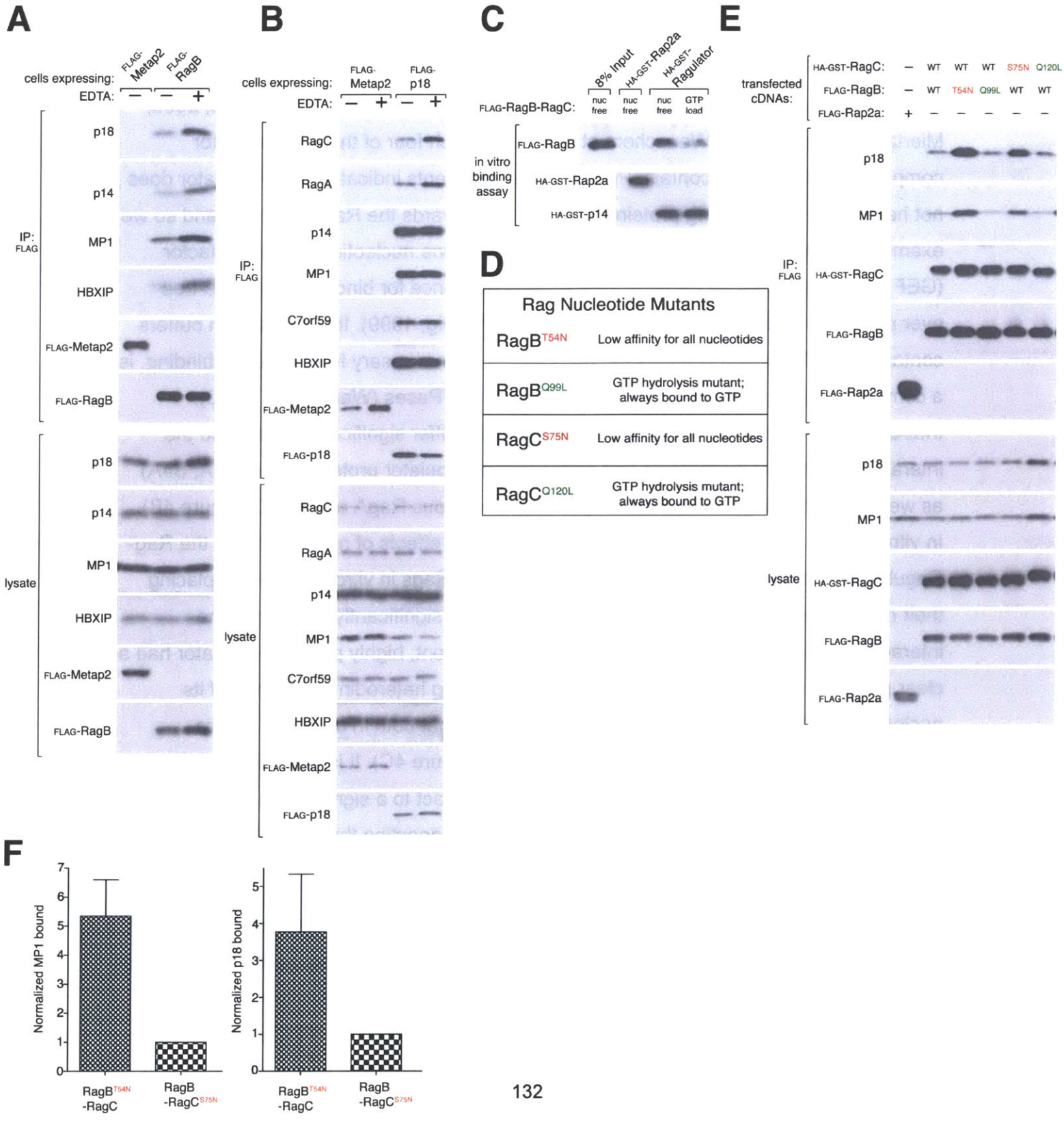
A
cells expressing:
FLAG-Metap2
FLAG-RagB
EDTA: – – +
IP: FLAG
p18
p14
MP1
HBXIP
FLAG-Metap2
FLAG-RagB
lysate
p18
p14
MP1
HBXIP
FLAG-Metap2
FLAG-RagB
B
cells expressing:
FLAG-Metap2
FLAG-p18
EDTA: – + – +
IP: FLAG
RagC
RagA
p14
MP1
C7orf59
HBXIP
FLAG-Metap2
FLAG-p18
lysate
RagC
RagA
p14
MP1
C7orf59
HBXIP
FLAG-Metap2
FLAG-p18
C
8% Input
HA-GST-Rap2a
HA-GST-Regulator
FLAG-RagB-RagC:
nuc free
nuc free
nuc free
GTP load
in vitro binding assay
FLAG-RagB
HA-GST-Rap2a
HA-GST-p14
D
Rag Nucleotide Mutants
RagB T54N — Low affinity for all nucleotides
RagB Q99L — GTP hydrolysis mutant; always bound to GTP
RagC S75N — Low affinity for all nucleotides
RagC Q120L — GTP hydrolysis mutant; always bound to GTP
E
transfected cDNAs:
HA-GST-RagC: – WT WT WT S75N Q120L
FLAG-RagB: – WT T54N Q99L WT WT
FLAG-Rap2a: + – – – – –
IP: FLAG
p18
MP1
HA-GST-RagC
FLAG-RagB
FLAG-Rap2a
lysate
p18
MP1
HA-GST-RagC
FLAG-RagB
FLAG-Rap2a
F
Normalized MP1 bound
0 1 2 3 4 5 6 7
RagB T54N -RagC
RagB -RagC S75N
Normalized p18 bound
0 1 2 3 4 5
RagB T54N -RagC
RagB -RagC S75N

Figure 4: Ragulator preferentially interacts with nucleotide-free RagB

A) EDTA increases the interaction between endogenous Ragulator and FLAG-RagB. HEK-293T cells stably expressing Flag-RagB were lysed in the absence or presence of EDTA and cell lysates and anti-FLAG immunoprecipitates analyzed by immunoblotting for the levels of the indicated proteins.

B) FLAG-p18 co-immunoprecipitates more endogenous Rags in the presence of EDTA. HEK-293T cells stably expressing FLAG-p18 were treated and analyzed as in (A).

C) Ragulator preferentially interacts with nucleotide-free Rags. In vitro binding assay in which immobilized HA-GST-Ragulator was incubated with nucleotide-free FLAG-RagB-RagC or Rag heterodimers loaded with GTP. HA-GST precipitates were analyzed for the levels of the indicated proteins.

D) Table summarizing Rag mutants used in this study.

E) The $RagB^{T54N}$ mutant preferentially interacts with endogenous Ragulator. Anti-FLAG immunoprecipitates were prepared from HEK-293T cells transfected with the indicated cDNAs in expression vectors and analyzed as in (A).

F) Quantification of endogenous MP1 and p18 binding to $RagB^{T54N}$-RagC and RagB-$RagC^{S75N}$. Each value represents the normalized mean ±SD for n=3. See also Figure S4.

Figure S4

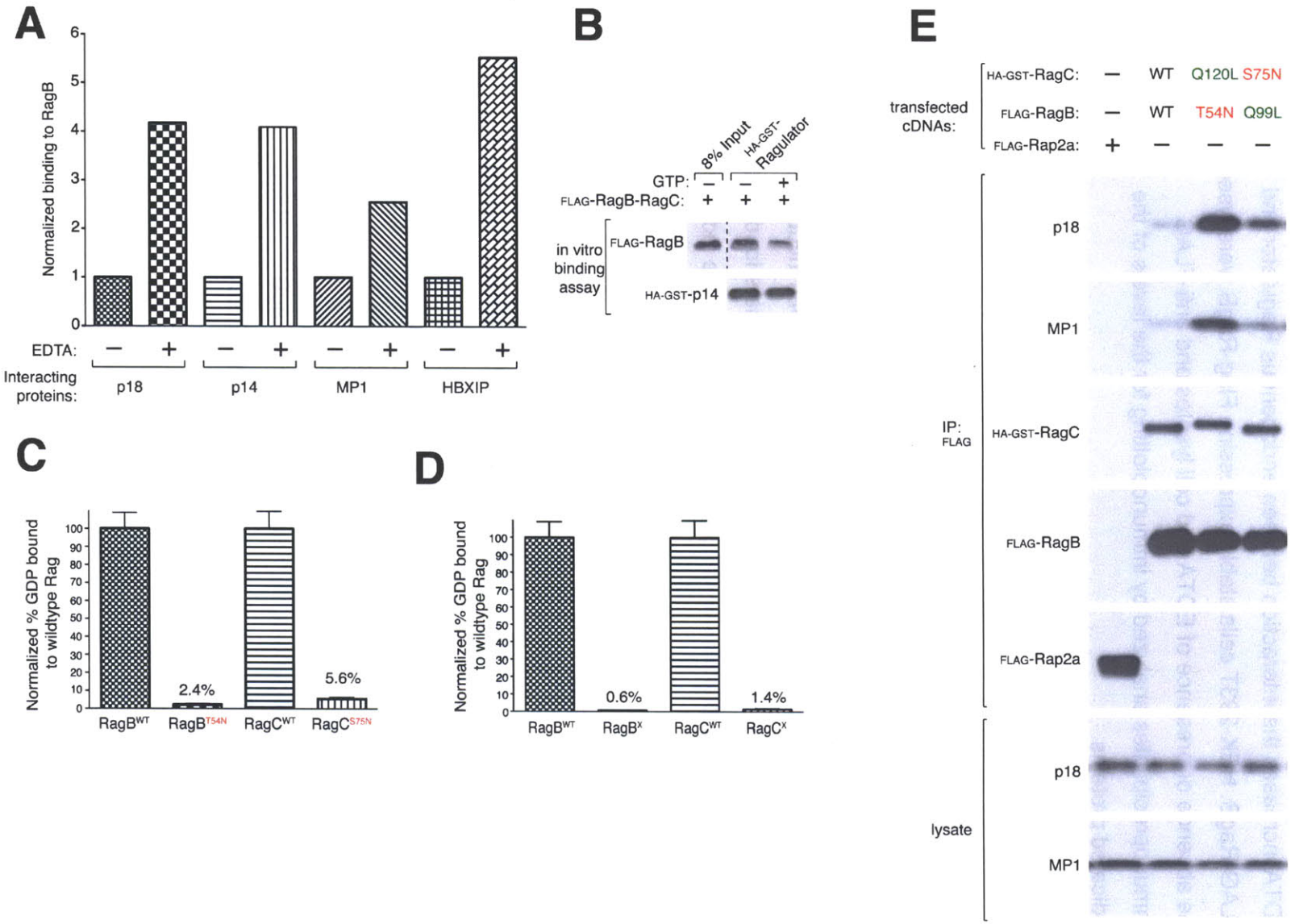
A
Normalized binding to RagB
EDTA:
Interacting proteins:
p18
p14
MP1
HBXIP
B
8% Input
HA-GST-Ragulator
GTP:
FLAG-RagB-RagC:
in vitro binding assay
FLAG-RagB
HA-GST-p14
C
Normalized % GDP bound to wildtype Rag
2.4%
5.6%
RagB^WT
RagB^T54N
RagC^WT
RagC^S75N
D
Normalized % GDP bound to wildtype Rag
0.6%
1.4%
RagB^WT
RagB^X
RagC^WT
RagC^X
E
transfected cDNAs:
HA-GST-RagC:
FLAG-RagB:
FLAG-Rap2a:
WT
Q120L
S75N
T54N
Q99L
IP: FLAG
p18
MP1
HA-GST-RagC
FLAG-RagB
FLAG-Rap2a
lysate
p18
MP1

Supplemental Figure 4: GTP destabilizes the Rag-Ragulator complex both in vitro and in vivo, related to Figure 4

A) Quantification of endogenous Ragulator proteins binding to recombinant RagB in the absence and presence of EDTA.

B) Excess GTP destabilizes the Rag-Ragulator interaction. In vitro binding assay in which FLAG-RagB-RagC was pre-bound to HA-GST-Ragulator and then further incubated in the absence or presence of GTPγS. HA-GST precipitates were analyzed by immunoblotting for the levels of the indicated proteins.

C) Quantification of the binding of GDP to $RagB^{T54N}$ or $RagC^{S75N}$. Proteins were loaded with [^{3}H]GDP and the amount of GDP bound was determined by filter-binding assays. Each value represents the normalized mean ±SD of four independent samples.

D) Quantification of binding to GDP to $RagB^{D163N}$ ($RagB^{X}$) or $RagC^{D181N}$ ($RagC^{X}$). Proteins were loaded with [^{3}H]GDP and the amount of GDP bound was determined by filter-binding assays. Each value represents the normalized mean ±SD of four independent samples.

E) The nucleotide binding state of RagB governs the Rag-Ragulator interaction. Anti-FLAG immunoprecipitates were prepared from HEK-293T cells transfected with the indicated cDNAs in expression vectors and cell lysates and immunoprecipitates were analyzed by immunoblotting for levels of indicated proteins.

resulting in mutants ($RagB^{T54N}$ and $RagC^{S75N}$) that bind negligible amounts of nucleotides (Figure S4C). The corresponding H-Ras mutant ($H\text{-}Ras^{S17N}$) also binds nucleotides poorly, but, interestingly, interacts with GEFs to a greater extent than the wild type protein (Feig, 1999; Feig and Cooper, 1988; John et al., 1993). Mutants in the second class are homologous to $H\text{-}Ras^{Q61L}$ and are constitutively bound to GTP because they lack GTPase activity ($RagB^{Q99L}$ and $RagC^{Q120L}$) (Frech et al., 1994; Krengel et al., 1990). Within cells the heterodimer of nucleotide-free RagB and wild-type RagC ($RagB^{T54N}$-RagC) interacted with Ragulator at levels 4-6 fold greater than the heterodimer of wild-type RagB and nucleotide-free RagC (RagB-$RagC^{S75N}$) (Figures 4E, 4F), suggesting that the presence or absence of nucleotide on RagB largely controls the Rag-Ragulator interaction. Consistent with this interpretation, a heterodimer of GTP-bound RagB and nucleotide-free RagC ($RagB^{Q99L}$-$RagC^{S75N}$) interacted with Ragulator much more weakly than a heterodimer with the opposite properties ($RagB^{T54N}$-$RagC^{Q120L}$) (Figure S4E). Thus, the nucleotide binding state of RagB is the major determinant of the strength of the interaction between Rag heterodimers and Ragulator.

Ragulator is a GEF for RagA and RagB

The binding properties of Ragulator are highly consistent with it having GEF activity towards RagB. To test this possibility, it was necessary to develop a way to measure GDP dissociation from one Rag and not the other. To this end, we mutated the conserved Asp to Asn in the Rag 'NKxD motif' ($RagB^{D163N}$ and $RagC^{D181N}$). This mutation changes the base specificity of a GTPase from guanine to xanthosine nucleotides (Hoffenberg et al., 1995; Schmidt et al., 1996), and we denote these mutants as $RagB^{X}$ or $RagC^{X}$ both of which bind less than 2% of the guanine nucleotides than their wild type counterparts (Figure S4D). Therefore, when we load $RagB^{X}$-RagC or RagB-$RagC^{X}$ with GDP or GTP in vitro, we know which of the Rag GTPases in the heterodimer is bound to the guanine nucleotide.

In vitro many GEFs displace GDP and GTP at similar rates from their cognate GTPases (Klebe et al., 1995; Lenzen et al., 1998; Zhang et al., 2005). Thus, we loaded

RagB^X-RagC or RagB-RagC^X heterodimers with labeled GDP or GTP and tested the effects of Ragulator on their dissociation. Ragulator did not affect GDP or GTP dissociation from the Rap2a control GTPase (Figure 5A). When tested on RagC within the RagB^X-RagC heterodimer, Ragulator modestly increased the release of GDP but not that of GTP (Figure 5B). In contrast, Ragulator greatly accelerated both GDP and GTP dissociation from RagB in the RagB-RagC^X heterodimer (Figure 5C, S5A) and did so in a dose-dependent manner (Figure S5C). As expected from the very high level of homology between RagA and RagB (Figure S1D), Ragulator also greatly increased guanine nucleotide dissociation from RagA in the RagA-RagC^X heterodimer (Figure 5D). Consistent with its function as a GEF, in a GTP binding assay in which we pre-bound RagB-RagC^X or RagA-RagC^X with unlabeled GDP and then incubated it with labeled GTP, Ragulator significantly increased GTP binding to RagB and RagA (Figure 5E, 5F, S5B).

Because the Rags function as a heterodimer, we wondered whether the nucleotide binding state of RagC might alter the function of Ragulator towards RagB. When the RagB-RagC^X heterodimer was co-loaded with either XDP or XTP in addition to GDP or GTP (Figure S5D, S5E), there was no difference in Ragulator-mediated GDP or GTP dissociation from RagB, suggesting that the nucleotide binding state of RagC does not alter Ragulator GEF activity towards RagB.

To determine if the exchange activity of Ragulator depends on a particular subunit, we tested p14-MP1, HBXIP-C7orf59, and p18 separately in the GDP exchange assay. Unlike the pentameric complex, none of these subassemblies increased GDP dissociation from RagB (Figure 5G). Likewise, trimeric Ragulators composed of either p14-MP1-p18 or HBXIP-C7orf59-p18 were no more effective at accelerating GTP dissociation from RagB than a control protein (Figure 5H). These results indicate that Ragulator is a GEF for RagA and RagB and that a pentameric Ragulator is required for this activity.

Recently, Vam6 was shown to act as a GEF for Gtr1p, the yeast ortholog of RagA and RagB, and to be necessary for the activation of the TORC1 pathway in yeast (Binda et al., 2009). However, we found that VPS39, the mammalian ortholog of VAM6, not only

Figure 5

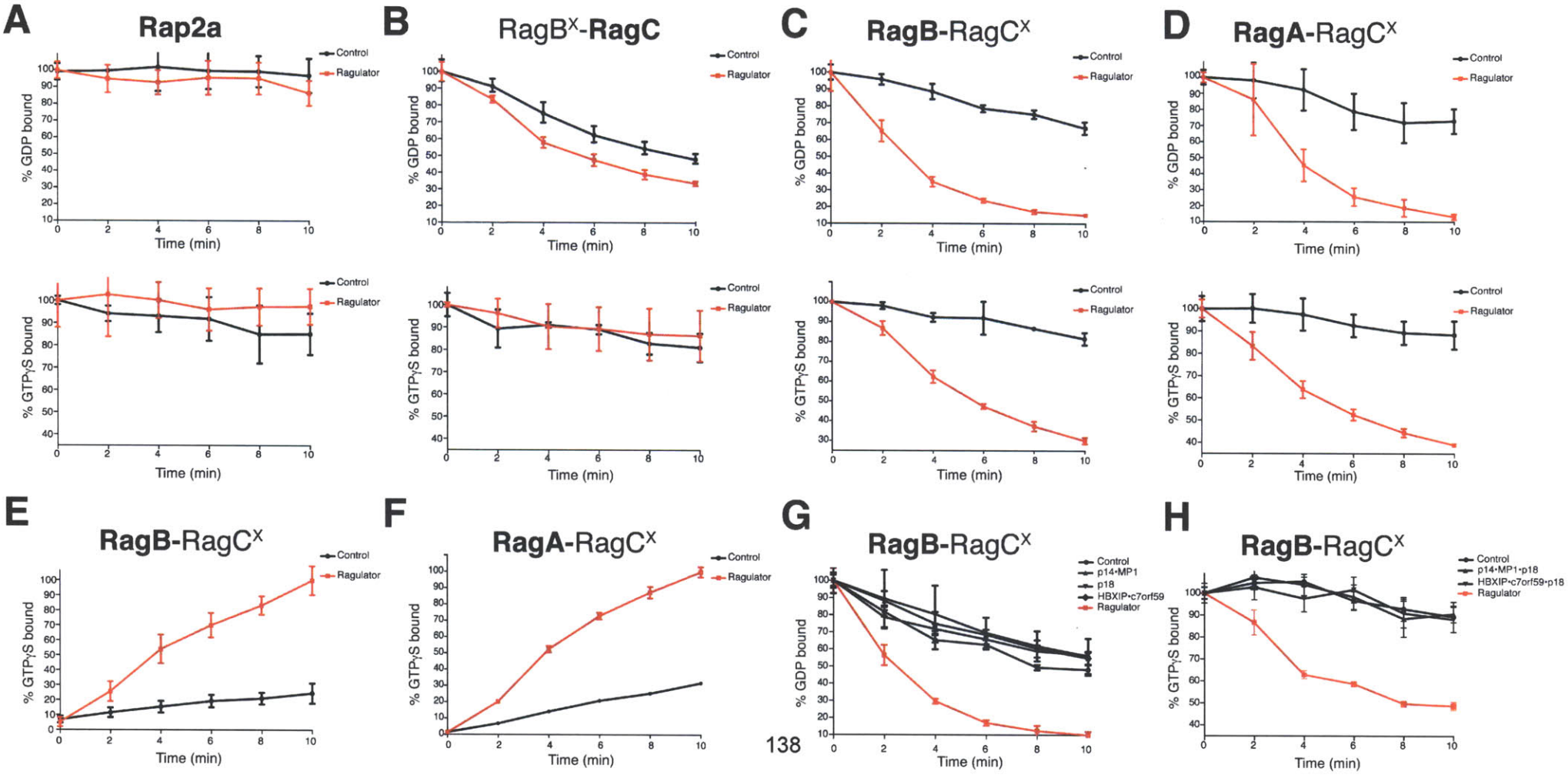
A
Rap2a
B
RagB^X-RagC
C
RagB-RagC^X
D
RagA-RagC^X
E
RagB-RagC^X
F
RagA-RagC^X
G
RagB-RagC^X
H
RagB-RagC^X
% GDP bound
% GTPγS bound
Time (min)
Control
Ragulator
p14•MP1
p18
HBXIP•c7orf59
p14•MP1•p18
HBXIP•c7orf59•p18

Figure 5: Ragulator is a GEF for RagA and RagB

A) Ragulator does not stimulate GDP or GTPγS dissociation from Rap2a. Nucleotide dissociation assay, in which Rap2a was loaded with either [^{3}H]GDP or [^{35}S]GTPγS, and incubated with Ragulator. Dissociation was monitored by a filter-binding assay. Each value represents the normalized mean ±SD for n=4.

B) Ragulator moderately stimulates GDP, but not GTPγS dissociation from RagC. RagB^{D163N}-RagC was loaded, incubated with Ragulator or a control and analyzed as in (A). Each value represents the normalized mean ±SD for n=4.

C) Ragulator greatly accelerates GDP and GTPγS dissociation from RagB. RagB-RagC^{D181N} was loaded, incubated with Ragulator or a control and analyzed as in (A). Each value represents the normalized mean ±SD for n=4.

D) Ragulator substantially increases GDP and GTPγS dissociation from RagA. RagA-RagC^{D181N} was loaded with nucleotide, incubated with Ragulator or a control and analyzed as in (A). Each value represents the normalized mean ±SD for n=4.

E) Ragulator accelerates GTPγS binding to RagB. RagB-RagC^{D181N} was loaded with GDP and incubated with Ragulator or a control and [^{35}S]GTPγS. [^{35}S]GTPγS binding was determined as in (A). Each value represents the normalized mean ±SD for n=4.

Figure S5

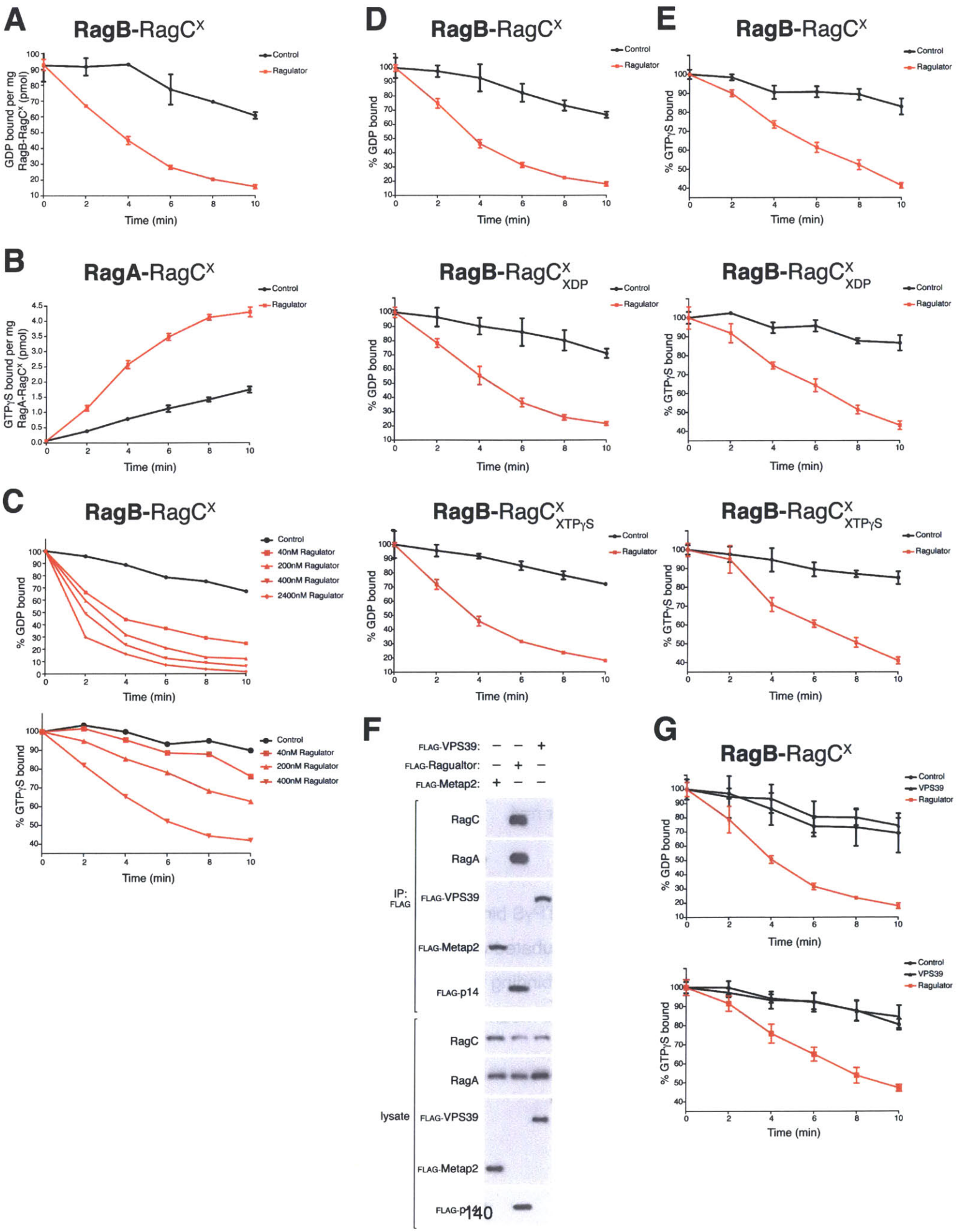
A
RagB-RagCX
GDP bound per mg RagB-RagCX (pmol)
Time (min)
Control
Ragulator
B
RagA-RagCX
GTPγS bound per mg RagA-RagCX (pmol)
C
RagB-RagCX
% GDP bound
% GTPγS bound
40nM Ragulator
200nM Ragulator
400nM Ragulator
2400nM Ragulator
D
RagB-RagCX
RagB-RagCX XDP
RagB-RagCX XTPγS
E
% GTPγS bound
F
FLAG-VPS39:
FLAG-Ragualtor:
FLAG-Metap2:
IP: FLAG
lysate
RagC
RagA
FLAG-VPS39
FLAG-Metap2
FLAG-p14
G
VPS39

Supplemental Figure 5: The nucleotide state of RagC does not alter Ragulator activity towards RagB and VPS39 does not function as a GEF for RagB, related to Figure 5

A) Ragulator stimulates GDP dissociation from RagB. Nucleotide dissociation assay in which RagB-RagC^{D181N} was loaded with [^{3}H]GDP and incubated with Ragulator or a control. Dissociation was monitored by a filter-binding assay and is reported as pmols of [^{3}H]GDP per mg of RagB-RagC^{D181N}. Each value represents the normalized mean ±SD for n=4.

B) Ragulator increases GTPγS binding to RagA. RagA-RagC^{D181N} loaded with GDP was incubated with Ragulator or a control and [^{35}S]GTPγS. [^{35}S]GTPγS binding was determined as in (A) and is reported as pmols of [^{35}S]GTPγS per mg of RagA-RagC^{D181N}. Each value represents the normalized mean ±SD for n=4.

C) Ragulator stimulates GDP and GTPγS dissociation in a dose dependent manner. Dissociation assay in which RagB-RagC^{D181N} was loaded with either [^{3}H]GDP or [^{35}S]GTPγS, and incubated with the indicated amounts of Ragulator and analyzed as in (A). Each value represents the normalized mean of two independent samples.

D) The nucleotide-binding state of RagC does not alter Ragulator-mediated GDP dissociation from RagB. Dissociation assay in which RagB-RagC^{D181N} was loaded with either XDP or XTPγS and [^{3}H]GDP and incubated with Ragulator or a control and analyzed as in (A). Each value represents the normalized mean ±SD for n=4.

E) Ragulator-mediated GTP dissociation from RagB is not affected by RagC nucleotide binding. Dissociation assay in which RagB-RagC^{D181N} was loaded with either XDP or XTPγS and [^{35}S]GTPγS and incubated with

Ragulator or a control and analyzed as in (A). Each value represents the normalized mean ±SD for n=4.

F) VPS39 does not interact with endogenous Rags. Anti-FLAG immunoprecipitates were prepared from HEK-293T cells transfected with the indicated cDNAs in expression vectors. Cell lysates and immunoprecipitates were analyzed by immunoblotting for levels of indicated proteins.

G) VPS39 does not stimulate GDP or GTP dissociation from RagB. Dissociation assay in which RagB-RagC^{D181N} was loaded with either [^{3}H]GDP or [^{35}S]GTPγS, and incubated with either VPS39, Ragulator or a control and analyzed as in (A). Each value represents the normalized mean ±SD for n=4.

failed to interact with endogenous RagA (Figure S5F) but also did not stimulate GDP or GTP dissociation from RagB (Figure S5G). These findings suggest that VPS39 is not a GEF for RagA or RagB and that the amino acid sensing mechanisms of yeast and higher eukaryotes have diverged.

The v-ATPase controls Ragulator function in cells

The v-ATPase is a positive regulator of the mTORC1 signaling pathway that acts downstream of amino acids and upstream of the Rags (Zoncu et al., 2011a). The v-ATPase consists of V0 and V1 domains, two multi-subunit complexes (Forgac, 2007), both of which interact with Ragulator (Zoncu et al., 2011a). Interestingly, amino acid starvation and re-stimulation strengthens and weakens the V1-Ragulator interaction, respectively, while v-ATPase inhibition prevents regulation of the interaction by locking it in the amino acid-free state. Because the v-ATPase, unlike Ragulator, is not required to maintain the Rag GTPases on the lysosomal surface (Zoncu et al., 2011a), it must have an important function distinct from the control of Rag localization. Given its regulated interaction with Ragulator, it seemed likely that the v-ATPase might regulate the GEF activity of Ragulator. To test this possibility, we used the amino acid-sensitive interaction between the Rag heterodimers and Ragulator as a marker of Ragulator GEF activity in cells. Consistent with the nucleotide loaded state of RagB determining the Rag-Ragulator interaction, in cells stably expressing the GTP-bound $RagB^{Q99L}$ mutant, the interaction between Ragulator and $RagB^{Q99L}$ was no longer regulated by amino acids and resembled the weak Rag-Ragulator interaction observed in amino acid stimulated cells (Figure 6A). Interestingly, pre-treatment of cells with the v-ATPase inhibitors Salicylihalamide A (SalA) (Xie et al., 2004) or Concanamycin A (ConA) (Bowman et al., 2004), prevented amino acid stimulation from weakening the Rag-Ragulator interaction, which remained at the strong level observed in the absence of amino acids (Figures 6A, 6B, S6A). Importantly, v-ATPase inhibition did not affect the already weak interaction between the $RagB^{Q99L}$ mutant and Ragulator (Figure 6A). Thus, regulation of the Rag-Ragulator interaction depends on the v-ATPase, which is necessary to transmit the amino acid signal to the GEF activity of Ragulator.

Figure 6

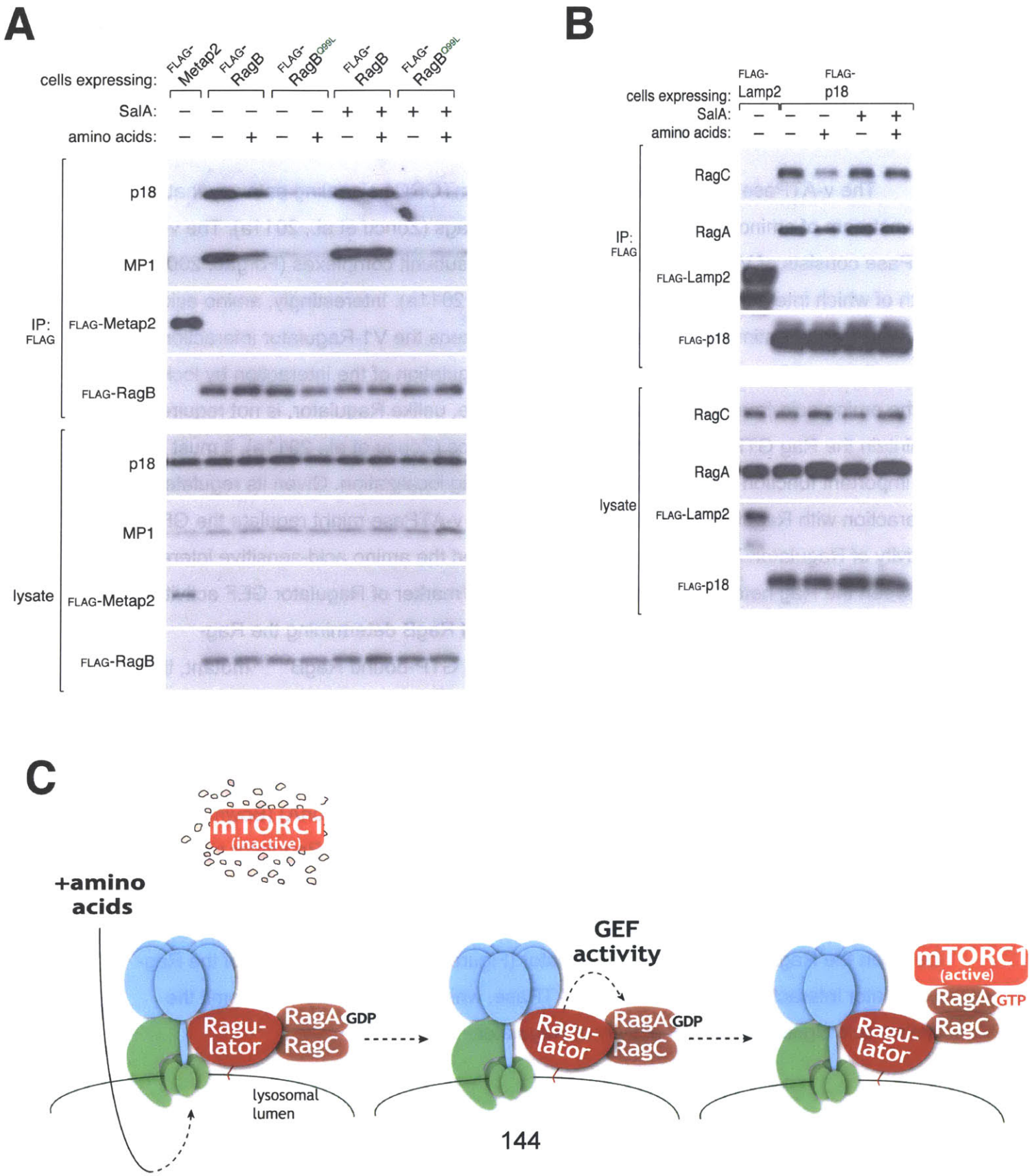
A
cells expressing:
FLAG-Metap2
FLAG-RagB
FLAG-RagB Q99L
FLAG-RagB
FLAG-RagB Q99L
SalA:
amino acids:
IP: FLAG
p18
MP1
FLAG-Metap2
FLAG-RagB
lysate
p18
MP1
FLAG-Metap2
FLAG-RagB
B
cells expressing:
FLAG-Lamp2
FLAG-p18
SalA:
amino acids:
IP: FLAG
RagC
RagA
FLAG-Lamp2
FLAG-p18
lysate
RagC
RagA
FLAG-Lamp2
FLAG-p18
C
mTORC1 (inactive)
+amino acids
Ragu-lator
RagA GDP
RagC
lysosomal lumen
GEF activity
Ragu-lator
RagA GDP
RagC
mTORC1 (active)
Ragu-lator
RagA GTP
RagC

Figure 6: The v-ATPase controls the function of Ragulator

A) The v-ATPase functions upstream of the regulated binding between Rags and Ragulator. HEK-293T cells stably expressing FLAG-RagB or FLAG-$RagB^{Q99L}$ were starved for 2 hours or starved and stimulated with amino acids for 15 min in the absence or presence of the v-ATPase inhibitor SalA. Cell lysates and anti-FLAG immunoprecipitates were analyzed by immunoblotting for the levels of the indicated proteins.

B) Inactivation of the v-ATPase blocks the amino acid dependent Rag-Ragulator interaction. HEK-293T cells stably expressing FLAG-p18 were treated as in (B). Anti-FLAG immunoprecipitates were analyzed for the levels of the indicated proteins.

C) Model for amino-acid induced mTORC1 activation. In the absence of amino acids the v-ATPase, Ragulator, and Rags exist in a tightly bound super complex and mTORC1 cannot associate with the lysosomal surface and remains inactive. Amino acid accumulation in the lysosomal lumen generates an activating signal that is transmitted in a v-ATPase-dependent fashion to activate the GEF activity of Ragulator towards RagA. Upon RagA-GTP loading, the Rag-Ragulator interaction weakens and mTORC1 is recruited to the lysosomal surface where it interacts with Rheb and becomes activated. Rheb is not shown.

Figure S6

A

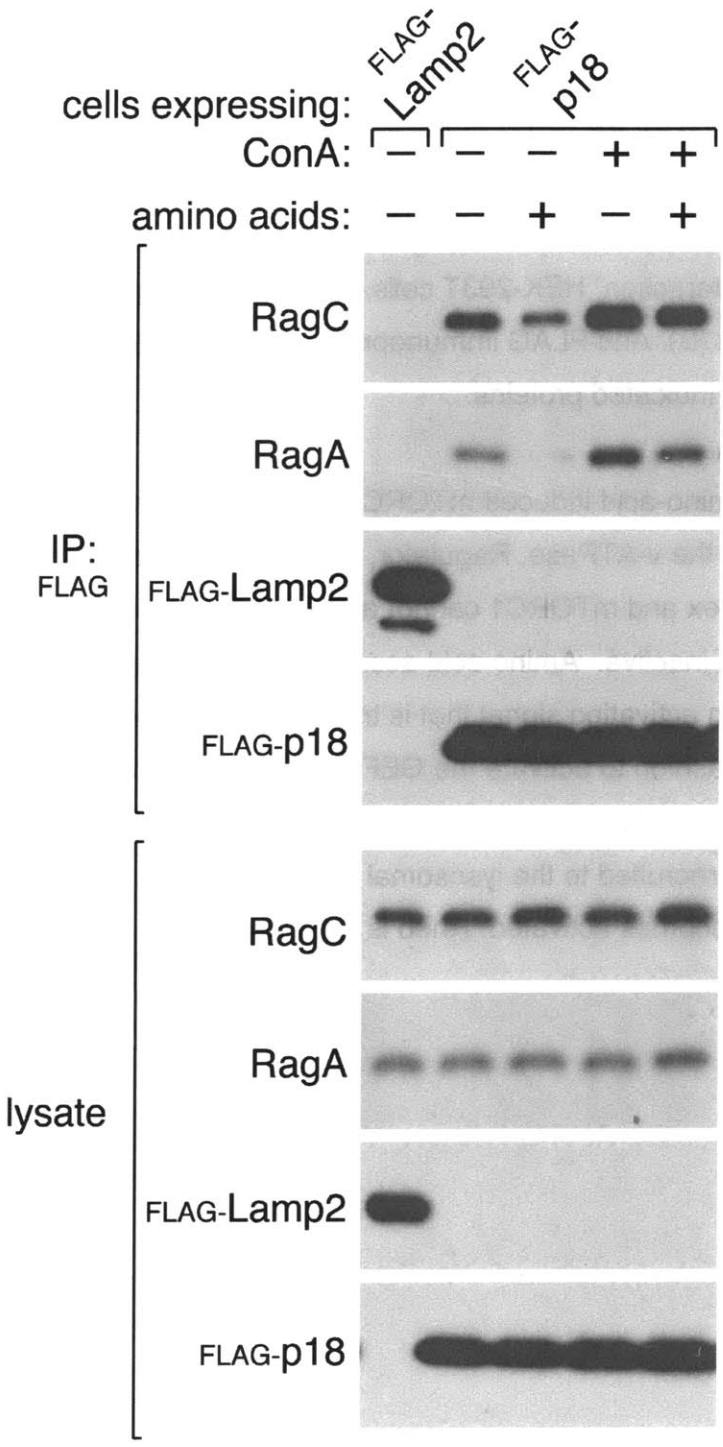
cells expressing:
FLAG-Lamp2
FLAG-p18
ConA: – – – + +
amino acids: – – + – +
IP: FLAG
RagC
RagA
FLAG-Lamp2
FLAG-p18
lysate
RagC
RagA
FLAG-Lamp2
FLAG-p18

Supplemental Figure 6: v-ATPase inhibition decreases the regulated interaction between Rags and Ragulator

A) Inactivation of the v-ATPase inhibits the amino acid dependent regulated interaction between Ragulator and Rags. HEK-293T cells stably expressing FLAG-p18 were starved for amino acids for 2 hours or starved and stimulated with amino acids for 15 min in the absence or presence of the v-ATPase inhibitor ConA. Cell lysates and anti-FLAG immunoprecipitates were analyzed by immunoblotting for the levels of the indicated proteins.

Discussion

In this study we identify HBXIP and C7orf59 as two novel components of the mTORC1 pathway. In association with known Ragulator proteins (p18, p14 and MP1), HBXIP and C7orf59 form a pentameric complex that is essential for localizing the Rag GTPases to the lysosomal surface and activating mTORC1 in response to amino acids. In addition to being a scaffold, Ragulator promotes nucleotide exchange of RagB and of the highly related RagA. Thus, we identify a key link in the signaling cascade that converts a signal emanating from amino acids into the nucleotide loading of the Rags and ultimately the recruitment of mTORC1 to the lysosomal surface. We suggest that C7orf59 and HBXIP be renamed LAMTOR4 and LAMTOR5, respectively, to reflect their critical roles in regulating the mTORC1 pathway and to be consistent with the naming convention of other Ragulator components.

Our in vitro binding results and secondary structure predictions, combined with available structural data, support the following molecular architecture for pentameric Ragulator: p18 is a lysosome-associated scaffold protein that binds two roadblock-containing heterodimers, p14-MP1 and HBXIP-C7orf59, and thereby tethers them to the lysosome. In vitro and in vivo data suggest that all five members of Ragulator must be present to efficiently interact with the Rag heterodimers, although the stoichiometry between the two complexes is unknown. The recently reported crystal structure of a Gtr1p-Gtr2p heterodimer, the yeast orthologs of mammalian Rags, reveals the presence of roadblock domains in the C-terminal portion of both GTPases, a structural feature that the C-terminal domains of the Rags are also predicted to have (Gong et al., 2011). Thus, the roadblock domain may represent the basic architectural element of the Ragulator-Rag complex.

Several proteins that interact with NTPases have a roadblock domain, suggesting that it may have regulatory functions as well as structural ones (Koonin and Aravind, 2000). The recently solved crystal structure of the bacterial GAP, MglB, shows that it contains a roadblock domain and may promote GTP hydrolysis through stabilization of the catalytic machinery of its cognate GTPase (Miertzschke et al., 2011). Consistent with a possible regulatory role for proteins with this domain, Ragulator prefers to bind to

nucleotide-free rather than nucleotide-bound RagB. These binding properties are characteristic of other GEF-GTPase interactions and suggested that Ragulator might be a GEF for RagA and RagB. To test this hypothesis, it was necessary to develop a system for monitoring the nucleotide bound to an individual Rag in a heterodimer containing two of them. To this end, we made use of Rag complexes containing a wild type Rag that binds guanine nucleotides and a Rag^X mutant that cannot. We suggest that the Rag^X mutants may be useful reagents for the identification of other factors that control the nucleotide-loading state of the Rags. Ragulator greatly increases both GDP and GTP dissociation from RagB and RagA but not RagC. The preferential GEF activity of Ragulator for RagB and RagA likely stems from differences between the RagA/B and the RagC switch I/II regions, which are known to serve as a critical recognition motif on a GTPase for its cognate GEF (Fiegen et al., 2006; Jonathan, 1998). In addition, the intrinsic rapid GDP dissociation capacity of RagC suggests that a GEF might not be necessary for it. Rather, other regulators, namely guanine dissociation inhibitors, which block GDP dissociation (Garcia-Mata et al., 2011; Jennings and Pavitt, 2010), might have a more prominent role in the regulation of GTP binding by RagC.

Protein scaffolds encompass one of the most diverse sets of signaling molecules in cells. Recent studies have suggested that in addition to bringing multiple proteins together, some scaffolds also have catalytic functions. *E. coli* uses the catalytic scaffold EspG to inhibit host intracellular trafficking by bringing together the Arf1 GTPase and Pak2 kinase as well as blocking Arf1-GAP assisted-GTP hydrolysis and activating Pak2 kinase activity (Selyunin et al., 2011). Similarly, by binding to both Rags and the v-ATPase, Ragulator not only physically connects two major regulators of mTORC1 but also transmits the amino acid signal from the v-ATPase to the Rags through its GEF activity.

Our inability to detect GEF activity in partial assemblies of Ragulator implies that multiple surfaces, which exist only on the pentameric Ragulator are required to endow it with exchange activity. Recently, TRAPPI, a multi-protein tethering complex was identified as a GEF for YPT1 (Jones et al., 2000; Wang et al., 2000). Like Ragulator, the

GEF activity of the TRAPPI complex is not contained in one subunit, but requires the presence of multiple components (Cai et al., 2008).

The likely presence of roadblock domains in the C-terminal regions of all four Rags raises the tantalizing possibility that one Rag may directly regulate the nucleotide cycle of the other. The solution of a Rag-Ragulator structure will greatly enhance our understanding of the function of the roadblock domain in this system and the precise mechanism by which Ragulator activates RagA and RagB. While Ragulator is the first factor identified that directly regulates Rag nucleotide binding, we anticipate the identification of other Rag regulatory proteins such as GAPs that will help explain how amino acid starvation inactivates the Rags and by extension the mTORC1 pathway.

The regulated interaction between Rags and Ragulator depends on amino acids and the nucleotide binding state of RagA and RagB and provides an in-cell output for the activity of Ragulator and the pathway downstream of it. Using this assay, we find that inhibition of the v-ATPase inactivates Ragulator. The fact that the v-ATPase is required for mTORC1 activation, functions downstream of amino acids but upstream of RagA/B nucleotide loading, and interacts with Ragulator, suggests a model in which the v-ATPase links an amino acid-generated signal to the activation of the Ragulator GEF activity (Figure 6C).

There are many possible functions for the regulated interaction between the Rags and Ragulator. In one model, the Rag-Ragulator complex exists in two conformations that are determined by amino acid availability: a tightly bound state, which cannot interact with mTORC1, and an open one that favors mTORC1 recruitment to the lysosomal surface. Upon amino acid stimulation, Ragulator promotes GTP loading of RagA/B, leading to a weakening of Ragulator-Rag binding and a conformation that may expose an mTORC1-binding surface on the Rag GTPases. A precedent for such a nutrient-dependent conformational change exists within mTORC1. Conditions that inhibit the mTORC1 pathway result in a stronger association between mTOR and raptor with a concomitant decrease in in vitro kinase activity, and conditions that activate result in a weaker interaction and greater in vitro activity (Kim et al., 2002).

Alternatively, or in addition to the first model, the regulated interaction might be necessary for the Rags to reversibly leave the lysosomal surface. During starvation conditions, Ragulator would hold Rags at the lysosome. Upon amino acid stimulation, Rags may dissociate from Ragulator when RagA/B binds GTP, capture mTORC1 in the cytoplasm, and then shuttle it back to the lysosome by re-associating with Ragulator. Many GTPases are known to cycle on and off membranes in a nucleotide dependent manner (Hutagalung and Novick, 2011), and Rag cycling may provide a physical means to ferry mTORC1 to the lysosome. Future work combining structural studies and dynamic live cell imaging will clarify the mechanistic aspects of the regulation of Rag-mTORC1 binding, and how mTORC1 is ferried to the lysosome.

Materials and Methods

Cell lysis and immunoprecipitation

Cells were rinsed once with ice-cold PBS and lysed with Chaps lysis buffer (0.3% Chaps, 10 mM β-glycerol phosphate, 10 mM pyrophosphate, 40 mM Hepes pH 7.4, 2.5 mM $MgCl_2$ and 1 tablet of EDTA-free protease inhibitor [Roche] per 25 ml). Where specified in the figures, Chaps lysis buffer was supplemented with 12.5 mM EDTA. When only cell lysates were required (i.e., no immunoprecipitation was to be performed), 1% Triton X-100 was substituted for Chaps. When the interaction between Ragulator and mTORC1 was interrogated, in cell cross-linking with DSP was preformed as described in (Sancak et al., 2008) prior to cell lysis. The soluble fractions of cell lysates were isolated by centrifugation at 13,000 rpm in a microcentrifuge for 10 minutes. For immunoprecipitations, primary antibodies were added to the cleared lysates and incubated with rotation for 1.5 hours at 4°C. 60 μl of a 50% slurry of protein G-sepharose was then added and the incubation continued for an additional 1 hour. Immunoprecipitates were washed three times with lysis buffer containing 150 mM NaCl. Immunoprecipitated proteins were denatured by the addition of 20 μl of sample buffer and boiling for 5 minutes, resolved by 8%–16% SDS-PAGE, and analyzed by immunoblotting as described (Kim et al., 2002). For anti-FLAG-immunoprecipitations, the FLAG-M2 affinity gel was washed with lysis buffer 3 times. 20 μl of a 50% slurry of the affinity gel was then added to cleared cell lysates and incubated with rotation for 2 hours at 4°C. The beads were washed 3 times with lysis buffer containing 150 mM NaCl. Immunoprecipitated proteins were denatured by the addition of 50 μl of sample buffer and boiling for 5 minutes.

For co-transfection experiments, 2,000,000 HEK293T cells were plated in 10 cm culture dishes. Twenty-four hours later, cells were transfected with the pRK5-based cDNA expression plasmids indicated in the figures in the following amounts: 100 ng or 1000 ng FLAG- or HA-HBXIP; 100 ng or 1000 ng FLAG- or HA-HBXIP; 100 ng or 1000 ng FLAG-p14; 100 ng HA-MP1; 100 ng or 1000 ng FLAG- or HA-p18; 100 ng or 1000 ng FLAG-Rap2a; 300 ng Flag-Metap2; 300 ng Flag-VPS39; 100 ng Flag- or HA-RagB and 100 ng HA- or HA-GST-RagC. The total amount of plasmid DNA in each transfection was

normalized to 2 µg with empty pRK5. Thirty-six hours after transfection, cells were lysed as described above.

Identification of HBXIP and C7orf59

Immunoprecipitates from HEK-293T cells stably expressing FLAG-p18, FLAG-p14, FLAG-RagB or FLAG-Metap2 were prepared using Chaps lysis buffer as described above. Proteins were eluted with the FLAG peptide (sequence DYKDDDDK) from the FLAG-M2 affinity gel, resolved on 4-12% NuPage gels (Invitrogen), and stained with simply blue stain (Invitrogen). Each gel lane was sliced into 10-12 pieces and the proteins in each gel slice digested overnight with trypsin. The resulting digests were analyzed by mass spectrometry as described (Sancak et al., 2008). Peptides corresponding to HBXIP and C7orf59 were identified in the FLAG-p14, FLAG-p18 and FLAG-RagB immunoprecipitates, while no peptides were detected in negative control immunoprecipitates of FLAG-Metap2.

Total amino acid starvation and stimulation, leucine starvation and stimulation, Salicylihalamide A and Concanamycin A treatment

HEK-293T cells in culture dishes or coated glass cover slips were rinsed with and incubated in amino acid-free RPMI or leucine-free RPMI for either 50 minutes or 2 hours, and stimulated with a 10X mixture of total amino acids or 10X leucine for 10-20 minutes, respectively. After stimulation, the final concentration of amino acids in the media was the same as in RPMI. The 10X mixture of total amino acids was prepared from individual powders of amino acids. Where drug treatment was performed, cells were incubated with 2.5 µm of Salicylihalamide A or 2.5 µm of Concanamycin A during the 2 hour starvation period and the 15 min stimulation period.

RNAi in mammalian cells

On day one, 200,000 HEK-293T cells were plated in a 6 well plate. Twenty-fours hours later, the cells were transfected with 250 nM of a pool of siRNAs [Dharmacon] targeting HBXIP or C7orf59, a non-targeting pool, or 125 nM of siRNAs targeting p14 or

p18. On day four, the cells were transfected again but this time with double the amount of siRNAs. On day five, the cells were either split onto coated glass cover slips or rinsed with ice-cold PBS, lysed and subjected to immunobloting as described above.

In vitro binding assays

For the binding reactions, 20 µl of a 50% slurry containing immobilized HA-GST-tagged proteins were incubated in binding buffer (1% Triton X-100, 2.5mM $MgCl_2$, 40 mM Hepes pH 7.4, 2 mM DTT and 1mg/ml BSA) with 2 µg of FLAG-tagged proteins in a total volume of 50 µl for 1 hour and 30 minutes at 4°C. In binding assays where HA-GST-Ragulator was used, HA-GST-p14-MP1 was pre-bound to FLAG-HBXIP-HA-C7orf59 and FLAG-p18 for 5 minutes at 4°C prior to the addition of other FLAG-tagged proteins. In experiments where the Flag-RagB-HA-RagC heterodimer was loaded with nucleotide, 2 µg of FLAG-RagB-HA-RagC was incubated at 25°C for 10 minutes in Rag loading buffer (0.3% Chaps, 40 mM Hepes pH 7.4, 5 mM EDTA, 2 mM DTT and 1 mg/ml BSA) supplemented with 1 mM GTPγS in a total volume of 10 µl. The Rag-nucleotide complex was stabilized by the addition of 20 mM $MgCl_2$ and incubated for an additional 5 minutes at 25°C. In assays with nucleotide free Rags, 2 µg of FLAG-RagB-HA-RagC was added to the binding assay with 3 µl of Calf-alkaline phosphatase (NEB). Binding assays in which Ragulator was incubated with nucleotide-loaded or -free Rags were conducted at 4°C for 45 minutes. For the nucleotide competition assay, 2 µg FLAG-RagB-HA-RagC was pre-bound to Ragulator proteins for 30 minutes followed by the addition of 1 mM GTPγS and further incubated for 1 hour and 30 minutes at 4°C. To terminate all binding assays, samples were washed 3 times with 1 ml of ice-cold binding buffer supplemented with 150 mM NaCl followed by the addition of 50 µl of sample buffer.

Nucleotide exchange (GEF) assays

40 pmols of FLAG-RagB^{D163N}-HA-RagC, FLAG-RagC^{D181N}-HA-RagB or FLAG-Rap2a were loaded with either 2 µM of [^{3}H]GDP (25-50 Ci/mmol), 10 µCi of [^{35}S]GTPγS

(1250 Ci/mmol), 2 mM GDP (for GTP binding assays), or co-loaded with guanine nucleotides and either 50 nM of XTPγS or 50 nM XDP (Ragulator GEF activity was maintained between a range of 5-500 nM xanthine nucleotide) in a total volume of 100 µl of Rag loading buffer as described above. The GTPase-[^{3}H]GDP-XDP/ XTPγS or GTPase-[^{35}S]GTPγS-XDP/ XTPγS and GTPase-GDP complexes were stabilized by addition of 20 mM $MgCl_2$ followed by a further incubation at 4°C for 12 hours or 25°C for 5 minutes, respectively. To initiate the GEF assay, 40 pmols of pentameric Ragulator, the indicated Ragulator subcomplexes or a control (FLAG-Metap2, FLAG-VPS39, or FLAG-HBXIP-HA-C7orf59) were added along with 200 µM GTPγS or 5 µCi of [^{35}S]GTPγS (for GTP binding assays) and incubated at 25°C. Samples were taken every 2 minutes and spotted on nitrocellulose filters, which were washed with 2 ml of wash buffer (40 mM Hepes pH 7.4, 150 mM NaCl and 5 mM $MgCl_2$). Filter-associated radioactivity was measured using a TriCarb scintillation counter (Perkin Elmer).

Materials

Reagents were obtained from the following sources: antibodies to ATP6V1B2 and LAMP2 from Abcam; antibodies to phospho-T389 S6K1, S6K1, RagA, RagC, p14, p18, MP1, C7orf59, HBXIP mTOR, phospho-T398 dS6K, and the FLAG epitope from Cell Signaling Technology; HRP-labeled anti-mouse, and anti-rabbit secondary antibodies from Santa Cruz Biotechnology; antibody to the HA tag from Bethyl laboratories; RPMI, FLAG M2 affinity gel, GTPγS, GDP, Chaps, Triton, and amino acids from Sigma Aldrich; [^{3}H]GDP and [^{35}S]GTPγS from Perkin Elmer; protein G-sepharose and immobilized glutathione beads from Pierce; FuGENE 6 and Complete Protease Cocktail from Roche; Alexa 488 and 568-conjugated secondary antibodies, Schneider's media, Express Five Drosophila-SFM, and Inactivated Fetal Calf Serum (IFS) from Invitrogen; amino acid-free RPMI, and amino acid free Schneider's media from US Biological; siRNAs targeting indicated genes and siRNA transfection reagent from Dharmacon; human cDNA encoding HBXIP from Open Biosystems; Concanamycin A from A. G. Scientific; nitrocellulose membrane filters from Advantec; calf-alkaline phosphatase from NEB. The dS6K antibody was a generous gift from Mary Stewart (North Dakota State University). Salicylihalamide A (SalA) was a generous gift from Jeff DeBrabander (UT

Southwestern).

RNAi in Drosophila S2 cells

dsRNAs against *Drosophila HBXIP* and *C7orf59* genes were designed as described in (Sancak et al., 2008). Primer sequences used to amplify DNA templates for dsRNA synthesis for dHBXIP and, dC7orf59 including underlined 5' and 3' T7 promoter sequences, are as follows:

dHBXIP (CG14812)
Forward primer:
GAATTAATACGACTCACTATAGGGAGAGGAGAAAGTCCTAGCGGAAATC
Reverse primer:
GAATTAATACGACTCACTATAGGGAGAGCTTGAAGATAACGCCTGTGAT

dC7orf59 (CG14977)
Forward primer:
GAATTAATACGACTCACTATAGGGAGACTGATACTAAAGGAAGATGGAGCAG
Reverse primer:
GAATTAATACGACTCACTATAGGGAGAGTATATTCTACGGTTGGACATGCAG

dsRNAs targeting GFP and dRagC were used as positive and negative controls, respectively. On day one, 4,000,000 S2 cells were plated in 6-cm culture dishes in 5 ml of Express Five SFM media. Cells were transfected with 1 μg of dsRNA per million cells using Fugene (Roche). Two days later, a second round of dsRNA transfection was performed. On day five, cells were rinsed once with amino acid-free Schneider's medium, and starved for amino acids by replacing the media with amino acid-free Schneider's medium for 1.5 hours. To stimulate with amino acids, the amino acid-free medium was replaced with complete Schneider's medium for 30 minutes. Cells were then washed with ice cold PBS, lysed, and subjected to immunoblotting for phospho-T398 dS6K and total dS6K.

Immunofluorescence assays

Immunofluorescence assays were performed as described in (Sancak et al., 2010). Briefly, 200,000 HEK-293T cells were plated on fibronectin-coated glass coverslips in 12-well tissue culture plates. Twenty-four hours later, the slides were rinsed with PBS once and fixed for 15 min with 4% paraformaldehyde in PBS at room temperature. The slides were rinsed twice with PBS and cells were permeabilized with 0.05% Triton X-100 in PBS for 5 min. After rinsing twice with PBS, the slides were incubated with primary antibody in 5% normal donkey serum for 1 hr at room temperature, rinsed four times with PBS, and incubated with secondary antibodies produced in donkey (diluted 1:1000 in 5% normal donkey serum) for 45 min at room temperature in the dark and washed four times with PBS. Slides were mounted on glass coverslips using Vectashield (Vector Laboratories) and imaged on a spinning disk confocal system (Perkin Elmer) or a Zeiss Laser Scanning Microscope (LSM) 710.

In immunofluorescence assays where HBXIP or C7orf59 were co-localized with p18, HEK-293T cells were seeded and processed as described above with the following exceptions. Immediately after seeding, cells were transfected with the following constructs (all cDNAs were expressed from pRK5 expression plasmid): 50 ng Flag-HBXIP, 50 ng HA-p14, 50 ng HA-MP1, 50 ng HA-C7orf59 and 50 ng HA-p18; or 50 ng Flag-C7orf59, 50 ng HA-p14, 50 ng HA-MP1, 50 ng HA-HBXIP and 50 ng HA-p18. The cells were processed the following day.

Cell size determinations

For measurements of cell size, HEK-293T cells treated with siRNAs as described above were harvested by trypsinization in a 4 ml volume and diluted 1:20 with counting solution (Isoton II Diluent, Beckman Coulter). Cell diameters were determined with a particle size counter (Coulter Z2, Beckman Coulter) running Coulter Z2 AccuComp software.

Protein purification of recombinant Rag heterodimers and Ragulator

To produce protein complexes used for GEF or in vitro binding assays, 4,000,000 HEK-293T cells were plated in 15 cm culture dishes. Forty-eight hours later, cells were transfected separately with the following constructs (all cDNAs were expressed from

pRK5 expression plasmid). For pentameric Ragulator: 4 µg Flag-p14, 8 µg HA-MP1, 8 µg HA-p18^{G2A} (a lipidation defective mutant), 8 µg HA-HBXIP, and 8 µg HA-C7orf59. For trimeric Ragulator complexes: 8 µg FLAG-p14, 16 µg HA-MP1 and 16 µg HA-p18^{G2A}; or 8 µg FLAG-HBXIP, 16 µg HA-C7orf59 and 16 µg HA-p18^{G2A}. For dimeric complexes: 8 µg FLAG-p14 and 16 µg HA-MP1; 8 µg FLAG-HBXIP and 16 µg HA-C7orf59; 8 µg of HA-GST-p14 and 16 µg of MP1; 8 µg FLAG-RagB^{D163N} and 16 µg HA-RagC; 8 µg FLAG-RagC^{D181N} and 16 µg HA-RagB; or 8 µg FLAG-RagB and 16 µg HA-RagC. For individual proteins: 10 µg Flag-p18^{G2A}; 10 µg Flag-Metap2; 15 µg Flag-VPS39; 10 µg HA-GST-HBXIP, 10 µg HA-GST-C7orf59; or 10 µg HAGST-Rap2a

Thirty-six hours post transfection cell lysates were prepared as described above and either 200 µl of a 50% slurry of glutathione affinity beads or 200 µl of a 50% slurry of FLAG-M2 affinity gel were added to lysates from cells expressing HA-GST-tagged or FLAG-tagged proteins, respectively. Recombinant proteins were immunoprecipitated for 3 hours at 4°C. Each sample was washed once with Triton lysis buffer, followed by 3 washes with Triton lysis buffer supplemented with 500 mM NaCl. Samples containing FLAG-tagged proteins were eluted from the FLAG-M2 affinity gel with a competing FLAG peptide as described above.

Monomeric Rag GDP loading

40 pmols of FLAG-RagB, FLAG-RagB^{S54N}, FLAG-RagB^{D163N}, FLAG-RagC, FLAG-RagC^{T75N} or FLAG-RagC^{D181N} were loaded with 2 µM of [^{3}H]GDP as described for Rag heterodimers, but $MgCl_2$ stabilization lasted for 5 min at 25°C. The amount of [^{3}H]GDP bound to monomeric Rags was determined with a filter binding assay and was normalized to [^{3}H]GDP binding by wild type RagB or RagC.

Acknowledgements

We thank all members of the Sabatini Lab for helpful suggestions and Eric Spooner for mass spectrometric analyses of samples. This work was supported by grants from the NIH (CA103866 and AI47389) and Department of Defense (W81XWH-07-0448) to D.M.S., awards from the LAM Foundation to D.M.S, and fellowship support from the LAM Foundation and from the Jane Coffin Childs Memorial Fund for Medical Research to R.Z. D.M.S. is an investigator of the Howard Hughes Medical Institute.

References

Binda, M., PÈli-Gulli, M.-P., Bonfils, G., Panchaud, N., Urban, J., Sturgill, T.W., Loewith, R., and De Virgilio, C. (2009). The Vam6 GEF Controls TORC1 by Activating the EGO Complex. Mol Cell *35*, 563-573.

Bos, J.L., Rehmann, H., and Wittinghofer, A. (2007). GEFs and GAPs: critical elements in the control of small G proteins. Cell *129*, 865-877.

Bowman, A.B., Patel-King, R.S., Benashski, S.E., McCaffery, J.M., Goldstein, L.S., and King, S.M. (1999). Drosophila roadblock and Chlamydomonas LC7: a conserved family of dynein-associated proteins involved in axonal transport, flagellar motility, and mitosis. J Cell Biol *146*, 165-180.

Bowman, E.J., Graham, L.A., Stevens, T.H., and Bowman, B.J. (2004). The bafilomycin/concanamycin binding site in subunit c of the V-ATPases from Neurospora crassa and Saccharomyces cerevisiae. J Biol Chem *279*, 33131-33138.

Cai, Y., Chin, H.F., Lazarova, D., Menon, S., Fu, C., Cai, H., Sclafani, A., Rodgers, D.W., De La Cruz, E.M., Ferro-Novick, S., *et al.* (2008). The Structural Basis for Activation of the Rab Ypt1p by the TRAPP Membrane-Tethering Complexes. Cell *133*, 1202-1213.

Cortez, D., Guntuku, S., Qin, J., and Elledge, S.J. (2001). ATR and ATRIP: Partners in Checkpoint Signaling. Science *294*, 1713-1716.

Dubouloz, F., Deloche, O., Wanke, V., Cameroni, E., and De Virgilio, C. (2005). The TOR and EGO protein complexes orchestrate microautophagy in yeast. Mol Cell *19*, 15-26.

Feig, L.A. (1999). Tools of the trade: use of dominant-inhibitory mutants of Ras-family GTPases. Nat Cell Biol *1*, E25-27.

Feig, L.A., and Cooper, G.M. (1988). Inhibition of NIH 3T3 cell proliferation by a mutant ras protein with preferential affinity for GDP. Mol Cell Biol *8*, 3235-3243.

Fiegen, D., Dvorsky, R., and Ahmadian, M.R. (2006). Structural Principles of Ras Interaction with Regulators and Effectors

RAS Family GTPases. In, C. Der, ed. (Springer Netherlands), pp. 45-66.

Fingar, D.C., Salama, S., Tsou, C., Harlow, E., and Blenis, J. (2002). Mammalian cell size is controlled by mTOR and its downstream targets S6K1 and 4EBP1/eIF4E. Genes Dev *16*, 1472-1487.

Forgac, M. (2007). Vacuolar ATPases: rotary proton pumps in physiology and pathophysiology. Nat Rev Mol Cell Biol *8*, 917-929.

Frech, M., Darden, T.A., Pedersen, L.G., Foley, C.K., Charifson, P.S., Anderson, M.W., and Wittinghofer, A. (1994). Role of glutamine-61 in the hydrolysis of GTP by p21H-ras: an experimental and theoretical study. Biochemistry *33*, 3237-3244.

Fujii, R., Zhu, C., Wen, Y., Marusawa, H., Bailly-Maitre, B., Matsuzawa, S., Zhang, H., Kim, Y., Bennett, C.F., Jiang, W., *et al.* (2006). HBXIP, cellular target of hepatitis B virus oncoprotein, is a regulator of centrosome dynamics and cytokinesis. Cancer Res *66*, 9099-9107.

Gao, M., and Kaiser, C.A. (2006). A conserved GTPase-containing complex is required for intracellular sorting of the general amino-acid permease in yeast. Nat Cell Biol *8*, 657-667.
Garcia-Mata, R., Boulter, E., and Burridge, K. (2011). The 'invisible hand': regulation of RHO GTPases by RHOGDIs. Nat Rev Mol Cell Biol *12*, 493-504.

Garcia-Saez, I., Lacroix, F.B., Blot, D., Gabel, F., and Skoufias, D.A. (2011). Structural characterization of HBXIP: the protein that interacts with the anti-apoptotic protein survivin and the oncogenic viral protein HBx. J Mol Biol *405*, 331-340.

Gong, R., Li, L., Liu, Y., Wang, P., Yang, H., Wang, L., Cheng, J., Guan, K.L., and Xu, Y. (2011). Crystal structure of the Gtr1p-Gtr2p complex reveals new insights into the amino acid-induced TORC1 activation. Genes Dev *25*, 1668-1673.

Good, M.C., Zalatan, J.G., and Lim, W.A. (2011). Scaffold proteins: hubs for controlling the flow of cellular information. Science *332*, 680-686.

Hara, K., Yonezawa, K., Weng, Q.P., Kozlowski, M.T., Belham, C., and Avruch, J. (1998). Amino acid sufficiency and mTOR regulate p70 S6 kinase and eIF-4E BP1 through a common effector mechanism. J Biol Chem *273*, 14484-14494.

Hirose, E., Nakashima, N., Sekiguchi, T., and Nishimoto, T. (1998). RagA is a functional homologue of S. cerevisiae Gtr1p involved in the Ran/Gsp1-GTPase pathway. J Cell Sci *111 (Pt 1)*, 11-21.

Hoffenberg, S., Nikolova, L., Pan, J.Y., Daniel, D.S., Wessling-Resnick, M., Knoll, B.J., and Dickey, B.F. (1995). Functional and structural interactions of the Rab5 D136N mutant with xanthine nucleotides. Biochem Biophys Res Commun *215*, 241-249.

Howell, J.J., and Manning, B.D. (2011). mTOR couples cellular nutrient sensing to organismal metabolic homeostasis. Trends Endocrinol Metab *22*, 94-102.

Hutagalung, A.H., and Novick, P.J. (2011). Role of Rab GTPases in membrane traffic and cell physiology. Physiol Rev *91*, 119-149.

Jennings, M.D., and Pavitt, G.D. (2010). eIF5 has GDI activity necessary for translational control by eIF2 phosphorylation. Nature *465*, 378-381.

John, J., Rensland, H., Schlichting, I., Vetter, I., Borasio, G.D., Goody, R.S., and Wittinghofer, A. (1993). Kinetic and structural analysis of the Mg(2+)-binding site of the guanine nucleotide-binding protein p21H-ras. J Biol Chem *268*, 923-929.

Jonathan, G. (1998). Structural Basis for Activation of ARF GTPase: Mechanisms of Guanine Nucleotide Exchange and GTP,ÄìMyristoyl Switching. Cell *95*, 237-248.

Jones, S., Newman, C., Liu, F., and Segev, N. (2000). The TRAPP complex is a nucleotide exchanger for Ypt1 and Ypt31/32. Mol Biol Cell *11*, 4403-4411.

Kim, D.-H., Sarbassov, D.D., Ali, S.M., King, J.E., Latek, R.R., Erdjument-Bromage, H., Tempst, P., and Sabatini, D.M. (2002). mTOR Interacts with Raptor to Form a Nutrient-Sensitive Complex that Signals to the Cell Growth Machinery. Cell *110*, 163-175.

Kim, E., Goraksha-Hicks, P., Li, L., Neufeld, T.P., and Guan, K.L. (2008). Regulation of TORC1 by Rag GTPases in nutrient response. Nat Cell Biol *10*, 935-945.

Klebe, C., Prinz, H., Wittinghofer, A., and Goody, R.S. (1995). The kinetic mechanism of Ran--nucleotide exchange catalyzed by RCC1. Biochemistry *34*, 12543-12552.

Koonin, E.V., and Aravind, L. (2000). Dynein light chains of the Roadblock/LC7 group belong to an ancient protein superfamily implicated in NTPase regulation. Curr Biol *10*, R774-776.

Krengel, U., Schlichting, I., Scherer, A., Schumann, R., Frech, M., John, J., Kabsch, W., Pai, E.F., and Wittinghofer, A. (1990). Three-dimensional structures of H-ras p21 mutants: molecular basis for their inability to function as signal switch molecules. Cell *62*, 539-548.

Kurzbauer, R., Teis, D., de Araujo, M.E., Maurer-Stroh, S., Eisenhaber, F., Bourenkov, G.P., Bartunik, H.D., Hekman, M., Rapp, U.R., Huber, L.A., *et al.* (2004). Crystal structure of the p14/MP1 scaffolding complex: how a twin couple attaches mitogen-activated protein kinase signaling to late endosomes. Proc Natl Acad Sci U S A *101*, 10984-10989.

Lenzen, C., Cool, R.H., Prinz, H., Kuhlmann, J., and Wittinghofer, A. (1998). Kinetic analysis by fluorescence of the interaction between Ras and the catalytic

domain of the guanine nucleotide exchange factor Cdc25Mm. Biochemistry *37*, 7420-7430.

Lunin, V.V., Munger, C., Wagner, J., Ye, Z., Cygler, M., and Sacher, M. (2004). The structure of the MAPK scaffold, MP1, bound to its partner, p14. A complex with a critical role in endosomal map kinase signaling. J Biol Chem *279*, 23422-23430.

Ma, X.M., and Blenis, J. (2009). Molecular mechanisms of mTOR-mediated translational control. Nat Rev Mol Cell Biol *10*, 307-318.

Marusawa, H., Matsuzawa, S., Welsh, K., Zou, H., Armstrong, R., Tamm, I., and Reed, J.C. (2003). HBXIP functions as a cofactor of survivin in apoptosis suppression. Embo J *22*, 2729-2740.

Melegari, M., Scaglioni, P.P., and Wands, J.R. (1998). Cloning and characterization of a novel hepatitis B virus x binding protein that inhibits viral replication. J Virol *72*, 1737-1743.

Miertzschke, M., Koerner, C., Vetter, I.R., Keilberg, D., Hot, E., Leonardy, S., Sogaard-Andersen, L., and Wittinghofer, A. (2011). Structural analysis of the Ras-like G protein MglA and its cognate GAP MglB and implications for bacterial polarity. Embo J *30*, 4185-4197.

Nada, S., Hondo, A., Kasai, A., Koike, M., Saito, K., Uchiyama, Y., and Okada, M. (2009). The novel lipid raft adaptor p18 controls endosome dynamics by anchoring the MEK-ERK pathway to late endosomes. Embo J *28*, 477-489.

Roccio, M., Bos, J.L., and Zwartkruis, F.J. (2006). Regulation of the small GTPase Rheb by amino acids. Oncogene *25*, 657-664.

Sancak, Y., Bar-Peled, L., Zoncu, R., Markhard, A.L., Nada, S., and Sabatini, D.M. (2010). Ragulator-Rag complex targets mTORC1 to the lysosomal surface and is necessary for its activation by amino acids. Cell *141*, 290-303.

Sancak, Y., Peterson, T.R., Shaul, Y.D., Lindquist, R.A., Thoreen, C.C., Bar-Peled, L., and Sabatini, D.M. (2008). The Rag GTPases bind raptor and mediate amino acid signaling to mTORC1. Science *320*, 1496-1501.

Schmidt, G., Lenzen, C., Simon, I., Deuter, R., Cool, R.H., Goody, R.S., and Wittinghofer, A. (1996). Biochemical and biological consequences of changing the specificity of p21ras from guanosine to xanthosine nucleotides. Oncogene *12*, 87-96.

Schurmann, A., Brauers, A., Massmann, S., Becker, W., and Joost, H.G. (1995). Cloning of a novel family of mammalian GTP-binding proteins (RagA, RagBs,

RagB1) with remote similarity to the Ras-related GTPases. J Biol Chem *270*, 28982-28988.

Sekiguchi, T., Hirose, E., Nakashima, N., Ii, M., and Nishimoto, T. (2001). Novel G proteins, Rag C and Rag D, interact with GTP-binding proteins, Rag A and Rag B. J Biol Chem *276*, 7246-7257.

Selyunin, A.S., Sutton, S.E., Weigele, B.A., Reddick, L.E., Orchard, R.C., Bresson, S.M., Tomchick, D.R., and Alto, N.M. (2011). The assembly of a GTPase-kinase signalling complex by a bacterial catalytic scaffold. Nature *469*, 107-111.

Smith, E.M., Finn, S.G., Tee, A.R., Browne, G.J., and Proud, C.G. (2005). The tuberous sclerosis protein TSC2 is not required for the regulation of the mammalian target of rapamycin by amino acids and certain cellular stresses. J Biol Chem *280*, 18717-18727.

Stocker, H., Radimerski, T., Schindelholz, B., Wittwer, F., Belawat, P., Daram, P., Breuer, S., Thomas, G., and Hafen, E. (2003). Rheb is an essential regulator of S6K in controlling cell growth in Drosophila. Nat Cell Biol *5*, 559-565.

Wang, F.Z., Sha, L., Zhang, W.Y., Wu, L.Y., Qiao, L., Li, N., Zhang, X.D., and Ye, L.H. (2007). Involvement of hepatitis B X-interacting protein (HBXIP) in proliferation regulation of cells. Acta Pharmacol Sin *28*, 431-438.

Wang, W., Sacher, M., and Ferro-Novick, S. (2000). TRAPP stimulates guanine nucleotide exchange on Ypt1p. J Cell Biol *151*, 289-296.

Wanschers, B., van de Vorstenbosch, R., Wijers, M., Wieringa, B., King, S.M., and Fransen, J. (2008). Rab6 family proteins interact with the dynein light chain protein DYNLRB1. Cell Motil Cytoskeleton *65*, 183-196.

Wen, Y., Golubkov, V.S., Strongin, A.Y., Jiang, W., and Reed, J.C. (2008). Interaction of hepatitis B viral oncoprotein with cellular target HBXIP dysregulates centrosome dynamics and mitotic spindle formation. J Biol Chem *283*, 2793-2803.

Wunderlich, W., Fialka, I., Teis, D., Alpi, A., Pfeifer, A., Parton, R.G., Lottspeich, F., and Huber, L.A. (2001). A novel 14-kilodalton protein interacts with the mitogen-activated protein kinase scaffold mp1 on a late endosomal/lysosomal compartment. J Cell Biol *152*, 765-776.

Xie, X.S., Padron, D., Liao, X., Wang, J., Roth, M.G., and De Brabander, J.K. (2004). Salicylihalamide A inhibits the V0 sector of the V-ATPase through a mechanism distinct from bafilomycin A1. J Biol Chem *279*, 19755-19763.

Zhang, B., Zhang, Y., Shacter, E., and Zheng, Y. (2005). Mechanism of the guanine nucleotide exchange reaction of Ras GTPase--evidence for a GTP/GDP displacement model. Biochemistry *44*, 2566-2576.

Zoncu, R., Bar-Peled, L., Efeyan, A., Wang, S., Sancak, Y., and Sabatini, D.M. (2011a). mTORC1 senses lysosomal amino acids through an inside-out mechanism that requires the vacuolar H(+)-ATPase. Science *334*, 678-683.

Zoncu, R., Efeyan, A., and Sabatini, D.M. (2011b). mTOR: from growth signal integration to cancer, diabetes and ageing. Nat Rev Mol Cell Biol *12*, 21-35.

Chapter 4

A tumor suppressor complex with GAP activity for the Rag GTPases that signal amino acid sufficiency to mTORC1

Liron Bar-Peled[1,2,8], Lynne Chantranupong[1,2,8], Andrew D. Cherniack[4], Walter W. Chen[1,2], Kathleen A. Ottina[1,2], Brian C. Grabiner[1,2], Eric D. Spear[7], Scott L. Carter[4], Matthew Meyerson[4,5,6], and David M. Sabatini[1,2,3,4]

[1]Whitehead Institute for Biomedical Research and Massachusetts Institute of Technology, Department of Biology, Nine Cambridge Center, Cambridge, MA 02142, USA

[2]Koch Institute for Integrative Cancer Research, 77 Massachusetts Avenue, Cambridge, MA 02139, USA

[3]Howard Hughes Medical Institute, Department of Biology, Massachusetts Institute of Technology, Cambridge, MA 02139, USA

[4]Broad Institute of Harvard and Massachusetts Institute of Technology, 7 Cambridge Center, Cambridge, Cambridge MA 02142, USA

[5]Department of Medical Oncology, Dana-Farber Cancer Institute, Harvard Medical School, 450 Brookline Avenue, Boston, MA 02215, USA.

[6]Department of Pathology, Harvard Medical School, 25 Shattuck Street, Boston, MA 02115, USA.

[7]Department of Cell Biology, John Hopkins University School of Medicine, Baltimore, MD 21205, USA.

[8]These authors contributed equally to this work

This work has been published in:
Bar-Peled L., Chantranupong L., Cherniack A. D., Chen W. W., Ottina K. A., Grabiner, Spear E. A., Carter S. L., Meyerson M., and Sabatini D. M. (2013). A tumor suppressor complex with GAP activity for the Rag GTPases that signal amino acid sufficiency to mTORC1. *Science* 340: 1100-1106.

Experiments in figures 1, 2, 3, 4, 5, S1, S2, S3, S4 and S5 were preformed by LBP. Experiments in figures 2, 4, 5, S1, S2, S3, S4 and S5 were preformed by LC. Analysis in figures 5 and S5 were preformed by ADC. Experiments in figure S5 were preformed by WWC.

Summary

The mTOR Complex 1 (mTORC1) pathway promotes cell growth in response to many cues, including amino acids, which act through the Rag GTPases to promote mTORC1 translocation to the lysosomal surface, its site of activation. Although progress has been made in identifying positive regulators of the Rags, it is unknown if negative factors also exist. Here, we identify GATOR as a complex that interacts with the Rags and is composed of two subcomplexes we call GATOR1 and 2. Inhibition of GATOR1 subunits (DEPDC5, Nprl2, and Nprl3) makes mTORC1 signaling resistant to amino acid deprivation. In contrast, inhibition of GATOR2 subunits (Mios, WDR24, WDR59, Seh1L, Sec13) suppresses mTORC1 signaling and epistasis analysis shows that GATOR2 negatively regulates DEPDC5. GATOR1 has GTPase activating protein (GAP) activity for RagA and RagB and its components are mutated in human cancer. In cancer cells with inactivating mutations in GATOR1, mTORC1 is hyperactive and insensitive to amino acid starvation and such cells are hypersensitive to rapamycin, an mTORC1 inhibitor. Thus, we identify a key negative regulator of the Rag GTPases and reveal that, like other mTORC1 regulators, Rag function can be deregulated in cancer.

Introduction

The mTOR complex 1 (mTORC1) kinase is a master regulator of growth and its deregulation is common in human disease, including cancer and diabetes (*1*). In response to a diverse set of environmental inputs, including amino acid levels, mTORC1 regulates many anabolic and catabolic processes, such as protein synthesis and autophagy (*1, 2*). The sensing of amino acids by mTORC1 initiates from within the lysosomal lumen (*3*) and requires a signaling machine associated with the lysosomal membrane that consists of the Rag GTPases (*4, 5*), the Ragulator complex (*6, 7*), and the vacuolar ATPase (v-ATPase) (*3*). The Rag GTPases exist as obligate heterodimers of RagA or RagB, which are highly homologous, with either RagC or RagD, which are also very similar to each other (*4, 5, 8*). Through a poorly understood mechanism requiring the v-ATPase, luminal amino acids activate the guanine nucleotide exchange factor (GEF) activity of Ragulator towards RagA/B that, when GTP-loaded, recruits mTORC1 to the lysosomal surface (*7*). There, mTORC1 interacts with its activator Rheb, which is regulated by many upstream signals, including growth factors (*1*). Upon amino acid withdrawal RagA/B become GDP-bound (*4*) and mTORC1 leaves the lysosomal surface, leading to its inhibition. The negative regulators that inactivate the Rag GTPases are unknown.

Results and Discussion

We suspected that important regulators of the Rags might have escaped prior identification because their interactions with the Rags are too weak to persist under standard purification conditions. Thus, to preserve unstable protein complexes (*9*), we treated human embryonic kidney (HEK)-293T cells expressing FLAG-tagged RagB with a chemical cross-linker, and identified via mass spectrometry proteins that co-immunoprecipitate with FLAG-RagB. This analysis revealed the presence in the immunoprecipitates of known Rag interacting proteins as well as Mios, a 100 kDa WD40-repeat protein not previously studied (Fig. S1A). Consistent with this finding, endogenous RagA and RagC co-immunoprecipitated with recombinant Mios expressed in HEK-293T cells and isolated under similar purification conditions (Fig. 1A). Suppression of Mios, by RNA interference (RNAi) in human cells, strongly inhibited the amino acid-induced activation of mTORC1, as detected by the phosphorylation state of its substrate S6K1 (Fig. 1B, S2B). Moreover, in *Drosophila* S2 cells, dsRNAs targeting Mio (*10*), the fly ortholog of Mios, ablated dTORC1 signaling and also reduced cell size (Fig. 1, C, and D). Thus, in human and fly cells, Mios is necessary for amino acid signaling to TORC1.

In vitro we failed to detect a strong interaction between purified Mios and the Rag heterodimers, suggesting that within cells other components exist that are needed for complex formation. Indeed, in FLAG-Mios immunoprecipitates prepared from HEK-293T cells, we detected 7 additional proteins (WDR24, WDR59, Seh1L, Sec13, DEPDC5, Nprl2, and Nprl3) by mass spectrometry. The proteins varied in abundance, however, with much greater amounts of WDR24, WDR59, Seh1L, and Sec13 co-immunoprecipitating with Mios than DEPDC5, Nprl2, and Nprl3 (Fig. S1B). In contrast, in FLAG-DEPDC5 immunoprecipitates, Nprl2 and Nprl3 were more abundant than Mios, WDR24, WDR59, Seh1L, and Sec13 and experiments with FLAG-Nprl2 gave analogous results (Fig. S1B). These findings suggest that two subcomplexes exist, one consisting of Mios, WDR24, WDR59, Seh1L, and Sec13, and the other of DEPDC5, Nprl2, and Nprl3. To test this notion, we co-expressed FLAG-WDR24 or FLAG-Nprl2

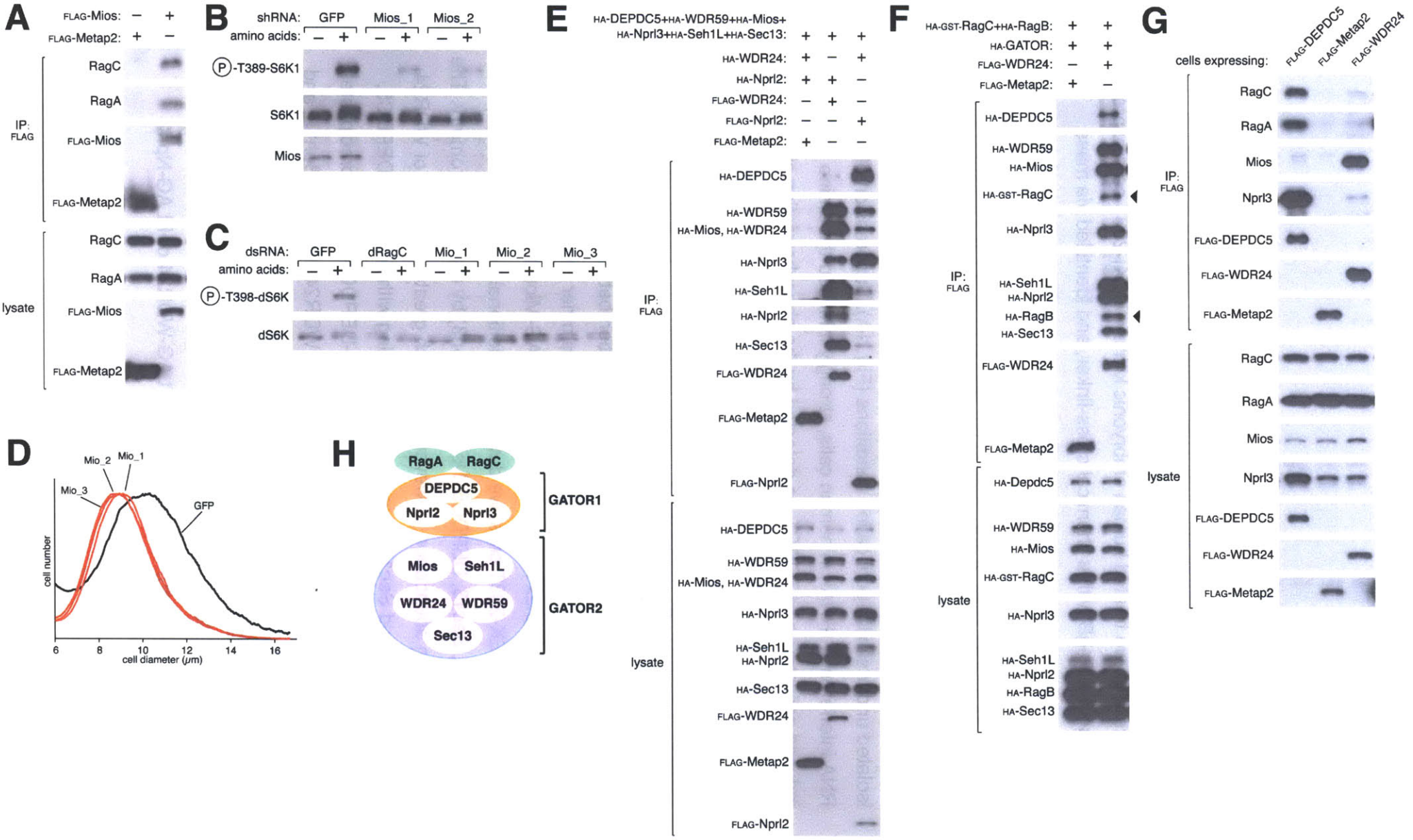
A
FLAG-Mios: – +
FLAG-Metap2: + –
IP: FLAG
RagC
RagA
FLAG-Mios
FLAG-Metap2
lysate
RagC
RagA
FLAG-Mios
FLAG-Metap2
B
shRNA: GFP Mios_1 Mios_2
amino acids: – + – + – +
P-T389-S6K1
S6K1
Mios
C
dsRNA: GFP dRagC Mio_1 Mio_2 Mio_3
amino acids: – + – + – + – + – +
P-T398-dS6K
dS6K
D
Mio_2
Mio_1
Mio_3
GFP
cell number
6 8 10 12 14 16
cell diameter (μm)
E
HA-DEPDC5+HA-WDR59+HA-Mios+
HA-Nprl3+HA-Seh1L+HA-Sec13: + + +
HA-WDR24: + – +
HA-Nprl2: + + –
FLAG-WDR24: – + –
FLAG-Nprl2: – – +
FLAG-Metap2: + – –
IP: FLAG
HA-DEPDC5
HA-WDR59
HA-Mios, HA-WDR24
HA-Nprl3
HA-Seh1L
HA-Nprl2
HA-Sec13
FLAG-WDR24
FLAG-Metap2
FLAG-Nprl2
lysate
HA-DEPDC5
HA-WDR59
HA-Mios, HA-WDR24
HA-Nprl3
HA-Seh1L
HA-Nprl2
HA-Sec13
FLAG-WDR24
FLAG-Metap2
FLAG-Nprl2
F
HA-GST-RagC+HA-RagB: + +
HA-GATOR: + +
FLAG-WDR24: – +
FLAG-Metap2: + –
IP: FLAG
HA-DEPDC5
HA-WDR59
HA-Mios
HA-GST-RagC
HA-Nprl3
HA-Seh1L
HA-Nprl2
HA-RagB
HA-Sec13
FLAG-WDR24
FLAG-Metap2
lysate
HA-Depdc5
HA-WDR59
HA-Mios
HA-GST-RagC
HA-Nprl3
HA-Seh1L
HA-Nprl2
HA-RagB
HA-Sec13
G
cells expressing:
FLAG-DEPDC5
FLAG-Metap2
FLAG-WDR24
IP: FLAG
RagC
RagA
Mios
Nprl3
FLAG-DEPDC5
FLAG-WDR24
FLAG-Metap2
lysate
RagC
RagA
Mios
Nprl3
FLAG-DEPDC5
FLAG-WDR24
FLAG-Metap2
H
RagA
RagC
DEPDC5
Nprl2
Nprl3
GATOR1
Mios
Seh1L
WDR24
WDR59
Sec13
GATOR2

Figure. 1. GATOR is a Rag-interacting complex, whose Mios component is necessary for the activation of mTORC1 by amino acids. (**A**) Mios interacts with endogenous RagA and RagC. HEK-293T cells were transfected with the indicated cDNAs in expression vectors. Cells were treated with a cell permeable chemical cross-linker, lysates were prepared and subjected to Flag immunoprecipitation (IP) followed by immunoblotting for the indicated proteins. (**B**) Mios is necessary for the activation of the mTORC1 pathway by amino acids. HEK-293T cells expressing shRNAs targeting GFP or Mios were starved of amino acids for 50 min or starved and then re-stimulated with amino acids for 10 min. Cell lysates were analyzed for the phosphorylation state of S6K1. (**C**) S2 cells treated with dsRNAs targeting Mio or GFP were starved of amino acids for 90 min or starved and re-stimulated with amino acids for 30 min. The indicated proteins were detected by immunoblotting. (**D**) Cell size histogram of S2 cells after dsRNA-mediated depletion of Mio. (**E**)-(**F**) GATOR is an octomeric complex defined by two distinct subcomplexes and interacts with the Rag GTPases. HEK-293T cells were transfected and processed as in (**A**) with the exclusion of the cross-linking reagent, and cell lysates and FLAG-immunoprecipitates were subjected to immunoblotting. (**G**) HEK-293T cells stably expressing FLAG-tagged DEPDC5 or WDR24 were lysed and cell lysates and FLAG immunoprecipitates were analyzed by immunoblotting for endogenous RagA, RagC, Mios and Nprl3. (**H**) Schematic summarizing GATOR-Rag interactions. GATOR2 (Mios, Seh1L, WDR24, WDR59 and Sec13) interacts with GATOR1 (DEPDC5, Nprl2 and Nprl3), which likely then binds the Rags.

A

Proteins in FLAG-RagB IP

	Protein	Peptide count
Ragulator	p18	217
	MP1	38
	p14	86
	HBXIP	68
	C7orf59	16
v-ATPase	V-type proton ATPase subunit G1	9
	V-type proton ATPase subunit E1	18
	Mios	6

B

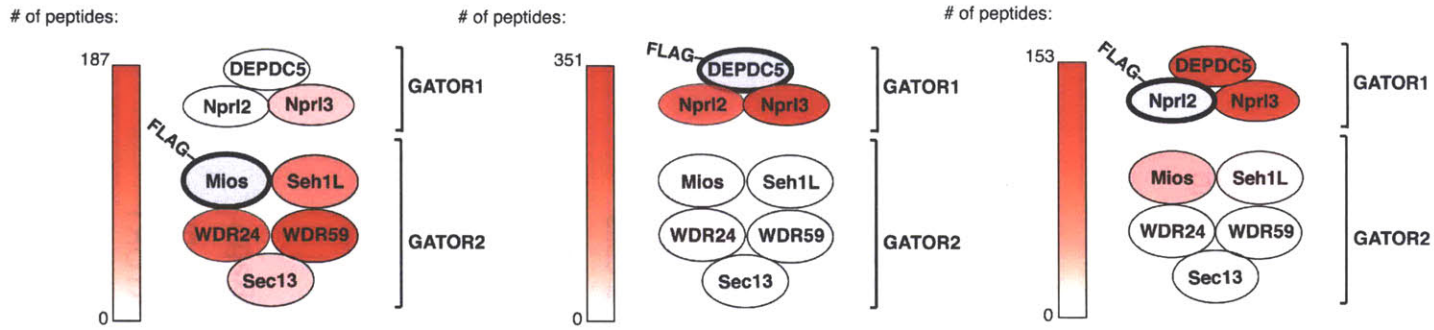

C

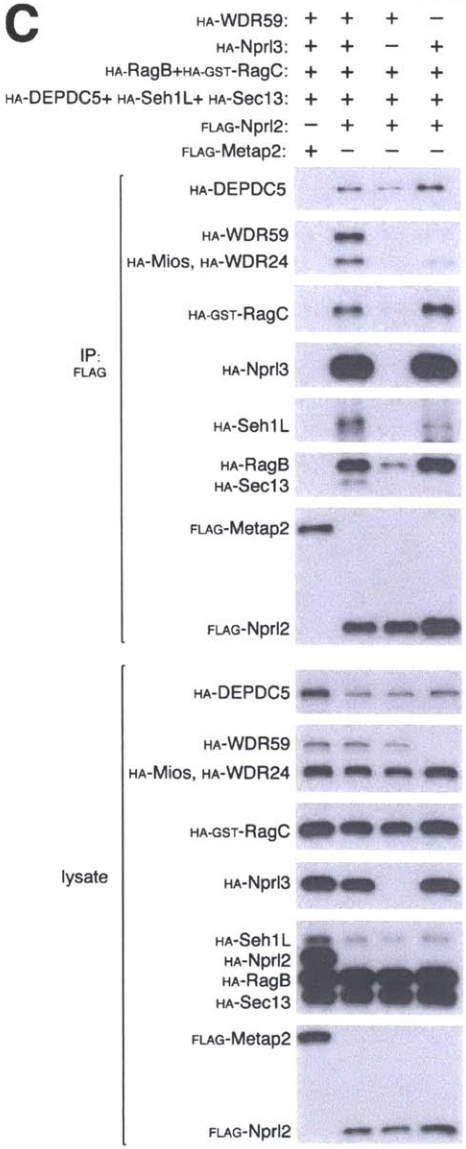

D

IP: FLAG-Mios

IP: FLAG-DEPDC5

		Peptide count	
		RagA	RagC
IP: FLAG	FLAG-DEDPC5	45	30
	FLAG-WDR24	2	0

E

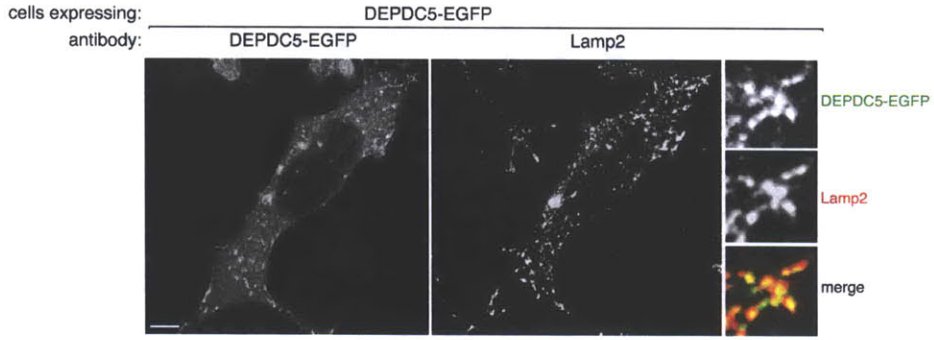

F

IP: FLAG-Nprl2

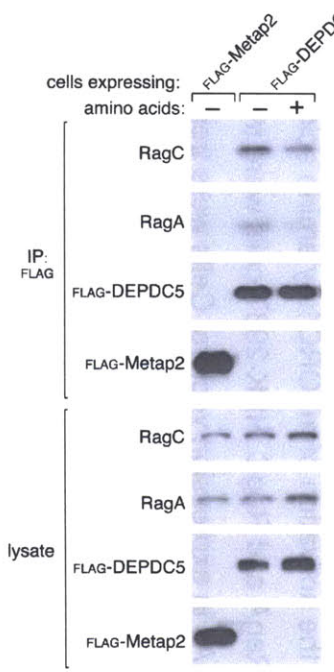

Figure S1. The octomeric GATOR complex is composed of two distinct subcomplexes. (**A**) Table summarizing peptide counts of proteins that co-immunoprecipitate with FLAG-RagB. HEK-293T cells stably expressing FLAG-RagB were treated with a chemical cross-linker and cell lysates were subject to FLAG-immunoprecipitation followed by mass spectrometry analysis of co-immunoprecipitated proteins. (**B**) Cartoon summarizing peptide counts from mass spectrometric analyses of anti-FLAG immunoprecipitates from HEK-293T cells expressing FLAG-Mios (left), FLAG-DEPDC5 (center) and FLAG-Nprl2 (right). GATOR subunits are color-coded according to their peptide counts. (**C**) The GATOR-Rag interaction is primarily mediated by the GATOR1 subcomplex. HEK-293T cells were transfected with the indicated cDNAs in expression vectors. Cell lysates were prepared and subjected to FLAG immunoprecipitation (IP) followed by immunoblotting for indicated proteins. (**D**) Table of peptide counts for the RagA and RagC proteins that co-immunoprecipitate with FLAG-DEPDC5 or FLAG-WDR24. HEK-293T cells stably expressing FLAG-tagged proteins were processed as described in (**A**). (**E**) DEPDC5 localizes to the lysosomal surface. Images of HEK-293T cells stably expressing DEPDC5-EGFP (green) and immunostained for Lamp2 (red). In all images, insets show selected fields that were magnified five times and their overlays. Scale bar represents 10 μM. (**F**) The GATOR1-Rag interaction is regulated by amino acids. HEK-293T cells stably expressing FLAG-tagged DEPDC5 were starved of amino acids for 2 hours or starved and restimulated for 10 minutes. Cell lysates were prepared and subjected to an anti-FLAG immunoprecipitation, which was analyzed as in (**C**).

together with HA-tagged versions of the other seven proteins. As expected, DEPDC5 and Nprl3 co-immunoprecipitated with Nprl2 much more strongly than with WDR24, while the opposite was true for Mios, WDR59, Seh1L, and Sec13 (Fig. 1E). For reasons described later, we call the 8-protein complex GATOR for GAP Activity Towards Rags and the two subcomplexes GATOR1 (DEPDC5, Nprl2, and Nprl3) and GATOR2 (Mios, WDR24, WDR59, Seh1L, and Sec13) (Fig. 1H).

When the eight proteins were co-expressed with RagB and RagC, GATOR interacted strongly with the Rag heterodimer (Fig. 1F) and, like the Rags and Ragulator (*6, 7*), its DEPDC5 component localized to the lysosomal surface (Fig. S1E). Experiments in which single GATOR proteins were omitted revealed complex relationships between the components, but suggested that GATOR1 mediates the GATOR-Rag interaction (Fig. S1C). Consistent with this conclusion, when stably expressed in HEK-293T cells, FLAG-DEPDC5 co-immunoprecipitated much more endogenous RagA and RagC than FLAG-WDR24, as detected by immunoblotting (Fig. 1G) and mass spectrometric analysis (Fig. S1D). Amino acid starvation increased the amount of RagA and RagC that co-immunoprecipitated with DEPDC5, suggesting a regulatory role for GATOR1 (Fig. S1F).

The finding that GATOR components interact with the Rag GTPases was intriguing because their likely budding yeast orthologs (IML1, NPR2, NPR3) positively regulate autophagasome formation, a TORC1-dependent process (*11*), and, at least in certain yeast strains, also inhibit TORC1 signaling upon nitrogen starvation (*12-14*). Recently the likely yeast orthologs of GATOR2 (Sea2, Sea3, Sea4, Seh1L, and Sec13) were shown to interact with IML1, NPR2, and NPR3 to form a complex that has been called SEA (*15*). However, unlike GATOR, the SEA complex does not appear to consist of two distinct subcomplexes as its components are found in stoichiometric amounts.

We used RNAi in HEK-293T and *Drosophila* S2 cells to examine the function of each GATOR component in amino acid sensing by mTORC1 and dTORC1, respectively. We excluded Sec13 from further analysis as it functions

in several protein complexes (*16*) and so its inhibition might have effects that are difficult to interpret. Consistent with Mios being required for amino acids to activate mTORC1 (Fig. 1B), depletion of other GATOR2 components or their *Drosophila* orthologs strongly blunted amino acid-induced activation of mTORC1 and dTORC1, respectively (Fig. 2, A, C, and D; S2, A, B, C, and D). In contrast, loss of GATOR1 proteins had the opposite effect and prevented the inactivation of mTORC1 and dTORC1 normally caused by amino acid deprivation (Fig. 2, B and E; S2, A, and D). Consistent with the opposite roles of GATOR1 and GATOR2 on dTORC1 signaling, dsRNAs targeting dSeh1L or dDEPDC5 decreased and increased, respectively, S2 cell size (Fig. 2F). To clarify the relationship between GATOR1 and GATOR2, we used RNAi to inhibit dDEPDC5 at the same time as Mio or dSeh1L in S2 cells. Interestingly, in the background of GATOR1 inhibition, loss of GATOR2 had no effect on dTORC1 activity, indicating that GATOR2 functions upstream of GATOR1 (Fig. 2, G and H). Thus, GATOR2 is an inhibitor of an inhibitor (GATOR1) of the amino acid sensing branch of the TORC1 pathway.

A key step in the amino acid-induced activation of mTORC1 is its recruitment to the lysosomal surface, an event that requires known positive components of the amino acid sensing pathway, like Ragulator (*7*) and the v-ATPase (*3*). Consistent with a positive role for GATOR2, in HEK-293T cells expressing shRNAs targeting Mios (Fig. 1B) or Seh1L (Fig. 2A) mTOR did not translocate to LAMP2-positive lysosomal membranes upon amino acid stimulation (Fig. 3A). In contrast, in cells expressing an shRNA targeting DEPDC5 (Fig. S2A), mTOR localized constitutively to the lysosomal surface regardless of amino acid availability (Fig. 3B). Moreover, just overexpression of DEPDC5 was sufficient to block the amino acid-induced translocation of mTOR to the lysosomal surface (Fig. 3C). Unlike Ragulator, which tethers the Rags to the lysosomal surface (*6-7*), GATOR2 is not needed for the proper Rag localization (Fig. S3A). Thus, GATOR1 and GATOR2 have opposite effects on the activity and subcellular localization of mTORC1.

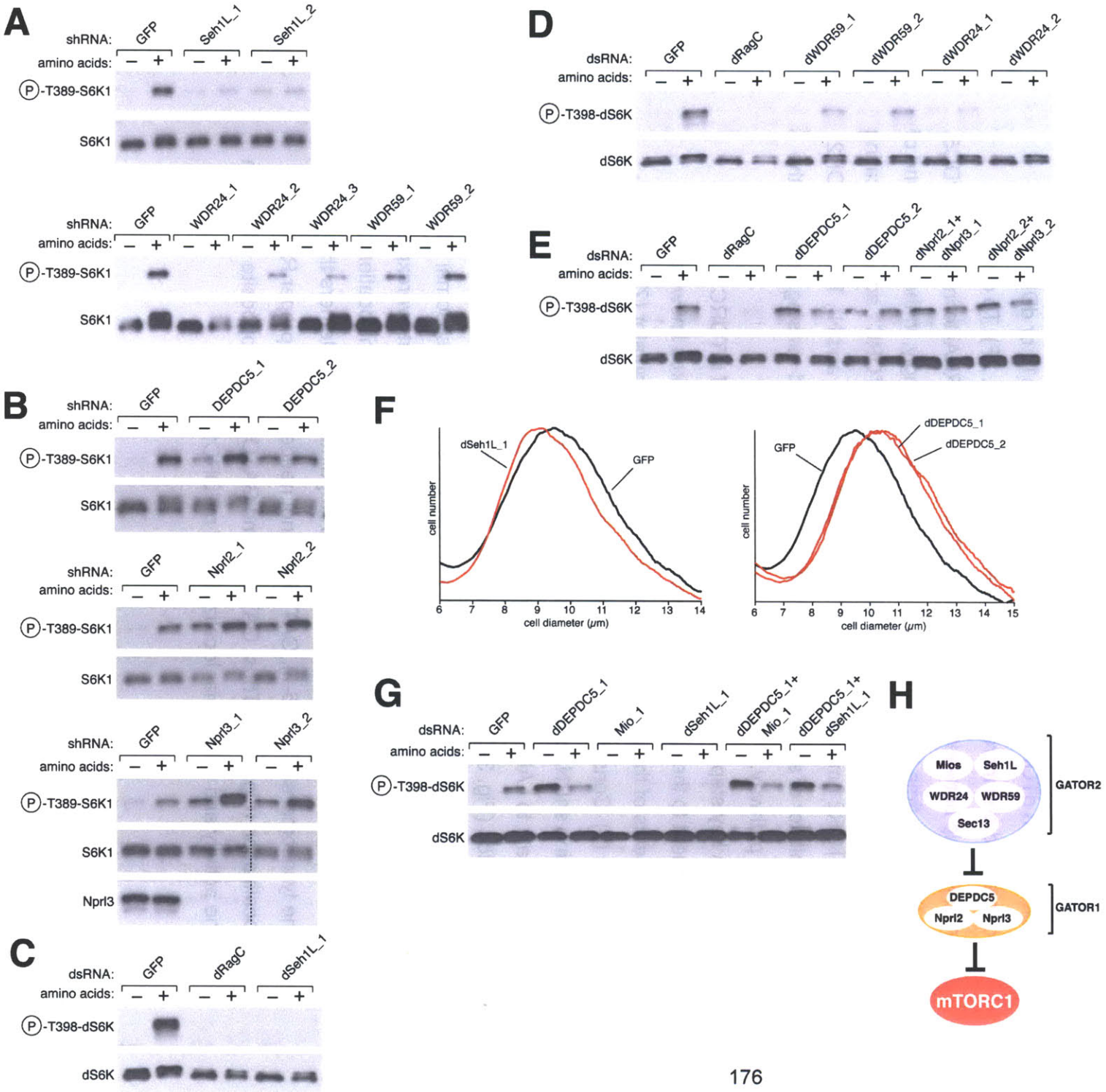
A
shRNA: GFP Seh1L_1 Seh1L_2
amino acids: – + – + – +
Ⓟ-T389-S6K1
S6K1
shRNA: GFP WDR24_1 WDR24_2 WDR24_3 WDR59_1 WDR59_2
amino acids: – + – + – + – + – + – +
Ⓟ-T389-S6K1
S6K1
B
shRNA: GFP DEPDC5_1 DEPDC5_2
amino acids: – + – + – +
Ⓟ-T389-S6K1
S6K1
shRNA: GFP Nprl2_1 Nprl2_2
amino acids: – + – + – +
Ⓟ-T389-S6K1
S6K1
shRNA: GFP Nprl3_1 Nprl3_2
amino acids: – + – + – +
Ⓟ-T389-S6K1
S6K1
Nprl3
C
dsRNA: GFP dRagC dSeh1L_1
amino acids: – + – + – +
Ⓟ-T398-dS6K
dS6K
D
dsRNA: GFP dRagC dWDR59_1 dWDR59_2 dWDR24_1 dWDR24_2
amino acids: – + – + – + – + – + – +
Ⓟ-T398-dS6K
dS6K
E
dsRNA: GFP dRagC dDEPDC5_1 dDEPDC5_2 dNprl2_1+ dNprl3_1 dNprl2_2+ dNprl3_2
amino acids: – + – + – + – + – + – +
Ⓟ-T398-dS6K
dS6K
F
dSeh1L_1
GFP
cell number
6 7 8 9 10 11 12 13 14
cell diameter (μm)
GFP
dDEPDC5_1
dDEPDC5_2
cell number
6 7 8 9 10 11 12 13 14 15
cell diameter (μm)
G
dsRNA: GFP dDEPDC5_1 Mio_1 dSeh1L_1 dDEPDC5_1+ Mio_1 dDEPDC5_1+ dSeh1L_1
amino acids: – + – + – + – + – + – +
Ⓟ-T398-dS6K
dS6K
H
Mios
Seh1L
WDR24
WDR59
Sec13
GATOR2
DEPDC5
Nprl2
Nprl3
GATOR1
mTORC1

Figure 2. The GATOR complex is required for the regulation of the TORC1 pathway by amino acids. (**A**) shRNA-mediated depletion of the GATOR2 components Seh1L, WDR24, or WDR59 in HEK-293T cells inhibits amino acid-induced S6K1 phosphorylation. (**B**) In HEK-293Ts expressing shRNAs targeting the GATOR1 components DEPDC5, Nprl2, and Nprl3, S6K1 phosphorylation is insensitive to amino acid withdrawal. In (**A**) and (**B**) cells were starved of amino acids for 50 min or starved and restimulated with amino acids for 10 min. Cell lysates were immunoblotted for the phosphorylation state of S6K1. dsRNA-mediated depletion in S2 cells of (**C**) dSeh1L; (**D**) dWDR59 and dWDR24; and (**E**) dDEPDC5, dNprl2, and dNprl3. S2 cells were treated with the indicated dsRNAs and were starved of amino acids for 90 min or starved and restimulated with amino acids for 30 min. Immunoblotting was used to detect the phosphorylation state of dS6K. (**F**) S2 cell sizes after dsRNA-mediated depletion of dSeh1L and dDEPDC5. (**G**) GATOR2 functions upstream of GATOR1. S2 cells were treated with the indicated combinations of dsRNAs and starved and restimulated with amino acids and analyzed as in (**C**)-(**E**). (**H**) Schematic depicting the relationship between GATOR1 and GATOR2 in their regulation of mTORC1.

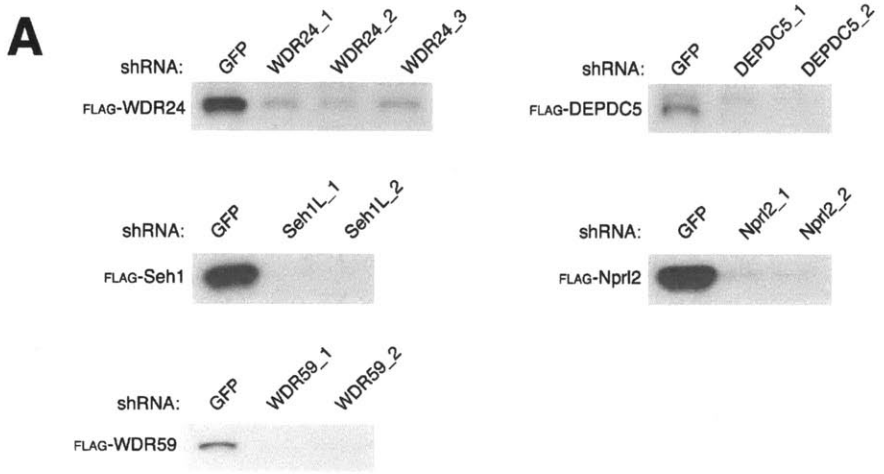
A
shRNA:
GFP
WDR24_1
WDR24_2
WDR24_3
FLAG-WDR24
shRNA:
GFP
DEPDC5_1
DEPDC5_2
FLAG-DEPDC5
shRNA:
GFP
Seh1L_1
Seh1L_2
FLAG-Seh1
shRNA:
GFP
Nprl2_1
Nprl2_2
FLAG-Nprl2
shRNA:
GFP
WDR59_1
WDR59_2
FLAG-WDR59

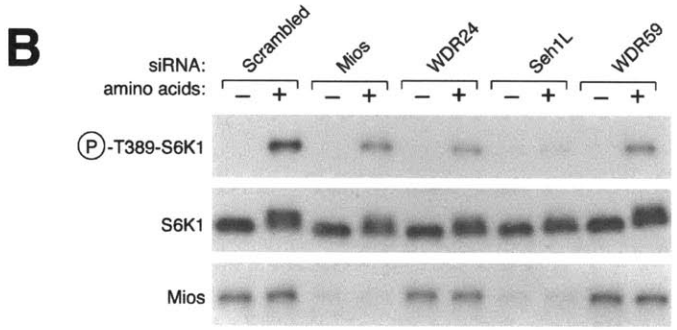
B
siRNA:
Scrambled
Mios
WDR24
Seh1L
WDR59
amino acids:
– + – + – + – + – +
Ⓟ-T389-S6K1
S6K1
Mios

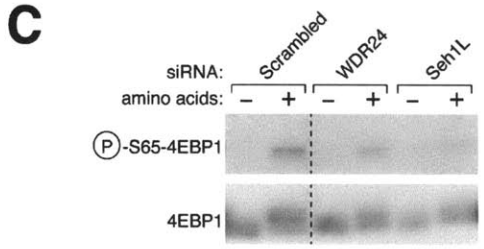
C
siRNA:
Scrambled
WDR24
Seh1L
amino acids:
– + – + – +
Ⓟ-S65-4EBP1
4EBP1

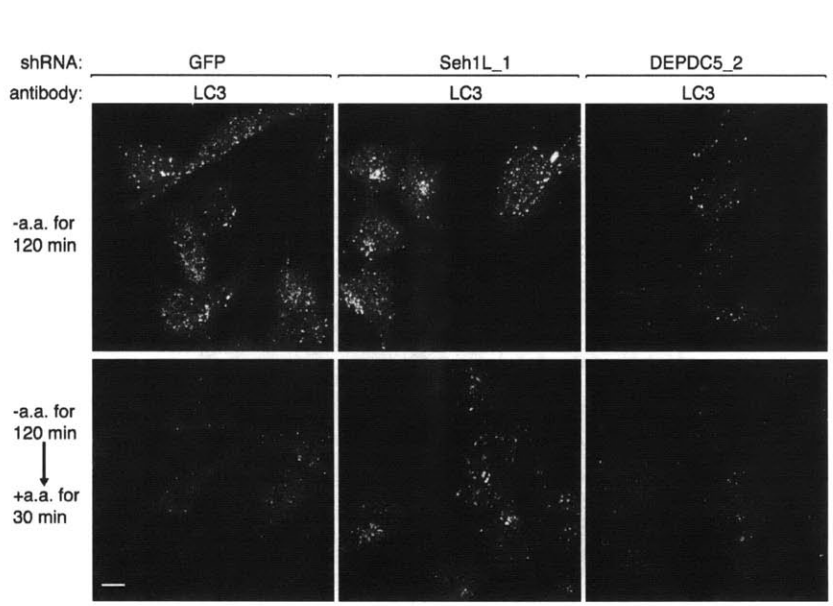
D
shRNA:
GFP
Seh1L_1
DEPDC5_2
antibody:
LC3
LC3
LC3
-a.a. for
120 min
-a.a. for
120 min
+a.a. for
30 min

Figure S2. Depletion of GATOR components regulates multiple mTORC1-dependent outputs. (**A**) Validation of shRNAs targeting GATOR components. HEK-293T cells were transfected with indicated cDNAs and corresponding shRNAs in expression vectors. Cell lysates were analyzed by immunoblotting to determine the extent of recombinant protein depletion by the indicated shRNAs. (**B-C**) siRNA mediated depletion of GATOR2 components indicates that these proteins are necessary for amino-acid induced activation of mTORC1. HEK-293T cells treated with the indicated siRNAs were starved of amino acids for 50 min or starved and restimulated with amino acids for 10 min. Cell lysates were prepared followed by immunoblotting to detect the levels of the indicated proteins. (**D**) The GATOR complex regulates autophagy. Images of HEK-293T cells, expressing the indicated shRNAs targeting Seh1L or DEPDC5, starved for amino acids for 2 hours or starved and restimulated for 30 minutes, were analyzed for LC3 puncta formation. Scale bar represents 10 μM.

Figure 3

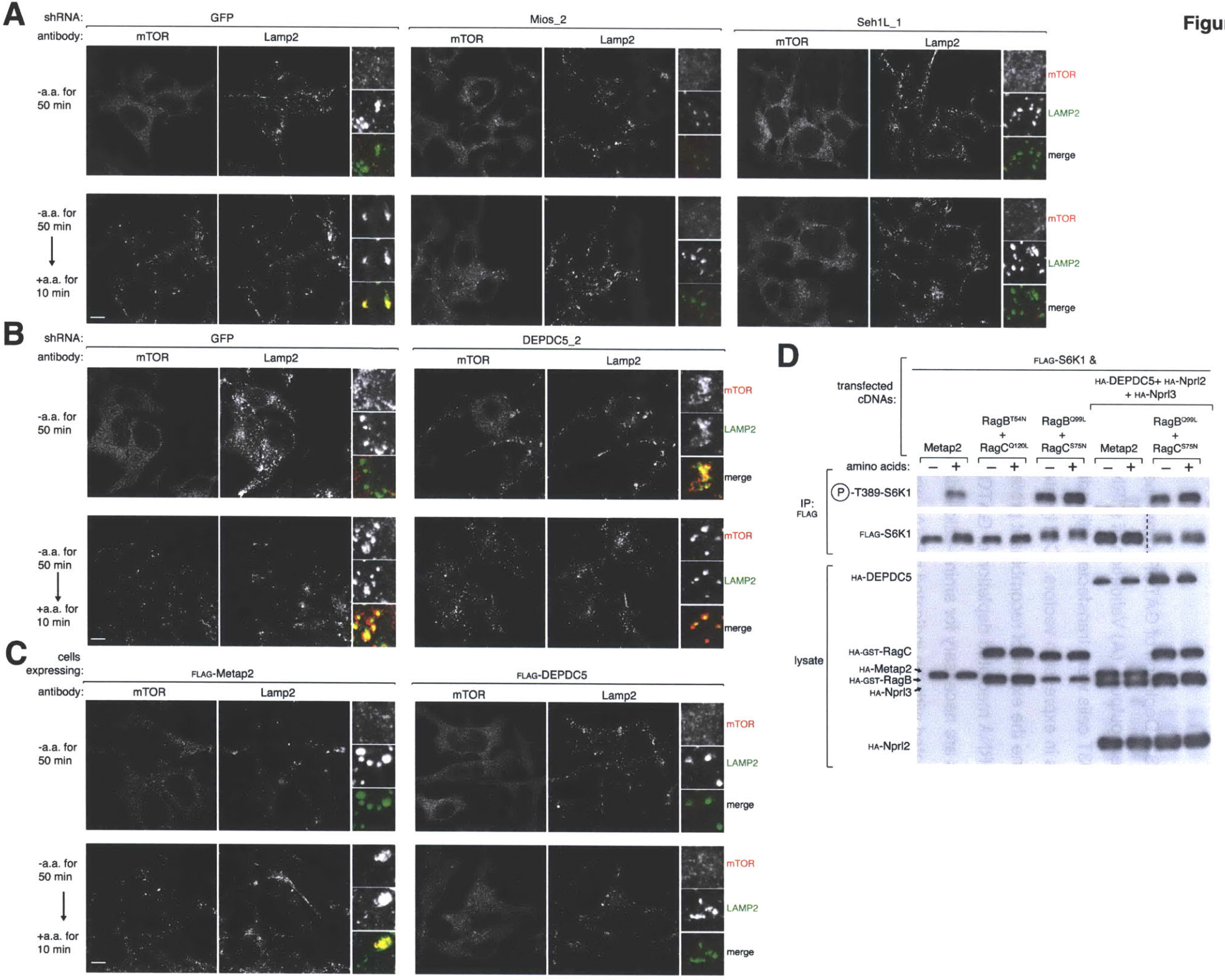
A
shRNA:
GFP
Mios_2
Seh1L_1
antibody:
mTOR
Lamp2
-a.a. for 50 min
+a.a. for 10 min
mTOR
LAMP2
merge
B
shRNA:
GFP
DEPDC5_2
antibody:
mTOR
Lamp2
-a.a. for 50 min
+a.a. for 10 min
mTOR
LAMP2
merge
C
cells expressing:
FLAG-Metap2
FLAG-DEPDC5
antibody:
mTOR
Lamp2
-a.a. for 50 min
+a.a. for 10 min
mTOR
LAMP2
merge
D
transfected cDNAs:
FLAG-S6K1 &
HA-DEPDC5+ HA-Nprl2 + HA-Nprl3
Metap2
RagBT54N + RagCQ120L
RagBQ99L + RagCS75N
Metap2
RagBQ99L + RagCS75N
amino acids:
– + – + – + – + – +
IP: FLAG
P-T389-S6K1
FLAG-S6K1
lysate
HA-DEPDC5
HA-GST-RagC
HA-Metap2
HA-GST-RagB
HA-Nprl3
HA-Nprl2

Figure 3. GATOR regulates mTORC1 localization to the lysosomal surface and functions upstream of the Rag GTPases. (**A**) RNAi-mediated depletion of the GATOR2 components Mios and Seh1L prevents amino acid-induced mTOR lysosomal translocation. HEK-293T cells expressing the indicated shRNAs were starved or starved and restimulated with amino acids for the specified times prior to co-immunostaining for mTOR (red) and Lamp2 (green). (**B**) Reduced expression of DEPDC5 in HEK-293T cells results in constitutive mTOR localization to the lysosomal surface. HEK-293T cells treated with the indicated lentiviral shRNAs were processed as described in (**A**). (**C**) Images of HEK-293T cells stably expressing FLAG-DEPDC5 starved for or starved and restimulated with amino acids. Cells were processed as described in (**A**). In all images, insets show selected fields that were magnified five times and their overlays. Scale bar equals 10 μM. (**D**) GATOR1 functions upstream of the nucleotide binding state of the Rags. HEK-293T cells transfected with the indicated cDNAs in expression vectors were starved of amino acids for 50 min or starved and restimulated with amino acids for 10 min. The indicated proteins were detected by immunoblotting.

Figure S3

A

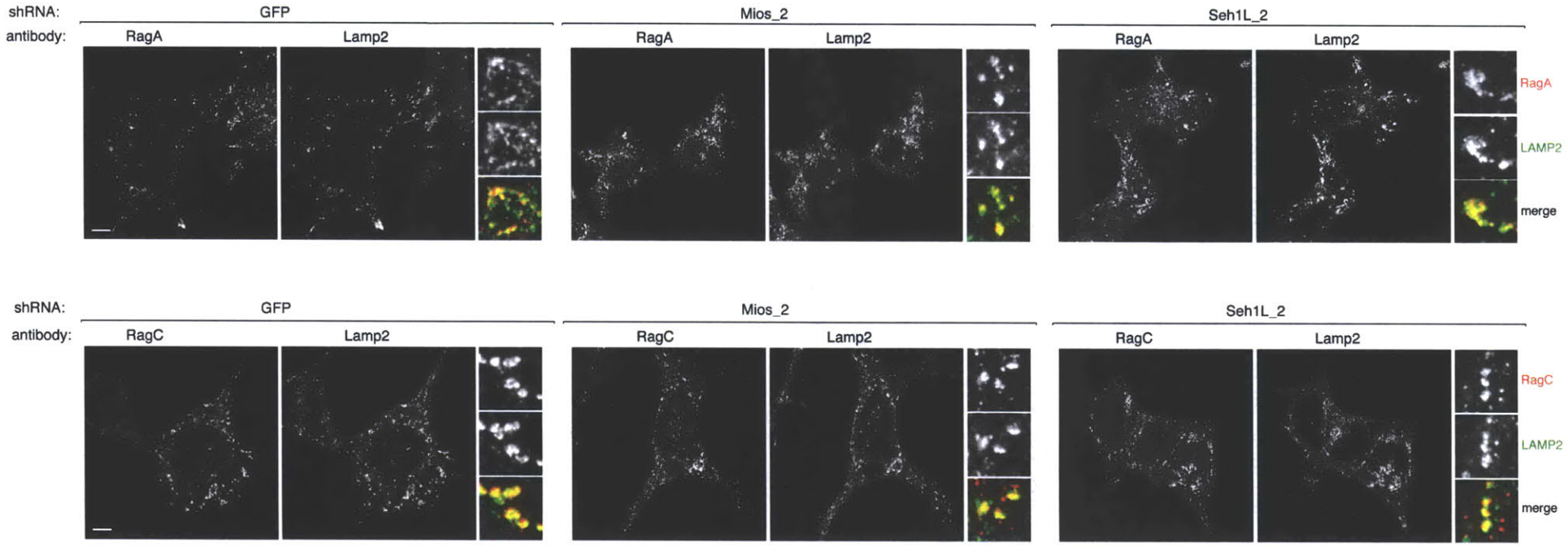
shRNA:
antibody:
GFP
RagA
Lamp2
Mios_2
RagA
Lamp2
Seh1L_2
RagA
Lamp2
RagA
LAMP2
merge
shRNA:
antibody:
GFP
RagC
Lamp2
Mios_2
RagC
Lamp2
Seh1L_2
RagC
Lamp2
RagC
LAMP2
merge

Figure S3. GATOR2 is not required for the localization of the Rag GTPases to the lysosomal surface. (**A**) Images of HEK-293T cells, expressing the indicated shRNAs targeting Mios or Seh1L, were co-immunostained for RagA or RagC (red) and Lamp2 (green). In all images, insets show selected fields that were magnified five times and their overlays. Scale bar represents 10 μM.

Consistent with GATOR1 being an inhibitor of the mTORC1 pathway, concomitant overexpression of its three components blocked the amino acid-induced activation of mTORC1 (Fig. 3D) to a similar extent as $RagB^{T54N}$-$RagC^{Q120L}$, a Rag heterodimer that is dominant negative because the $RagB^{T54N}$ mutant cannot bind GTP (*7*). In contrast, expression of the dominant active $RagB^{Q99L}$-$RagC^{S75N}$ heterodimer blocked not only amino acid deprivation but also GATOR1 overexpression from inhibiting mTORC1 signaling. Because $RagB^{Q99L}$ is constitutively bound to GTP (*17*) and $RagC^{S75N}$ cannot bind GTP (*7*), this result suggests that GATOR1 functions upstream of the regulation of the nucleotide binding state of the Rags.

To test the possibility that GATOR1 is a guanine nucleotide exchange factor (GEF) or a GTPase activating protein (GAP) for the Rags we prepared Rag heterodimers consisting of a wild-type Rag and a Rag^X mutant (see methods) (*7*). The Rag^X mutants are selective for xanthosine rather than guanine nucleotides, allowing us to prepare heterodimers in vitro in which the wild-type Rag is loaded with radiolabeled GTP or GDP while the Rag^X partner is bound to XDP or XTP (*7*). In vitro, purified GATOR1 (Fig. S4E) did not stimulate the dissociation of GDP from RagB or RagC when each was bound to its appropriate Rag^X partner (Fig. S4, A, and B), ruling out its function as a GEF. In contrast, GATOR1 strongly increased, in a time and dose-dependent manner, GTP hydrolysis by RagA or RagB within $RagC^X$-containing heterodimers, irrespective of which nucleotide $RagC^X$ was loaded with (Fig. 4, A, B and E; S4, C and D). GATOR1 also slightly boosted GTP hydrolysis by RagC within a $RagB^X$-RagC heterodimer (Fig. 4C), but had no effect on the GTPase activity of Rap2a (Fig. 4D). LRS, a putative GAP for RagD (*18*), did not alter the basal GTP hydrolysis by RagA, RagB or RagC (Fig 4, A, B and C). Consistent with the binding preference of many GAPs for the GTP-loaded state of target GTPases, in vitro GATOR1 preferentially interacted with the $RagB^{Q99L}$-containing heterodimer (Fig. 4F). Thus, the GATOR1 complex has GAP activity for RagA/B, providing a mechanism for its inhibitory role in mTORC1 signaling.

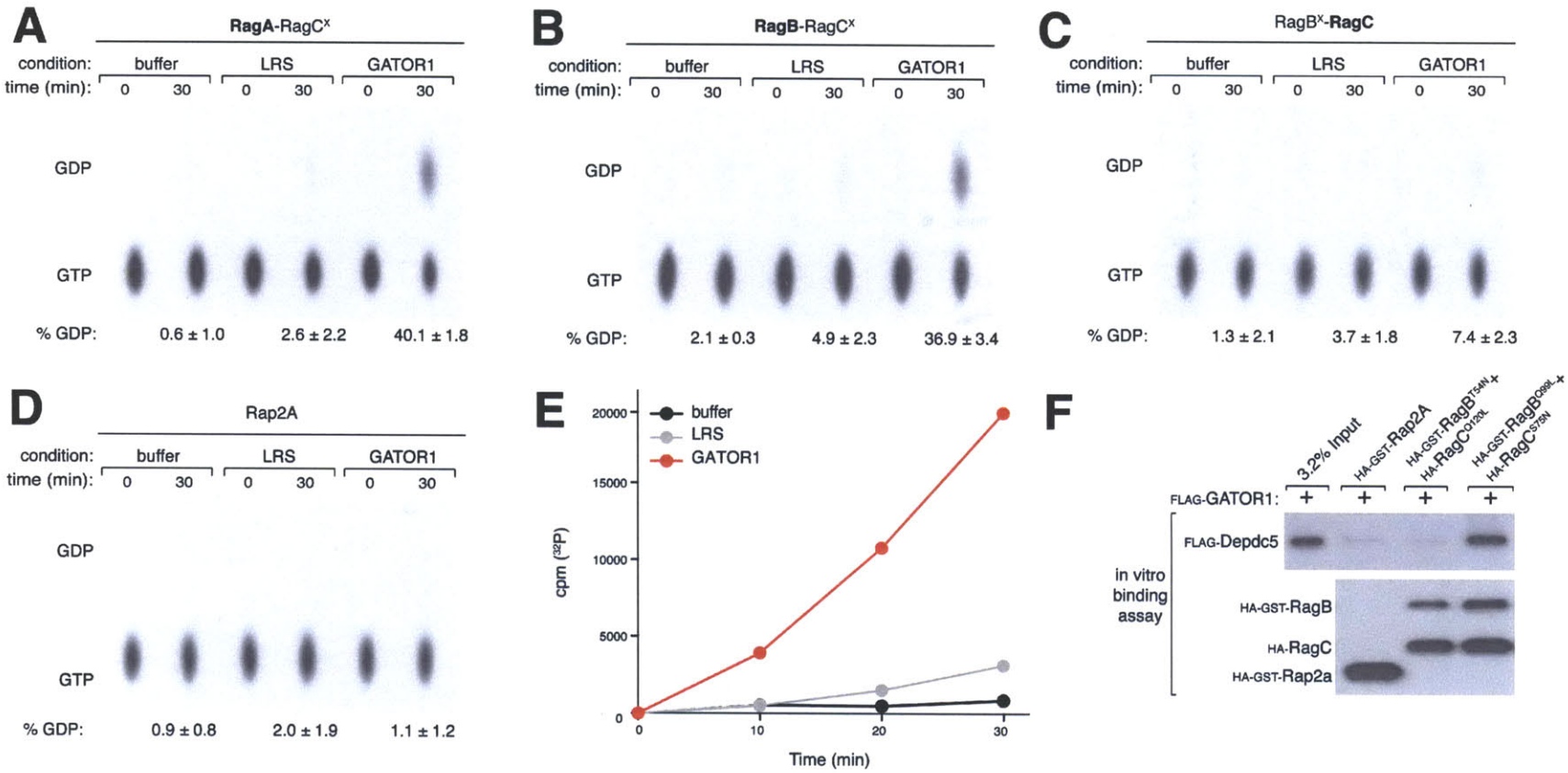
A
RagA-RagC^X
condition: buffer LRS GATOR1
time (min): 0 30 0 30 0 30
GDP
GTP
% GDP: 0.6 ± 1.0 2.6 ± 2.2 40.1 ± 1.8
B
RagB-RagC^X
condition: buffer LRS GATOR1
time (min): 0 30 0 30 0 30
GDP
GTP
% GDP: 2.1 ± 0.3 4.9 ± 2.3 36.9 ± 3.4
C
RagB^X-RagC
condition: buffer LRS GATOR1
time (min): 0 30 0 30 0 30
GDP
GTP
% GDP: 1.3 ± 2.1 3.7 ± 1.8 7.4 ± 2.3
D
Rap2A
condition: buffer LRS GATOR1
time (min): 0 30 0 30 0 30
GDP
GTP
% GDP: 0.9 ± 0.8 2.0 ± 1.9 1.1 ± 1.2
E
buffer
LRS
GATOR1
cpm (32P)
20000
15000
10000
5000
0
0 10 20 30
Time (min)
F
3.2% Input
HA-GST-Rap2A
HA-GST-RagB^T54N+
HA-RagC^Q120L
HA-GST-RagB^Q99L+
HA-RagC^S75N
FLAG-GATOR1: + + + +
in vitro binding assay
FLAG-Depdc5
HA-GST-RagB
HA-RagC
HA-GST-Rap2a

Figure 4

Figure 4. GATOR1 is a GTPase activating protein complex for RagA and RagB. (**A**)-(**D**) GATOR1 stimulates GTP hydrolysis by RagA and RagB. RagA-RagC^{X}, RagB-RagC^{X}, RagC-RagB^{X} or the control GTPase Rap2a were loaded with [α-^{32}P] GTP and incubated with GATOR1 (20 pmols) or the control Leucyl tRNA synthetase (LRS) (20 pmols). GTP hydrolysis was determined by thin layer chromatography (see methods). Each value represents the normalized mean ± SD (*n* = 3). (**E**) GATOR1 increases GTP hydrolysis by RagB in a time dependent manner. RagB-RagC^{X} was loaded with [γ-^{32}P]GTP, incubated with GATOR1 or a control and hydrolysis was determined by phosphate capture (see methods) Each value represents the normalized mean ± SD (*n* = 3). (**F**) GATOR1 preferentially interacts with the dominant active Rag heterodimer. In vitro binding assay in which FLAG-GATOR1 was incubated with immobilized HA-GST-tagged RagB^{T54N}-RagC^{Q120L} (dominant negative), RagB^{Q99L}-RagC^{S75N} (dominant active) or Rap2a. HA-GST precipitates were analyzed by immunoblotting for the levels of FLAG-GATOR1.

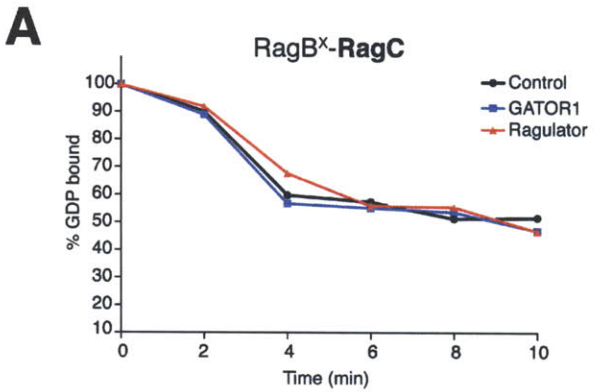
A
RagB^X-RagC
Control
GATOR1
Ragulator
% GDP bound
Time (min)

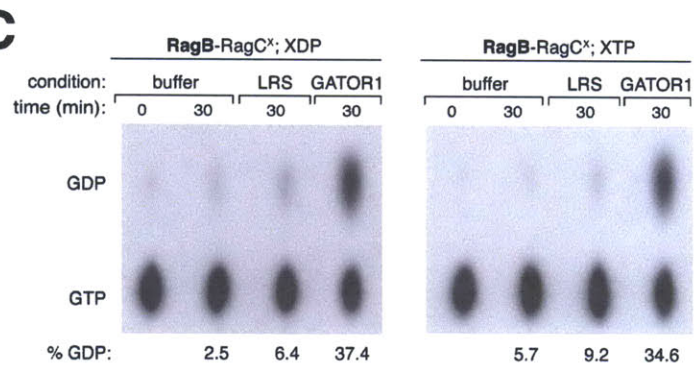
C
RagB-RagC^X; XDP
RagB-RagC^X; XTP
condition:
buffer
LRS
GATOR1
time (min):
0
30
GDP
GTP
% GDP:
2.5
6.4
37.4
5.7
9.2
34.6

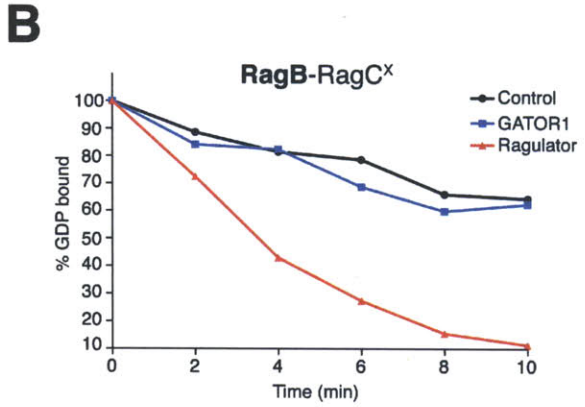
B
RagB-RagC^X
Control
GATOR1
Ragulator
% GDP bound
Time (min)

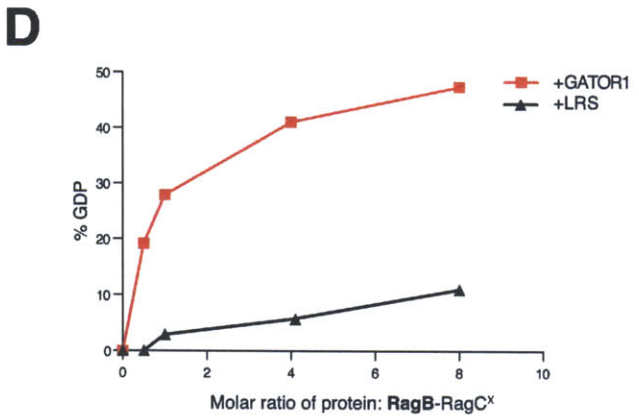
D
+GATOR1
+LRS
% GDP
Molar ratio of protein: RagB-RagC^X

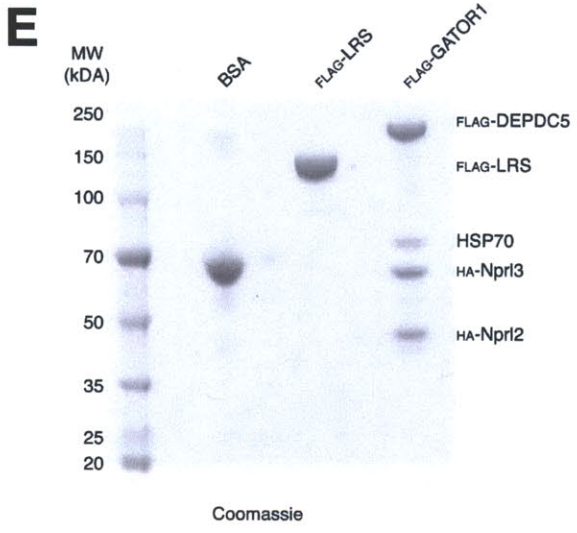
E
MW (kDA)
BSA
FLAG-LRS
FLAG-GATOR1
FLAG-DEPDC5
FLAG-LRS
HSP70
HA-Nprl3
HA-Nprl2
Coomassie

Figure S4. GATOR1 does not promote nucleotide dissociation from RagB or RagC. (**A**) GATOR1 does not alter GDP dissociation by RagC. GDP dissociation assay, in which RagC-RagB^{X} was loaded with [^{3}H]GDP and incubated with GATOR1, Ragulator, or a control. Dissociation was monitored by a filter-binding assay. Each value represents the normalized mean for n=2. (**B**) GATOR1 does not alter GDP dissociation by RagB. RagB-RagC^{X} was loaded with [^{3}H]GDP, incubated with GATOR1, Ragulator, or a control protein and analyzed as in (**A**). Each value represents the normalized mean for n=2. (**C**) The nucleotide-bound state of RagC does not alter GATOR1-GAP activity for RagB. RagB-RagC^{X} was loaded with [α-^{32}P] GTP and XDP or XTP and incubated with GATOR1 or a control protein. GTP hydrolysis was determined by thin layer chromatography. (**D**) GATOR1 stimulates GTP hydrolysis of RagB in a dose dependent manner. RagB-RagC^{X} was loaded with [α-^{32}P]GTP and incubated with the indicated molar amount of GATOR1 or a control protein. GTP hydrolysis was determined as described in (**C**). (**E**) Coomassie blue stained SDS-PAGE of purified LRS and GATOR1. Identity of indicated proteins was validated by immunoblotting. HSP70, which co-purifies with GATOR1, does not stimulate RagB-mediated GTP hydrolysis.

Because the pathways that convey upstream signals to mTORC1 are frequently deregulated by mutations in cancer (reviewed in (*19*)), we thought it possible that GATOR1 components might be mutated in human tumors. Indeed previous studies identified in lung and breast cancers deletions of a 630 kb region of 3p21.3 that includes *NPRL2* (*20, 21*), and one study reported two cases of glioblastoma with deletions in a three-gene region of 22q12.2 that contains *DEPDC5* (*22*). Moreover, in cancer cells with 3p21.3 deletions, expression of Nprl2 inhibited their capacity to grow as tumor xenografts, identifying it as a tumor suppressor (*21, 23*). Our analyses of publically available data from the cancer genome atlas (TCGA) identified a subset of glioblastomas and ovarian cancers with nonsense or frameshift mutations or truncating deletions in *DEPDC5* or *NPRL2.* In most of these tumors, *DEPDC5* or *NPRL2* also underwent an LOH event, indicating that the tumors were unlikely to retain a functional copy of the gene products (Fig. 5, A, B and C; S5A). In addition, in both tumor types, focal homozygous or hemizygous deletions, as well as missense mutations accompanied by LOH, were also detected in *DEPDC5* and *NPRL2* (Fig. 5A). *NPRL3* is located too proximal to the 16p telomere to adequately access copy number alterations in it using high-density microarray analysis. In aggregate, inactivating mutations in GATOR1 components are present in low single digit percentages of glioblastomas and ovarian cancers, frequencies that may change upon better assessment of *NPRL3*.

In order to study the effects of GATOR1 loss on cancer cells, we used the Cosmic and CCLE resources (see methods) to identify human cancer cell lines with homozygous deletions in *DEPDC5*, *NPRL2*, or *NPRL3*, which we confirmed via immunoblotting or PCR of genomic DNA (Fig. S5, B, C, and F). In seven such lines, but not in Jurkat or HeLa cells, mTORC1 signaling was hyperactive and completely insensitive to amino acid deprivation and V-ATPase inhibition, irrespective of which GATOR1 component was lacking (Fig. 5D; S5, D, E, and I). Furthermore, in GATOR1-null cells mTOR localized to the lysosomal surface even in the absence of amino acids (Fig. 5E). When DEPDC5 and Nprl2 were re-introduced into cancer cell lines lacking them, the mTORC1 pathway regained

sensitivity to amino acid regulation (Fig. 5F; S5, G, and H), indicating that it is indeed the loss of GATOR1 proteins that is driving aberrant mTORC1 signaling in these cells.

The proliferation of the GATOR1-null cancer cells was very sensitive to the mTORC1 inhibitor rapamycin, with IC_{50s} in the 0.1-0.4 nM range (Fig. 5G). These values are many orders of magnitude less than for cell lines that are not considered rapamycin sensitive, like HeLa and HT29 cells, and at the low end of cancer cell lines, like PC3 and Jurkat cells, which have lost *PTEN* function (*24-26*), an established negative regulator of the mTORC1 pathway. In addition, the forced expression of DEPDC5 in the MRKNU1 ($DEPDC5^{-/-}$) cell line led to a marked reduction in its proliferation (Fig. S5J).

In conclusion, we identify the octomeric GATOR complex as a critical regulator of the pathway that signals amino acid sufficiency to mTORC1 (Fig. 5G). The GATOR1 subcomplex has GAP activity for RagA and RagB and its loss makes mTORC1 signaling insensitive to amino acid deprivation. Inactivating mutations in GATOR1 are present in cancer and may help identify tumors likely to respond to clinically-approved pharmacological inhibitors of mTORC1.

A

Tumor: Glioblastoma
Sample size: (283)

	LOH	Homozygous focal deletion	Hemizygous focal deletion	Biallelic inactivation
DEPDC5	4 (1.41%)	1 (0.35%)	1 (0.35%)	1 (0.35%)
NPRL2	1 (0.35%)	0	0	0

Tumor: Ovarian cancer
Sample size: (441)

	LOH	Homozygous focal deletion	Hemizygous focal deletion
DEPDC5	4 (0.91%)	1 (0.23%)	1 (0.23%)
NPRL2	0	0	4 (0.91%)

B

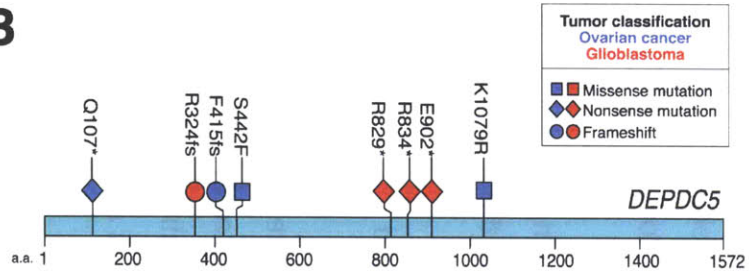

C

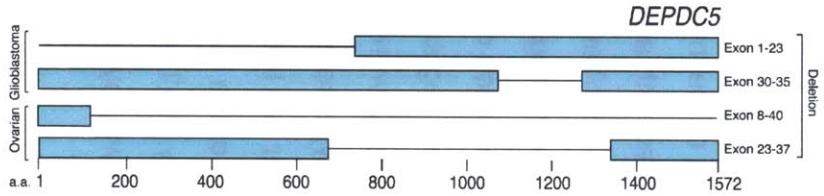

D

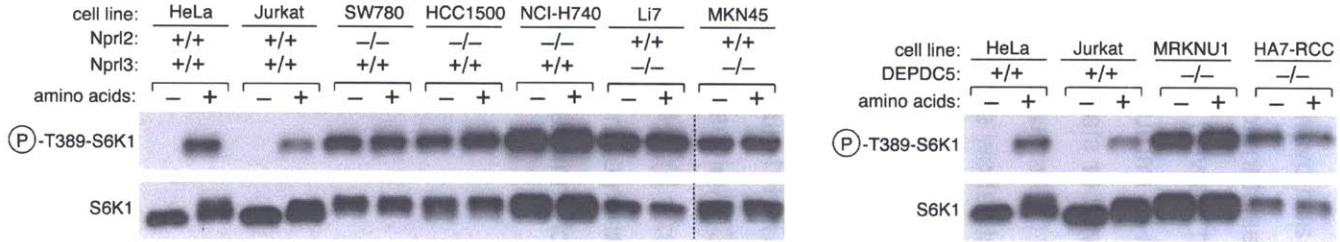

E

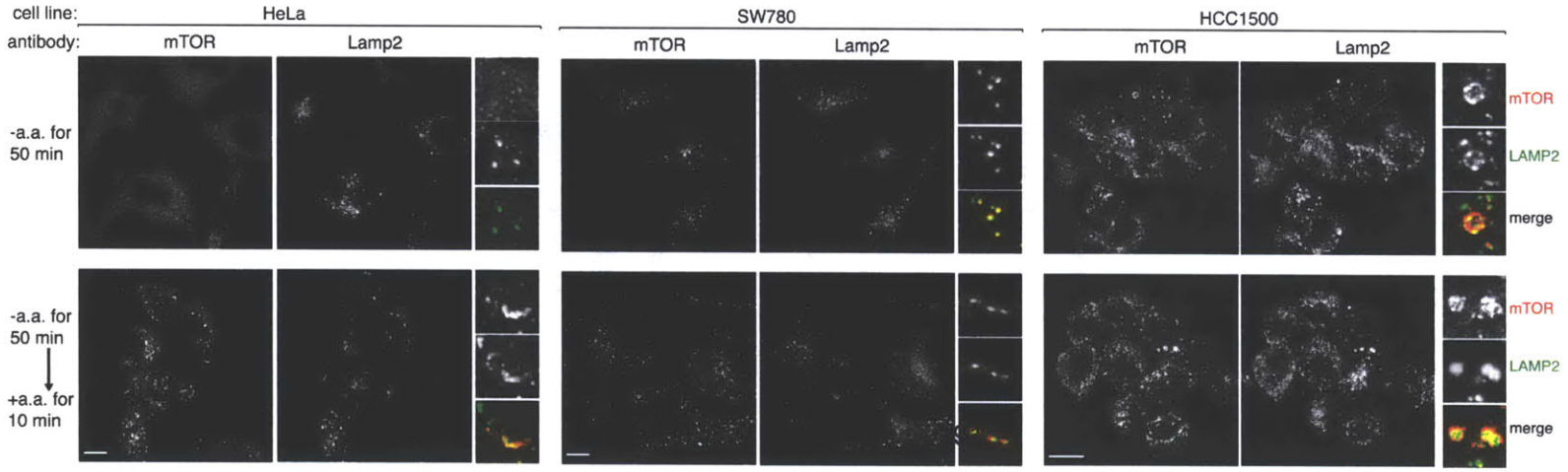

F

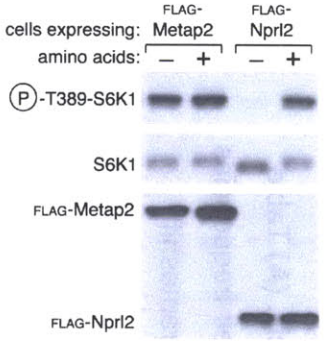

G

Cancer Cell	GATOR1 Deletion	Rapamycin IC_{50} (nM)
HeLa	–	>4000
HT29	–	>4000
Jurkat	–	16 - 194
PC3	–	0.23 ± 0.01
HCC1500	*NPRL2*$^{-/-}$	0.19 ± 0.02
SW780	*NPRL2*$^{-/-}$	0.44 ± 0.08
Li7	*NPRL3*$^{-/-}$	0.42 ± 0.16
MRKNU1	*DEPDC5*$^{-/-}$	0.14 ± 0.04
HA7-RCC	*DEPDC5*$^{-/-}$	0.38 ± 0.06

H

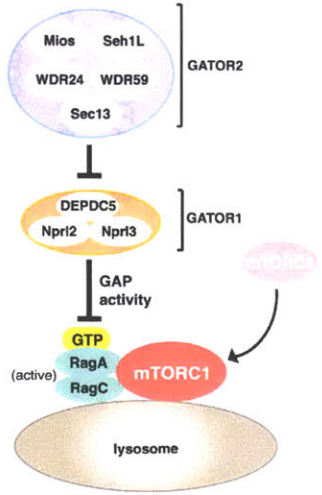

Figure. 5. GATOR1 components are mutated in cancer and GATOR1-null cancer cells are hypersensitive to the mTORC1 inhibitor rapamycin. (**A**) Table summarizing genomic alterations in *DEPDC5* and *NPRL2* and their frequencies in glioblastoma and ovarian cancer. The ratios of nonsense and frameshift mutations to missense mutations in *DEPDC5* (p-value = 0.00015) and *NPRL2* (p-value = 0.00342) in glioblastoma differ significantly from the ratio of all nonsense and frameshift mutations to missense mutations in glioblastoma genomes as determined by a fisher exact test. (**B**)-(**C**) Mutations and deletions identified in *DEPDC5* in glioblastomas and ovarian cancers. (**D**) In GATOR1-null cancer cells the mTORC1 pathway is resistant to amino acid starvation. Cells were starved of amino acids for 50 min and starved and restimulated with amino acids for 10 min. Cell lysates were analyzed by immunoblotting for levels of the indicated proteins. (**E**) Cancer cells were starved or starved and restimulated with amino acids for the specified times prior to co-immunostaining for mTOR (red) and Lamp2 (green). In all images, insets show selected fields that were magnified five times and their overlays. Scale bar equals 10 μM. (**F**) Re-introduction of Nprl2 into the SW780 cell line (*NPRL2*$^{-/-}$) restores amino acid-dependent regulation of mTORC1. Cells stably expressing a control protein or Nprl2 were treated and analyzed as in (**D**). (**G**) GATOR1-null cancer cells are hypersensitive to Rapamycin. Rapamycin IC_{50} values for indicated cancer cell lines. Values are presented as mean ± SD (n = 3). (**H**) Model for the role of the GATOR complex in the amino acid sensing branch of the mTORC1 pathway. GATOR2 is a negative regulator of GATOR1, which inhibits the mTORC1 pathway by functioning as a GAP for RagA.

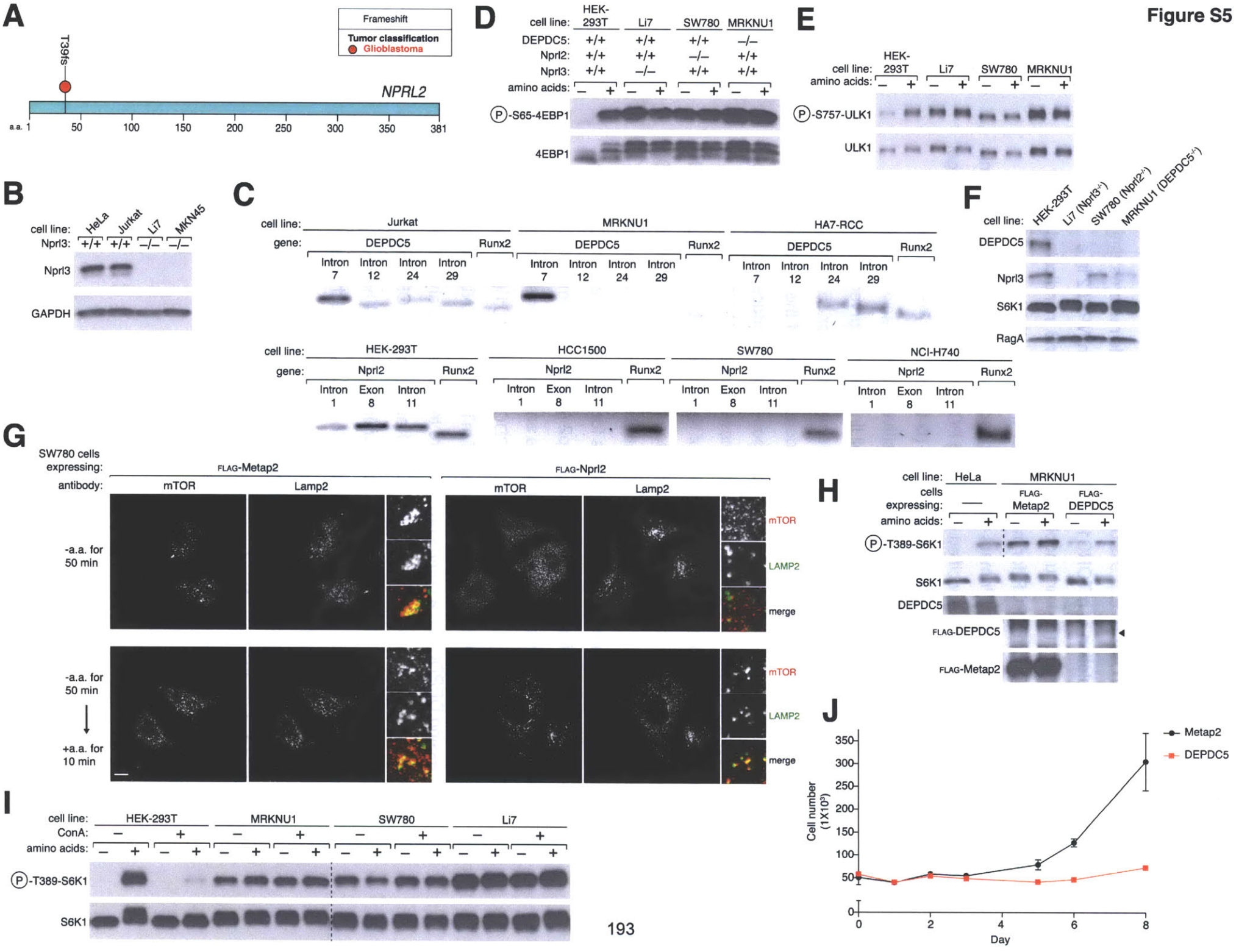
A
Frameshift
Tumor classification
Glioblastoma
T39fs
NPRL2
a.a. 1
50
100
150
200
250
300
350
381
B
cell line: HeLa Jurkat Li7 MKN45
Nprl3: +/+ +/+ –/– –/–
Nprl3
GAPDH
C
cell line: Jurkat MRKNU1 HA7-RCC
gene: DEPDC5 Runx2
Intron 7 Intron 12 Intron 24 Intron 29
cell line: HEK-293T HCC1500 SW780 NCI-H740
gene: Nprl2 Runx2
Intron 1 Exon 8 Intron 11
D
cell line: HEK-293T Li7 SW780 MRKNU1
DEPDC5: +/+ +/+ +/+ –/–
Nprl2: +/+ +/+ –/– +/+
Nprl3: +/+ –/– +/+ +/+
amino acids: – + – + – + – +
P-S65-4EBP1
4EBP1
E
cell line: HEK-293T Li7 SW780 MRKNU1
amino acids: – + – + – + – +
P-S757-ULK1
ULK1
F
cell line: HEK-293T Li7 (Nprl3+/-) SW780 (Nprl2+/-) MRKNU1 (DEPDC5+/-)
DEPDC5
Nprl3
S6K1
RagA
G
SW780 cells expressing: FLAG-Metap2 FLAG-Nprl2
antibody: mTOR Lamp2 mTOR Lamp2
-a.a. for 50 min
+a.a. for 10 min
mTOR
LAMP2
merge
H
cell line: HeLa MRKNU1
cells expressing: — FLAG-Metap2 FLAG-DEPDC5
amino acids: – + – + – +
P-T389-S6K1
S6K1
DEPDC5
FLAG-DEPDC5
FLAG-Metap2
I
cell line: HEK-293T MRKNU1 SW780 Li7
ConA: – + – + – + – +
amino acids: – + – + – + – + – + – + – + – +
P-T389-S6K1
S6K1
J
Cell number (1X10³)
350
300
250
200
150
100
50
0
0 2 4 6 8
Day
Metap2
DEPDC5

Figure S5. GATOR1 re-expression in GATOR1-null cells restores amino acid-dependent regulation of mTORC1. (**A**) Mutation found in *NPRL2* in a glioblastoma tumor. (**B**) Immunoblot for the levels of Nprl3 in indicated cancer cell lines. (**C**) Genomic PCR for indicated *DEPDC5* and *NPRL2* regions from various cancer cell lines. Primers were designed to amplify the indicated intronic or exonic regions of the specified genes and PCR products were resolved by gel electrophoresis. Runx2 is a positive control. (**D-E**) mTORC1-dependent translation control and autophagy are insensitive to amino acid deprivation in GATOR1-null cells. The indicated cancer cell lines were starved of amino acids for 2 hours or starved and restimulated with amino acids for 15 min. Cell lysates were prepared and immunoblotting used to detect levels of the indicated proteins. (**F**) Cells missing a GATOR1 component have reduced expression of remaining GATOR1 proteins. Immunoblot shows levels of Nprl3 and DEPDC5 in the indicated cell lines. (**G**) Re-introduction of Nprl2 into SW780 (*NPRL2*$^{-/-}$) cells restores the amino acid-dependent localization of mTORC1. Images of SW780 cells stably expressing FLAG-Nprl2 or a control protein were starved of or starved of and restimulated with amino acids for the indicated times. Cells were co-immunostained for mTOR (red) and Lamp2 (green). In all images, insets show selected fields that were magnified five times and their overlays. Scale bar represents 10 μM. (**H**) Re-expression of DEPDC5 in MRKNU1 (*DEPDC5*$^{-/-}$) cells restores amino acid-dependent regulation of mTORC1. MRKNU1 cells stably expressing DEPDC5 or a control protein were treated and analyzed as in (**D**). (**I**) v-ATPase inhibition does not inhibit mTORC1 activity in GATOR1-null cells. The indicated cancer cell lines were deprived of amino acids for 4 hours in the presence or absence of 2.5 μM Concanamycin A (ConA) and then stimulated with amino acids for 15 minutes. Cell lysates were prepared and analyzed as described in (**D**). (**J**) Re-introduction of DEPDC5 into MRKNU1 (*DEPDC5*$^{-/-}$) cells inhibits their proliferation. Number of MRKNU1 cells expressing DEPDC5 or a control protein was determined on indicated days. Values are presented as mean ± SD (n = 3-9).

Materials and Methods

Materials

Reagents were obtained from the following sources: antibody to Nprl3 from Atlas Antibodies; HRP-labeled anti-mouse and anti-rabbit secondary antibodies from Santa Cruz Biotechnology; antibodies to phospho-T389 S6K1, S6K1, RagA and RagC, phospho-T398 dS6K, mTOR, LC3, and FLAG epitope from Cell Signaling Technology; the antibody to Mios and DEPDC5 was produced in collaboration with Cell Signaling Technology; antibodies to the HA epitope from Bethyl laboratories. RPMI, FLAG M2 affinity gel, ATP, GDP, and amino acids from Sigma Aldrich; DMEM from SAFC Biosciences; Xtremegene 9, Fugene 6 and Complete Protease Cocktail from Roche; Alexa 488 and 568-conjugated secondary antibodies; Schneider's media, Express Five-SFM, and Inactivated Fetal Calf Serum (IFS) from Invitrogen; amino acid-free RPMI, and amino acid free Schneider's media from US Biological; Cellulose PEI TLC plates from Sorbent Technologies; [^{3}H]GDP, [α-^{32}P]GTP, and [γ-^{32}P]GTP from Perkin Elmer; GTP, XTP and XDP from Jena Biosciences; siRNAs targeting indicated genes and siRNA transfection reagent from Dharmacon; nitrocellulose membrane filters from Advantec; DSP from Pierce. The dS6K antibody was a generous gift from Mary Stewart (North Dakota State University).

Cell lines and tissue culture

HEK-293T, HeLa, and HT-29 cells were cultured in DMEM 10% IFS; Jurkat, HCC1500, NCI-H740 and Li7 cells were cultured in RPMI supplemented with 10% FBS; MRKNU1 cells were cultured in DMEM supplemented with 10% FBS and 2 mM glutamine; SW780 and HA7RCC cells were cultured in IMDM supplemented with 10% FBS; MKN45 were cultured in RPMI supplemented with 20% FBS; S2 cells were cultured in Express-Five SFM. All cell lines were maintained at 37°C, 5% CO2, with the exception of S2 cells which were grown at 25°C. HCC1500, NCI-H740 and SW780 cells were obtained from the American

Type Culture Collection (ATCC), Li7 cells from the Riken Bio Resource Center, MRKNU1 from the Health Science Research Resources Bank (HSRRB), MKN45 cells from Deutsche Sammlung von Mikroogranismen and Zellkulturen (DSMZ) and HA7RCC cells were a generous gift from Benoît Vandeneynde (de Duve Institute and Université catholique de Louvain and Ludwig Institute for Cancer Research).

Cell lysis and immunoprecipitation

HEK-293T cells transiently transfected with cDNA expression vectors (see below) were rinsed once with ice-cold PBS and lysed with Triton lysis buffer (1% Triton X-100, 10 mM β-glycerol phosphate, 10 mM pyrophosphate, 40 mM HEPES pH 7.4, 2.5 mM $MgCl_2$ and 1 tablet of EDTA-free protease inhibitor [Roche] (per 25 ml buffer)). Lysis of HEK-293T cells stably expressing FLAG-tagged DEPDC5, WDR24 or Metap2, was identical to the procedure described in *(7)*. The soluble fractions of cell lysates were isolated by centrifugation at 13,000 rpm in a microcentrifuge for 10 minutes. For anti-FLAG-immunoprecipitations, the FLAG-M2 affinity gel was washed with lysis buffer 3 times. 20 μl of a 50% slurry of the affinity gel was then added to cleared cell lysates and incubated with rotation for 2 hours at 4°C. The beads were washed 3 times with lysis buffer containing 150 mM NaCl. Immunoprecipitated proteins were denatured by the addition of 50 μl of sample buffer and boiling for 5 minutes as described (*27*), resolved by 8%–16% SDS-PAGE, and analyzed by immunoblotting.

For co-transfection experiments, 2,000,000 HEK-293T cells were plated in 10 cm culture dishes. Twenty-four hours later, cells were transfected using Xtremegene 9 transection reagent with the pRK5-based cDNA expression plasmids indicated in the Figures in the following amounts: 100 ng HA-RagB; 100 ng HA- or HA-GST-RagC; 300 ng HA-GST-$RagB^{Q99L}$ or 300 ng HA-GST-$RagB^{T54N}$; 300 ng HA-GST-$RagC^{S75N}$ or 300 ng HA-GST-$RagC^{Q120L}$; 500 ng HA- or 100-1000 ng Flag-Metap2; 2000 ng Flag- or 100 ng HA-Mios; 300 ng Flag- or 100 ng HA-WDR24; 200 ng Flag- or 100-300 ng HA-Nprl2; 100 ng HA-WDR59; 100-300 ng HA-Nprl3; 100 ng HA-Seh1L; 100 ng HA-Sec13, 3 ng Flag-S6K. The

total amount of plasmid DNA in each transfection was normalized to 2 μg with empty pRK5. Thirty-six hours after transfection, cells were lysed as described above.

Mass spectrometric analyses

HEK-293T cells stably expressing FLAG-tagged Metap2, RagB, Mios, DEPDC5, WDR24, or Nprl2 were chemically crosslinked with DSP prior to cell lysis with Triton lysis buffer as described in (*6*). Cell lysates and FLAG-immunoprecipitations were prepared as described above. Proteins were eluted with the FLAG peptide (sequence DYKDDDDK) from the FLAG-M2 affinity gel, resolved on 4-12% NuPage gels (Invitrogen), and stained with simply blue stain (Invitrogen). Each gel lane was sliced into 10-12 pieces and the proteins in each gel slice digested overnight with trypsin. The resulting digests were analyzed by mass spectrometry as described (*4*). Peptides corresponding to GATOR members, Ragulator, v-ATPase or Rags were detected in the FLAG-RagB, FLAG-Mios, FLAG-DEPDC5, FLAG-Nprl2 and FLAG-WDR24 immunoprecipitates, while no peptides were detected in negative control immunoprecipitates of FLAG-Metap2.

Amino acid starvation and stimulation and concanamycin A treatment of cell lines

HEK-293T cells in culture dishes or coated glass cover slips were rinsed with and

incubated in amino acid-free RPMI for either 50 minutes or 2 hours and stimulated with a 10X mixture of amino acids for 10-30 minutes. After stimulation, the final concentration of amino acids in the media was the same as in RPMI. The 10X mixture was prepared from individual powders of amino acids. Amino acid starvation for other cancer cell lines cells was identical to the procedure described above, with the addition of 10% dialyzed IFS to amino acid-free RPMI. When concanamycin A (ConA) was used, cells were incubated with 2.5 μM of ConA during the 4 hr amino acid starvation and 15 min amino acid stimulation

periods.

RNAi in Drosophila S2 cells

dsRNAs against *Drosophila GATOR* genes were designed as described in (*4*). Primer sequences used to amplify DNA templates for dsRNA synthesis for Mio, dSeh1L, dWDR24, dWDR59, dDEPDC5, dNprl2, and dNprl3 including underlined 5' and 3' T7 promoter sequences, are as follows:

Mio (CG7074)

Forward primer CG7074_1F:

GAATTAATACGACTCACTATAGGGAGATGCCTTATATATCCGTGAACTACCT

Reverse primer CG7047_1R:

GAATTAATACGACTCACTATAGGGAGACTCAATGTCCCAGATGGTGAT

Forward primer CG7074_2F:

GAATTAATACGACTCACTATAGGGAGAAGATGATAAAGCTGTTCGATCTGAG

Reverse primer CG7047_2R:

GAATTAATACGACTCACTATAGGGAGACAATTAACAAACGAAAACTTTCCAC

Forward primer CG7074_3F:

GAATTAATACGACTCACTATAGGGAGAATCGCTTTATAGACCAGTTGTATGC

Reverse primer CG7047_3R:

GAATTAATACGACTCACTATAGGGAGAAGCTTGGTCTCCGATAGATATTTG

dSeh1L (CG8722)

Forward primer CG8722_1F:

GAATTAATACGACTCACTATAGGGAGAGAAAGTGCGTTAAAATCGATACTGT

Reverse primer CG8722_1R:

GAATTAATACGACTCACTATAGGGAGACAATTGTGCTCGCTAAACTTAATG

dWDR59 (CG4705)

Forward primer CG4705_1F:

GAATTAATACGACTCACTATAGGGAGAAGGCAGAGCAACAAATACTATGAAC

Reverse primer CG4705_1R:

GAATTAATACGACTCACTATAGGGAGAAGTCCCAAATATGAGAAAATGTGTC

Forward primer CG4705_2F:

GAATTAATACGACTCACTATAGGGAGACATTATGGAGAAGACAGTTCGACTT

Reverse primer CG4705_2R:

GAATTAATACGACTCACTATAGGGAGAATTGATCAAACAGTGGCATCTTAGT

dWDR24 (CG7609)

Forward primer CG7609_1F:

GAATTAATACGACTCACTATAGGGAGATGTACAAATTCATGGTAAACGACAC

Reverse primer CG7609_1R:

GAATTAATACGACTCACTATAGGGAGAGTGAGTTCATTGGATTCTTTTGATT

Forward primer CG7609_2F:

GAATTAATACGACTCACTATAGGGAGAAATCAAAAGAATCCAATGAACTCAC

Reverse primer CG7609_2R:

GAATTAATACGACTCACTATAGGGAGAAAGAGCTCAAAGTTGTCAAAGGTAA

dDEPDC5 (CG12090)

Forward primer CG12090_1F:

GAATTAATACGACTCACTATAGGGAGAGGACTTGGTGATGAATCTAAAGGAT

Reverse primer CG12090_1R:

GAATTAATACGACTCACTATAGGGAGATGAAGGTAATCTCTATCGAGTCCAG

Forward primer CG12090_2F:

GAATTAATACGACTCACTATAGGGAGATCGAAAAGCATTACTTGGATAGAAC

Reverse primer CG12090_2R:

GAATTAATACGACTCACTATAGGGAGAATCAAAGAGCGAGTTGTGCTTATAC

dNprl2 (CG9104)

Forward primer CG9104_1F:

GAATTAATACGACTCACTATAGGGAGAATGTGTTCGATGCTATCAATGTTTA

Reverse primer CG9104_1R:

GAATTAATACGACTCACTATAGGGAGATATATAAGGCAGGATCTGTTGTGTG

Forward primer CG9104_2F:

GAATTAATACGACTCACTATAGGGAGATGCATACAGAATCTGGTCTACTACG

Reverse primer CG9104_2R:

GAATTAATACGACTCACTATAGGGAGACACTTCCAGATCACAGTCACATTC

dNprl3 (CG8783)

Forward primer CG8783_1F:
GAATTAATACGACTCACTATAGGGAGACTGTACAGGTATCCGTACCAGACTC
Reverse primer CG8783_1R:
GAATTAATACGACTCACTATAGGGAGAATAGCTGTGGTTTAACAGCAAACAG
Forward primer CG8783_2F:
GAATTAATACGACTCACTATAGGGAGAATCTTCCATGATCTATGCACCAC
Reverse primer CG8783_2R:
GAATTAATACGACTCACTATAGGGAGAACGAGCTTATAAACATGCTCGATAC

dsRNAs targeting GFP and dRagC were used as negative and positive controls, respectively. On day one, 4,000,000 S2 cells were plated in 6 cm culture dishes in 5 ml of Express Five SFM media. Cells were transfected with 1 µg of dsRNA per million cells using Fugene 6 (Roche). Two days later, a second round of dsRNA transfection was performed. On day five, cells were rinsed once with amino acid-free Schneider's medium, and starved for amino acids by replacing the media with amino acid-free Schneider's medium for 1.5 hours. To stimulate with amino acids, the amino acid-free medium was replaced with complete Schneider's medium for 30 minutes. Cells were then washed with ice cold PBS, lysed, and subjected to immunoblotting for phospho-T398 dS6K and total dS6K.

Mammalian RNAi

On day one, 200,000 HEK-293T cells were plated in a 6 well plate. Twenty-fours hours later, the cells were transfected with 250 nM of a pool of siRNAs [Dharmacon] targeting Mios, WDR24, WDR59 or Seh1L or a non-targeting pool. On day four, the cells were transfected again but this time with double the amount of siRNAs. On day five, the cells were either split onto coated glass cover slips or rinsed with ice-cold PBS, lysed and subjected to immunobloting as described above.

Lentiviral shRNAs targeting Mios, WDR24, WDR59, Seh1L, DEPDC5, Nprl2, Nprl3 and GFP were obtained from the TRC. The TRC number for each

shRNA is as follows:

Human Mios shRNA_1: TRCN0000303645

Human Mios shRNA_2: TRCN0000370186

Human WDR24 shRNA_1: TRCN0000130142

Human WDR24 shRNA_2: TRCN0000416122

Human WDR24 shRNA_3: TRCN0000445462

Human WDR59 shRNA_1: TRCN0000156940

Human WDR59 shRNA_2: TRCN0000156869

Human Seh1L shRNA_1: TRCN0000330510

Human Seh1L shRNA_2: TRCN0000330507

Human Nprl2 shRNA_1: TRCN0000234677

Human Nprl2 shRNA_2: TRCN0000234673

Human Nprl3 shRNA_2: TRCN0000135594

Human DEPDC5 shRNA_1: TRCN0000137523

The following shRNAs targeting Nprl3 and DEPDC5 were made in the lab and cloned into pLKO.1 vector as described (*28*).

The target sequence for the Nprl3 shRNA:

Human Nprl3 shRNA_1: GATGTTATTCTGGCAACAATT

The target sequence for the DEPDC5 shRNA:

Human DEPDC5 shRNA_2: CAGGTATTTGAAGAGTTTATT

shRNA-encoding plasmids were co-transfected with the Delta VPR envelope and CMV VSV-G packaging plasmids into actively growing HEK-293T cells using Xtremegene 9 transfection reagent as previously described (*28*). Virus-containing supernatants were collected 48 hours after transfection, filtered to eliminate cells and target cells were infected in the presence of 8 μg/ml polybrene. 24 hours later, cells were selected with puromycin and analyzed on the 2^{nd} or 3^{rd} day after infection.

Immunofluorescence assays

Immunofluorescence assays were performed as described in (*6*). Briefly, 200,000 HEK-293T (infected with lentiviral shRNAs) cells or 75,000 cells for other cell lines used (HeLa, SW780, HCC1500) were plated on fibronectin-coated glass coverslips in 12-well tissue culture plates. Twenty-four hours later, the slides were rinsed with PBS once and fixed for 15 min with 4% paraformaldehyde in PBS at room temperature. The slides were rinsed twice with PBS and cells were permeabilized with 0.05% Triton X-100 in PBS for 5 min. In assays requiring the LC3 primary antibody, cells were fixed and permeabilized in ice-cold MeOH for 10 min. After rinsing twice with PBS, the slides were incubated with primary antibody in 5% normal donkey serum for 1 hr at room temperature, rinsed four times with PBS, and incubated with secondary antibodies produced in donkey (diluted 1:1000 in 5% normal donkey serum) for 45 min at room temperature in the dark and washed four times with PBS. Slides were mounted on glass coverslips using Vectashield (Vector Laboratories) and imaged on a spinning disk confocal system (Perkin Elmer) or a Zeiss Laser Scanning Microscope (LSM) 710.

S2 cell size determinations

For measurements of cell size, S2 cells treated with dsRNAs as described above, were harvested in a 4 ml volume and diluted 1:20 with counting solution (Isoton II Diluent, Beckman Coulter). Cell diameters were determined with a particle size counter (Coulter Z2, Beckman Coulter) running Coulter Z2 AccuComp software.

Purification of recombinant Rag heterodimers, GATOR1, and Ragulator for GAP/GEF/In-vitro binding assays

To produce protein complexes used for GAP or GEF assays, 4,000,000 HEK-293T cells were plated in 15 cm culture dishes. Forty-eight hours later, cells

were transfected with the following combination of constructs (all cDNAs were expressed from pRK5 expression plasmid). For FLAG-GATOR1: 4 µg FLAG-DEPDC5, 8 µg HA-Nprl2 and 8 µg HA-Nprl3. For FLAG-Ragulator: 4 µg Flag-p14, 8 µg HA-MP1, 8 µg HA-p18^{G2A} (a lipidation defective mutant), 8 µg HA-HBXIP, and 8 µg HA-C7orf59. For RagA/B-RagC^{X}: 16 µg HA-RagB or HA-RagA and 8 µg Flag-RagC^{D181N}; for RagB^{X}-RagC: 8 µg FLAG-RagB^{D163N} and 16 µg HA-RagB. For Rags used in in-vitro binding assays: 8 µg HA-GST-RagB^{T54N} and 16 µg HA-RagC^{Q120L}; 4 µg HA-GST-RagB^{Q99L} and 8 µg HA-RagC^{S75N}. For individual proteins: 10 µg Flag- or HA-GST-Rap2a, 15 µg of FLAG-Leucyl tRNA synthetase (LRS), or 10 µg Flag-Metap2.

Thirty-six hours post transfection cell lysates were prepared as described above, with the exception that for all FLAG-GATOR1 and FLAG-LRS purifications, 1 mM ATP was added to the lysis buffer. 200 µl of a 50% slurry of FLAG-M2 affinity gel or immobilized glutathione beads were added to lysates from cells expressing FLAG-tagged proteins or HA-GST tagged proteins, respectively. Recombinant proteins were immunoprecipitated for 3 hours at 4°C. Each sample was washed once with Triton lysis buffer, followed by 3 washes with Triton lysis buffer supplemented with 500 mM NaCl. For FLAG-LRS and FLAG-GATOR1 an additional wash was preformed and samples were incubated in Triton lysis buffer supplemented with 500mM NaCl for 30 min. Finally samples were washed 4 times with CHAPS buffer (40 mM Hepes pH 7.4, 0.3% CHAPS) supplemented with 2.5 mM $MgCl_2$ for GTPase purifications. FLAG-tagged proteins were eluted from the FLAG-M2 affinity gel with a competing FLAG peptide for 1 hour as described above. Proteins were subsequently purified on a HiLoad 16/60 Superdex 200 FPLC column (GE) pre-equilibrated with CHAPS buffer supplemented with 150 mM NaCl. The peak corresponding to the desired complex was concentrated with 10,000 MW CO columns (Amicon), snap frozen in CHAPS buffer supplemented with 10% glycerol and stored at -80°C. In some Rag GAP assays, FLAG-GATOR1 and FLAG-LRS were not further purified by FPLC and instead stored in CHAPS buffer supplemented with 10% glycerol

immediately following elution with FLAG peptide. The FPLC-purified and -non-purified GATOR1 had very similar levels of GAP activity towards RagB.

In Vitro Binding Assays

For the binding reactions, 20 µl of a 50% slurry containing immobilized HA-GST-tagged proteins were incubated in binding buffer (1% Triton X-100, 2.5 mM MgCl2, 40 mM HEPES [pH 7.4], 2 mM DTT, and 1 mg/ml BSA) with 2 µg of FLAG-GATOR1 in a total volume of 50 µl for 1 hr and 30 min at 4°C. To terminate binding assays, samples were washed three times with 1 ml of ice-cold binding buffer supplemented with 300 mM NaCl followed by the addition of 50 µl of sample buffer.

Rag GTP hydrolysis assays

14 µg of the indicated Rag heterodimers or Rap2a were incubated for 2 hours at 4°C with 20 µl of FLAG-M2 affinity gel prewashed in CHAPS loading buffer (4 mM HEPES pH 7.4, 30 mM NaCl, 0.3% CHAPS). The resin was then washed 3 times with CHAPS loading buffer to remove unbound protein. The GTPases were loaded in 100 µl CHAPS loading buffer containing 0.1 µM XDP or 0.1 µM XTP, 70 pmols of the specified radioactive GTP species ([α-^{32}P]GTP for TLC assays or [γ-^{32}P]GTP for phosphate capture assays), 2 mM DTT, 0.01 µg/µl BSA, and 5 mM EDTA at 25°C for 10 minutes. Following nucleotide loading, $MgCl_2$ was added to a final concentration of 20 mM and the GTPases were incubated overnight at 4°C. The GTPases were washed 6 times with GTPase wash buffer (4 mM HEPES pH 7.4, 5 mM $MgCl_2$, 20 mM NaCl, 0.3% CHAPS, 2 mM DTT, 0.01 µg/µl BSA) to remove unbound nucleotide. 30 µl of competing FLAG-peptide was then added and the GTPases were eluted from the affinity gel for 2 hours. Protein concentrations were determined prior to use.

For the TLC-based GTP hydrolysis assay, 5 pmols of the indicated Rag heterodimer or Rap2a loaded with xanthosine nucleotides and [α-^{32}P]GTP were added to 20 pmols Flag-LRS or Flag-GATOR1 in 45 µl of GTPase wash buffer. The reaction was incubated at 25°C for the indicated time. The assay was

terminated upon addition of 5 µl of 6X Elution Buffer (6.7 mM GTP, 6.7 mM GDP, 100 mM EDTA, 2% SDS) followed by further incubation for 5 minutes at 65°C at 1,400 rpm. Chloroform was added to separate the nucleotides from denatured proteins and the sample was spun at 13,200 rpm in a microcentrifuge for 1 min to separate the aqueous and organic phases. 30 µl of the aqueous layer was removed. Samples were spotted on a PEI Cellulose TLC plates and developed for 2.5 hours in 0.5 M KH_2PO_4 pH 3.4. Plates were exposed to film and spot densities were quantified with Multi Gauge V2.2 (Fujifilm).

For the phosphate capture GTP hydrolysis assay, Flag-RagC^{D181N}-HA-RagB was loaded with [γ-^{32}P]GTP and XDP as described above. A total of 48 pmols of loaded Flag-RagC^{D181N}-HA-RagB was added to GTPase wash buffer containing Flag-LRS or FLAG-GATOR1 in a total volume of 140 µl and incubated at 25°C. At the indicated time points three aliquots of 10 µl were taken and quenched by addition of 500 µl of activated charcoal mixture (5% activated charcoal, Norit® (Sigma) in 50 mM NaH_2PO_4). This mixture was then vortexed and spun at 13200 rpm in a microcentrifuge for 10 minutes at 4°C. 375 µl of the supernatant was added to 3.5 ml of Optifluor scintillation fluid and free $^{32}P_i$ was measured using a TriCarb scintillation counter (Perkin Elmer).

Nucleotide Exchange Assays

These assays were essentially performed as described in (7). Briefly, 40 pmols of FLAG-RagB^{X}-HA-RagC or FLAG-RagC^{X}-HA-RagB were loaded with 2 µM of [^{3}H]GDP (25-50 Ci/mmol). The GTPase-[^{3}H]GDP were stabilized by addition of 20 mM $MgCl_2$ followed by a further incubation at 4°C for 12 hours. To initiate the GEF assay, 40 pmols of the indicated proteins were added along with 200 µM GTPγS and incubated at 25°C. Samples were taken every 2 minutes and spotted on nitrocellulose filters, which were washed with 2 ml of wash buffer (40 mM HEPES pH 7.4, 150 mM NaCl and 5 mM $MgCl_2$). Filter-associated radioactivity was measured using a TriCarb scintillation counter (Perkin Elmer).

Identification of *DEPDC5* and *NPRL2* genomic alterations in glioblastoma

and ovarian tumors

Mutations and chromosome alterations in the TCGA dataset of Glioblastoma and Serous Ovarian tumors are available at cancergenome.nih.gov (*29, 30*). *DEDPC5* and *NPRL2* mutation identification came from analysis of exome sequencing data and copy number alternations were based on Affiymatrix SNP 6.0 microarray data. Tumors chosen for analysis had point mutations or focal deletions encompassing all or a portion of either *DEPDC5* or *NPRL2*. Loss of heterozygosity, biallelic inactivation, hemizygous and homozygous deletions in these tumors were determined using the ABSOLUTE algorithm (*31*).

Identification of GATOR1-null cancer cell lines

To identify cancer cell lines null for GATOR1 components we searched the following publically available databases: Cancer Cell Line Encyclopedia (CCLE) (http://www.broadinstitute.org/ccle/home) and Cancer Genome Project (CPG) (http://www.sanger.ac.uk/cgi-bin/genetics/CGP/conan/search.cgi). GATOR1 null cell lines were identified in CCLE based on a value <-4 when sorted by deletion of the indicated GATOR1 genes. GATOR1-null cells were identified at CGP based on copy number analysis using CONAN. *NPRL3*-null cells were verified by immunoblotting for the Nprl3 protein. *DEPDC5*- and *NPRL2*-null cells were verified by genomic PCR as follows. Genomic DNA from cancer cells was extracted using the QiAmp DNA Mini kit Blood and Tissue (Qiagen) and used in PCR reactions with the gene-specific primers listed below. Runx2 is a positive control.

Runx2_exon6_fwd: CGCATTCCTCATCCCAGTATG
Runx2_exon6_rev: AAAGGACTTGGTGCAGAGTTCAG
DEPDC5_intron7_fwd: CCAAGCAACTAAAGCACAACCCAA
DEPDC5_intron7_rev: CAGGCTTCCTGACCCTGGATAC
DEPDC5_intron12_fwd: TGGGCCATCTGCTGTACTGAC
DEPDC5_intron12_rev: CAGAAGAGCTCTCATGGTTCCTGG
DEPDC5_intron24_fwd: AGTGACTTTCCTTTCAAGCCATCCT
DEPDC5_intron24_rev: CCTTAGCACAGTGCCTAGAGTTCA

DEPDC5_intron29_fwd: TGAAGCTCAGGGATGACGTGC
DEPDC5_intron29_rev: AATCAGGCGTCACAAAGCTACCA
NRPL2_intron1_fwd: GCTCCCAATGTGGCAGGGAA
NRPL2_intron1_rev: TCACCTTCTGTGGGACCTGGA
NRPL2_exon8_fwd: CTGATCCCTGGCACCCACAG
NRPL2_exon8_rev: CCAATGAGGTCTCGCACGGT
NRPL2_intron11_fwd: GAGCTGGATGAGCGGCTTGA
NRPL2_intron11_rev: AGGAGGGACTACCCACAGCA

Rapamycin sensitivity assays

The indicated cancer cell lines were seeded in 96 well plates (Corning). Rapamycin, (0.4 pM – 4 μM), was added 24 hours post-seeding, and DMSO was used as the control. Cell viability was measured 4 days after drug addition with CellTiter Glo luminescent viability assay (Promega). Readings were normalized to the untreated cells and IC_{50} values calculated with Prism 5 (Graphpad). All assays were performed in triplicate.

Cell proliferation assays

On day minus 1 of the assay, 1,000,000 MRKNU1 cells were electroporated using a Lonza Nucleofector II following the manufacturers recommendation (Buffer L, program L029) with pRK5-based cDNA expression plasmids in the following amounts: 2.5 μg of FLAG-Metap2 and 2.5 μg of Empty pRK5; 5 μg FLAG-DEPDC5. On day 0, 40,000 electroporated cells were seeded in a 12-well in 2 mL of the appropriate media. Cell numbers were counted on subsequent days. At each time point, assays were repeated 3-9 times.

Acknowledgements

We thank all members of the Sabatini Lab for helpful suggestions, Eric Spooner for the mass spectrometric analysis of samples and Nora Kory for technical assistance. This work was supported by grants from the NIH (CA103866 and AI47389) and Department of Defense (W81XWH-07-0448) to D.M.S. and the NCI (U24CA143867) to M.L.M., and awards from the David H. Koch Graduate Fellowship Fund to L.B.P., the NSF Graduate Research Fellowship Program to L.C., the Harvard-MIT Health, Sciences, and Technology IDEA^2 program to W.W.C., and the American Cancer Society to B.C.G. D.M.S. is an investigator of the Howard Hughes Medical Institute.

References

1. M. Laplante, D. M. Sabatini, mTOR signaling in growth control and disease. *Cell* **149**, 274 (Apr 13, 2012).
2. X. M. Ma, J. Blenis, Molecular mechanisms of mTOR-mediated translational control. *Nat Rev Mol Cell Biol* **10**, 307 (May, 2009).
3. R. Zoncu *et al.*, mTORC1 senses lysosomal amino acids through an inside-out mechanism that requires the vacuolar H(+)-ATPase. *Science* **334**, 678 (Nov 4, 2011).
4. Y. Sancak *et al.*, The Rag GTPases bind raptor and mediate amino acid signaling to mTORC1. *Science* **320**, 1496 (Jun 13, 2008).
5. E. Kim, P. Goraksha-Hicks, L. Li, T. P. Neufeld, K. L. Guan, Regulation of TORC1 by Rag GTPases in nutrient response. *Nat Cell Biol* **10**, 935 (Aug, 2008).
6. Y. Sancak *et al.*, Ragulator-Rag complex targets mTORC1 to the lysosomal surface and is necessary for its activation by amino acids. *Cell* **141**, 290 (Apr 16, 2010).
7. L. Bar-Peled, L. D. Schweitzer, R. Zoncu, D. M. Sabatini, Ragulator Is a GEF for the Rag GTPases that Signal Amino Acid Levels to mTORC1. *Cell* **150**, 1196 (Sep 14, 2012).
8. T. Sekiguchi, E. Hirose, N. Nakashima, M. Ii, T. Nishimoto, Novel G proteins, Rag C and Rag D, interact with GTP-binding proteins, Rag A and Rag B. *J Biol Chem* **276**, 7246 (Mar 9, 2001).
9. G. Mattson *et al.*, A practical approach to crosslinking. *Mol Biol Rep* **17**, 167 (Apr, 1993).
10. T. Iida, M. A. Lilly, missing oocyte encodes a highly conserved nuclear protein required for the maintenance of the meiotic cycle and oocyte identity in Drosophila. *Development* **131**, 1029 (Mar, 2004).
11. R. Loewith, M. N. Hall, Target of rapamycin (TOR) in nutrient signaling and growth control. *Genetics* **189**, 1177 (Dec, 2011).
12. T. K. Neklesa, R. W. Davis, A genome-wide screen for regulators of TORC1 in response to amino acid starvation reveals a conserved Npr2/3 complex. *PLoS Genet* **5**, e1000515 (Jun, 2009).
13. X. Wu, B. P. Tu, Selective regulation of autophagy by the Iml1-Npr2-Npr3 complex in the absence of nitrogen starvation. *Mol Biol Cell* **22**, 4124 (Nov, 2011).
14. M. Graef, J. Nunnari, Mitochondria regulate autophagy by conserved signalling pathways. *Embo J* **30**, 2101 (Jun 1, 2011).
15. S. Dokudovskaya *et al.*, A conserved coatomer-related complex containing Sec13 and Seh1 dynamically associates with the vacuole in Saccharomyces cerevisiae. *Mol Cell Proteomics* **10**, M110 006478 (Jun, 2011).
16. N. C. Leksa, T. U. Schwartz, Membrane-coating lattice scaffolds in the nuclear pore and vesicle coats: commonalities, differences, challenges. *Nucleus* **1**, 314 (Jul-Aug, 2010).

17. U. Krengel *et al.*, Three-dimensional structures of H-ras p21 mutants: molecular basis for their inability to function as signal switch molecules. *Cell* **62**, 539 (Aug 10, 1990).
18. J. M. Han *et al.*, Leucyl-tRNA synthetase is an intracellular leucine sensor for the mTORC1-signaling pathway. *Cell* **149**, 410 (Apr 13, 2012).
19. D. M. Sabatini, mTOR and cancer: insights into a complex relationship. *Nat Rev Cancer* **6**, 729 (Sep, 2006).
20. M. I. Lerman, J. D. Minna, The 630-kb lung cancer homozygous deletion region on human chromosome 3p21.3: identification and evaluation of the resident candidate tumor suppressor genes. The International Lung Cancer Chromosome 3p21.3 Tumor Suppressor Gene Consortium. *Cancer Res* **60**, 6116 (Nov 1, 2000).
21. J. Li *et al.*, Functional characterization of the candidate tumor suppressor gene NPRL2/G21 located in 3p21.3C. *Cancer Res* **64**, 6438 (Sep 15, 2004).
22. T. J. Seng *et al.*, Complex chromosome 22 rearrangements in astrocytic tumors identified using microsatellite and chromosome 22 tile path array analysis. *Genes Chromosomes Cancer* **43**, 181 (Jun, 2005).
23. L. Ji *et al.*, Expression of several genes in the human chromosome 3p21.3 homozygous deletion region by an adenovirus vector results in tumor suppressor activities in vitro and in vivo. *Cancer Res* **62**, 2715 (May 1, 2002).
24. M. S. Neshat *et al.*, Enhanced sensitivity of PTEN-deficient tumors to inhibition of FRAP/mTOR. *Proc Natl Acad Sci U S A* **98**, 10314 (Aug 28, 2001).
25. M. Y. Wang *et al.*, Mammalian target of rapamycin inhibition promotes response to epidermal growth factor receptor kinase inhibitors in PTEN-deficient and PTEN-intact glioblastoma cells. *Cancer Res* **66**, 7864 (Aug 15, 2006).
26. F. Meric-Bernstam *et al.*, PIK3CA/PTEN mutations and Akt activation as markers of sensitivity to allosteric mTOR inhibitors. *Clin Cancer Res* **18**, 1777 (Mar 15, 2012).
27. D.-H. Kim *et al.*, mTOR Interacts with Raptor to Form a Nutrient-Sensitive Complex that Signals to the Cell Growth Machinery. *Cell* **110**, 163 (2002).
28. D. D. Sarbassov, D. A. Guertin, S. M. Ali, D. M. Sabatini, Phosphorylation and regulation of Akt/PKB by the rictor-mTOR complex. *Science* **307**, 1098 (Feb 18, 2005).
29. Comprehensive genomic characterization defines human glioblastoma genes and core pathways. *Nature* **455**, 1061 (Oct 23, 2008).
30. Integrated genomic analyses of ovarian carcinoma. *Nature* **474**, 609 (Jun 30, 2011).
31. S. L. Carter *et al.*, Absolute quantification of somatic DNA alterations in human cancer. *Nat Biotechnol* **30**, 413 (May, 2012).

Chapter 5

Future Directions and Discussion

Amino acids not only function as substrates for metabolic processes but are key signaling molecules required for activation of the mTORC1 pathway. Despite their essential roles, surprisingly little is known about how they are sensed and stimulate mTORC1. The discovery that mTORC1 shuttles to the lysosomal surface in response to amino acid-mediated activation of the Rag GTPases represented a breakthrough in our understanding of mTORC1 regulation. It makes intuitive sense for mTORC1 signaling to occur at the lysosome since this organelle is the end point of many catabolic pathways, thus allowing mTORC1 to assess the metabolic state of the cell.

The findings presented in this thesis make significant contributions to our mechanistic understanding of how amino acids are sensed by this pathway. The discovery of Ragulator, GATOR2 and GATOR1 not only represent the first positive and negative regulators of the Rag GTPases, but also shed light on how deregulation of amino acid sensing can underlie human disease. The ineffectiveness of rapamycin as a broad cancer therapeutic has been partially attributed to a lack of appropriate biomarkers for mTORC1-driven cancers. Our discovery that GATOR1 deficient cancer cells are hypersensitive to rapamycin portends its use as a biomarker to identify patients whose tumors may be sensitive to rapamycin treatment. In the following section we discuss several questions motivated by this work.

Why do the Rags function as heterodimers?

This is one of the most puzzling questions in the amino acid sensing field. We can speculate that heterodimerization may afford this pathway a greater degree of signal modulation. Canonical signal transduction pathways (growth factor signaling, vesicular transport) rely on GTPases that exist in either an on (GTP-bound) or off (GDP-bound) state, thus providing a switch-like mechanism in response to an input. Joining two Rag GTPases together yields four different

nucleotide-bound states, potentially extending their signaling dynamics from a simple (i.e. on, off) system to a more nuanced one (i.e. partially on). While there is overwhelming evidence that the nucleotide states of RagA and RagB take precedence in regulating their interaction with mTORC1, the nucleotide states of RagC and RagD must also be critical in regulating mTORC1 in order for the above hypothesis to work. Studies in yeast reveal that the GTP-locked mutant of GTR2 (RagC) inactivates the pathway regardless of the nucleotide loaded state of GTR1 (RagA) (*1*). The importance of RagC has also been observed in mammalian cells, where the GTP mutant of RagB activates the pathway to the greatest degree when expressed concomitantly with the RagC-GDP mutant (*2*). At the mechanistic level we find that raptor strongly binds to GDP-loaded RagC (in a Rag heterodimer) but not when RagC is bound to GTP (LBP, unpublished data). Thus the strongest interaction between mTORC1 and Rags occurs when RagA is GTP-bound and RagC is GDP-loaded. The other nucleotide states of the Rags may interact with mTORC1 at different affinities, allowing the heterodimer to function as a dimmer in its control of mTORC1, rather than a switch.

These results imply that upstream regulatory factors that mediate the amino acid signal such as GEFs and GAPs must also exist for RagC and RagD. While there is little doubt that this will be the case, one potential form of regulation that has been largely overlooked may come from within the Rag heterodimer. Precedence for heterodimeric G proteins regulating the nucleotide bound state of their partners comes from the signal recognition particle (SRP)-SRP receptor (SR) system. SRP and SR function as GAPs for each other when both are loaded with GTP, ensuring proper translocon docking (*3*). The recently solved crystal structure of GTR1-GTR2 demonstrates that the G domain of GTR2 undergoes significant structural re-arrangements in its transition from the GTP to GDP bound state. This results in the GTR2 G domain contacting the G domain of GTR1 and hints at a possible regulation of one GTR (Rag) by the other (*4, 5*). Solution of the crystal structure of GTR1 bound to GDP within the GTR1-GTR2 heterodimer and use of Rag^{X} mutants that allow for Rag specific nucleotide loading (*6*) will help test this hypothesis.

How does the v-ATPase regulate the activity of Ragulator?

The identification of v-ATPase as a direct positive regulator of mTORC1 came as a surprise, as its role in lysosomal acidification is independent of its function in amino acid sensing (*7*). The amino acid-dependent conformational changes between Ragulator and the V1 domain of the v-ATPase offers some insight into how this complex relays the amino acid signal. When cells are starved of amino acids the V1 and Ragulator subunits strongly interact with each other (*7*). This result can be mimicked with pharmacological inhibitors of the v-ATPase that jam V1-V0 rotation (*8*) and block mTORC1 signaling (*7*). Upon amino acid stimulation, the V1-Ragulator interactions weaken, presumably activating Ragulator GEF activity. How the tight interaction between Ragulator and V1 inhibits the GEF activity is not clear, but it suggests that the physical manipulation of Ragulator by V1 modulates Ragulator activity. Interestingly, negative regulation of GEFs appears to be mediated through proteins that stabilize autoinhibitory domains common to many GEFs (*9-11*), which may also be found in Ragulator.

While stabilization of V1-Ragulator interactions imply an inhibitory role for the v-ATPase, depletion of V0 subunits inactivates the mTORC1 pathway, proposing a bimodal function for this complex. Given the constitutively strong binding between V0 and Ragulator, it is likely the V0 domain will also be required for activation of Ragulator. This model suggests that V1, in addition to being a direct inhibitor of Ragulator, negatively regulates V0 activation of Ragulator when cells are starved for amino acids. Careful in vitro Ragulator GEF assays incorporating highly purified v-ATPase complexes will delineate the precise mechanisms the v-ATPase uses to control Ragulator.

Recent studies suggest that the hydrolytic activity of the v-ATPase, responsible for V0-V1 rotation should be altered by the amino acid signal (*7*). However v-ATPase activity in aggregate, as measured by lysosomal acidification, does not change upon amino acid starvation or stimulation. While lysosome acidification is a good proxy for ATP hydrolysis it by no means defines it.

Moreover, a large fraction of v-ATPase complexes do not interact with Ragulator, making the above results difficult to interpret in the context of amino acid signaling. Ongoing studies directly measuring ATP hydrolysis by the Ragulator-bound fraction of v-ATPase will likely shed light on this important question.

Is there a broader significance to the regulated interaction between Rags and Ragulator?

We find that amino acid starvation strengthens the Rag-Ragulator interaction, whereas stimulation weakens it, paralleling the change in the nucleotide bound state of RagA/B from GDP to GTP. We interpret this change in affinity as an outcome of the GEF activity of Ragulator towards RagA/B, which is consistent with the poor interactions observed between GEFs and nucleotide-bound versions of their cognate GTPases. The weakening of the Rag-Ragulator interaction could expose an mTORC1-binding site on the Rags. Temptingly, it could also reflect the reversible departure of the Rags from the lysosomal surface, a cycle dependent on the nucleotide state of RagA and RagB. Why might the Rags leave the lysosome? Perhaps the simplest explanation would be to retrieve mTORC1 from the cytoplasm and return it back to its site of activation. How mTORC1 transits to the lysosome remains unknown. Live-cell microscopy suggests that mTORC1 does not shuttle to the lysosome along actin or tubulin tracks. Furthermore, treatment of cells with the microtubule depolymerizing drug nocodazole, does not perturb mTORC1 activation by amino acids (LBP and RZ, unpublished results). While mTORC1 could associate with lysosomal membranes through Brownian motion, the speed with which mTORC1 translocates to the lysosome argues for a directed process rather than random diffusion. Studies involving dynamic live cell imaging will be essential in elucidating whether the Rags leave the lysosomal surface to capture mTORC1 upon amino acid stimulation.

How does GATOR2 regulate GATOR1?

Genetic interaction mapping reveals that GATOR2 is an upstream inhibitor of GATOR1. The weakening of the interaction between Rags and GATOR1 after amino acid stimulation, is consistent with many potential mechanisms for its inhibition by GATOR2. One possibility is that GATOR2 simply prevents the interaction between GATOR1 and the Rags, protecting them from GTP hydrolysis. Another possibility is that GATOR2 directly inhibits GATOR1 GAP activity by mimicking other inhibitors of GAPs. Fortunately, both of these scenarios are easy to test. Spatial regulation might also be employed by GATOR2 to ferry GATOR1 away from lysosomes. This idea is consistent with the spatial regulation of TSC2 by growth factors (*12*) and is plausible given that the COPII coat protein Sec13 is a member of GATOR2.

Is there cross-talk between the v-ATPase-Ragulator and GATOR branches?

A major question stemming from this work is how Rag activating and inactivating pathways are coordinated. Preliminary experiments using pharmacological inhibitors of the v-ATPase in GATOR1-deficient cells revealed that mTORC1 was still insensitive to amino acid regulation, the same result obtained in cells expressing the GTP-mutant of RagA. This finding suggests that GATOR1 and the v-ATPase-Ragulator branch either function in parallel pathways to regulate the Rags or that GATOR1 lies downstream of v-ATPase-Ragulator. We favor the former possibility, as these parallel mechanisms of regulation are often encountered in other GTPase networks such as those of Ras and Arf (*14*). The persistent mTORC1 activity upon v-ATPase inhibition is the consequence of the slow rate of GTP hydrolysis of RagA/B in cells lacking GATOR1, dispensing the need for activation by Ragulator. Whether the amino acid signal is split between the GATOR and v-ATPase-Ragulator or whether both pathways are controlled by the same hierarchical amino acid sensor is the subject of intense scrutiny.

Conclusions

At present, we have only begun to scratch the surface of the vast mTORC1-signaling network. From a molecular perspective, the work described here sheds light on one of the oldest eukaryotic signaling pathways. The onus will now be to identify the amino acid sensor(s) that controls the lysosome based signaling platform required for mTORC1 shuttling. By following a bottom up approach it is likely that this question will be addressed in the years to come.

From a physiological perspective, mTOR catalytic inhibitors and the generation of pathway specific knockout mice promise to unravel both the cellular and organismal programs under the control of mTORC1. The genomic revolution also ensures that many orphan diseases once lacking a defined molecular basis will undoubtedly be linked back to this pathway. One can only anticipate what new biology studying the mTORC1 pathway will reveal.

References

1. M. Binda *et al.*, The Vam6 GEF Controls TORC1 by Activating the EGO Complex. *Mol Cell* **35**, 563 (2009).
2. Y. Sancak *et al.*, The Rag GTPases bind raptor and mediate amino acid signaling to mTORC1. *Science* **320**, 1496 (Jun 13, 2008).
3. D. Akopian, K. Shen, X. Zhang, S. O. Shan, Signal Recognition Particle: An Essential Protein-Targeting Machine. *Annu Rev Biochem*, (Feb 13, 2013).
4. R. Gong *et al.*, Crystal structure of the Gtr1p-Gtr2p complex reveals new insights into the amino acid-induced TORC1 activation. *Genes Dev* **25**, 1668 (Aug 15, 2011).
5. J. H. Jeong *et al.*, Crystal structure of the Gtr1p(GTP)-Gtr2p(GDP) protein complex reveals large structural rearrangements triggered by GTP-to-GDP conversion. *J Biol Chem* **287**, 29648 (Aug 24, 2012).
6. L. Bar-Peled, L. D. Schweitzer, R. Zoncu, D. M. Sabatini, Ragulator Is a GEF for the Rag GTPases that Signal Amino Acid Levels to mTORC1. *Cell* **150**, 1196 (Sep 14, 2012).
7. R. Zoncu *et al.*, mTORC1 senses lysosomal amino acids through an inside-out mechanism that requires the vacuolar H(+)-ATPase. *Science* **334**, 678 (Nov 4, 2011).
8. X. S. Xie *et al.*, Salicylihalamide A inhibits the V0 sector of the V-ATPase through a mechanism distinct from bafilomycin A1. *J Biol Chem* **279**, 19755 (May 7, 2004).
9. D. Ron, G. Graziani, S. A. Aaronson, A. Eva, The N-terminal region of proto-dbl down regulates its transforming activity. *Oncogene* **4**, 1067 (Sep, 1989).
10. S. Katzav, J. L. Cleveland, H. E. Heslop, D. Pulido, Loss of the amino-terminal helix-loop-helix domain of the vav proto-oncogene activates its transforming potential. *Mol Cell Biol* **11**, 1912 (Apr, 1991).
11. A. Schmidt, A. Hall, Guanine nucleotide exchange factors for Rho GTPases: turning on the switch. *Genes Dev* **16**, 1587 (Jul 1, 2002).
12. S. L. Cai *et al.*, Activity of TSC2 is inhibited by AKT-mediated phosphorylation and membrane partitioning. *J Cell Biol* **173**, 279 (Apr 24, 2006).
14. J. L. Bos, H. Rehmann, A. Wittinghofer, GEFs and GAPs: critical elements in the control of small G proteins. *Cell* **129**, 865 (Jun 1, 2007).